

AD/A-004 886

WATER ELECTROLYSIS PROPULSION SYS-
TEM TESTING

John G. Campbell, et al

Marquardt Company

Prepared for:

Air Force Rocket Propulsion Laboratory

November 1974

DISTRIBUTED BY:

NTIS

National Technical Information Service
U. S. DEPARTMENT OF COMMERCE

UNCLASSIFIED

SECURITY CLASSIFICATION OF THIS PAGE (When Data Entered)

AD/A004886

REPORT DOCUMENTATION PAGE		READ INSTRUCTIONS BEFORE COMPLETING FORM
1. REPORT NUMBER AFRPL-TR-74-72	2. GOVT ACCESSION NO.	3. RECIPIENT'S CATALOG NUMBER
4. TITLE (and Subtitle) Water Electrolysis Propulsion System Testing		5. TYPE OF REPORT & PERIOD COVERED Final Report October 72 - July 74
7. AUTHOR(s) John G. Campbell R. Carl Stechman, Jr.		6. PERFORMING ORG. REPORT NUMBER
9. PERFORMING ORGANIZATION NAME AND ADDRESS The Marquardt Company 16555 Saticoy Street Van Nuys CA 91409		8. CONTRACT OR GRANT NUMBER(s) F04611-73-C-0006
11. CONTROLLING OFFICE NAME AND ADDRESS AFRPL/LKDA Edwards CA 93523		10. PROGRAM ELEMENT, PROJECT, TASK AREA & WORK UNIT NUMBERS PE-62302F; Proj-3058; Task-11 Work Unit-AFRPL-3058-11-VW
14. MONITORING AGENCY NAME & ADDRESS (if different from Controlling Office)		12. REPORT DATE November 1974
		13. NUMBER OF PAGES 208 211
		15. SECURITY CLASS. (of this report) UNCLASSIFIED
		15a. DECLASSIFICATION/DOWNGRADING SCHEDULE
16. DISTRIBUTION STATEMENT (of this Report) Approved for Public Release; Distribution Unlimited.		
17. DISTRIBUTION STATEMENT (of the abstract entered in Block 20, if different from Report) Reproduced by NATIONAL TECHNICAL INFORMATION SERVICE U.S. Department of Commerce Springfield, VA. 22151		
18. SUPPLEMENTARY NOTES		
19. KEY WORDS (Continue on reverse side if necessary and identify by block number) Gaseous O ₂ ; Gaseous H ₂ ; Bipropellant; Water Electrolysis; Satellite Propulsion; Attitude Control; Five-Pound Thrust; One-Tenth Pound Thrust; Blowdown		
20. ABSTRACT (Continue on reverse side if necessary and identify by block number) A twenty-four month program was conducted to demonstrate the life capability of a water electrolysis propulsion system and to develop lightweight 5-lbf and 0.1-lbf GO ₂ /GH ₂ thrusters. A water electrolysis propulsion system was tested for 33 weeks at an accelerated rate to demonstrate its capabilities. The electrolysis unit experienced a loss of voltage on one cell after 19 weeks of testing. Design modifications and repairs were made after which an additional 14 weeks of testing were accomplished with no degradation in performance. The lightweight 5 lbf engine accumulated 152,015 pulses and 4.16 hours of firing		

PRICES SUBJECT TO CHANGE

UNCLASSIFIED

SECURITY CLASSIFICATION OF THIS PAGE(When Data Entered)

Item 20. Abstract. (Continued)

demonstrating a steady state Isp of 355 seconds. The flightweight 0.1-lbf engine demonstrated a steady state Isp of 331 seconds while accumulating 301,726 pulses and 10.07 hours of firing time. A chamber coating failure which occurred just before the end of the 0.1-lbf life testing was attributed to corrosion effects due to the high spark energy from the spark plug igniter. The results of the system and engine tests have shown that a water electrolysis propulsion system is feasible and could provide significant weight advantages over mono-propellant systems for high total impulse long-life satellite missions.

ia

UNCLASSIFIED

SECURITY CLASSIFICATION OF THIS PAGE(When Data Entered)

NOTICES

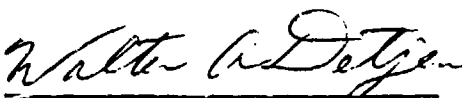
When U.S. Government drawings, specifications, or other data are used for any purpose than a definitely related Government procurement operation, the Government thereby incurs no responsibility nor any obligation whatsoever, and the fact that the Government may have formulated, furnished, or in any way supplied the said drawings, specifications, or other data, is not to be regarded by implication or otherwise, or in any manner licensing the holder or any other person or corporation, or conveying any rights or permission to manufacture, use or sell any patented invention that may in any way be related thereto.

This report was submitted by The Marquardt Company, Van Nuys, California, under Contract No. F04611-73-C-0006, Job Order No. 305811VW with the Air Force Rocket Propulsion Laboratory, Edwards, California 93523.

This report has been reviewed by the Information Office/DOZ and is releasable to the National Technical Information Service (NTIS). At NTIS it will be available to the general public, including foreign nations.

This technical report has been reviewed and is approved for publication.


MELVIN V. ROGERS
Project Engineer


WALTER A. DETJEN, Chief
Engine Development Branch


CHARLES E. SIEBER, Lt Colonel, USAF
Chief, Liquid Rocket Division

ACCESSION for	
NTIS	White Section <input checked="" type="checkbox"/>
	Buff Section <input type="checkbox"/>
UNCLASSIFIED	<input type="checkbox"/>
JCS INFORMATION	
BY	
DISTRIBUTION/AVAILABILITY CODES	
Dis.	Avail. and/or SPECIAL
A	

SUMMARY

A complete water electrolysis satellite propulsion system was tested for 33 weeks. The system consumed 201 pounds of water and produced an impulse of 70,000 pound-seconds.

A lightweight 0.1 pound thrust engine (Figure 1) and a lightweight five pound thrust engine (Figure 2) were developed and tested to demonstrate life capability and performance.

1. SYSTEM LIFE TESTING

The water electrolysis propulsion system had been assembled and given performance tests on a preceding contract (Reference 1). The system consisted of an electrolysis unit, made by General Electric Company, a water storage tank, gaseous hydrogen and oxygen storage tanks, a five-pound thrust heavyweight and a 0.1 pound thrust heavyweight engine.

The propellant supply system shown in Figure 3, consisting of the electrolysis unit, water tank, and gaseous propellant storage tanks, included a series of pressure switches which automatically turned the electrolysis system off and on, depending on the pressure in the propellant storage tanks.

An electronic pulser was designed to control engine firings for a prescribed duty cycle intended to produce, in 10 months, the total impulse of the seven-year satellite mission shown in Table 1. The system operated around the clock, seven days a week, with additional safety controls to turn off the electrolysis unit in case of system malfunction.

The initial electrolysis unit was tested for 19 weeks, producing an impulse of 41,000 pound-seconds, after which a failure of one of the six electrolysis cells occurred. The electrolysis unit was modified by General Electric Company. The modified unit was tested for 14 weeks and produced an impulse of 29,000 pound-seconds without any change in performance. The life testing demonstrated the capability of the electrolysis system for long-life operation as a satellite propulsion system.

2. FIVE-POUND THRUST ENGINE

A lightweight five-pound thrust engine was developed and life tested for 152,015 pulses and a total firing time of 4.16 hours. A test summary is given in Table 2. The engine was in excellent condition after completion of the life test program. Design changes made in the heavyweight five-pound engine developed on the previous contract resulted in an improvement of specific impulse from 345 seconds to 355 seconds. The engine performance is shown in Figure 4.

1. Stechman, R. C., Jr., and Campbell, J. G., "Water Electrolysis Satellite Propulsion System," AFRPL-TR-72-132, January, 1973

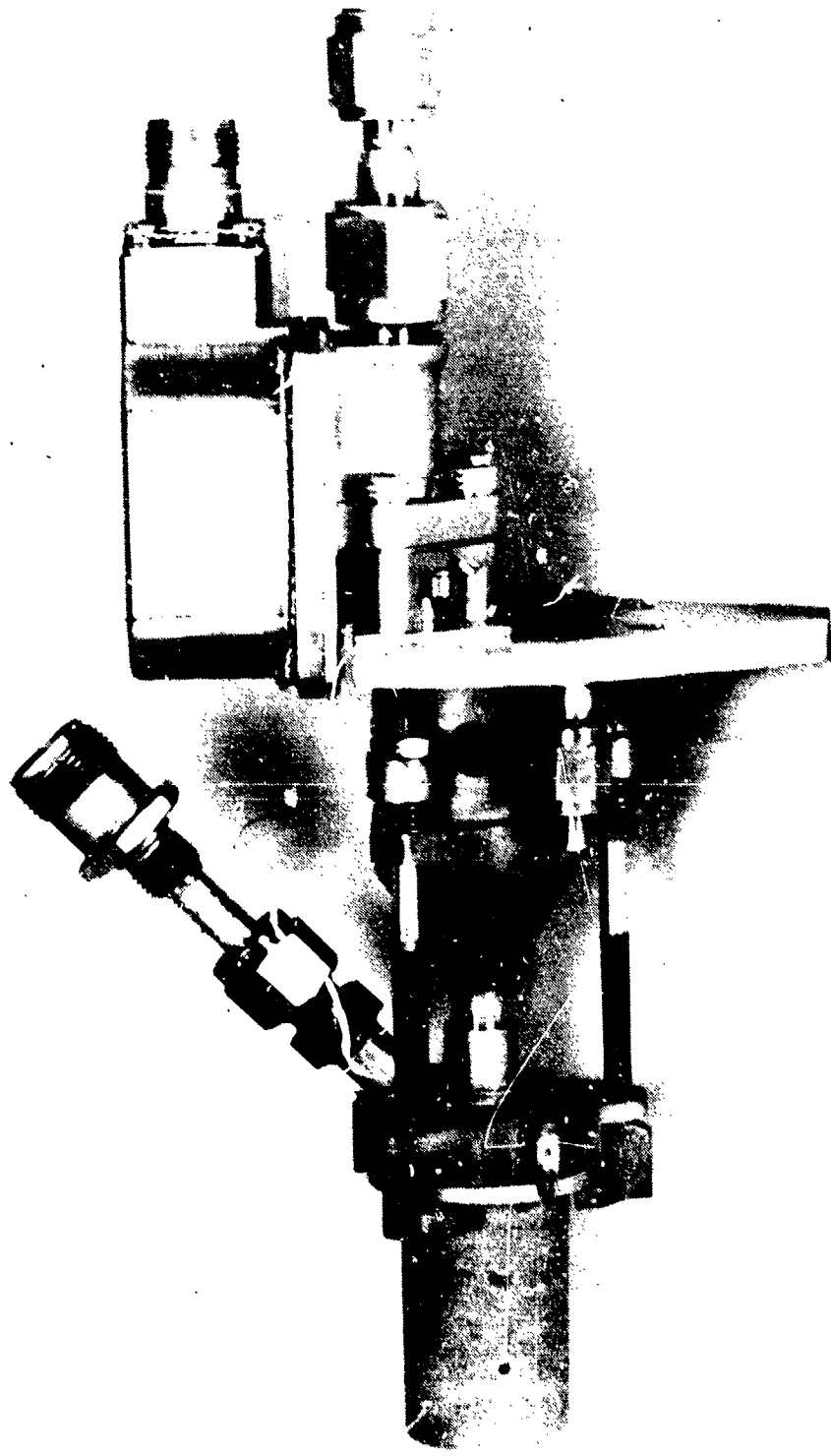
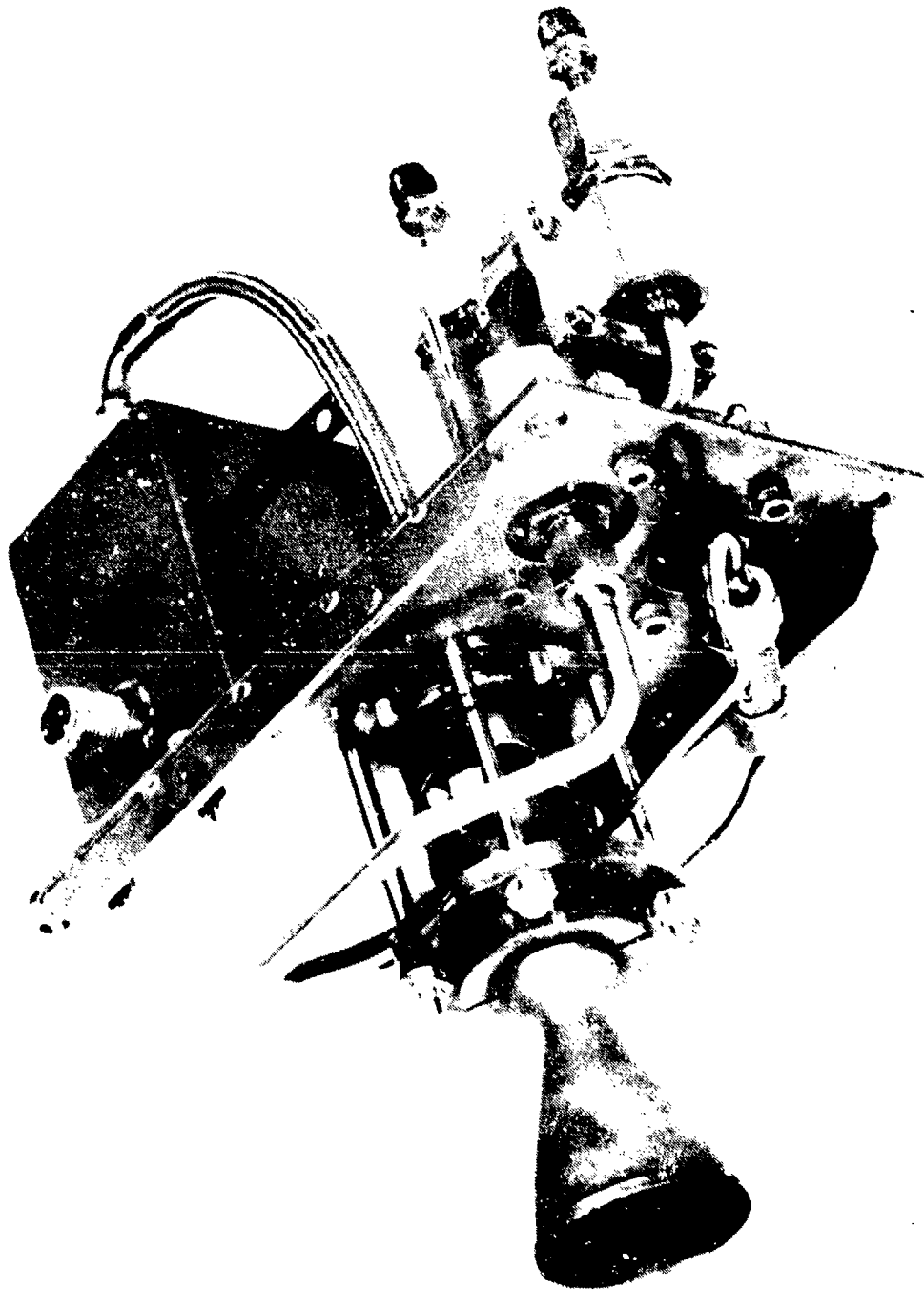


Figure 1. Flightweight 0.1 Lbf. Engine After Test Firings



REF ID: A64196

Figure 2. Flightweight 5 Lbf. Engine and Igniter

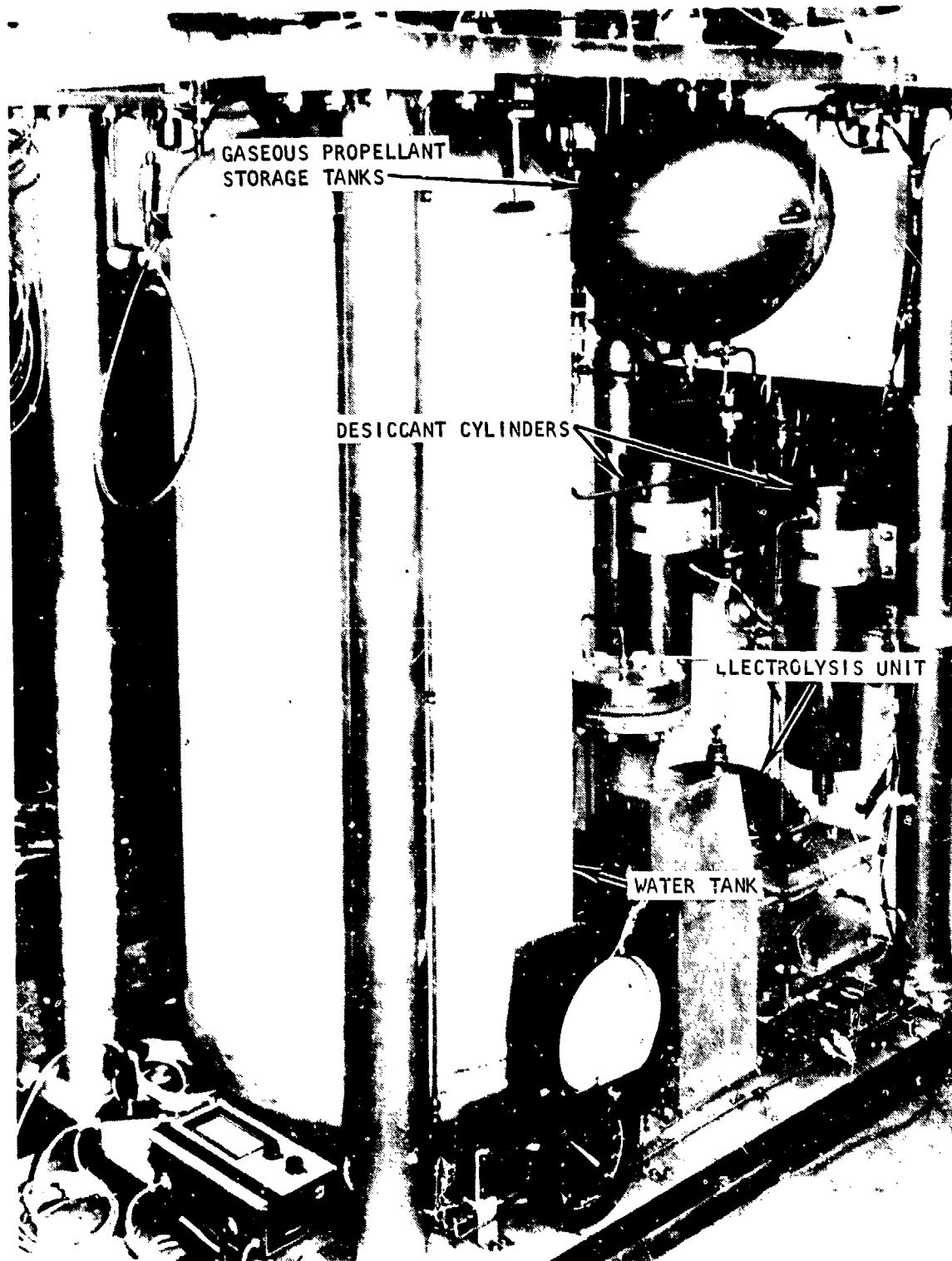


Figure 3. Water Electrolysis Propellant Supply System

TABLE 1. MISSION REQUIREMENTS

Maneuver or Mission Event	RFR Requirement	Satellite Weight (lbs.)	Operational Mode	Time	Electrolysis Power (Watts)	Total Impulse (lb.-sec.)	Est. Avg. Specific Impulse (sec.)	Required Propellants (lbs.)
Booster Injection Errors • Top-off Rate • Position & Velocity	2.0 Degree/sec. (in all Axes)	2400	Blowdown (Generated Prior to Launch)	20 min.	0	10 - 12	320	0.035
	$\Delta V = 80$ fps	2400	Blowdown (Generated After Launch at a Rate of 2.3 lbm/d.)	8 days	230	3,000	300	10.0
Station-Keeping	$\Delta V = 157$ fps/yr. E-W/N-S R.R. 3.3 x 10 ¹⁰ ft/sec ²	2200 (Avg.)	Generated as Required (Avg. Requirement = 0.00 lbm/day)	7 years	18	70,000	340	221.0
Attitude Control Requirements	$I_p = 3000$ lb.-sec. Spin: $\pm 0.5^\circ$ W.D. 3 Axes: $\pm 0.1^\circ$ O.D.	2200 (Avg.)	Generated as Required (Avg. Requirement = 0.0037 lbm/day)	7 years	18	3,000	275	15.0
Repositioning	$\Delta V = 200$ fps	2200	Generated Blowdown (Generated at a Rate of 2.3 lbm/day)	15 days	230	10,000	350	60.0
Contingency		2200	Generated as Required	As Required	18	300	320	1.27
TOTALS	$\Delta V = 1400$ fps					100,000	330 (Avg.)	244.00

TABLE 2. FLIGHTWEIGHT ENGINE TEST SUMMARY

	0.1 LB THRUST	5 LB THRUST
THRUST (POUNDS)	0.037-0.1	1-7
CHAMBER PRESSURE (PSIA)	25-70	7-50
SPECIFIC IMPULSE, STEADY STATE	331	355
SPECIFIC IMPULSE, 50 MILLISECONDS	300	-
PULSING DUTY CYCLES	0.1 SEC ON/0.1 SEC OFF	0.05 AND 0.10 SEC ON AT 10% TO 25% DUTY CYCLE
MAXIMUM RUN DURATION	30 MINUTES	1 HOUR
TOTAL RUN TIME	10.07 HOURS	4.16 HOURS
TOTAL FIRINGS	301,726	152,015

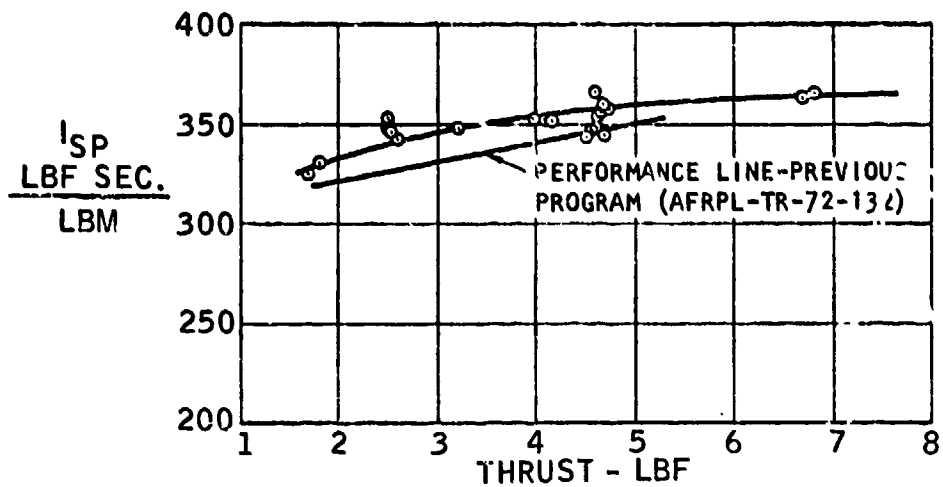


Figure 4. ISP of Flightweight 5 Lbf. Engine

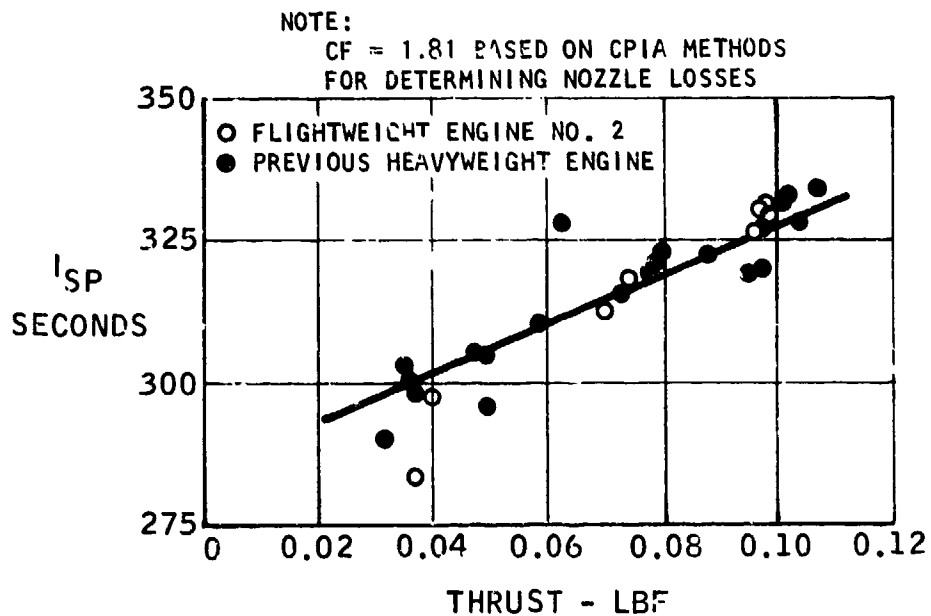


Figure 5. ISP of Flightweight 0.1 Lbf. Engine

The flightweight five-pound engine, shown in Figure 2, consists of a coated molybdenum combustion chamber, a nickel injector with six coaxial premixed elements, and 24 chamber film cooling orifices, a Marquardt bipropellant valve and a modified Champion FHE spark plug. Several components, such as the valve and mounting plate, were heavier than flightweight components. A flightweight igniter made by General Laboratory Associates (GLA) energizes the spark plug. Propellant flow rates are controlled by sonic orifices located downstream of the bipropellant valve. The nominal mixture ratio is 7.934 to match the proportions of oxygen and hydrogen produced by electrolysis of water. The nominal chamber pressure varies from 50 psia down to 16 psia, corresponding to a range of propellant tank pressures varying from 200 psia down to 67 psia. The weight of the flightweight five-pound thrust engine was 4.5 pounds, excluding the igniter. A completely flightweight engine would weigh 2.9 pounds. The flightweight GLA igniter weighs 1.71 pounds and the cable weighs 0.17 pounds.

3. 0.1 POUND THRUST ENGINE

Two flightweight 0.1 pound thrust engines were designed and tested. One of the two designs, shown in Figure 1, completed a test program of 301,726 pulses and 10.0⁷ hours of hot firing time. This 0.1 pound engine consisted of a coated C-103 columbium chamber, a single coaxial, premixed injector element, a MOOG bipropellant valve, with downstream sonic orifices, and a modified Champion FHE 231 spark plug. A flightweight GLA igniter energized the spark plug. The engine operates at chamber pressures from 70 psia down to 25 psia, depending on the propellant supply pressure. The nominal mixture ratio is 7.934. The weight of the flightweight engine, not including igniter, is projected to be 1.7 pounds using a flightweight valve and injector. It is expected that one flightweight igniter, weighing 1.7 pounds, could provide spark energy to a number of 0.1 pound engines on a satellite with engine selection controls.

The columbium chamber suffered a coating failure during the last half hour of the 10-hour life test. The test results with the columbium chamber and a molybdenum chamber which failed after 3.52 hours of hot firings suggest that the cause of coating failure may be due to excessively high energy release by the spark plug. In that case, longer life could be obtained by using the lower spark energy which was successfully used with the heavyweight engine on the preceding contract (Reference 1).

The 0.1 pound thrust engine demonstrated a C* efficiency of 82%, corresponding to an Isp of 331 seconds. The performance at various mixture ratios is plotted in Figure 5.

4. IGNITER

A flightweight igniter shown in Figure 6 was designed by GLA. Three identical units were delivered to Marquardt. The ignition system used to ignite the gaseous oxygen

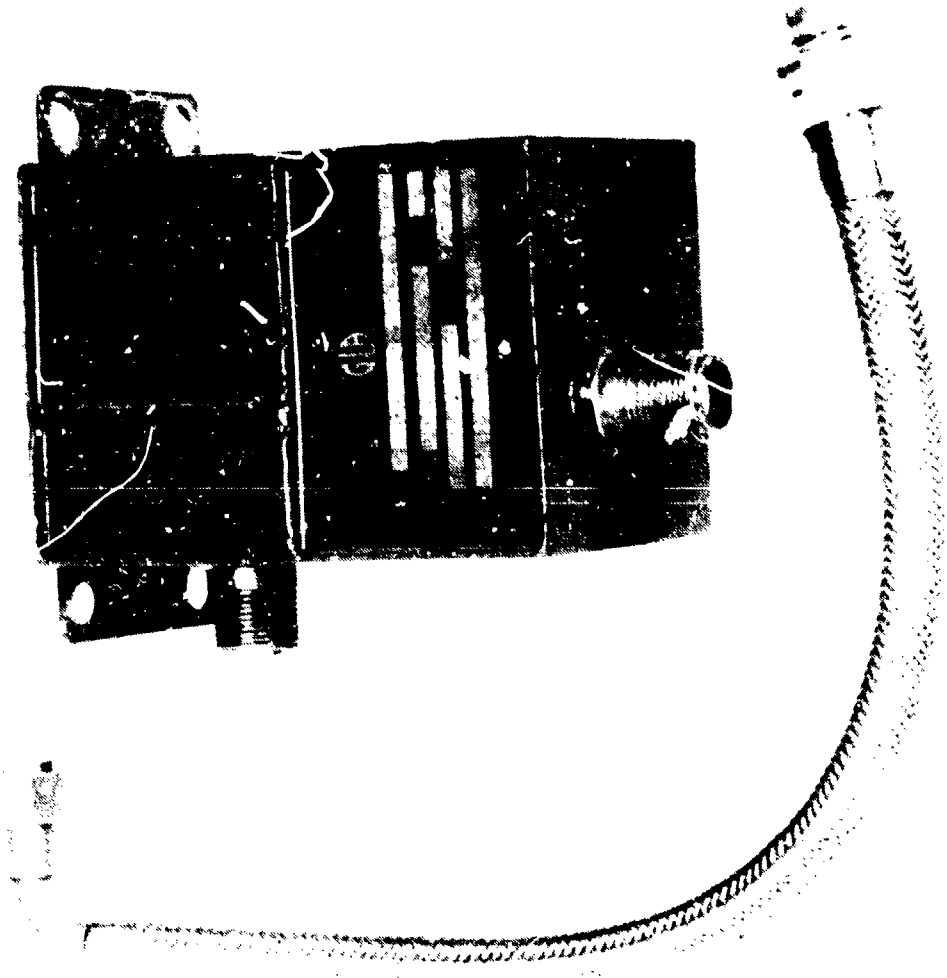


Figure 5. Flightweight Igniter and Cable

and hydrogen combination in the combustion chamber of the 5 lbf. and 0.1 lbf. rocket engine consists of a Champion FHE 231A spark plug with energy for the spark discharge supplied by a General Laboratory Associates (GLA) exciter. The exciter shown in Figure 6 provides a basic spark rate of 400 sparks/second at 28 vdc. The energy supplied to the spark plug at each discharge is 10 millijoules. In addition, the spark exciter system met the requirements for conducted and radiated EMI in accordance with the limits of MIL-STD-461-A, except during some switching transients. The exciter systems successfully completed the engine test firing sequences and provided greater than 1,000,000 sparks in both the 5.0 and 0.1 test programs.

TABLE OF CONTENTS

<u>SECTION</u>	<u>TITLE</u>	<u>PAGE</u>
	SUMMARY	1
I	INTRODUCTION	15
II	SYSTEM LIFE TESTING	17
III	5-POUND THRUST ENGINE	59
	1. Summary of Results From Program	59
	2. Engine Design	59
	3. Test Program	66
	4. Test Results	68
IV	ONE-TENTH POUND THRUST ROCKET ENGINE	111
	1. Flightweight Design No. 1	111
	2. Flightweight Design No. 2	120
V	SPARK IGNITION AND EXCITER SYSTEM	153
	1. System Description	153
	2. Test Program Results	153
VI	CONCLUSIONS	158
VII	RECOMMENDATIONS	159
Appendix A	FLIGHTWEIGHT IGNITER	161
Appendix B	TEST OF EXCITER CHARACTERISTICS	176

LIST OF ILLUSTRATIONS

<u>FIGURE</u>	<u>TITLE</u>	<u>PAGE</u>
1	Flightweight 0.1 Lbf. Engine After Test Firings	2
2	Flightweight 5 Lbf. Engine and Igniter	3
3	Water Electrolysis Propellant Supply System	4
4	Isp of Flightweight 5 Lbf. Engine	6
5	Isp of Flightweight 0.1 Lbf. Engine	6
6	Flightweight Igniter and Cable	8
7	Electrolysis Propulsion System	15
8	Comparison of Satellite Propulsion System Weights	15
9	Electrolysis Process	18
10	Water Electrolysis Cell Schematic	18
11	Simple Blowdown System	19
12	Water Electrolysis Ground Test System Schematic	21
13	Water Electrolysis Feed System	22
14	System Control Logic	25
15	Instrumentation Panel for Life Test	28
16	Pad D Life Test Location	29
17	PRL Control Room	30
18	Engine Firing Timer	31
19	5 Lbf. Workhorse Engine	33
20	0.1 Lbf. Workhorse Engine	34
21	Typical Pressure Cycle	37
22	Hydrogen Embrittlement of Hydrogen-Side Screen Assembly	42
23	Corrosion and Rust on Inner Surface of Top Endplate	43
24	Indentation on Screen Protector Ring Oxygen Eyelet	45
25	Niobium Deposit on Water Screen Assembly	46
26	Failure Pattern on Cell No. 4	47
27	Disassembled Carpenter 20 Check Valve After 14 Week Life Test	54
28	Oxygen Desiccant Cartridge at End of Life Testing	55
29	Hydrogen Desiccant Cartridge at End of Life Testing	56
30	5 Lbf. Thruster No. 3 After Test Program	60
31	Performance of 5 Lbf. Engine	61
32	5 Lbf. Engine ISP Vs. Electrical Pulse Width	62
33	5 Lbf. Injector Assembly	65
34	Cell 9 Schematic	67
35	5 Lbf. Thruster, Configuration No. 1 (X29069)	69
36	Flange and Injector for 5 Lbf. Thruster, Configuration No. 1	70
37	Outer Injector and Flange - 5 Lbf. Thruster, Configuration No. 1	71

LIST OF ILLUSTRATIONS (Continued)

<u>FIGURE</u>	<u>TITLE</u>	<u>PAGE</u>
38	5 Lbf. Thruster Injector, Configuration No. 1	72
39	5 Lbf. Thruster Assembly, Configuration No. 1	73
40	5 Lbf. Injector, Configuration No. 1, After Test	74
41	5 Lbf. Combustor, Configuration No. 1, After Test	75
42	Outside of 5 Lbf. Combustor, Configuration No. 1, After Test	76
43	5 Lbf. Thruster, Configuration No. 2	78
44	Injector for 5 Lbf. Thruster, Configuration No. 2	79
45	Exploded View of 5 Lbf. Thruster, Configuration No. 2	80
46	Partially Assembled 5 Lbf. Thruster, Configuration No. 2	81
47	5 Lbf. Thruster Installed in Cell 9 Thrust Stand	82
48	5 Lbf. Combustor, Configuration No. 2, After Test	86
49	Columbium Injector After Test	87
50	5 Lbf. Thruster, Configuration No. 3	88
51	Assembled 5 Lbf. Thruster, Configuration No. 3	90
52	5 Lbf. Thruster, Configuration No. 3	91
53	Performance of 5 Lbf. Thruster, Configuration No. 3	93
54	Impulse Bit of 5 Lbf. Thruster, Configuration No. 3	99
55	Valve Response Vs. Thrust Level	100
56	5 Lbf. GO ₂ /GH ₂ Rocket Engine Firing Record, 50 Ms Firing	101
57	5 Lbf. GO ₂ /GH ₂ Rocket Engine Firing Record, 100 Ms Firing	102
58	5 Lbf. GO ₂ /GH ₂ Rocket Engine Firing Record, 250 Ms Firing	103
59	5 Lbf. GO ₂ /GH ₂ Rocket Engine Firing Record, Steady State	104
60	Maximum Combustor Temperature of 5 Lbf. Thruster	105
61	Disassembled 5 Lbf. Thruster, Configuration No. 3, After Test	107
62	5 Lbf. Injector Face, Configuration No. 3, After Test	108
63	Spark Plug from 5 Lbf. Thruster, Configuration No. 3, After Test	108
64	5 Lbf. Combustor, Configuration No. 3, After Test	110
65	Flightweight 0.1 Lbf. Engine No. 1 Design	113
66	Assembled 0.1 Lbf. Flightweight Engine No. 1	114
67	0.1 Lbf. Engine Temperatures Vs. Injector Effective Radiation Area	117
68	0.1 Lbf. Engine Temperatures Vs. Spacer Thermal Resistance	118
69	0.1 Lbf. Engine Temperatures Vs. Combustor Effective Radiation Area	119
70	Flightweight 0.1 Lbf. Engine No. 1 With Radiation Fin	123
71	Flightweight 0.1 Lbf. Engine No. 2 Design	126
72	Components of Flightweight 0.1 Lbf. Engine No. 2	127
73	Flightweight 0.1 Lbf. Engine No. 2 Assembly	128

LIST OF ILLUSTRATIONS (Continued)

<u>FIGURE</u>	<u>TITLE</u>	<u>PAGE</u>
74	Location of Thermocouples on Flightweight Engine No. 2	130
75	Performance of 0.1 Lbf. Flightweight Engine No. 2	135
76	Flightweight 0.1 Lbf. Engine No. 2 During Firing	138
77	Cutaway View of 0.1 Lbf. Molybdenum Chamber After Firing	139
78	Spark Plug After Run 239 (28,918 Accumulated Pulses)	141
79	Spark Plug After Run 237 (71,152 Accumulated Pulses)	142
80	Deposit in Throat of 0.1 Lbf. Columbium Chamber	148
81	Cutaway View of 0.1 Lbf. Columbium Chamber After Firing	149
82	Spark Plug After Run 255 (301,728 Accumulated Pulses)	150
83	0.1 Lbf. Engine Chamber Pressure Rise	152
84	Champion Spark Plug FHE231A	154
85	Acceptance Test Record for S/N 001 Exciter	155
86	Acceptance Test Record for S/N 002 Exciter	156
87	Acceptance Test Record for S/N 004 Exciter	157
A1	Flight Type Exciter	162
A2	Schematic Wiring Diagram for Flightweight Igniter	163
A3	Installation Drawing of Flightweight Exciter	164
A4	Block Diagram of Flightweight Exciter	165
A5	Resonant Charging Components	167
A6	Resonant Charging Circuit	169
A7	Voltage and Current Transients	170
A8	Oscillatory Discharge Circuit	171
A9	Characteristics of Oscillatory Discharge Circuit	172
A10	Unidirectional Discharge Circuit	173
A11	Characteristics of Unidirectional Discharge Circuit	174
B1	Test Setup	182
B2	Solid State Switch	183
B3	EMI Levels Vs. Frequency, Positive D. C. Input	185
B4	EMI Levels Vs. Frequency, Negative D. C. Input	186
B5	Radiated Levels Vs. Frequency	187

LIST OF TABLES

<u>TABLE NO.</u>	<u>DESCRIPTION</u>	<u>PAGE</u>
1	Mission Requirements	5
2	Flightweight Engine Test Summary	5
3	Safety Controls	26
4	Life Test Engine Firing Schedule	32
5	Electrolysis Unit Performance Data	52
6	5 Lbf. Thruster Design Characteristics	64
7	Summary of Data from C-103 Injector Tests	84
8	5 Lbf. Thruster Part Number and Weight Summary	92
9	Steady State Performance, 5 Lbf., Configuration No. 3	95
10	Pulse Performance, 5 Lbf., Configuration No. 3	98
11	Design Characteristics, Flightweight 0.1 Pound Thrust Engine	112
12	Steady State Temperature With 0.1 Lbf. Molybdenum Chamber	136
13	Run Summary for Life Test of 0.1 Pound Columbium Chamber	144
14	Steady State Temperature With 0.1 Pound Columbium Chamber	145

SECTION I

INTRODUCTION

A water electrolysis satellite propulsion system uses satellite electrical power and an electrolysis unit which slowly separates water from a storage tank into hydrogen and oxygen. The separated gases are stored in small tanks for use by oxygen/hydrogen rocket engines as needed for satellite attitude control or orbit maneuvers. The system is shown schematically in Figure 7.

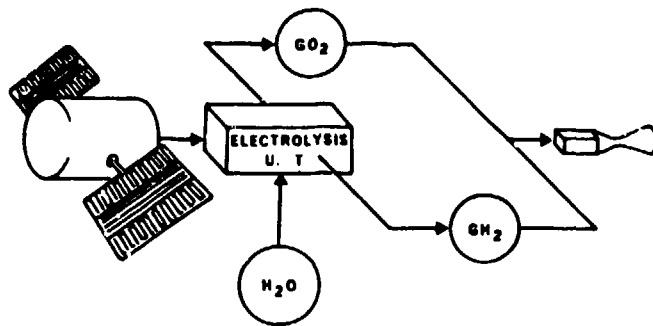


Figure 7. Electrolysis Propulsion System

A water electrolysis satellite propulsion system is especially advantageous for long life satellites which require a large total impulse to be supplied over a long period of time. The system is applicable to either spin stabilized or three-axis stabilized satellites. Comparisons of propulsion system weights for a typical seven-year satellite mission are shown in Figure 8.

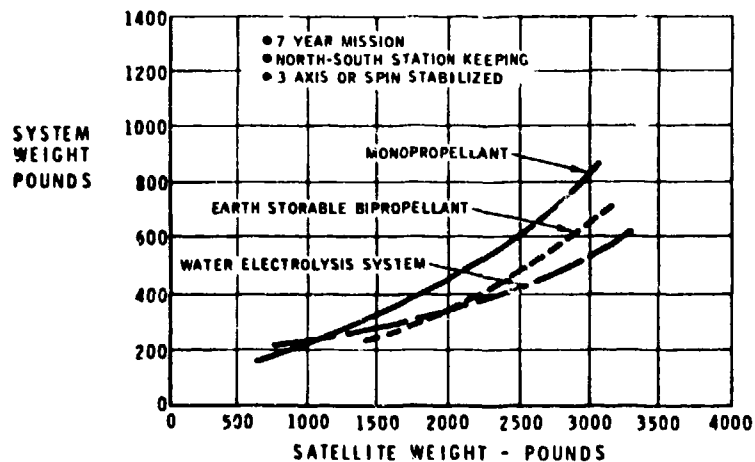


Figure 8. Comparison of Satellite Propulsion System Weights

The water electrolysis system (350 Isp) is much lighter than a monopropellant system (230 Isp) for satellites weighing over 1,500 pounds, and is also lighter than an earth storable bipropellant system (300 Isp) for satellites weighing over 2,400 pounds.

The electrical power requirements can be minimized by tailoring the size of the water electrolysis system to the propulsion requirements of a specific mission. For example, all station-keeping and attitude control of a 2,450 pound satellite can be accomplished with less than 20 watts continuous power. Repositioning maneuvers can be accomplished in one to two weeks by temporarily higher power consumption up to 235 watts.

Some of the advantages of a water electrolysis satellite propulsion system are as follows:

- . Lighter Weight System
- . Low Impulse Bit Capability
- . High reliability with an effective service life in space of up to 10 years
- . Bulk of propellants stored as inert water
- . Nontoxic, noncorrosive propellants
- . An exhaust plume consisting of water vapor
- . Safety aspects of a low pressure, separated gas system
- . Multi-operational mode flexibility to accomplish the various mission propulsive requirements in the most efficient and effective manner
- . Low power consumption

This report presents the results of a program to demonstrate the long-life capability of a water electrolysis propulsion system and to develop flightweight 5 lbf and 0.10 lbf thrusters.

This program was an extension of the effort performed by Marquardt under Air Force Contract F04611-71-C-0055, "Water Electrolysis Satellite Propulsion System," reported in Reference 1.

1. Stechman, R. C., Jr. and Campbell, J. G., "Water Electrolysis Satellite Propulsion System," AFRPL-TR-72-132, January 1973.

SECTION II

SYSTEM LIFE TESTING

A complete water electrolysis propulsion system, consisting of a propellant feed system, a five-pound thrust engine and a 0.10 pound thrust engine, was tested for 19 weeks, producing an impulse of 41,000 pound-seconds, after which a failure of one of the six electrolysis cells occurred. The electrolysis unit was modified by General Electric Company. The modified unit was tested for 14 weeks and produced an impulse of 29,000 pound-seconds without any change in performance.

An electrolysis unit, which is the critical component of the propellant feed system, separates water into hydrogen and oxygen by the process shown conceptually in Figure 9. The electrolysis unit made by General Electric Company contained six electrolysis cells as described in Reference 1. The basic construction of a single electrolysis cell is shown in Figure 10.

The propellant feed system was essentially the same as that described in the final report for the preceding contract (Reference 1), modified to operate only in the simple blowdown mode. A safety override system was also added, consisting of pressure transducers, thermocouples, and voltage signals from the system being monitored by API meters for automatic shutdown in case the limit values were exceeded.

1. SIMPLE BLOWDOWN SYSTEM

Three different modes of operation were possible with the ground test system built under the previous contract (Reference 1), depending on the method of pressurizing the water tank. Those modes were: (1) simple blowdown, (2) repressured blowdown, and (3) oxygen pressurized. The simple blowdown system was chosen for the life test on this program. A schematic diagram of a simple blowdown system is shown in Figure 11. The water is stored in a tank which is initially pressurized with helium. The water and helium may be separated by a flexible bladder or surface tension screens might be used in the tank to feed water to the electrolysis unit. In either case, as water is consumed, the volume in the tank to be filled by helium will increase, and the pressure will drop. The tank volume and initial pressure will be such that the water tank pressure when all water is consumed will equal the minimum pressure required to supply water to the electrolysis unit.

A latch valve located between the water tank and the electrolysis unit is closed whenever the electrolysis unit is turned off. Check valves are located on the hydrogen and oxygen outlets from the electrolysis unit. These check valves prevent the hydrogen and oxygen from flowing back into the electrolysis unit when the electrolysis unit is turned off. This prevents the hydrogen and oxygen from recombining into water on the catalytic surfaces in the electrolysis unit.

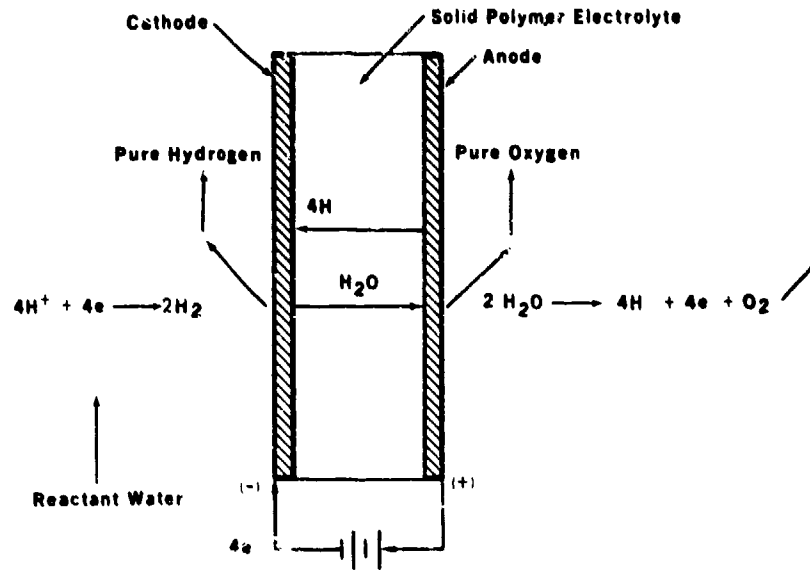


Figure 9. Electrolysis Process

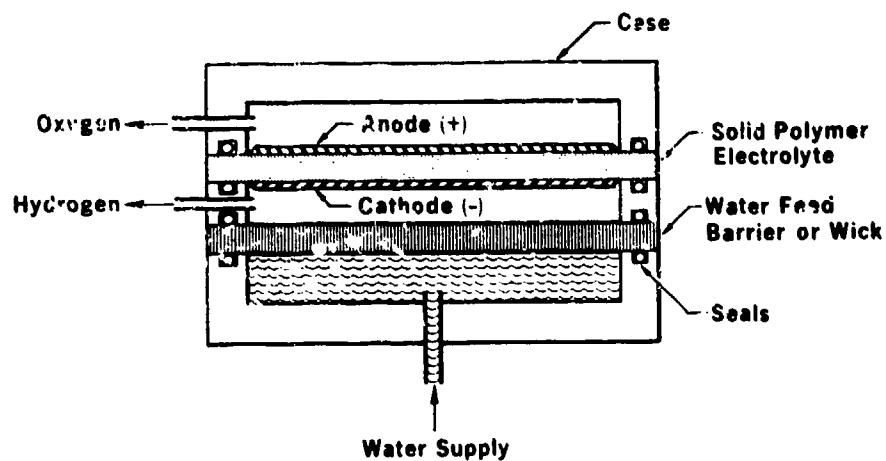


Figure 10. Water Electrolysis Cell Schematic

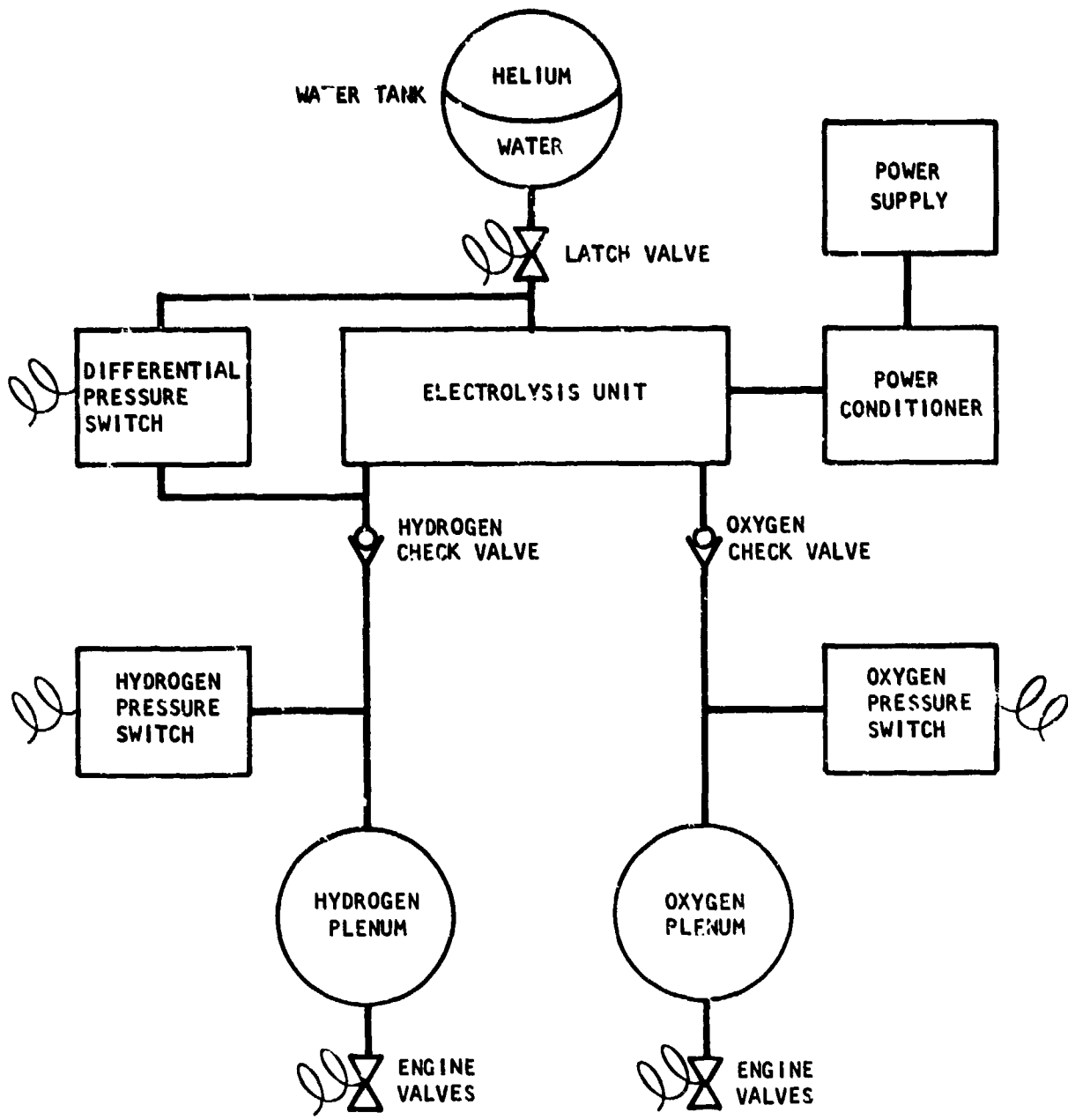


Figure 11. Simple Blowdown System

2. PROPELLANT FEED SYSTEM

The propellant feed system was modified for ground testing on this contract in the simple blowdown mode. The ground test system schematic diagram is shown in Figure 12. The electrolysis unit being tested did not have the capability of operating under as large a pressure drop from water inlet to hydrogen cell as would be required for a flight system operating in the simple blowdown mode. Therefore, the helium tank was repressurized manually several times during the life test program. The current in the low power mode, which is adjustable from 0.1 to 9.6 amps, was set at 0.6 amps to accommodate the maximum possible pressure drop, water to hydrogen cell, for low power mode testing. A number of hand valves, solenoid valves, and pressure transducers were added to the system for ease of operation and performance checks.

The major components in the propellant feed system are a water tank, an electrolysis unit, and gaseous propellant storage tanks.

a. Water Tank

The water tank, shown in Figure 13, is made of 321 stainless steel. It has an inside diameter of 24 inches, a height of 65 inches, and a volume of 15 ft³. Ultra pure water supplied by Arrowhead Puritas with a resistance above 10 megohms was loaded into the tank. The ultra pure water is deionized, sterilized by ultraviolet light and filtered through a 0.45 micron filter. The tank and all other parts of the water system were cleaned thoroughly before using. The design goal was to maintain 2 megohm resistance of the water without particulate or ionic contamination.

b. Electrolysis Unit

The electrolysis unit which separates the water into hydrogen and oxygen is shown in Figure 13. The electrolysis unit was made by General Electric Company. A number of design changes (described on page 50), were made by General Electric Company to correct deficiencies in the original design described in Reference 1.

c. Gaseous Propellant Plenum Tanks

The two hydrogen tanks and one oxygen tank, shown in Figure 13, were spherical and had a volume of 1 ft³. The tanks were made of 321 stainless steel.

d. Water Filter

A Millipore Filter XX45-047-00 is located in the water line between the water tank and the electrolysis unit to prevent any particulate matter from reaching the latch valve which controls water supply to the electrolysis unit. An 0.8 micron filter element was used.

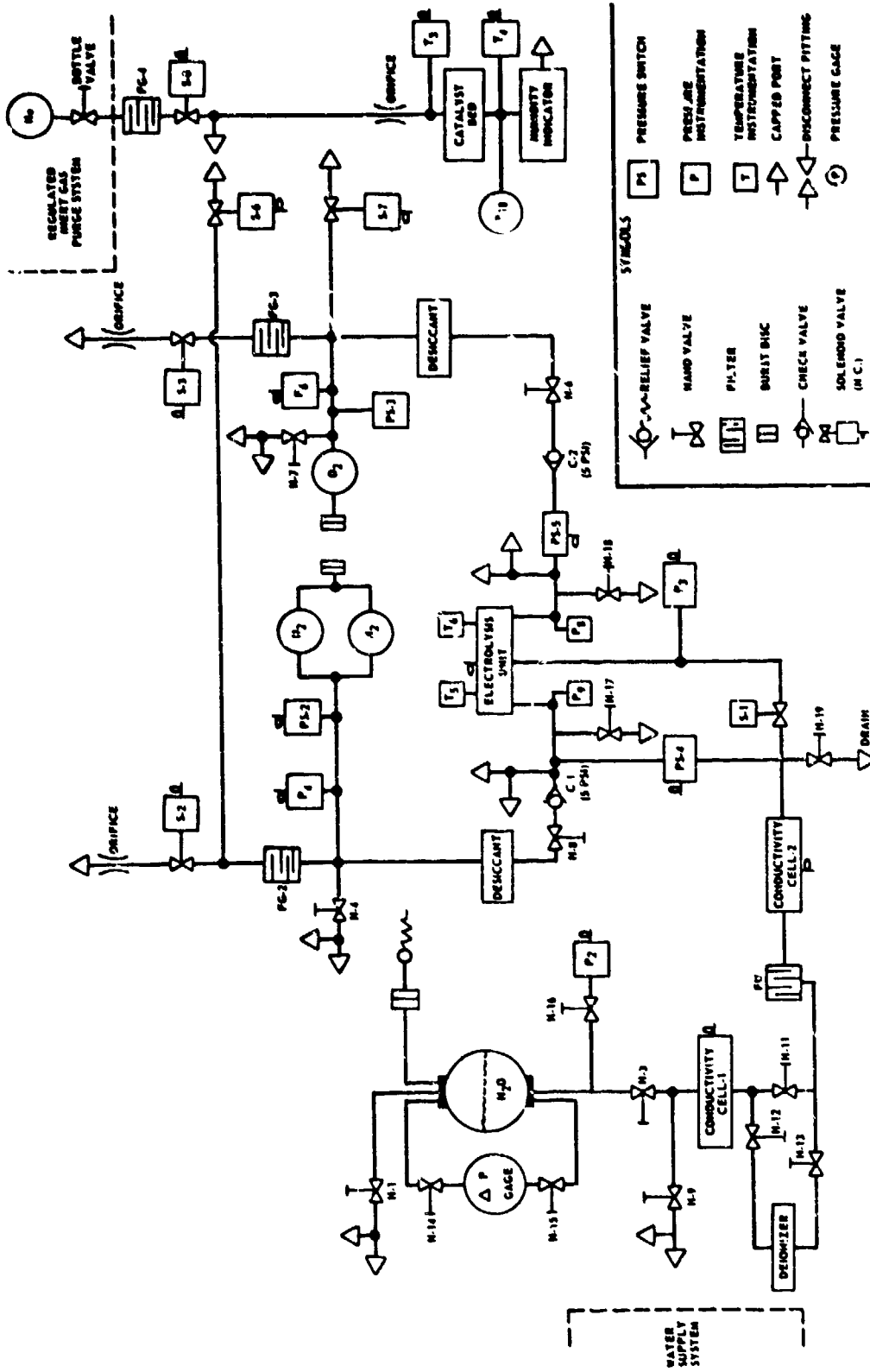


Figure 12. Water Electrolysis Ground Test System Schematic

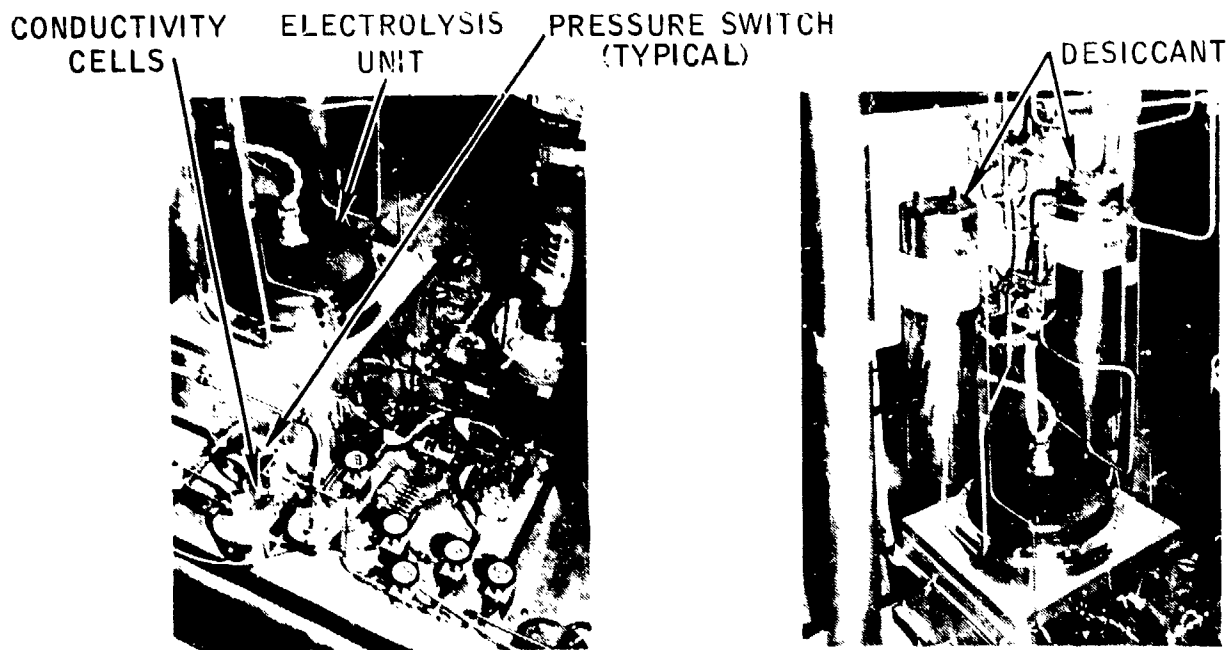
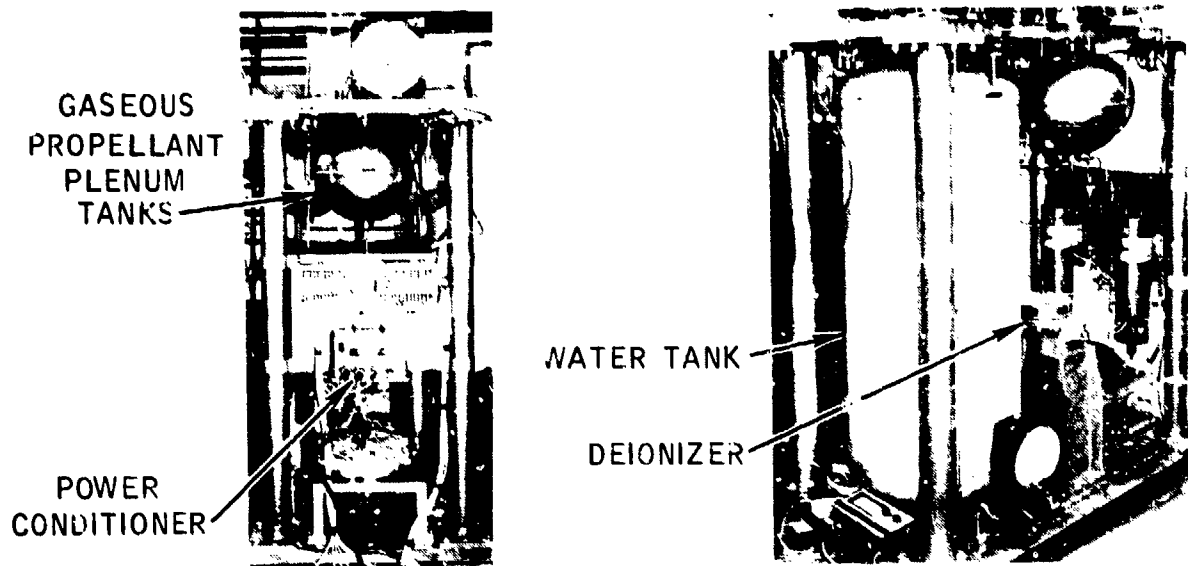


Figure 13. Water Electrolysis Feed System

e. Desiccant

Cylindrical desiccants made by Air Dry Corporation are located in the hydrogen and oxygen lines downstream from the electrolysis unit. The desiccants used in the ground test contained Linde Type 4A molecular sieve pellets. The desiccants removed the water vapor from the propellant gases produced by the water electrolysis unit. The desiccant cylinders are shown in Figure 13.

f. Conductivity Cells

Two conductivity cells made by Balsbaugh, Model No. 900-0.01T-HP, were placed in the water line between the water tank and the electrolysis unit to allow measurements of the electrical resistance of the water.

g. Deionizer

A deionizer installed in the water line between the water tank and the electrolysis unit was bypassed during the life testing because it was found that a water resistance near 2 megohms was maintained in the stainless steel water system without passing the water through the deionizer.

h. Humidity Indicator

The relative humidity of the hydrogen and oxygen after passing through the desiccants is determined by passing the gases through an Air Dry Corporation Model No. 7275 humidity indicator. The relative humidity is indicated by observing the color change in an indicating desiccant.

i. Hydrogen/Oxygen Gas Mixing

Any small amount of mixing of hydrogen and oxygen in either the hydrogen or oxygen systems is indicated by passing the gases through an Englehard Industries Deoxo catalytic gas purifier, Model D-10-2500. Any temperature rise of the gas flowing through the catalyst bed indicates the presence of some amount of mixed gases. The General Electric electrolysis unit produces completely separated gases in normal operation.

3. SYSTEM CONTROLS

The propellant feed system is controlled automatically by several pressure switches to provide hydrogen and oxygen as required to maintain the propellant storage tanks within maximum and minimum pressure limits. A power conditioner provides electric current to the electrolysis unit on one of three levels, (1) high, (2) low, or (3) standby. The proper current at any time is controlled by an electrical signal transmitted to one of three terminals on the power conditioner. The proper terminal is

selected automatically by four pressure switches in the system. The logic diagram for the pressure switches is shown in Figure 14. The pressure limits shown in Figure 14 are for maximum propellant supply pressures of 200 psia.

The pressure switch PS-2 on the hydrogen plenum system is in position "A" when the hydrogen pressure is below 180 psia, and is in position "B" when the hydrogen pressure is above 200 psia. Pressure switch PS-3 on the oxygen system is set at the same limits.

If both the oxygen and hydrogen tank pressures are below 180 psia, the control logic dictates that current be supplied to the electrolysis unit and the water inlet latch valve be opened. However, the amount of current is regulated by pressure switch PS-4, which measures the pressure differential between the inlet water pressure and the hydrogen cell (outlet) pressure.

A low current of about 6 amps will be supplied unless PS-4 measures a pressure differential greater than 70 psi, in which case a high current of about 23 amps will be supplied to the electrolysis unit.

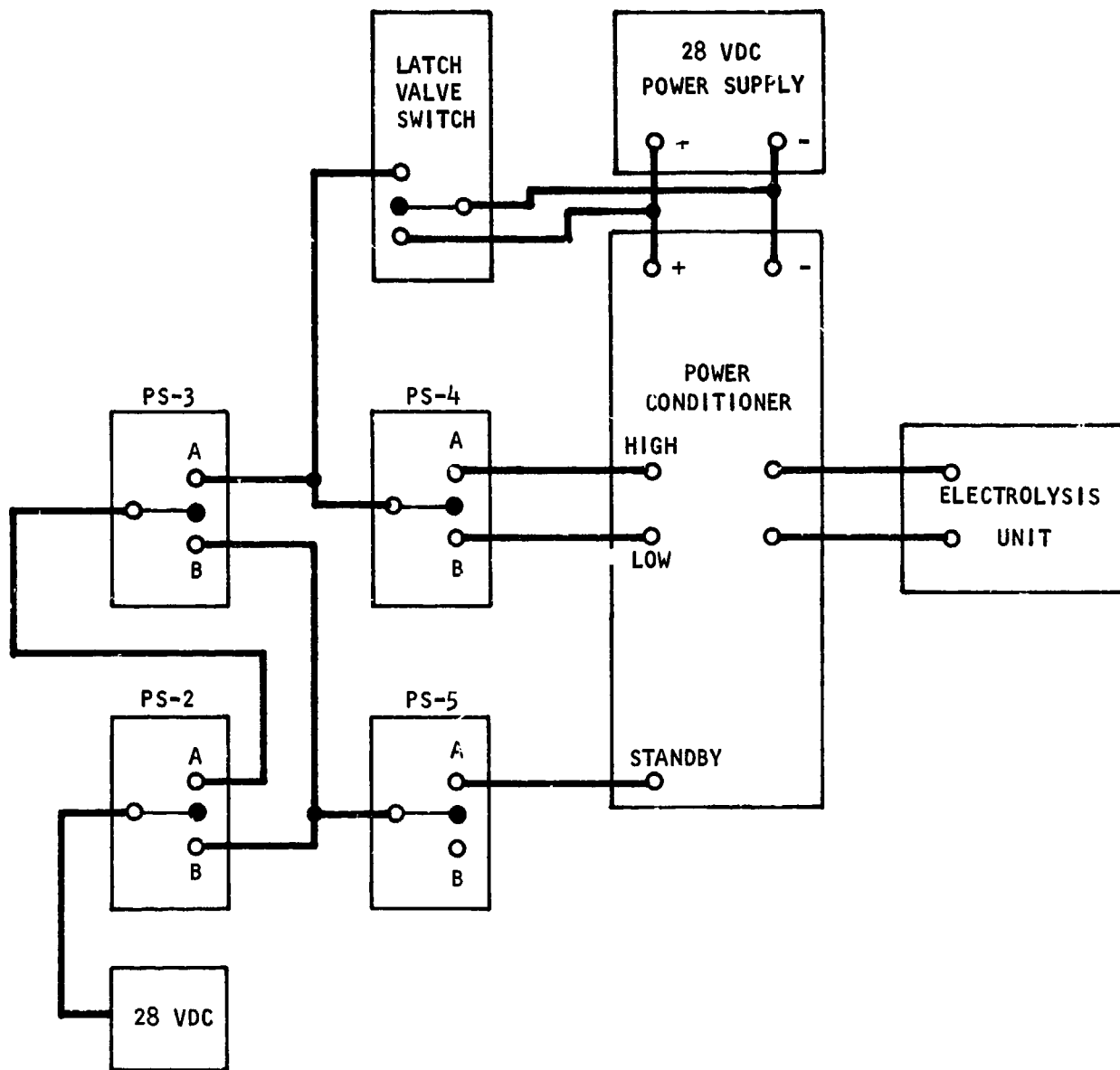
A manually operated relay is also placed between pressure switch PS-4 and the power conditioner to allow override selection of the current to high or low power level. This relay may be used after blowdown of the gaseous propellants in order to keep the electrolysis unit operating in the high power mode until one of the gas tanks has reached 200 psia. A remotely operated relay could be used in a flight system to keep the electrolysis system operating in the high power mode during a period of repetitive blowdowns as during a ΔV maneuver.

If either the hydrogen or oxygen tank pressure exceeds 200 psia, PS-5, a pressure switch on the oxygen cell (outlet) pressure, is activated. If the oxygen cell pressure drops below 145 psia, PS-5 is in position "A" and transmits a signal to the standby terminal of the power conditioner. In this case, a current of one amp will be transmitted to the electrolysis unit. If the oxygen cell pressure is above 180 psia, PS-5 is in position "B", and current to the electrolysis unit is turned off.

4. SAFETY CONTROLS

The propellant feed system was operated continuously around the clock, seven days a week. The test was unattended except for daily monitoring during the regular work week. Therefore, a safety control system was installed to automatically shut off the electrolysis unit in case certain safety limits were exceeded. The parameters monitored by the safety control system are shown in Table 3.

Electrical outputs from the pressure transducers measuring P_8 , the oxygen outlet cell pressure, and P_9 , the hydrogen cell outlet pressure, were connected to API Instruments Company's millivolt limit switches. If either pressure exceeded 250 psig, an electrical signal went to a Visi-Con Mark V-12 annunciator and the



COMPONENT	SENSES	CONTINUITY WHEN	
		(A)	(B)
PS - 2	H ₂ TANK PRESSURE	$P_{H_2} \leq 180 \text{ PSIA}$	$P_{H_2} \geq 200 \text{ PSIA}$
PS - 3	O ₂ TANK PRESSURE	$P_{O_2} \leq 180 \text{ PSIA}$	$P_{O_2} \geq 200 \text{ PSIA}$
PS - 4	$P_{H_2O} - P_{H_2}$	$P_{H_2O} - P_{H_2} \geq 70 \text{ PSIA}$	$P_{H_2O} - P_{H_2} \leq 70 \text{ PSIA}$
PS - 5	O ₂ CELL PRESSURE	$P_{O_2} \leq 145 \text{ PSIA}$	$P_{O_2} \geq 180 \text{ PSIA}$

Figure 14. System Control Logic

TABLE 3. SAFETY CONTROLS

Parameter	Description	Limit	Control Instrument	Action
P ₉	H ₂ Cell Pressure	250 psig	Transducer Output	Turn Off System Power
P ₈	O ₂ Cell Pressure	250 psig	Transducer Output	Turn Off System Power
P ₉ - P ₈	H ₂ - O ₂ Cell Pressure	70 psi	Transducer Output	Turn Off System Power
T ₅	E. U. Top Plate Temperature	170° F	API Temp. Control	Turn Off System Power
V ₁	Cell No. 1 Voltage	2.2 volts	API Voltage Control	Turn Off System Power
V ₂	Cell No. 2 Voltage	2.2 volts	API Voltage Control	Turn Off System Power
V ₃	Cell No. 3 Voltage	2.2 volts	API Voltage Control	Turn Off System Power
V ₄	Cell No. 4 Voltage	2.2 volts	API Voltage Control	Turn Off System Power
V ₅	Cell No. 5 Voltage	2.2 volts	API Voltage Control	Turn Off System Power
V ₆	Cell No. 6 Voltage	2.2 volts	API Voltage Control	Turn Off System Power

electrolysis unit was turned off. The time at which any of the safety limits were exceeded was shown on an Esterline-Angus Model AW operation recorder which was in continuous operation with a paper speed of three inches per hour. The API limit switches, the Visi-Con annunciator and the Esterline-Angus recorder are shown in Figure 15.

Ten different parameters were monitored by the annunciator. The first channel to exceed limits is indicated by a flashing light on the annunciator to aid in any subsequent failure analysis.

Another parameter monitored by the safety system was the absolute pressure differential between the hydrogen and oxygen cells. A differential above 70 psi would shut down the system.

A thermocouple on the top plate inside the electrolysis unit was monitored, with automatic shutdown if the temperature exceeded 170^oF. Any higher temperature would damage the solid polymer electrolytes in the electrolysis unit.

Each of the six cell voltages in the electrolysis unit was monitored to turn off the electrolysis unit in case any cell voltage exceeded 2.2 volts. Such a condition would indicate some type of failure within the electrolysis unit.

5. ENGINES

A five-pound thrust engine and a 0.1 pound thrust engine were installed in the Pad D test cell of the Precision Rocket Laboratory (PRL), adjacent to the propellant feed system as shown in Figure 16. The PRL control room is shown in Figure 17. Propellant lines were run from the hydrogen and oxygen tanks to the engines. Each engine had its own engine valves and spark plug igniters, which were activated by an automatic pulser shown in Figure 18. The pulser was designed and fabricated by Marquardt to provide engine firings over a period of 28 days with the duty cycles shown in Table 4. At the end of 28 days, the pulser shut down and was manually started to repeat the engine firings in Table 4. The pulser was also shut down by the safety system whenever the electrolysis unit was turned off by the safety system.

The five-pound thrust workhouse engine (Figure 19) and the 0.1 pound thrust workhouse engine (Figure 20) developed on the previous contract (Reference 1) were installed in Pad D for the life testing. A Bel Air Engineering fixed energy igniter unit described in Reference 1 was used with each engine.

6. TEST PREPARATION

The initiation of life testing was scheduled for February 1973. However, when the final check of the system was made, a leak was discovered in the mating joint of the electrolysis unit between the dome flange and the aluminum pressure plate. Thin

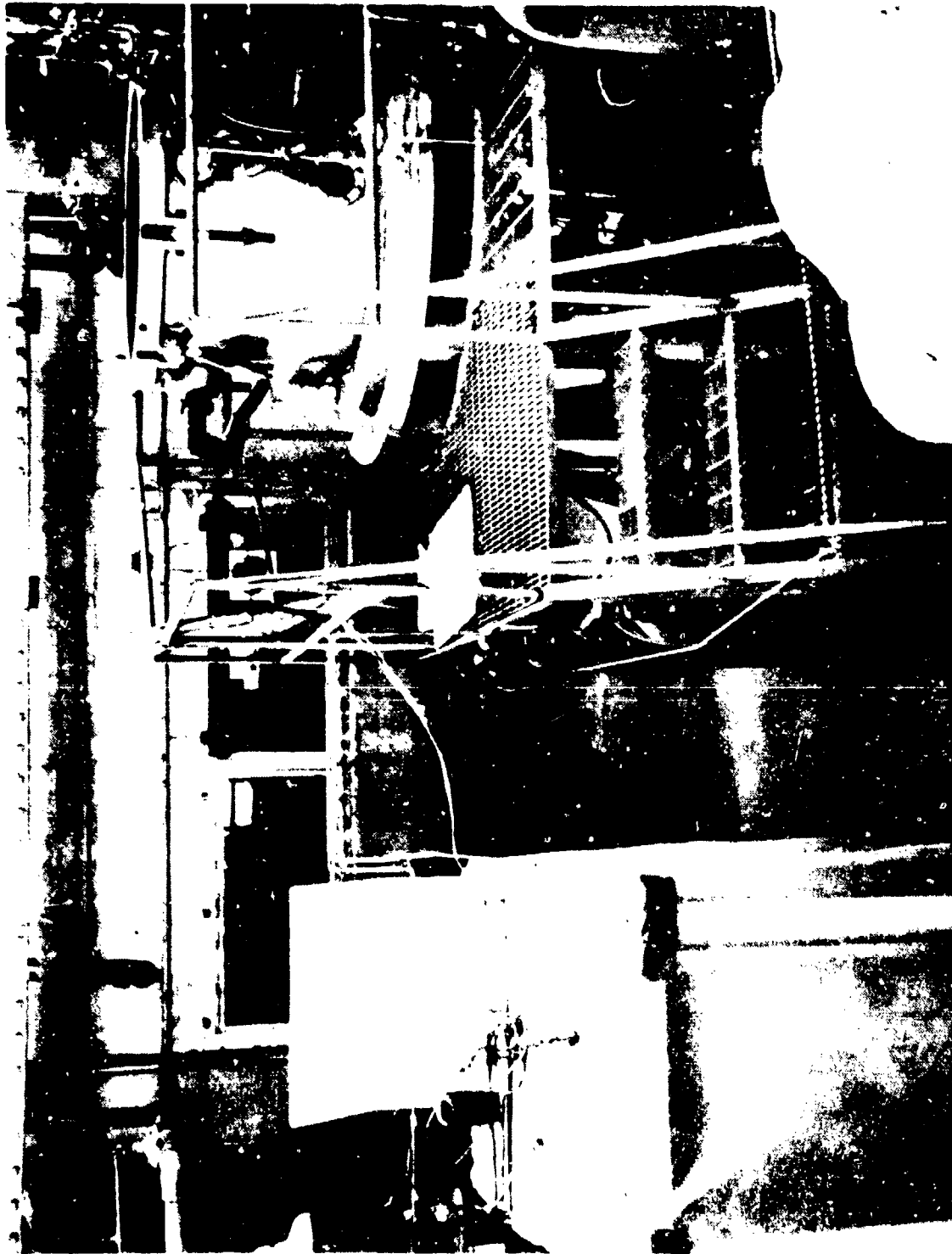


Figure 16, Pad D Life Test Location



Figure 17. PRL Control Room

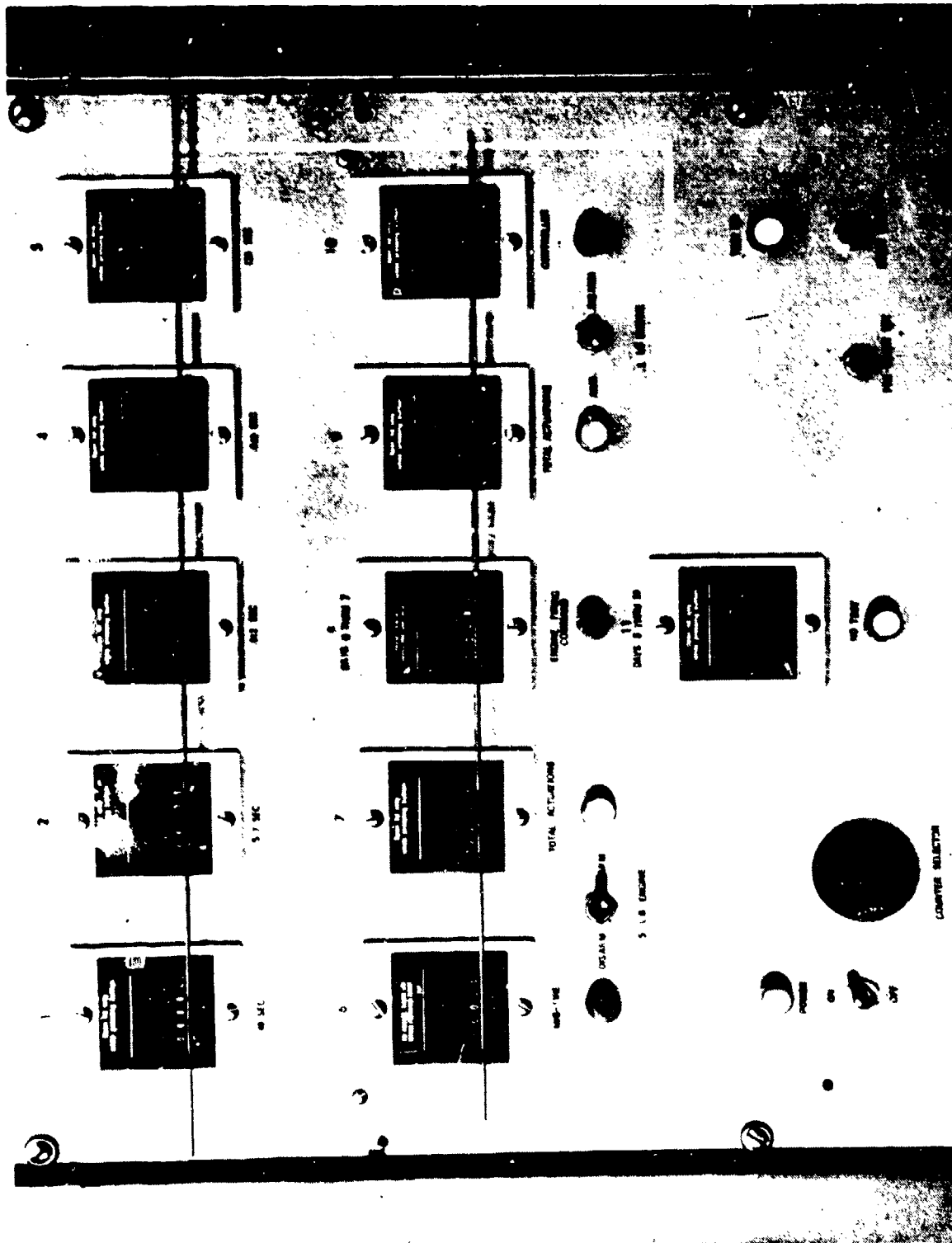


Figure 18. Engine Firing Timer

TABLE 4. LIFE TEST ENGINE FIRING SCHEDULE

	DAY																												
	1	2	3	4	5	6	7	8	9	10	11	12	13	14	15	16	17	18	19	20	21	22	23	24	25	26	27	28	
1. HIGH POWER MODE TESTING (2 LB. H ₂ O/DAY) REPETITIVE BLOWDOWN 5 LB. ENGINE, 40 SEC. FIRING EVERY 4 HRS.																													
2. LOW POWER MODE TESTING (0.5 LB. H ₂ O/DAY) CONTINUOUS CYCLE FIRING 5 LB. ENGINE, 5.7 SEC. FIRING EVERY 4 HOURS 0.1 LB. ENGINE, 29 PULSE TRAIN, 60 MS. ON, 940 MS. OFF, EVERY HOUR 0.1 LB. ENGINE, 0.012 SEC. FIRING EVERY 3 MIN. 0.1 LB. ENGINE, 120 SEC. FIRING EVERY 24 HOURS																													
3. SYSTEM MONITORING INTERMITTANT DATA RECORDING																													
4. COMPLETE DATA RECORDING																													

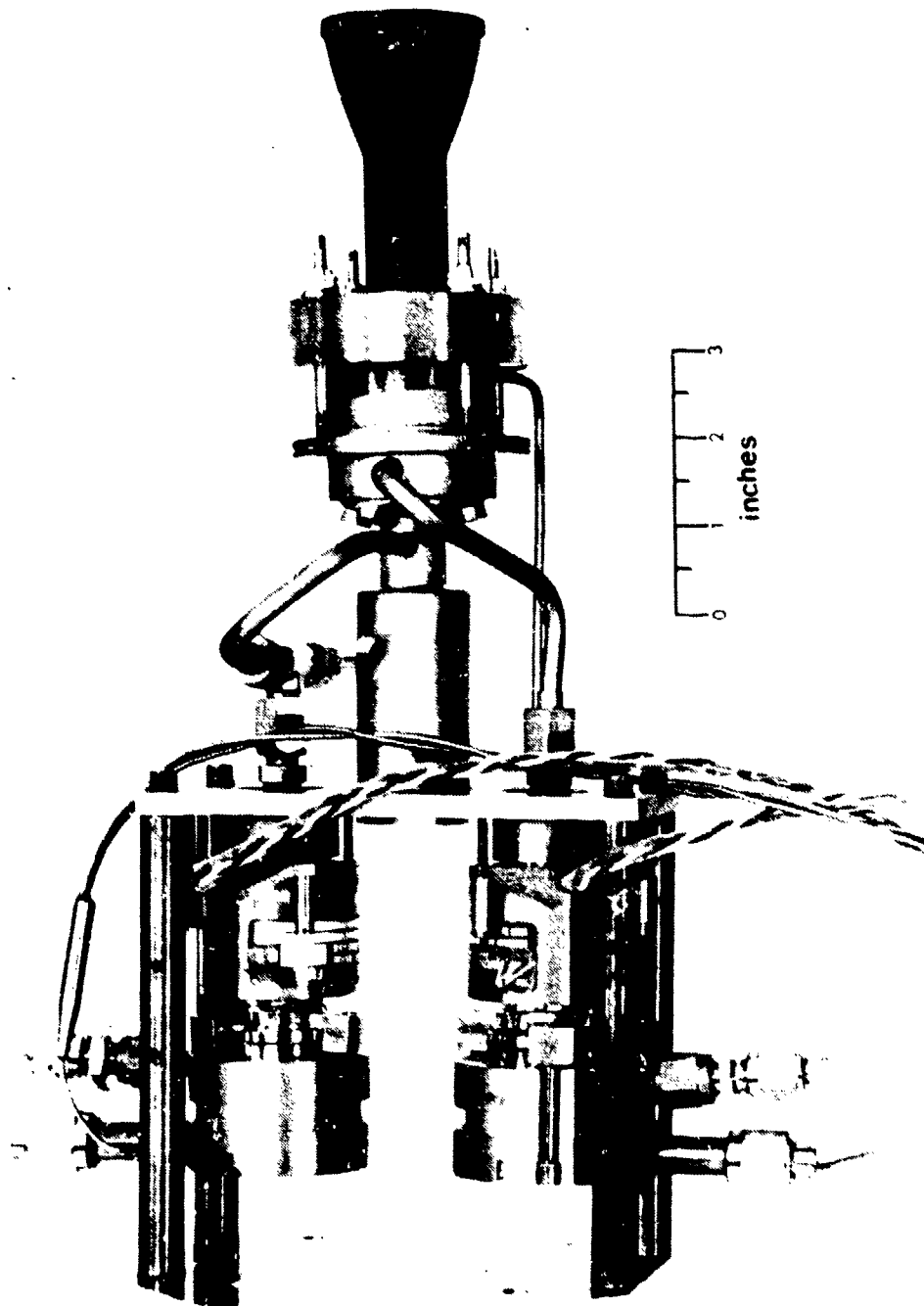


Figure 19. 5 Lbf. Workhorse Engine

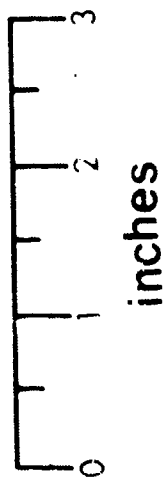
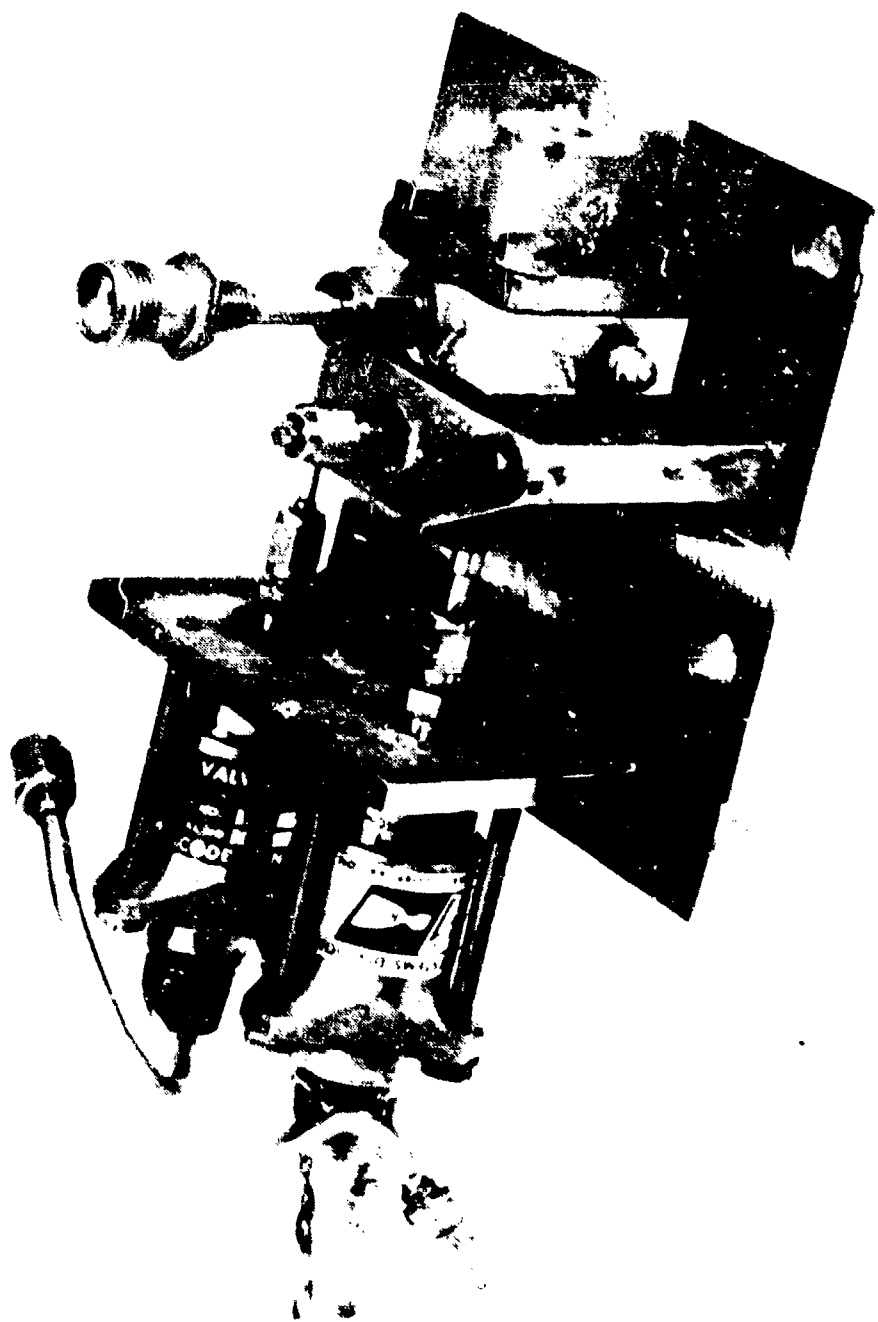


Figure 20. 0.1 Lbf. Workhorse Engine

columbium foil had been bonded with epoxy to the aluminum pressure plate to avoid contact between water and oxygen and the aluminum pressure plate. However, it was found that leak paths had developed between the columbium foil and the aluminum, allowing leakage of hydrogen.

The electrolysis unit was shipped to General Electric Company where the aluminum pressure plate was replaced by a stainless steel pressure plate. The inner surface of the dome was cleaned of rust and coated with teflon to eliminate further rusting. Some partial blockage of the water passage to Cell 4 was also eliminated. This blockage was caused by lateral extrusion of the adjacent polymer during assembly.

After the electrolysis unit had been returned to Marquardt, the system was reactivated preparatory to starting life tests. At this time a leak developed in one of the hydrogen tanks.

The leak developed in the end boss about 0.150 inch from the boss weld. This tank had been in intermittent service with hydrogen at 186 psig for ten months without any leakage. The leak was through a 0.050 inch long crack with raised edges giving the appearance of a small blister. The three tanks were removed from the system and given the following series of tests:

a. Ultrasonic Inspection of Boss

Transverse and axial ultrasonic inspection of the bosses did not reveal any stringers or other imperfections. The known flaw could not be detected because of reflections from the adjacent weld.

b. X-Ray Inspection

Radiographic inspection of the bosses was made by holding narrow film strips inside the boss. The known flaw was clearly shown and a similar flaw which had not carried to the surface was found in the other boss of the same tank. The flaws were characterized as forging (or extrusion) bursts, inherent flaws in the boss parent material and unrelated to welding. The weld x-rays which had been taken during the initial fabrication and inspection of the tanks was reexamined. The flaws were not visible because the x-rays had been focused on the weld.

c. Dye-Penetrant Inspection

Dye-penetrant inspection on the tanks and bosses did not reveal any flaw other than the one leaking crack.

The two flaws in the end bosses were repaired by countersinking 0.125 inch diameter flat bottom holes within .030/.060 inch of the inside surface, inserting a 321 pin and E. B. welding. The tank was subsequently proof-tested to 650 psig and showed no leakage.

7. TEST HISTORY -- ORIGINAL ELECTROLYSIS UNIT

a. June 13, 1973

Life testing of the electrolysis system was initiated on June 13, 1973. Initial tests of the two boilerplate system thrusters at the simulated altitude condition of approximately 80,000 feet indicated that both of the engines failed to ignite. Further investigation of the ignition system indicated that arcing of the spark occurred in the connector and could not be corrected. Rather than delay the life test, the decision was made to initiate the test and run the engines at sea level. Further tests indicated satisfactory ignition of the five-pound engine, but unsatisfactory 0.1-pound ignitions. Tests at 60 ms on/940 ms off could produce random ignitions. This again, was the fault of the igniter. Tests conducted in January 1973, indicated that the igniter required a longer duration to recharge, but this fact was neglected in setting up the test sequence.

During the second day of the test program, an unscheduled shutdown of the system occurred when Cell #6 voltage indicated greater than two volts. This occurred at 12:51 on June 14. The data had been visually recorded at 12:20 and 12:40 and Cell #6 indicated a constant 1.82 volts DC. The system was reset manually and no other anomalies occurred.

During the second week of operation, a significant oxygen leak occurred (20 psi decay in tank pressure/day). Investigation of the leak indicated: (1) a pinhole leak in the burst diaphragm of the oxygen tank, and (2) a small leak in the 0.1-pound O₂ valve.

A silver burst diaphragm was replaced with a nickel diaphragm, since the silver diaphragm showed signs of corrosion. The 0.1 lbf engine valve seat, with an accumulated 200,000 cycles (neglecting the cycles accumulated during the MOL Program where it was originally used), was replaced.

The life testing continued for 19 weeks with no indication of any deterioration of performance of the electrolysis unit, although the unit was shut down a number of times by peripheral causes such as city power failures or over-voltage spikes on some of the cell voltages. The cause of the voltage spikes was not determined conclusively, but was thought to be caused by stray electrical surges through the safety system rather than being generated by the electrolysis unit.

A typical history of electrolysis system pressures is shown in Figure 21. This data, taken July 11, 1973, shows buildup of pressures due to operation of the electrolysis unit in the high power mode. After 290 minutes, the oxygen tank reaches the maximum pressure and the electrolysis unit is shut off by the pressure switch PS-3. The electrolysis unit operates in the standby

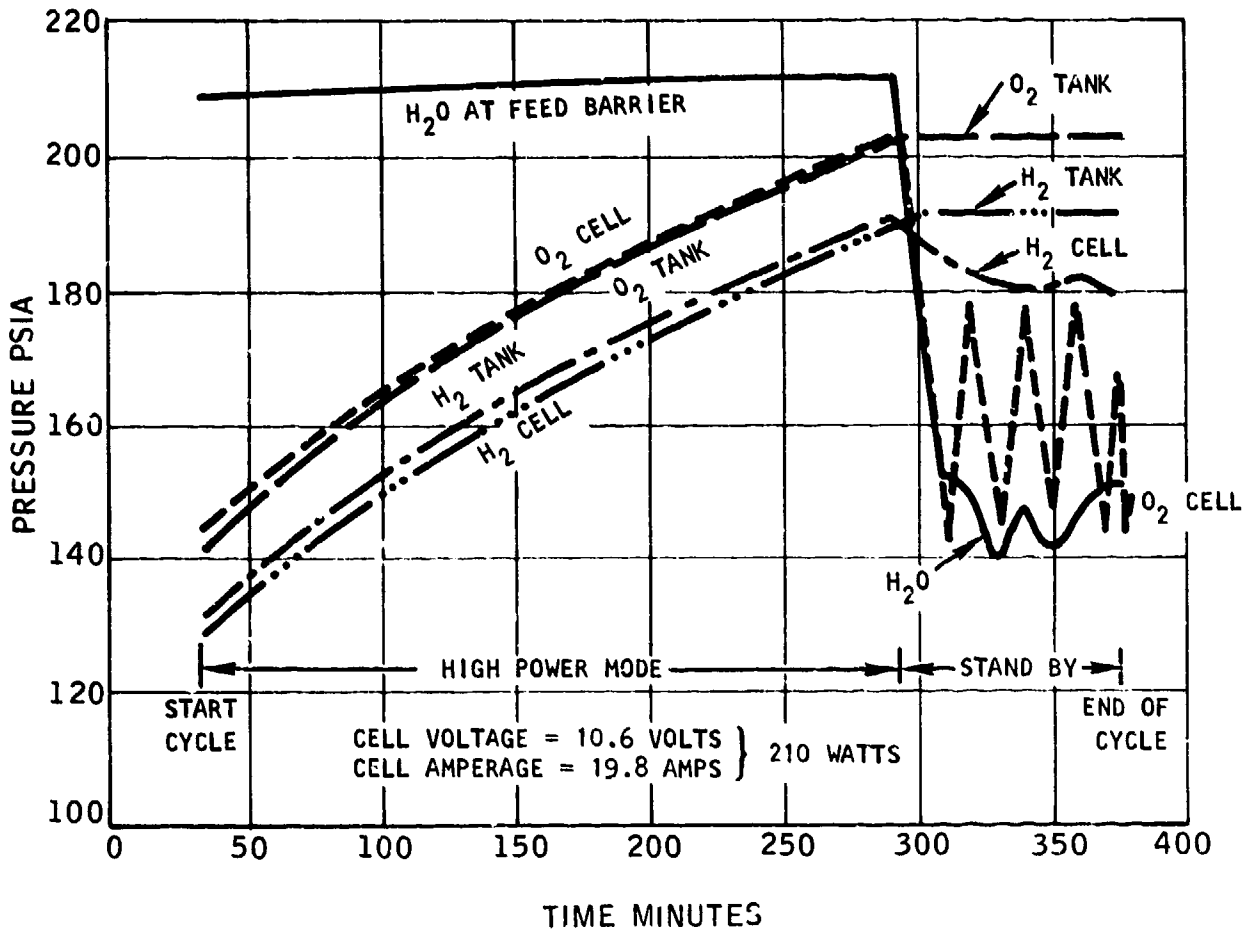


Figure 21. Typical Pressure Cycle

mode thereafter, with oscillations of the oxygen cell pressure as controlled by pressure switch PS-5. During standby operation, the pressure of the water isolated between the closed latch valve S-1 and the water feed barrier in the electrolysis unit drops lower than the hydrogen cell pressure. This means that no water will be transported across the water feed barrier during standby operation, which is a desirable situation. However, hydrogen can diffuse across the water feed barrier from the hydrogen cell to the water supply cell, possibly forming a bubble of hydrogen which would block access of water to the water feed barrier when the electrolysis unit is later turned on and the latch valve is opened. The water tank pressure, which is always higher than the hydrogen cell pressure, will force any hydrogen bubbles across the water feed barrier into the hydrogen cell and normal operation should result. This situation occurred frequently during life testing and no difficulties were ever encountered.

b. July 18, 1973

The check valve on the oxygen cell outlet was found to be stuck open on July 18. The 316 stainless steel check valve was removed from the system and found to be badly rusted. It was replaced by a clean valve.

c. July 20, 1973

Samples of hydrogen and oxygen were passed through the humidity indicator and the catalyst bed. No indication of mixed gases or humidity was observed. The lack of color change in the humidity indicator showed that the dew point of the gases after going through the desiccants was below -70°F .

d. August 17, 1973

The electrolysis unit was shut down for several hours so that the malfunctioning oxygen cell pressure transducer could be replaced. It was found that the 1/4 inch diameter line going to the transducer was blocked by rusty sediment.

e. August 17, 1973

The top plate temperature inside the electrolysis unit recorded 150°F , much higher than normal. The electrolysis unit continued to operate.

f. September 1973

The safety system shut the electrolysis unit off on several occasions during this time. Either Cell 6 voltage or the pressure differential between oxygen and hydrogen cells were shown on the annunciator to be responsible for the shutdown.

The oxygen outlet check valve was again found to be rusty at this time and was replaced.

During September, the PS-5 pressure switch began to operate erratically. The contact points were cleaned, after which normal operation was resumed.

On September 28, the overvoltage cutoff on the power conditioner repeatedly shut down whenever an attempt was made to start the electrolysis unit. The unit was finally started in low power after 49 attempts over a period of 75 minutes. The unit was then manually switched to high power after an hour of operation in the low power mode.

g. October 5, 1973

Cell 4 voltage was found to be abnormally low while the electrolysis unit was operating in the low power mode. All six cells were at about 1.62 volts, while Cell 4 was only 1.01 volts.

The oxygen cell pressure was about 20 psi lower than the hydrogen cell pressure, as had been the case after operating for a week or more in low power mode. A slight O/F unbalance of the sonic orifices on the 0.10 pound thrust engine was thought to be the cause.

The electrolysis unit was shut down manually. A cross membrane leakage test with the hydrogen cell pressurized 75 psig above the oxygen cell gave a flow rate of 14 cc/minute. Normal flow rate is 7 cc/minute and a flow up to 20 cc/minute would be acceptable. It was found that the low voltage on Cell 4 was eliminated when the electrolysis unit was operated with hydrogen cell pressure equal to or greater than the oxygen cell pressure. It was concluded that some leakage was occurring past the gasket seals between the hydrogen and oxygen cells. However, the cross membrane leakage test with hydrogen pressure greater than oxygen pressure was acceptable. After evaluating these results, General Electric Company recommended that the life tests be resumed with hydrogen pressure kept above oxygen pressure.

h. October 10, 1973

The life test was resumed, keeping hydrogen cell pressure higher than oxygen cell pressure by occasional manual blowdown of the oxygen tanks. Cell #4 voltage was normal.

i. October 24, 1973

Time 1406 -- The electrolysis unit was found shut down. Unit was turned on, resulting in Cell #4 being low in performance until O₂ pressure was manually lowered below H₂.

Time 1430 -- Cell #4 suddenly dropped to 0.45 VDC with all other cells normal at 19 amps and 1.67 VDC and H₂>O₂ by 5 to 10 psi.

Time 1440 -- Cell #4 suddenly returned to normal performance at 1.64 VDC.

Time 1645 -- Cell #4 suddenly dropped to 0.34 VDC with the unit base plate temperature on one side rising to 150°F. The base plate temperature on the other side was 115°F.

Time 1770 -- Electrolysis unit continued to operate in high power mode. Hydrogen cell pressure was 8 psi higher than oxygen cell pressure. Cell #4 voltage continued to slowly drop to 0.28 volts. Other cells maintained steady voltages of about 1.67 volts.

Time 1705 -- Unit was manually shut down with Cell #4 voltage immediately dropping to zero and other cells decaying rapidly. All cells (except Cell #5) reached zero volts in five minutes. Hydrogen pressure was 5 psi higher than oxygen pressure. The following cell performances were noted prior to shutdown:

		<u>Voltage, VDC</u>					
<u>Current</u>	<u>Cell Nos.</u>	<u>1</u>	<u>2</u>	<u>3</u>	<u>4</u>	<u>5</u>	<u>6</u>
19.3 amps		1.76	1.67	1.68	0.28	1.67	1.75

A gas cross membrane leakage test performed on the unit gave a rate of 300 cc/minute. The unit was then shipped to General Electric Company.

8. UNIT DISASSEMBLY AND INSPECTION

The following tests and observations were made by General Electric during the failure analysis from November 7 to 16, 1973:

- a. Cell ohmic resistances were as follows:

<u>Cell Nos.</u>	<u>1</u>	<u>2</u>	<u>3</u>	<u>4</u>	<u>5</u>	<u>6</u>
	0.0049	0.0046	0.0052	0.0049	0.005	0.0059

- b. All cells charged normally using the Simpson meter technique.
- c. Three of the four negative terminal current leads were electrically open.

d. A helium leakage test, with water and hydrogen cells 75 psi above oxygen cell pressure, showed gross leakage across the stack (250 cc/minute). This test determines the leakage rate in all twelve membranes (electrolysis cells and water transport membranes).

e. A helium leakage test with the water inlet 75 psi higher than hydrogen and oxygen cells showed a normal diffusion rate of 5 cc/minute. This test determines the leakage rate in the six water transport membranes.

f. Measurement of oxygen manifold gasket thicknesses showed the following compared to the initial average of 0.011 inch:

<u>Cell Nos.</u>	<u>1</u>	<u>2</u>	<u>3</u>	<u>4</u>	<u>5</u>	<u>6</u>
	0.011	0.0117	0.011	0.0106	0.010	0.0114

g. Measurement of water manifold gasket thicknesses showed the following compared to the initial average of 0.010 inch:

<u>Cell Nos.</u>	<u>1</u>	<u>2</u>	<u>3</u>	<u>4</u>	<u>5</u>	<u>6</u>
	0.0105	0.0099	0.0099	0.0097	0.0119	0.010

h. Measurement of oxygen-side cell gasket thicknesses showed the following averages compared to an initial average of 0.014 inch:

<u>Cell Nos.</u>	<u>1</u>	<u>2</u>	<u>3</u>	<u>4</u>	<u>5</u>	<u>6</u>
	0.0137	0.0142	0.0141	0.0133	0.0135	0.0137

i. Measurement of water-side cell gasket thicknesses showed the following compared to an initial average of 0.045 inch:

<u>Cell Nos.</u>	<u>1</u>	<u>2</u>	<u>3</u>	<u>4</u>	<u>5</u>	<u>6</u>
	0.0435	0.0445	0.0432	0.0446	0.0453	0.045

j. Hydrogen embrittlement was present on the hydrogen-side screen assemblies as shown in Figure 22. The material flaking shown in Figure 22 occurred during disassembly. Prior to disassembly, the screen assemblies appeared normal.

k. There was a band of corrosion about 1/8 inch wide on the outer diameter of the top endplate which is adjacent to the negative terminal plate. Rust and surface corrosion extended about one inch around the inner surface of the top endplate as shown in Figure 23. No corrosion was noted on the outer surface of the top endplate.

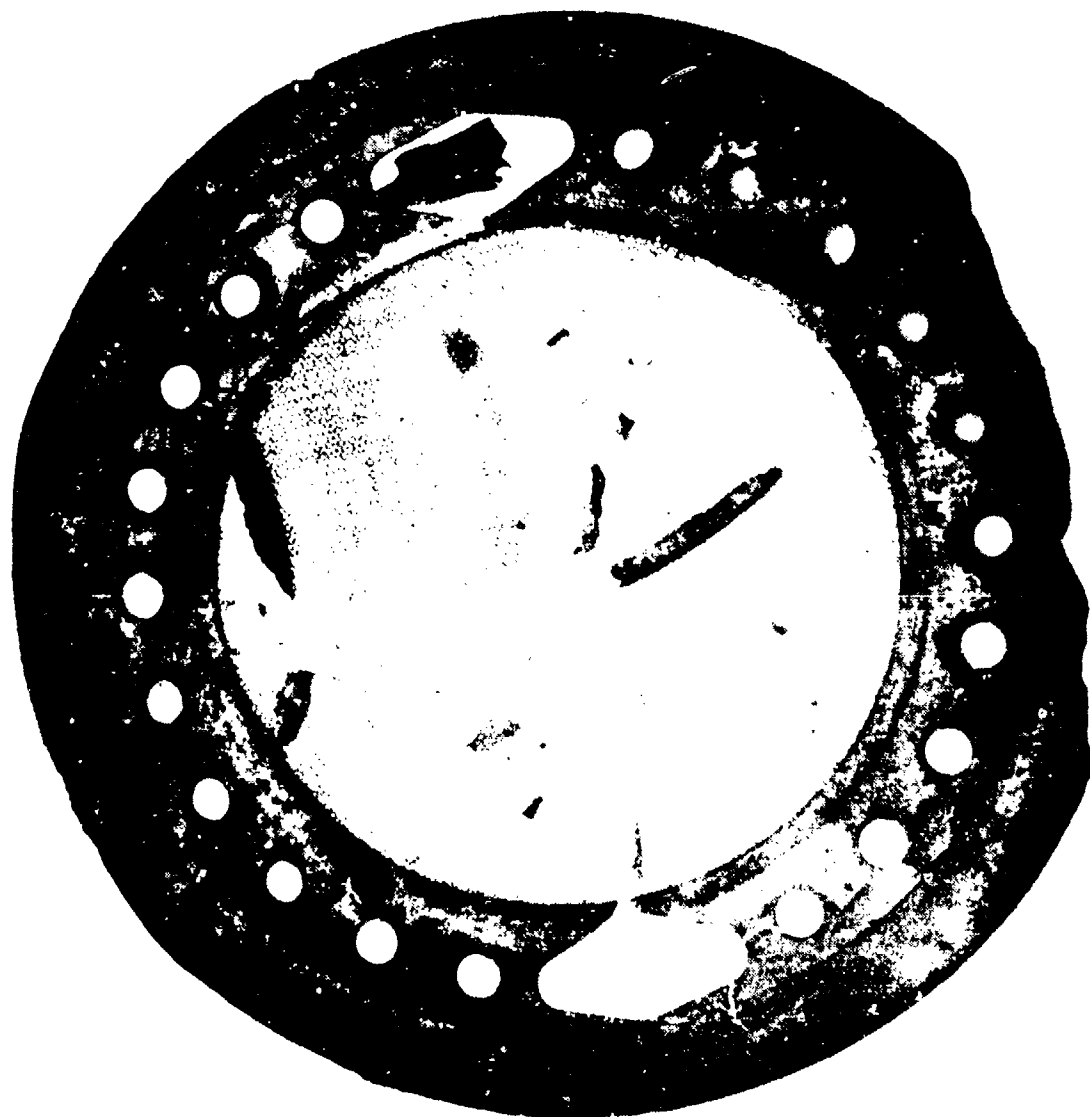


Figure 22. Hydrogen Embrittlement of Hydrogen-Side Screen Assembly

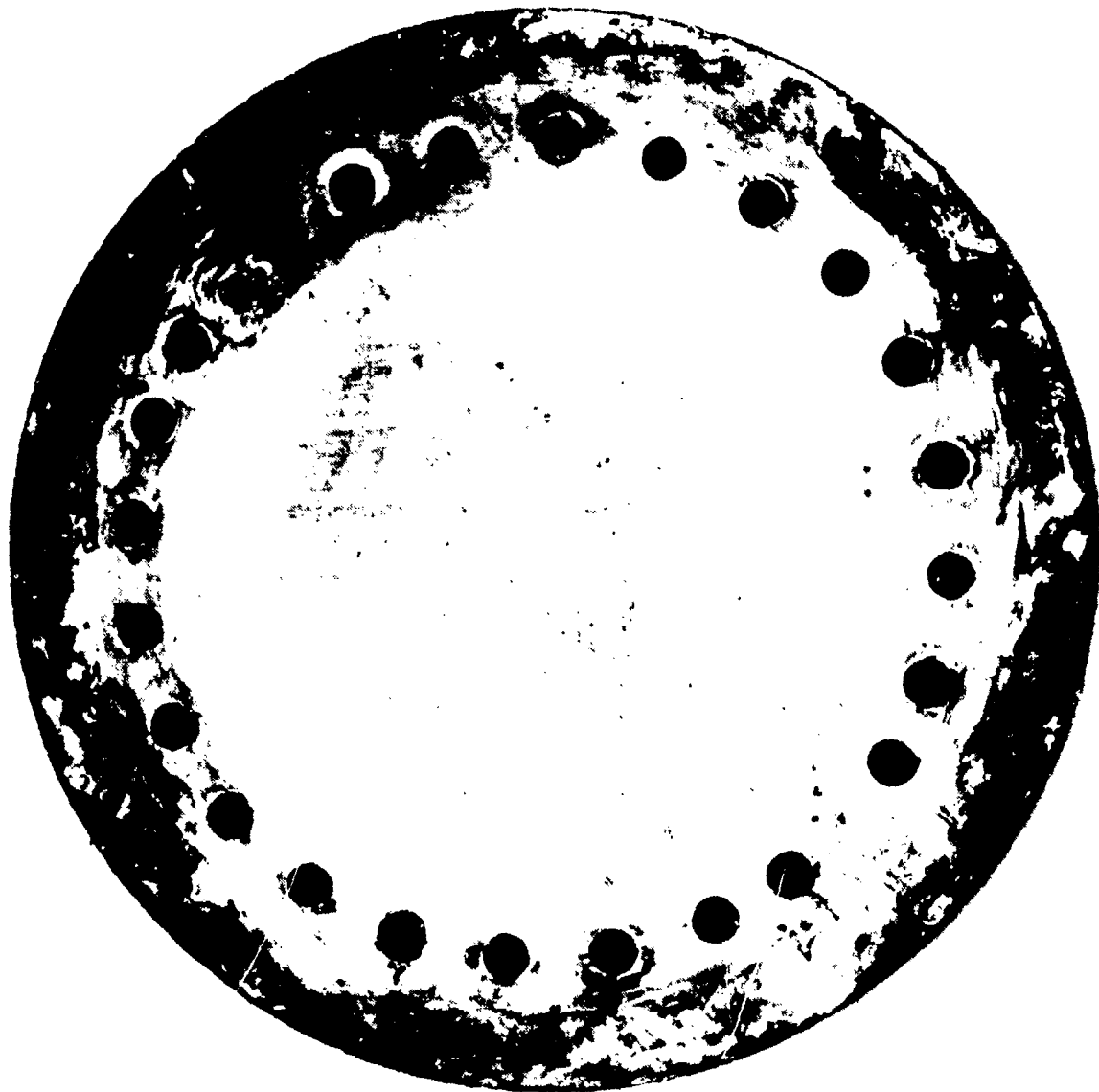


Figure 23. Corrosion and Rust on Inner Surface of Top Endplate

- l. A line indentation (0.005 inch deep) existed on the screen protector ring oxygen eyelets of Cell Nos. 4 and 5. Figure 24 is a photograph of the indentation and the mating oxygen manifold gasket which was also indented or creased from compression over the indentation.
- m. A whitish deposit (later analyzed to be niobium) was present on all the water screen assemblies and water transport membranes. Figure 25 shows a typical deposit on Cell No. 4; the deposit being at the top of the photo 180° opposite the water inlet manifold. In the assembled unit, this niobium deposit would be adjacent to the oxygen outlet port. The niobium screens were discolored with what appeared to be an oxide film.
- n. Each cell was individually leak checked by pressurizing one side at 3 psi helium while submerged in several inches of water. Only Cell No. 4 showed leakage, this occurring through two single pinholes in the membrane. These holes were approximately 0.5 inch apart and located 1.0 inch inside the perimeter of the active area adjacent to the water inlet manifold. The membrane was stripped in aqua regia and microscopically inspected. The two holes were cratered or depressed from the oxygen side and the surrounding area had a scorched or burned appearance on the hydrogen side. Some burning was also visible on the oxygen side adjacent to the oxygen outlet ports. The burning that occurred on the oxygen side appeared to have been considerably hotter than that on the hydrogen side around the two pinholes. Figure 26 is a sketch of the failure pattern observed on Cell No. 4.
- o. Approximately 5 cc's of condensate water were present in the hydrogen side volume of the unit enclosure after removal of the pressure dome. The water was analyzed as follows:

<u>Property</u>	<u>Analysis</u>
pH	1.7
F-	140 mg/liter
Iron	265 mg/liter

- p. Torque on the stack tie rod nuts prior to disassembly averaged 65 inch-pounds as compared to the initial installation of 80 inch-pounds.
- q. Disassembly of the potted electrical connections in the plastic cup on top of the stack revealed that the three open current leads from the negative terminal plate were due to an interface coating of the epoxy potting material which flowed between the electrical spade tab and the three current lead connections.

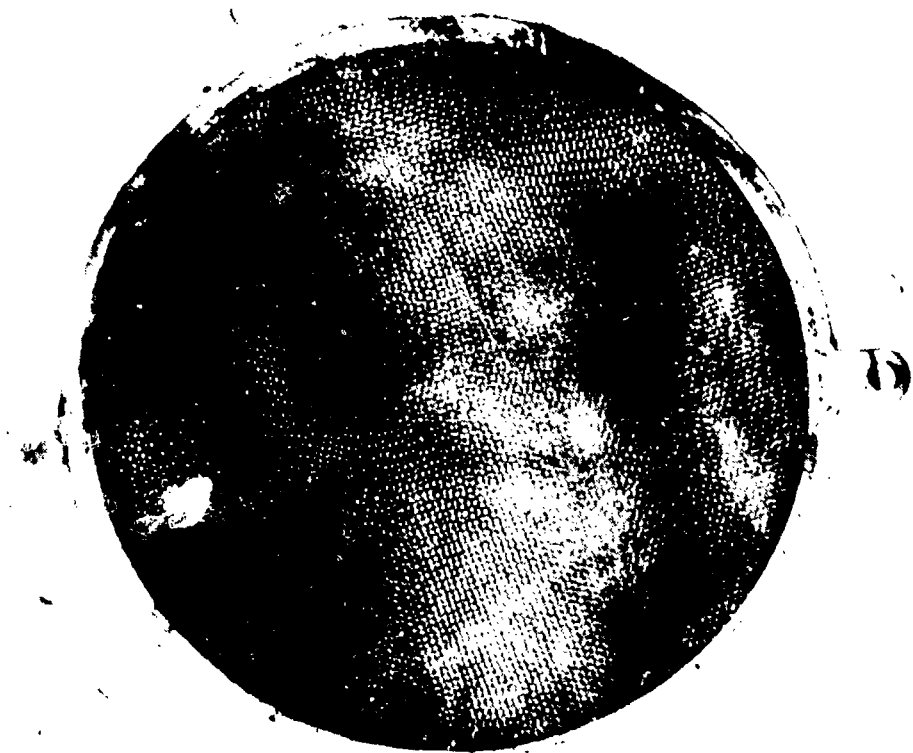


Figure 24. Indentation on Screen Protector Ring Oxygen Outlet

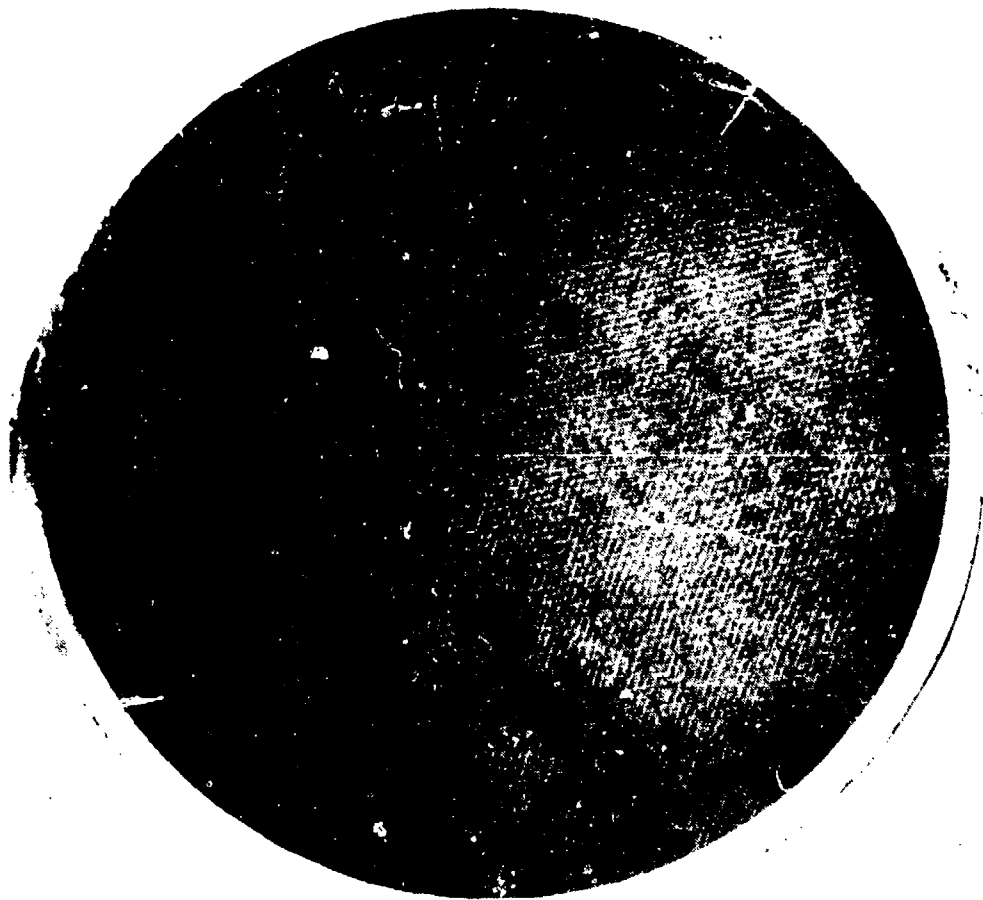


Figure 5. Niobium Deposit on Water Section Assembly

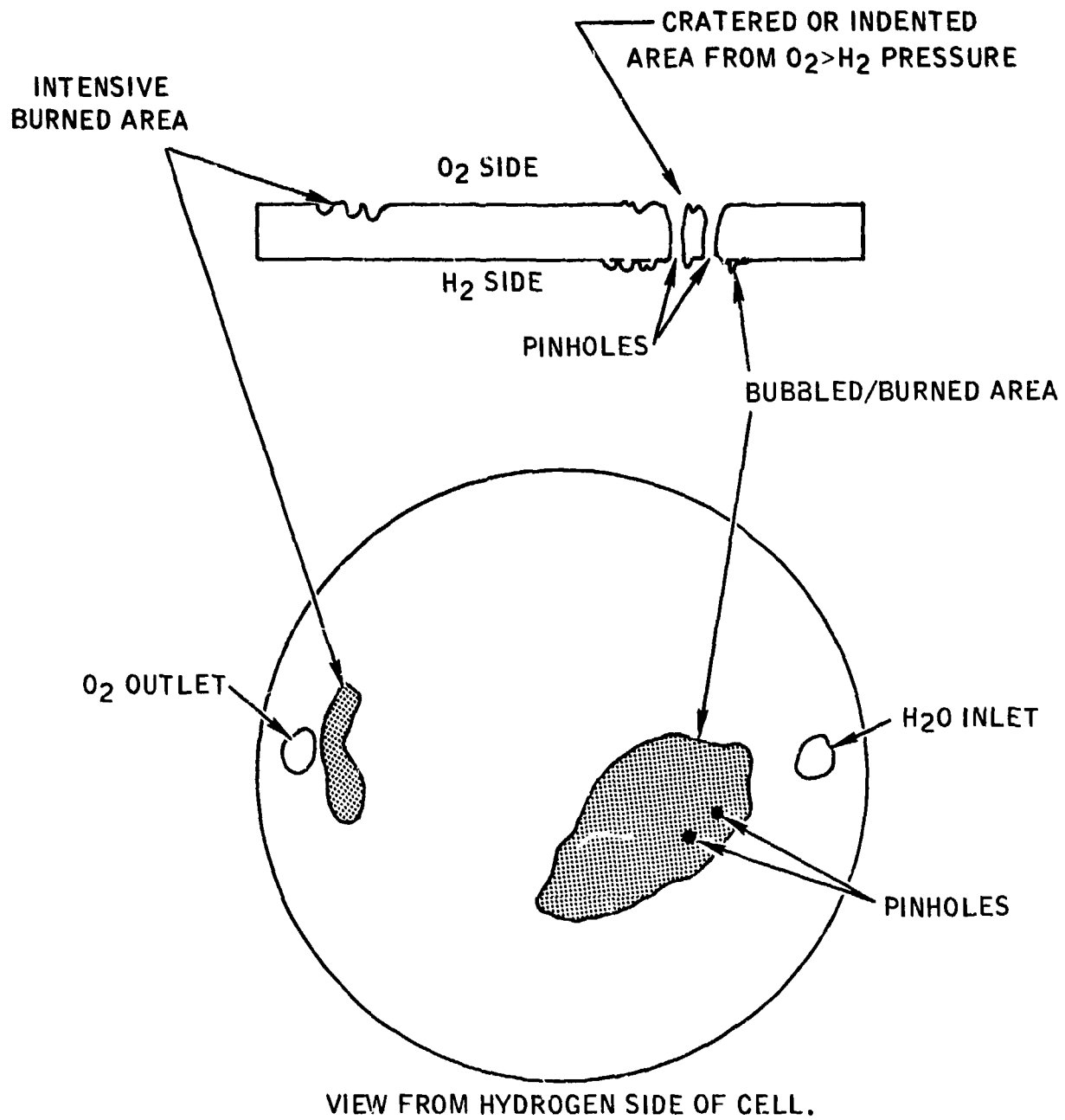


Figure 26. Failure Pattern on Cell No. 4

- r. The power conditioner was operated successfully as a component exhibiting no inability to hold high current on unit startup as was experienced at Marquardt. Simulation of the open current leads by carrying the current in only one of the negative terminal pins in the harness increased the startup voltage on the power conditioner.
- s. Evidence of burning was noted throughout the oxygen outlet manifold within the stack. The polysulfone sheet adjacent to the top endplate showed scorching in the oxygen manifold location.
- t. The 3/0 screen pattern from the oxygen side manifold eyelet area to the mating oxygen side of each cell was reflected by diamond indentations on the cell membrane surfaces. The water transport membranes showed no evidence of this pattern.
- u. Chemical analysis of a water transport membrane revealed the presence of iron in the membrane with the whitened area showing a larger concentration of iron (1.4 mg/g vs. 0.4 mg/g). The water content was normal (21.2%). Due to the presence of iron, the contamination level cannot be estimated from the IEC (ion exchange capacity) data. The whitish deposit area of the membrane was chemically analyzed to have an IEC of 0.89 while an unaffected area had an IEC of 0.86.

9. CAUSE OF THE VARIOUS FAILURE PHENOMENA

- a. It is concluded that the two pinholes observed in Cell No. 4 would cause the final operation symptoms. A failed cell of this nature would result in the inability to hold voltage due to depolarization of the electrode by gas mixing on the catalyst surface.
- b. The repeated tripping out of the power conditioner which occurred on September 28, 1973, was caused by the increased IR drop in the negative terminal circuit from the electrolysis module to the power conditioner. The loss of three of the four power leads caused an increased electrical resistance, thus a higher voltage output requirement from the power conditioner. This condition combined with the attempted module startup from a cold start on September 28 resulted in a high voltage startup requirement, particularly in the high current mode. This exceeded the 15 VDC power conditioner overvoltage shutdown setting, thus the inability to hold load.
- c. The hydrogen embrittlement observed on the hydrogen screen assemblies was anticipated as a result of teardown observations made on other long-life electrolysis units. To date, no electrolysis failure has been attributed to this phenomenon. No broken screen strands were observed in the Marquardt unit that would cause the two pinholes that were observed in Cell No. 4. The delamination and flaking of the sheet metal as shown in Figure 22 was the result of flexing of the material after unit disassembly.

- d. The rust and surface corrosion observed at the interface of the top endplate to the polysulfone insulating sheet and terminal plate were caused by the highly acidic condensate water which accumulated on top of the mylar insulating ring located adjacent to this area. Accumulated water condensate eventually bridged the gap (0.040 inch) to the endplate and caused corrosion from the presence of the voltage difference between the terminal plate and the endplate.
- e. The niobium oxide formation in the water transport compartment of each cell was caused by the reaction of the niobium screen material, fluoride dissolved in the water, and entrapped air or oxygen in the presence of extreme heat. The oxide pattern observed on the water screen assembly increased in intensity from the water inlet manifold to the opposite side of the compartment. Since the opposite side is the most water stagnant region of the compartment, the fluoride content would be at the greatest concentration. Any iron contamination in the feed water would also accumulate in this region as observed in the chemical analysis of the water transport membrane. Since the water content and IEC of the membrane were normal, the water transport properties of the membrane were not affected.
- f. The intermittent low performance or low cell voltage observed on Cell No. 4 and eventual pinhole failure probably occurred over a longer period of time (October 3 to 24). The indented impression in the oxygen manifold eyelet area of the screen protector ring on Cell No. 4 (Figure 24) is considered the most likely cause of failure. Difficulty in gasket sealing in this area has been experienced in previous buildups. A gasket leak probably occurred on October 3, resulting in oxygen entering the hydrogen side of Cell No. 4 and burning in the observed pinhole area of the cell. This resulted in a localized high membrane temperature and softening of the material. The observed cratering or indentations at the pinholes as viewed from the oxygen side was caused by the high overpressure of oxygen over hydrogen (23 psi). It is probable that the two pinholes occurred at this time but were small enough to reseal when the oxygen pressure was lowered. This is also true for the initial manifold leak.

The stack leakage test performed on October 5, 1973, revealed no excessive stack leakage when the hydrogen side pressure is greater than the oxygen side (up to 75 psi). The pinholes evidently were very small and thus could easily have been sealed with water or deformed and sealed in the opposite direction by the H_2/O_2 pressure differential.

Since the manifold gasket leakage was intermittent (as demonstrated by the erratic performance of Cell No. 4), this leakage was also not revealed with the October 5, 1973, leakage test. Continued operation in the hydrogen over oxygen pressure mode for the next 15 days with the failed pinhole area in Cell No. 4 eventually caused a larger pinhole leak and depolarization of the

electrode. It is evident from the improved performance of the unit prior to failure and the 150°F recorded base plate temperature, that overheating was occurring in the unit for some time on October 24. The oxygen manifold and oxygen outlet area of each cell experienced severe burning due to the operation in the hydrogen overpressure mode, causing hydrogen to enter the oxygen manifold and into the entrance of the oxygen side of each cell. The severe oxidation of the niobium water screen assemblies probably occurred at this time.

10. MODIFICATION OF ELECTROLYSIS UNIT

The electrolysis unit was modified by General Electric Company with the following changes:

- a. Substitution of a double-sided silicone adhesive manifold gasket in place of the elastomeric design.
- b. Substitution of a 4/0 screen pattern as top layer against the membrane electrode on the oxygen screen assembly. This insured that the gasket is positioned adjacent to the manifold slot to eliminate eyelet cover creasing.
- c. Replacement of the hydrogen screen assemblies and addition of a 4/0 screen pattern in place of a 3/0 pattern.
- d. Fabrication of six new membrane electrode assemblies.
- e. Fabrication of six new water transport membranes.
- f. Fabrication of six new water side gaskets.
- g. Connection of the internal harness directly to the terminal plates.
- h. Coating of the top endplate with TFE to 0.007 inch thickness.
- i. Addition of a gas leakage test to the assembly procedure, with oxygen pressure greater than hydrogen pressure.
- j. Reduction of the mylar insulation overlap width beyond stack perimeter.

The modified electrolysis unit was shipped to Marquardt on February 4, 1974.

11. TEST HISTORY-MODIFIED ELECTROLYSIS UNIT

The life test of the modified electrolysis unit was begun on March 12, 1974. After 25 minutes of operation in the high power mode (21.9 amps), the unit was shut off by the safety system because Cell No. 1 voltage had exceeded 2.2 volts. The

ambient temperature at this time was 48°F. This low temperature was at least partly responsible for the overvoltage of Cell No. 1, because the electrolysis unit was designed to operate in an ambient temperature near 70°F. After three shutdowns by excessive Cell 1 voltage, and consultation with General Electric Company, the current was adjusted to 15 amps and life testing was resumed.

Typical cell voltages in a 62°F ambient temperature at 15 amps were:

<u>Cell Nos.</u>	<u>1</u>	<u>2</u>	<u>3</u>	<u>4</u>	<u>5</u>	<u>6</u>
Voltages	1.87	1.74	1.73	1.73	1.75	1.78

At an ambient temperature of 76°F, the cell voltages were as follows:

<u>Cell Nos.</u>	<u>1</u>	<u>2</u>	<u>3</u>	<u>4</u>	<u>5</u>	<u>6</u>
Voltages	1.81	1.71	1.71	1.71	1.72	1.75

Those data indicate that Cell No. 1 voltage is more sensitive to ambient temperature than the other cells. The data also indicates that the high voltage in Cell No. 1 cannot be attributed entirely to the ambient temperature, because the voltage is higher than normal even at an ambient temperature of 76°F.

The life test was continued with a high power current of 15 to 16 amps. The low power current of 5 to 6 amps was maintained according to the original plans. The life test continued without incident through the planned completion date of June 20, 1974. The modified electrolysis unit and propellant feed system operated normally during the 14 weeks of testing.

a. Performance

The electrolysis unit performance data shown in Table 5 indicates that performance of the electrolysis unit remained unchanged during the 14 weeks of testing. Cell No. 1 maintained a somewhat higher voltage than the other cells during operation at 15-16 amps. The voltage increment became less as ambient temperature increased. There was no difference in voltage among the six cells during low power operation. It appears that a slight blockage of the water passage to Cell No. 1 was responsible for its higher voltage in high power operation.

b. Gas Separation

Tests of oxygen and hydrogen flowing through the catalyst bed and the humidity indicator at the end of the 14-week test showed that there was no mixing of hydrogen and oxygen within the electrolysis unit, and the dew-point of the gases was below -70°F after the gases passed through the desiccant cartridges.

TABLE 5. ELECTROLYSIS UNIT PERFORMANCE DATA

Fourteen-Week Test of Modifier Unit

Date	Operational Mode	Ambient Temperature °F	Current amps	Voltage VDC	Cell Voltage - VDC						Pressures - psia		
					#1	#2	#3	#4	#5	#6	Water Cell	Hydrogen Cell	Oxygen Cell
3-13-74	High Power	53	14.5	10.7	1.92	1.75	1.74	1.74	1.76	1.79	214	181	176
3-20-74	Low Power	55	5.1	9.8	1.69	1.65	1.66	1.66	1.66	1.69	210	182	180
4-11-74	High Power	58	15.1	10.4	1.92	1.74	1.74	1.75	1.76	1.81	215	168	170
4-15-74	Low Power	58	5.0	9.7	1.68	1.65	1.65	1.66	1.66	1.70	210	173	171
5-10-74	High Power	62	15.8	10.4	1.89	1.73	1.73	1.75	1.75	1.81	214	125	135
5-17-74	Low Power	59	5.2	9.8	1.70	1.56	1.66	1.67	1.67	1.72	210	168	197
6-11-74	High Power	70	15.8	10.1	1.82	1.71	1.70	1.71	1.71	1.75	214	154	182
6-18-74	Low Power	66	6.0	9.6	1.66	1.64	1.64	1.64	1.64	1.67	212	185	182

c. Rust in Oxygen Outlet

The check valve C-2 on the oxygen outlet from the electrolysis unit had failed to function on two occasions during the life test of the original electrolysis unit because of rust buildup. The check valve, made of 316 stainless steel, was cleaned and reinstalled twice during the 19 weeks of testing of the original electrolysis unit.

Another check valve of the same model, but made from Carpenter 20, was procured from Circle Seal for use with the modified electrolysis unit. This check valve did not rust and operated satisfactorily during the 14-week life test of the repaired electrolysis unit, indicating that substitution of Carpenter 20 for 316 stainless steel eliminated the problem of rusting. The disassembled Carpenter 20 check valve after 14 weeks of testing is shown in Figure 27.

d. Examination of Desiccant Cartridges

The two desiccant cartridges were opened and examined after 19 weeks of testing the original electrolysis unit and also after 14 weeks of testing the modified electrolysis unit.

The oxygen desiccant cartridge, made of tin plated steel, was badly rusted by the oxygen as shown in Figure 28.

The desiccant cartridge in the hydrogen outlet was not rusted, but at the conclusion of testing of the modified electrolysis unit, a pool of liquid smelling like vinegar was found on the top of the inner cartridge, as shown in Figure 29. The pH of the liquid was 4.2.

The weight of water collected by the hydrogen desiccant cartridge was 0.57 pounds and an additional 0.93 pounds of water was found between the cartridge and the case which is separated from the gas outlet. The desiccant was therefore working properly. The desiccant cartridge can remove a minimum of 1.2 pounds of water from the gas stream and was therefore not saturated, as evidenced by the -70°F measured dewpoint of the hydrogen.

The weight of water from the saturated hydrogen depends on the temperature of the electrolysis unit, which was generally between 80°F and 120°F during the life test. A total of 201 pounds of water were electrolyzed during the entire life test program, which would be expected to produce between 0.51 pounds of water at 80°F to 1.73 pounds of water at 120°F . Therefore, the total of 1.5 pounds of water collected in the hydrogen desiccant is consistent with the theoretical predictions.

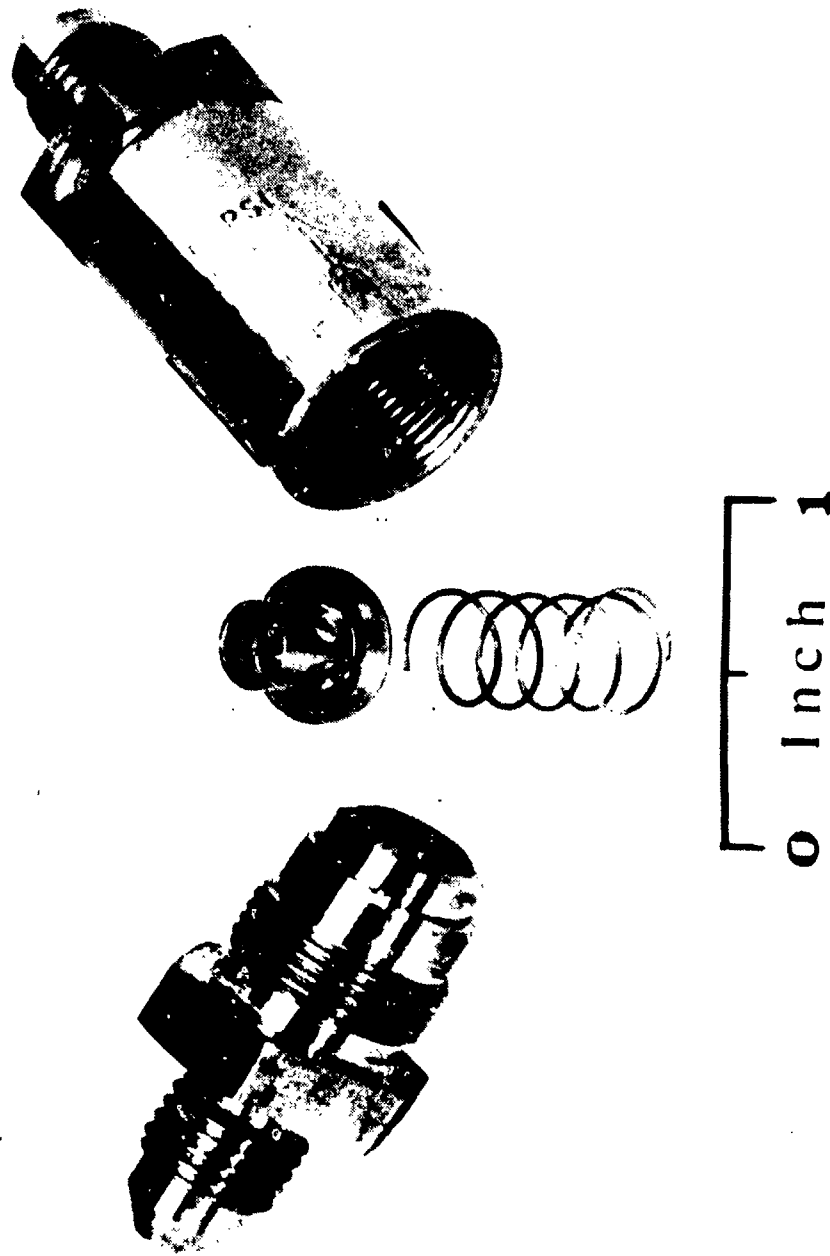


Figure 27. Disassembled Carpenter 20 Check Valve After 14 Week Life Test



Fig. 10.

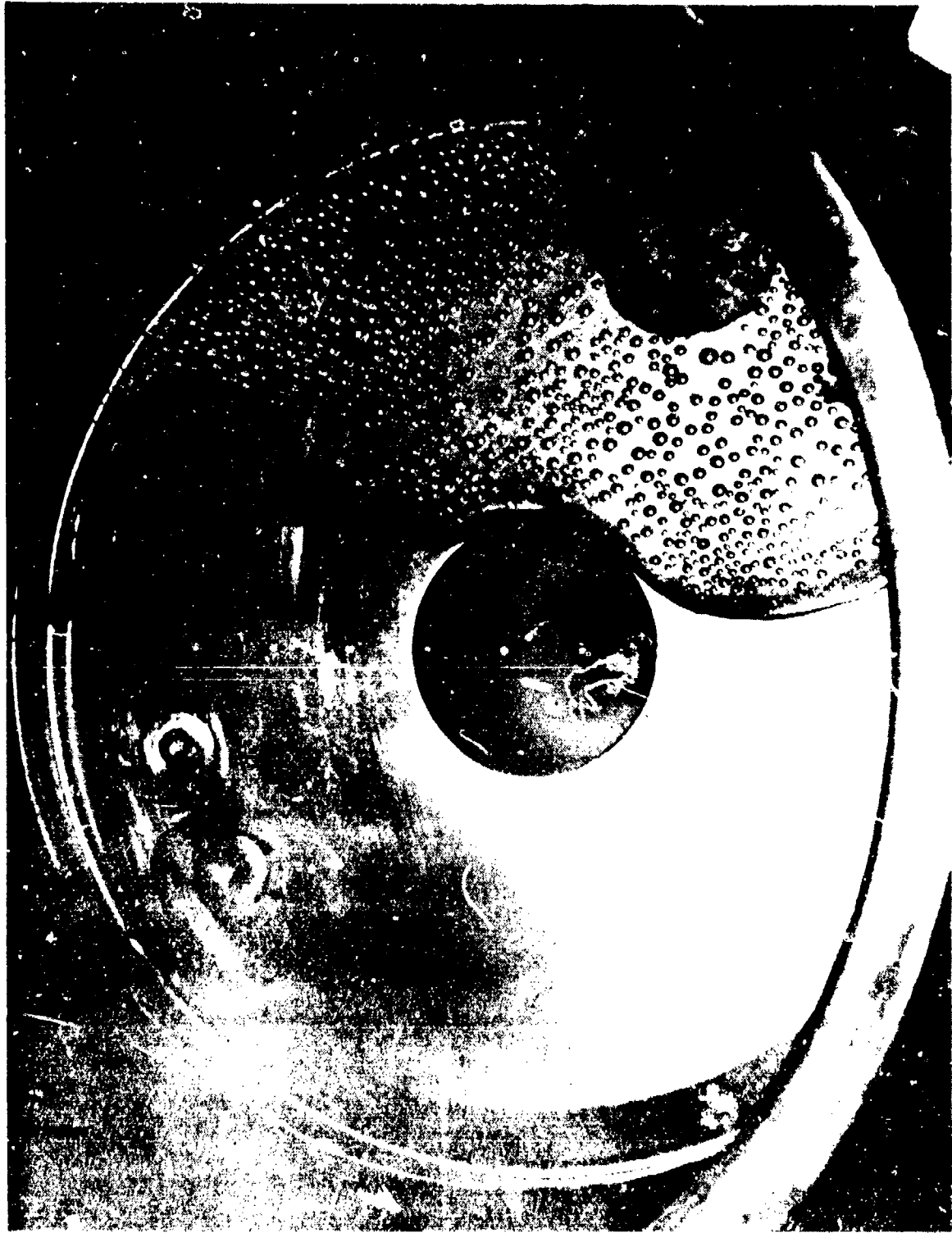


Fig. 1. (a) Lens of the Camera of the End of Life 1. (b)

The weight of water collected by the oxygen desiccant could not be determined because the extensive rusting of the tin plated cartridge prevented removal of the cartridge. A Carpenter 20 cartridge would be required for the oxygen cartridge to avoid rusting.

e. Water Purity

The solid polymer electrolyte (SPE) in the electrolysis unit is an ion exchange medium. Therefore, the water supplied to the SPE should have low levels of ionic and particulate contamination so that the ion exchange capacity of the SPE will be maintained.

General Electric Company specified that ionic contamination of the water should be low enough that the electrical resistance of the water should be 2 megohm-cm. By use of a stainless steel water supply system and strict cleaning procedures, it was shown during the life test program that this requirement for low ionic contamination can be met without using a deionizer.

A Millipore filter was also placed in the water supply system to prevent particulate contamination from reaching the electrolysis unit. A filtration test was made on the water after being stored in the stainless steel water tank for seven months. A colloidal tan colored deposit weighing 0.5 milligrams was collected from 7058 grams of water. A semiquantitative analysis showed that the principal constituents of the deposit were iron, silicon and magnesium.

General Electric Company made an analysis of the effect of this level of particulate contamination on the electrolysis unit if the Millipore filter was not used in the water supply system. In that case, the water feed barrier membranes, with an area of 0.23 ft² per cell, would filter ionic or particulate contamination from the water and thereby protect the SPE membrane from any effect of contamination. The analysis determined that if all such contamination from the 300 pounds of water were concentrated in one WFB (water feed barrier), a very conservative assumption, the only effect would be to decrease the WFB hydraulic permeability by 17 percent. However, water transport across the WFB does not depend on hydraulic permeability, but can be accomplished by evaporation even with small pressure drop across the WFB. Therefore, the somewhat decreased hydraulic permeability has a completely negligible effect on the SPE, with a predicted change in voltage of less than 0.001 volts.

12. SUMMARY OF LIFE TEST RESULTS

The results of the life test lead to the following conclusions:

- a. The propellant supply system operated satisfactorily throughout ambient sea level temperatures from 44°F to 100°F.

- b. The propellant supply system underwent 256 blowdown cycles, during which all pressure switches operated satisfactorily.
- c. The electrolysis unit entered the standby mode 230 times during the life test, during which time the system operated satisfactorily.
- d. The modified electrolysis unit operated for 14 weeks, consumed 83 pounds of water, and produced propellants with an impulse of 29,000 pound seconds, without any change in performance.
- e. One of the six cells of the modified electrolysis unit had abnormally high voltage in the high power mode. This condition could have been avoided by more extensive acceptance testing.
- f. No problems were encountered during life testing of the modified electrolysis unit which would prevent satisfactory long life operation.
- g. The propellant supply system does not require a deionizer.
- h. The propellant supply system does not require a water filter.
- i. Rusting of the lines, check valve, pressure transducer and desiccant cartridge in the oxygen outlet system can be eliminated by using Carpenter 20 components. No rusting occurred anywhere in the hydrogen system or in the oxygen system downstream of the desiccant.

SECTION III

5-POUND THRUST ROCKET ENGINE

The objective of the 5-pound thrust engine program was to develop a flight type gaseous oxygen-gaseous hydrogen rocket engine which operates on the oxygen and hydrogen produced by the electrolysis system. The design goal for the thruster was 350 seconds of specific impulse at a mixture ratio of 8. The thruster must have the capability of operating at 50 milliseconds pulse width to steady state operation and a life in excess of 150,000 firings and 5 hours of accumulated burn time.

1. SUMMARY OF RESULTS FROM PROGRAM

During this program, three thrusters were built and tested under simulated spacecraft environmental and feed system conditions.

Thruster No. 1 (P/N X29069) was used as the system test thruster and accumulated 1,210 pulses and 4.35 hours of firings using propellants generated by the electrolysis system.

Thruster No. 2 (P/N X29385) was the first flight type thruster tested. The injector was fabricated of Columbian C-103. This thruster's test program was terminated after 20,309 firings due to a brittle stress failure of the injector. The total accumulated burn time on this thruster was 2,684 seconds.

Thruster No. 3 (P/N X28680) was the final flight configuration to be tested and is shown in Figure 30 after the completion of the test program. This thruster's injector was fabricated of Nickel 200. The test program was completed satisfactorily with 150,025 ignitions and 4.25 hours of burn time. Performance of the thruster with a 40:1 exit nozzle expansion area ratio was 355 seconds (Figure 31) as documented by thrust measurements. At 1/3 of nominal thrust, the specific impulse was 325 seconds. At 50 ms electrical pulse width, the I_{sp} was greater than 320 seconds (Figure 32). Variability of the I_{sp} at short pulse widths was significant and affected by valve response and inlet pressure. Ignition of the thruster was 100% reliable down to inlet pressures of 50 psia or 1/4 of the nominal inlet pressure.

2. ENGINE DESIGN

The design of the 5-pound thrust rocket engine used in the three test series was based on the results of the test program conducted on the Development Rocket Engine which is described in Reference 1. The basic effort in this program was to further verify the adequacy of the design criteria while orienting the actual design toward a flight type configuration.

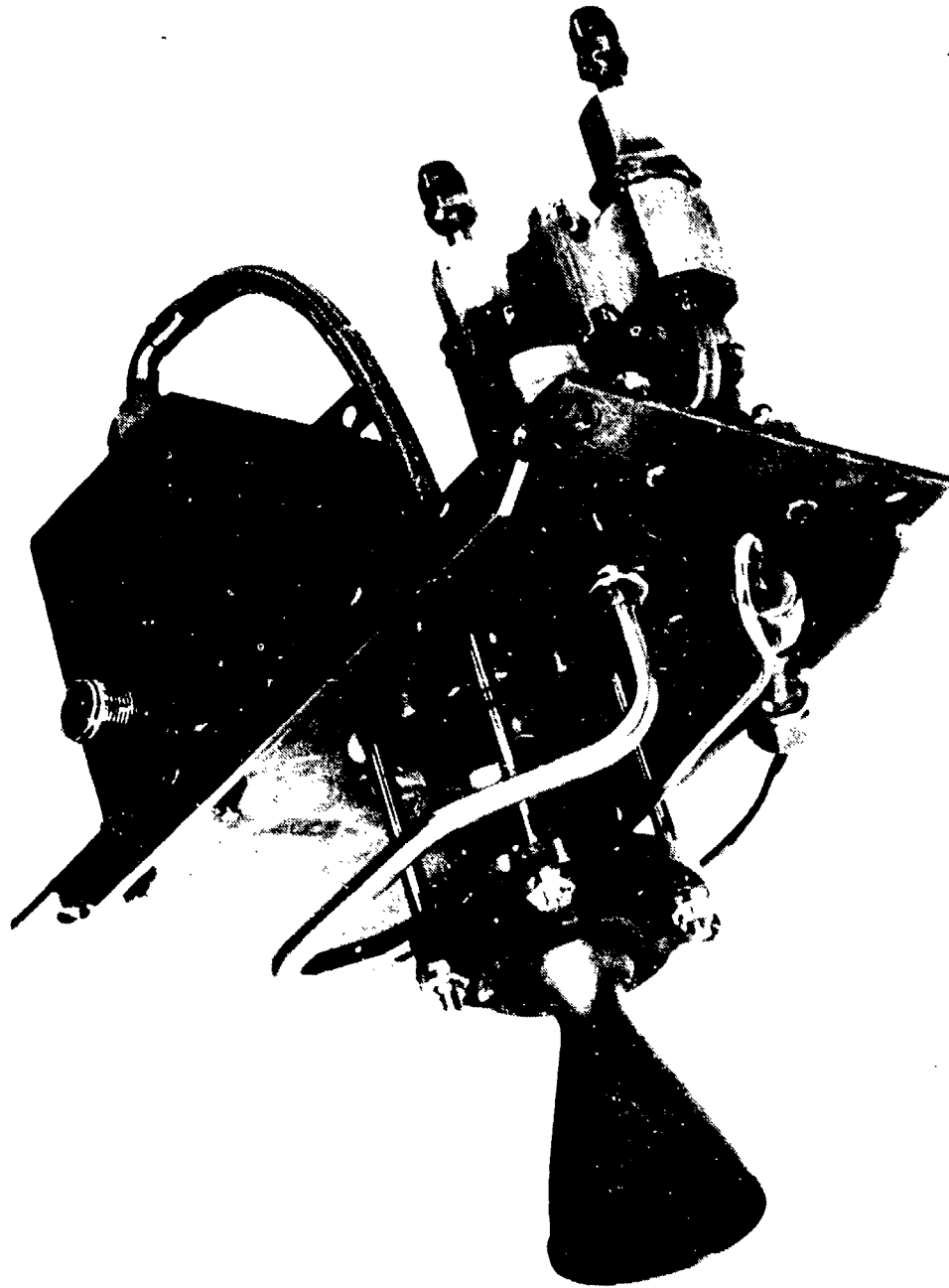


Figure 30. 5 Lbf. Thruster No. 3 After Test Program

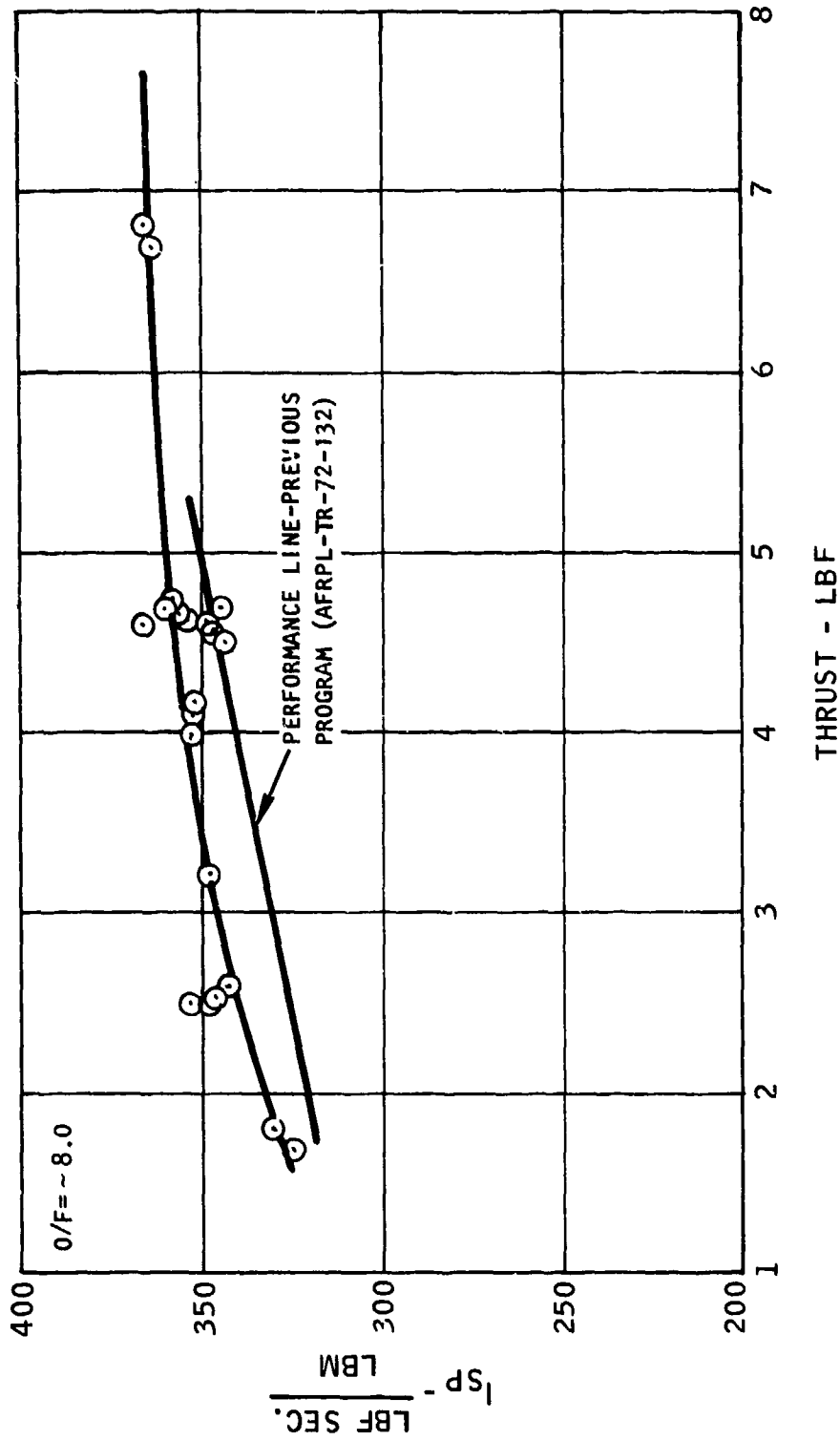


Figure 31. Performance of 5 Lbf. Engine

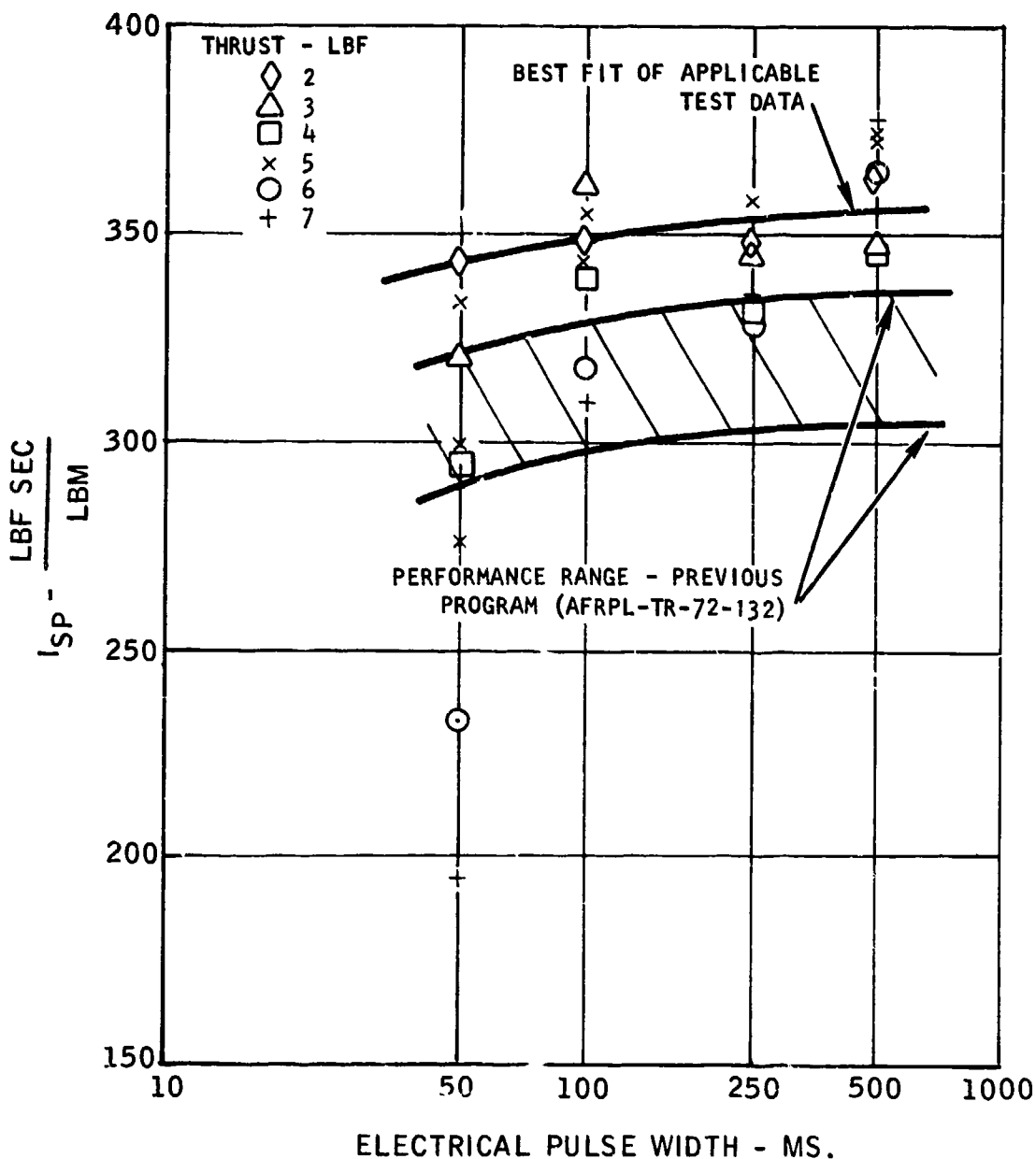


Figure 32. 5 Lbf. Engine ISP Vs. Electrical Pulse Width

a. **Basic Design Criteria**

The basic design characteristics of the 5-pound thrust rocket engine are shown in Table 6. The configuration represents Thruster No. 3 which successfully demonstrated the requirements of the program (150,000 seconds and 5 hours of burn time).

The thruster consists of individual elements which are bolted together. The major elements are:

- . Nickel 200 injector
- . Molybdenum combustion chamber
- . Marquardt propellant valve
- . General Laboratory Associates spark exciter

Injector

The 5-pound thrust engine injector consists of 6 coaxial premix injection elements surrounded by thirty-six 0.25 in. diameter film cooling holes. Each premix element consists of a .075 in. diameter oxidizer orifice surrounded by three .025 in. diameter H₂ orifices. The hydrogen is impinged on the oxygen using a plate which has a .075 in. diameter hole.

The hydrogen orifices are located on a 0.13 in. diameter, thus forcing the gas to turn a 90° angle into the oxygen gas. The gap between the injector and premix plate (see Figure 33, Drawing X29380) is 0.175 to 0.18 inches deep.

Approximately 60% of the hydrogen gas is used as film cooling and is controlled by an orifice which can be adjusted to the individual requirements.

This injector design was used on all three configurations and is nearly identical to the previously referred "development thruster." The only difference between the "development thruster" and the three thrusters tested is that the six premix orifices are parallel to the thruster axis, while the development thruster had the six premix orifices turned inward at 15°.

Spark Plug

The spark plug used in the 5-pound engine is a Champion (FHE-231A) type with the shunt (semiconductor) material removed. The spark plug or "igniter" is located in the center of the injector surrounded by the six elements. The tip of the plug is approximately 0.05 in. inside of the injector face and a 0.062 in. diameter hole separates the tip from the combustion chamber.

TABLE 6. 5-LBF THRUSTER DESIGN CHARACTERISTICS

1. 5 lbf at 50 psia Chamber Pressure
2. Blowdown Capability to 15 psia (1.5lbf)
3. Combustion Chamber - Exit Nozzle
 - a. Molybdenum Coated with MoSi_2
 - b. Contraction Area Ratio - 10:1
 - c. Expansion Area Ratio - 40
4. Fuel Film 60% - Radiation Cooled
5. Nickel 200 Injector
 - a. Six Premix Coaxial Elements
 - b. FHE 231A Spark Igniter (Champion) Modified
6. Low Power Bipropellant Valve (Marquardt)

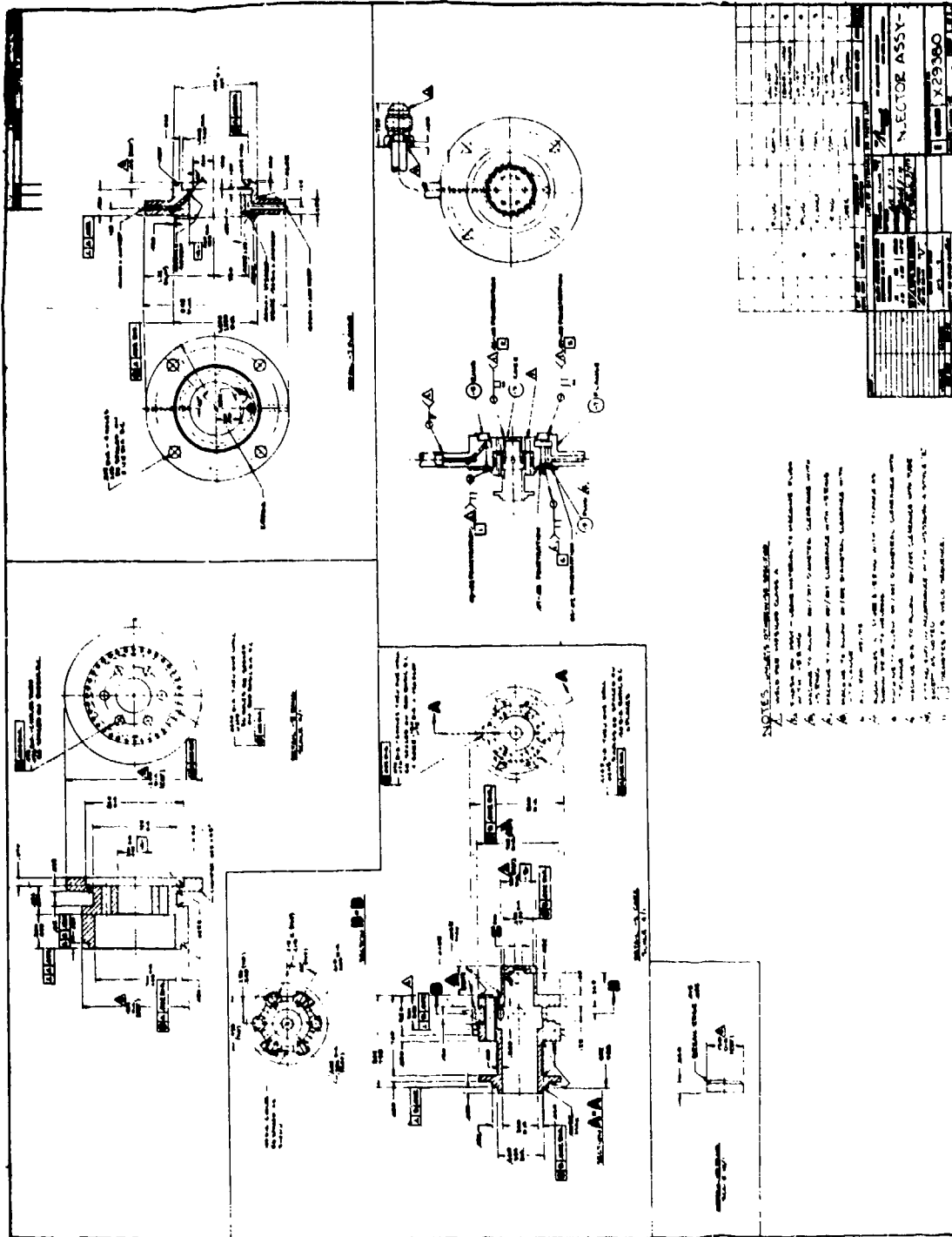


Figure 33. 5 Lbf. Injector Assembly

Valve

The valves used in Configuration 1 were the Marquardt R-4D coaxial valves which consume 50 watts/valve. The sealing surface is composed of a soft flexible Teflon seal and a metal to metal backup.

The Marquardt bipropellant valve, X29258, was used for Configurations 2 and 3. This valve is a modified version of the X24572 bipropellant valve developed under Air Force contract. The original valve had a power consumption of 56 watts and utilized a hard seat for sealing. The design was revised to incorporate a soft seat TFE and the power consumption was reduced to 21 watts through the use of a 39 ohm coil. In turn, the response of valve was significantly lengthened. The valve opening time with the revised coil is on the order of 30-40 ms, compared to 10-15 ms for the 56 watt valve.

Combustion Chamber

The combustion chamber and exit nozzle are constructed of MoSi₂ coated molybdenum. The design of the thruster is nearly identical to that used in the development thruster except that the thick section at the throat previously used was reduced in thickness to minimize thermal stresses. Two combustors were evaluated during this program, with the only variation being L*. The L*'s of the two were 4.2 inches and 5 inches with the larger L* combustor used for the Configuration No. 3 tests.

General Configuration and Design Criteria

The thruster and valves are designed for ease of disassembly while maintaining zero leakpaths.

The valves, injector, and combustor are connected by AN fittings and conventional bolts. The spark plug is installed in the thruster through a threaded fitting.

3. TEST PROGRAM

a. Test Facility

Marquardt's Test Cell 9 was used for all hot firing tests conducted on the three thrusters. The test cell is a 4,000 cubic foot steel sphere, 20 feet in diameter, rated for pressures from 0.0009 to 160 psia. Vacuum capability is provided by a 5-stage steam ejector system. The feed system and engine flow schematic for the thruster is shown on Figure 34.

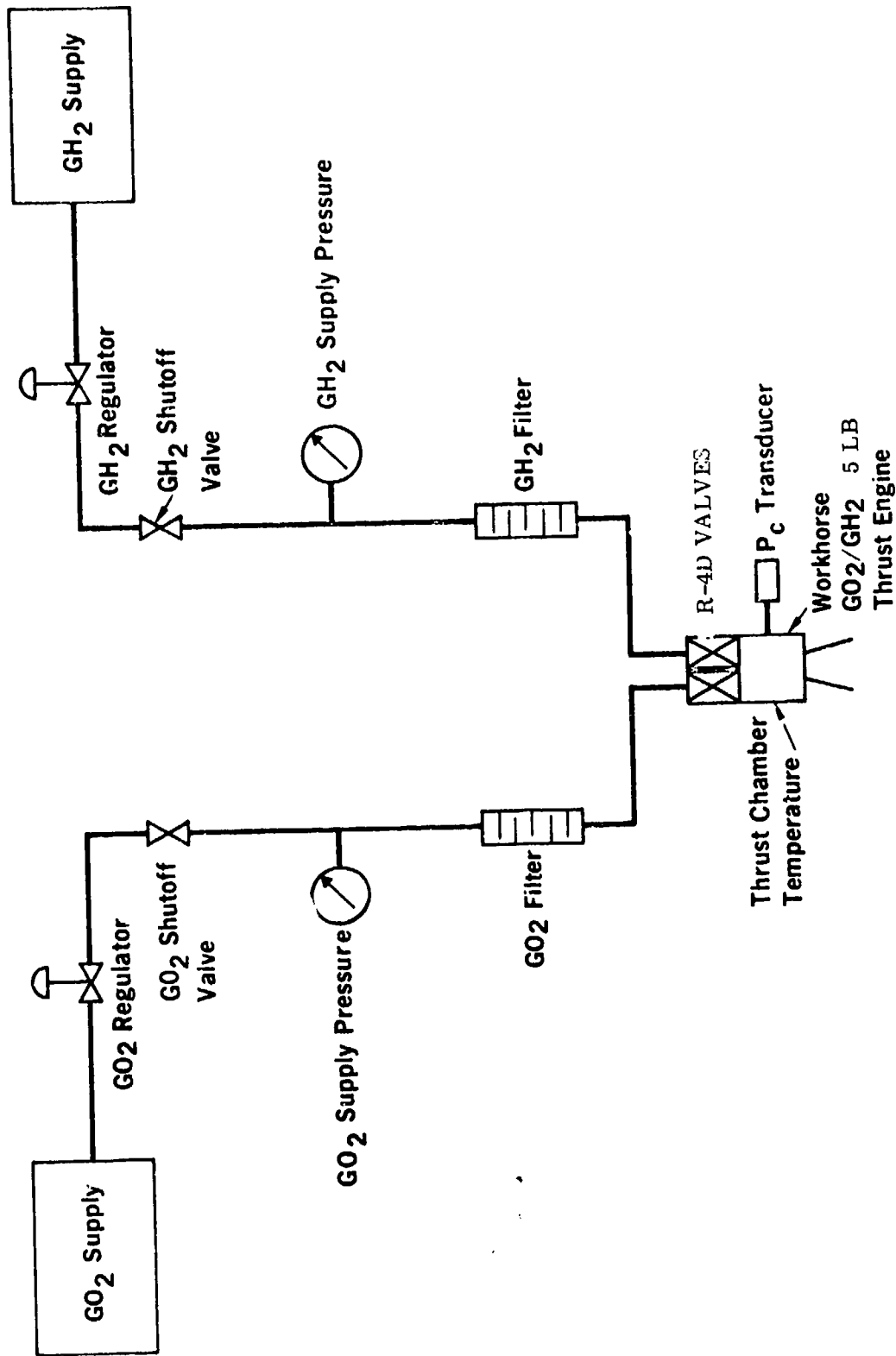


Figure 34. Cell 9 Schematic

b. Test Sequence

The test program for Thruster No. 1 which was used in the system life test consisted of a series of steady state and pulsing runs to document its capability to operate in the System Test.

The test program conducted on Thrusters No. 2 and 3 were designed to document the performance over a range of pressures, temperatures, and duty cycles. The basic requirements are:

- (1) Performance and thermal characterization.
- (2) Duty cycle demonstration by performing 150,000 pulses ranging from 50 ms. to steady state and the accumulation of 5 hours of burn time.

All tests conducted on the 5-pound thrust rocket engine utilized the GLA spark exciter which provided approximately 10 millijoules of energy per spark.

4. TEST RESULTS

a. Configuration No. 1

The P/N X29069 Thruster shown in Figure 35 was designed to be used in the water electrolysis system and to replace the previous program's thruster which failed after 70,000 cycles. The details of the injector are shown on Figures 36 and 37. Figures 38 and 39 (which were taken after conclusion of the life test) show the injector and assembly (less spark exciter). This thruster was tested in Cell 9 prior to inclusion in the system test. The test results indicated a specific impulse of 350 seconds at 5 pounds thrust dropping to 315 seconds at 2 pounds. The equilibrium wall temperature at the throat was 2500°F at the end of a 40-second firing. A total of 40 firings were conducted on the thruster prior to its transfer to Pad D for the life test program.

The Configuration No. 1 was used for the entire life test sequence, where it accumulated 1,210 firings and 4.35 hours of burn time.

At the completion of the test program, the engine was removed from the system and examined. Figures 40, 41, and 42 show the injector and combustor. The nickel injector shows a slight erosion around the spark plug hole and one crack is evident on a premix orifice at the 9 o'clock position. The spark plug tip was apparently corroded or galled within the injector and could not be removed. This was probably caused by the small clearance. The clearance was increased on the final design and the spark plug did not stick in the injector. The throat section of the combustor was not eroded, but as shown in Figure 42, a significant amount of "pockmarks" are evident on the outside and some were also on the inside. Although a significant amount of testing was accomplished at sea level,

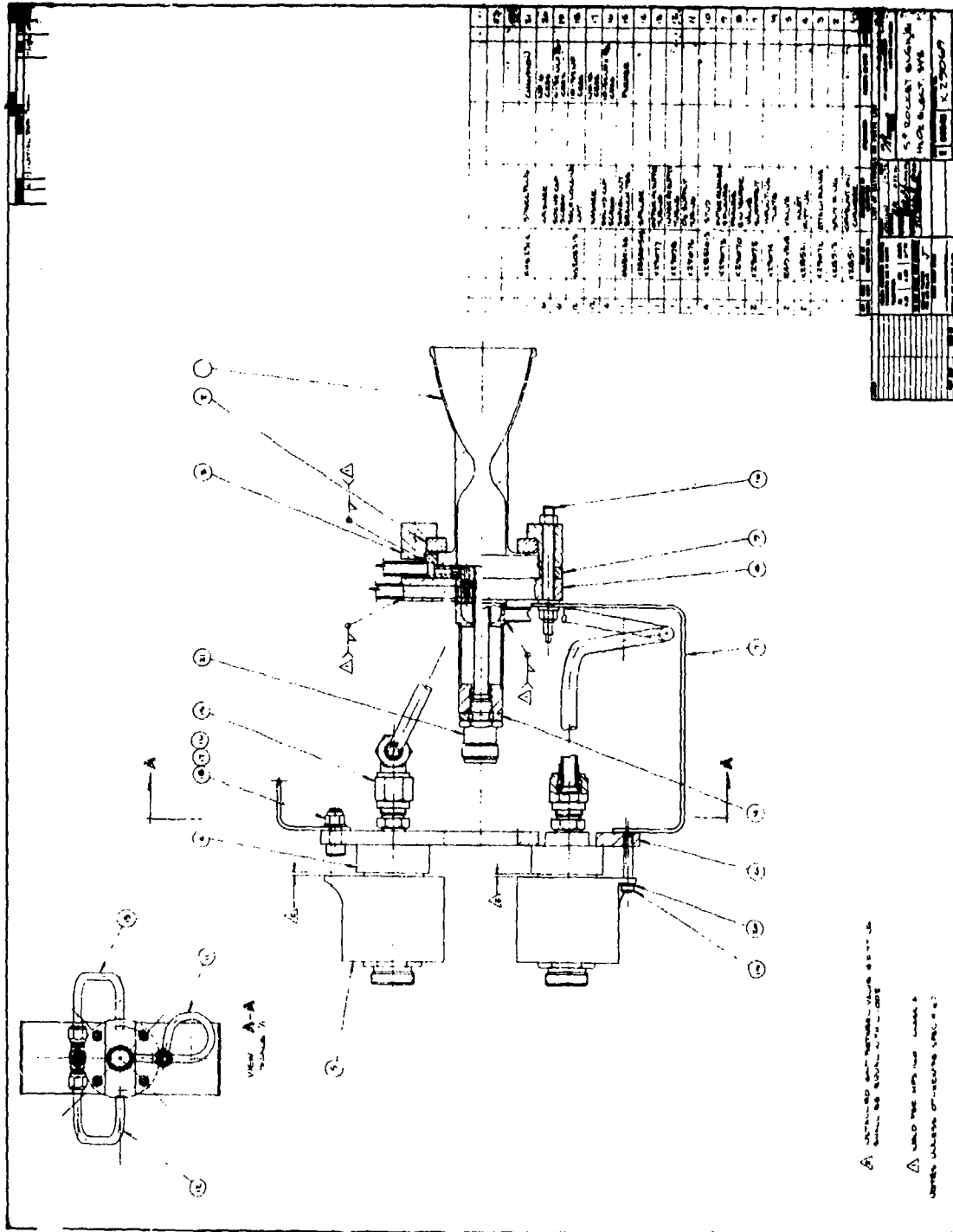


Figure 35. 5 Lbf. Thruster, Configuration No. 1 (X29069).

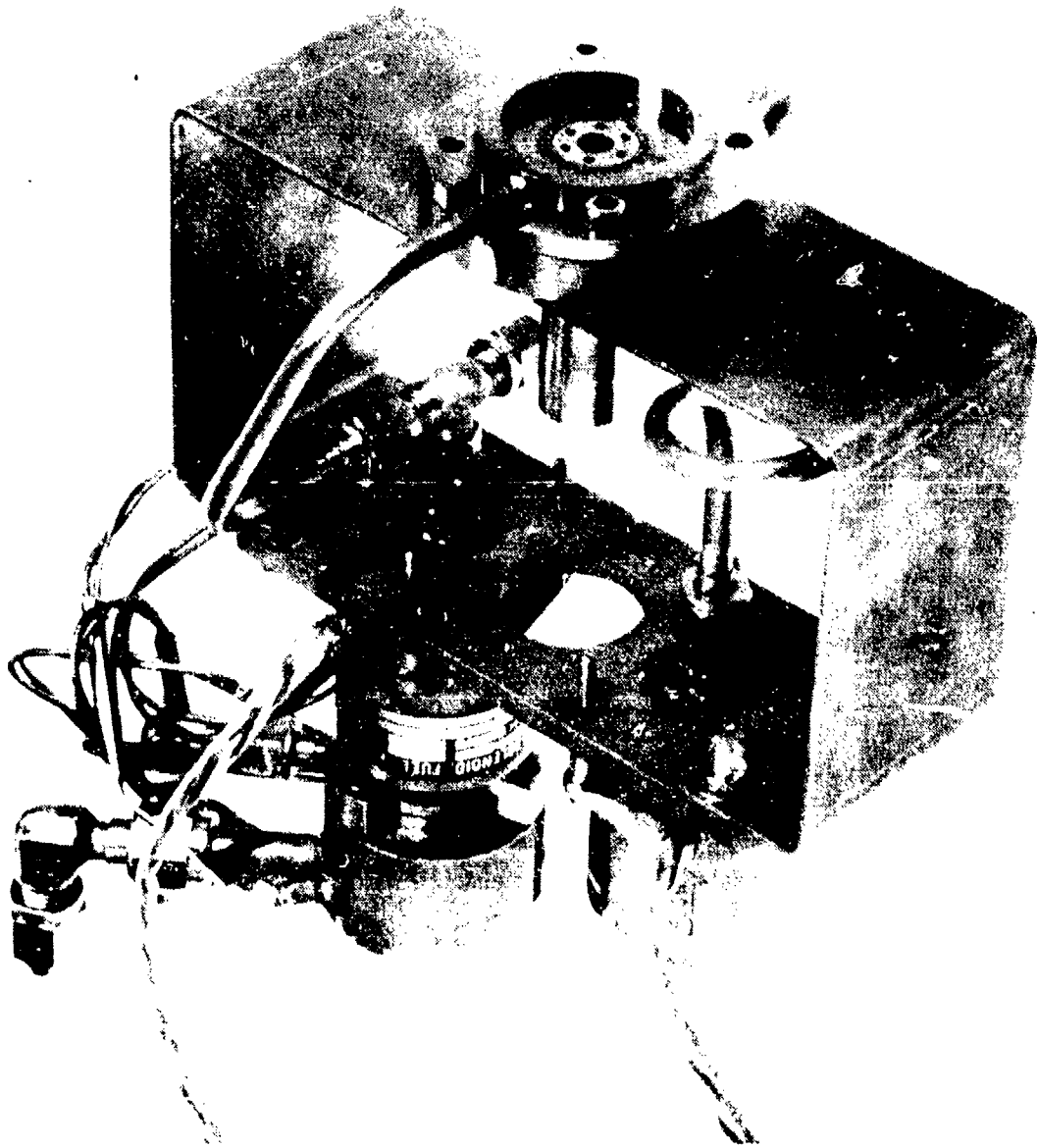


Figure 38. 5 lbf. Thruster Injector, Configuration No. 1

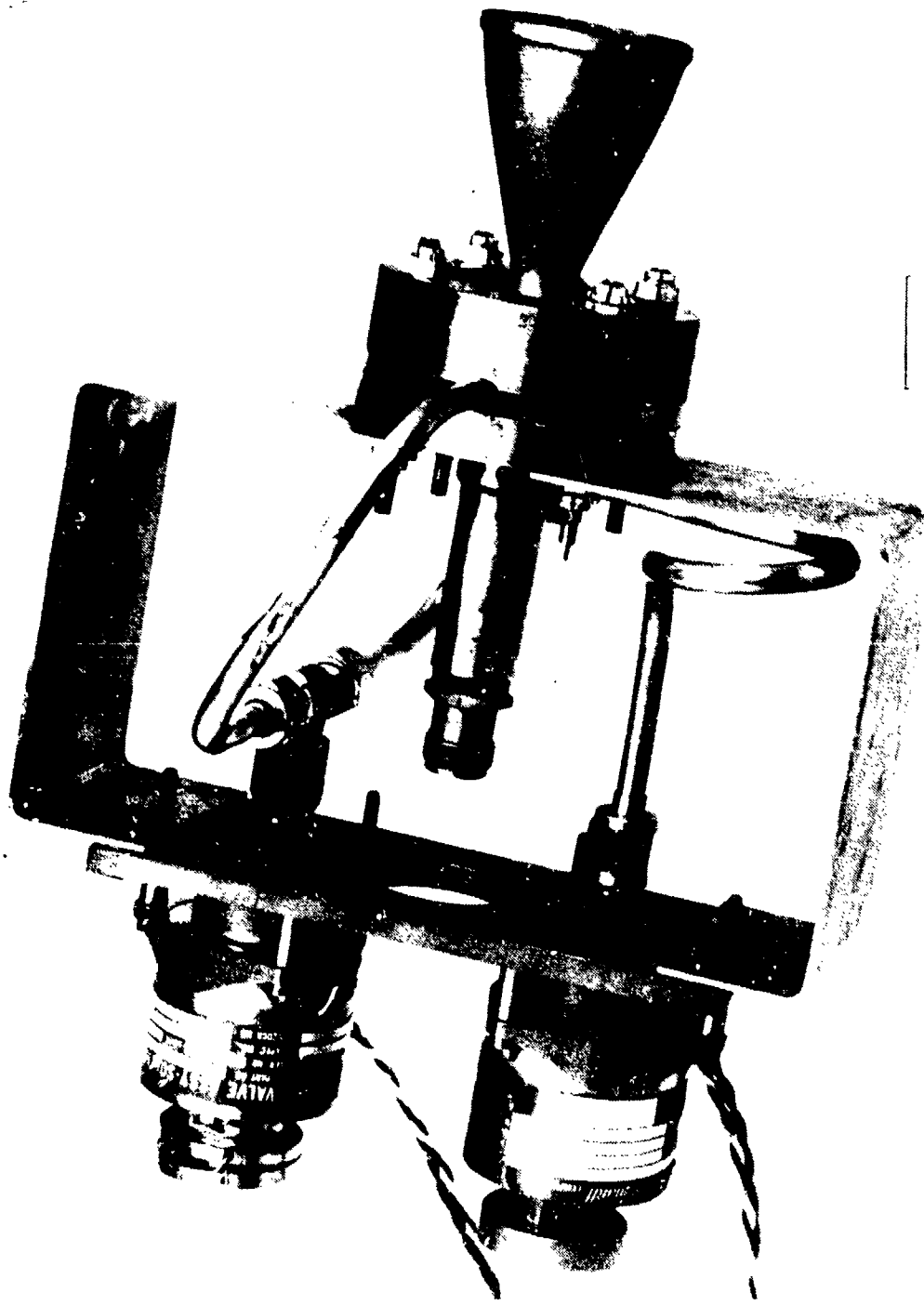


Figure 39. 5 Lbf. Thruster Assembly, Configuration No. 1



Figure 40. 5 Lbf. Injector, Configuration No. 1, After Test

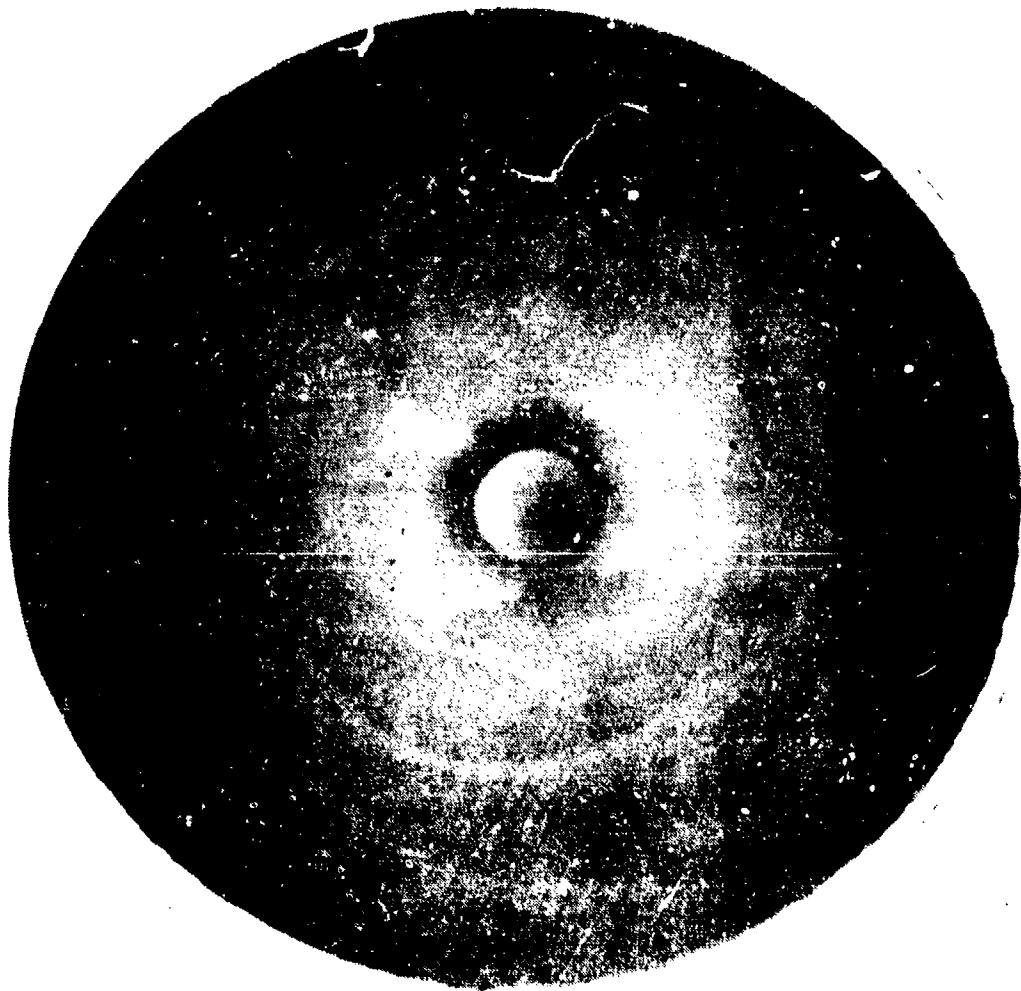


Figure 11. 5461, Combustor, Configuration No. 1



0 Inch 1

Figure 42. Outside of 5 Lbf Combustor, Configuration No. 1, After Test

the loss of coating did not degrade the thruster's ability to operate. The corrosion shown was observed halfway through the program, and it is hypothesized that improper cleaning procedures were used in coating the molybdenum as only 1/2 of the exit nozzle shows this corrosion. The other side (not shown) was relatively void of the corrosion.

Leakage checks of the two valves indicated zero leakage in snoop with GN₂ pressurant and no liquid leakage. The valve response data indicated no change in opening or closing time.

b. Configuration No. 2

Configuration No. 2 was the initial flight type configuration to be tested. Figure 43 shows Thruster, P/N X29385, and the injector details, P/N X29380, are shown in Figure 33. The design of the thruster was oriented toward high temperature capability material. Thus C-103 Columbium and 6AL-4V titanium were used in the injector while molybdenum was used for the combustor. As discussed previously, the Marquardt bipropellant valve was used to control the propellant and the propellant mixture was ignited using the GLA spark exciter which is described in detail in Appendix A.

The injector assembly and the individual components used to make up this thruster are shown in Figures 44, 45, and 46. Figure 44 shows the main injector with the 6 oxygen and 18 hydrogen jets (lower left of photo), the pre-mix section and 36 hydrogen film cooling holes (upper left), and the feed manifold and attach flange. The latter is fabricated of titanium and the two former of C-103 Columbium. Figure 45 shows the complete exploded view of the thruster (less exciter), and Figure 46 shows the partially assembled thruster. Figure 47 shows the thruster installed in the Cell 9 test facility.

(1) Cold Flow and Orifice Calibration

Cold flow calibration was made to determine the sizes of both the main trim orifice and the split of hydrogen between the main orifices and the film cooling orifice. The thruster is designed to operate at 50 psia with a 200 psia inlet, thus sonic or choked orifices are used to control the flow. These two sharp edged orifices are installed between the valve and the injector feed tubes.

Downstream of the sonic hydrogen orifice, two subsonic orifices are located which are sized to provide the right amount of film cooling. In the case of this design, 60 percent H₂ film cooling is used.

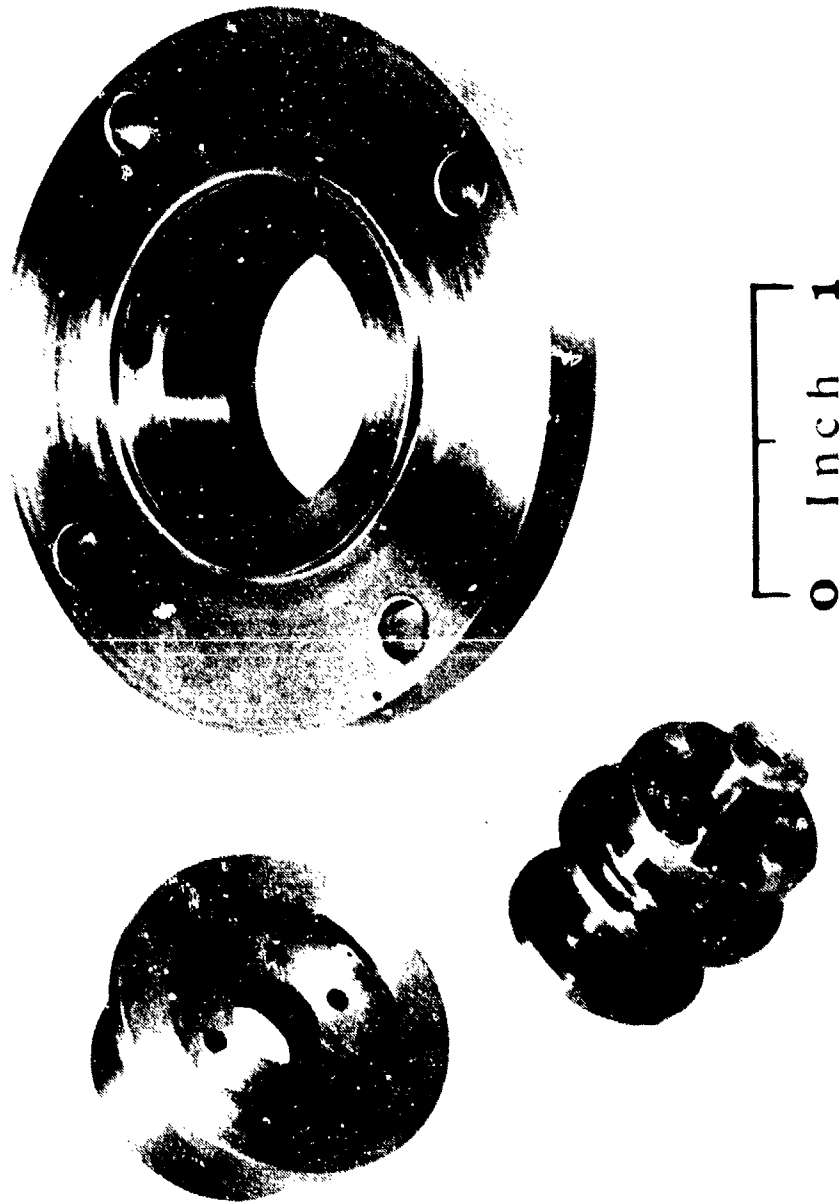


Figure 44. Injector for 5 Lbf. Thruster, Configuration No. 2

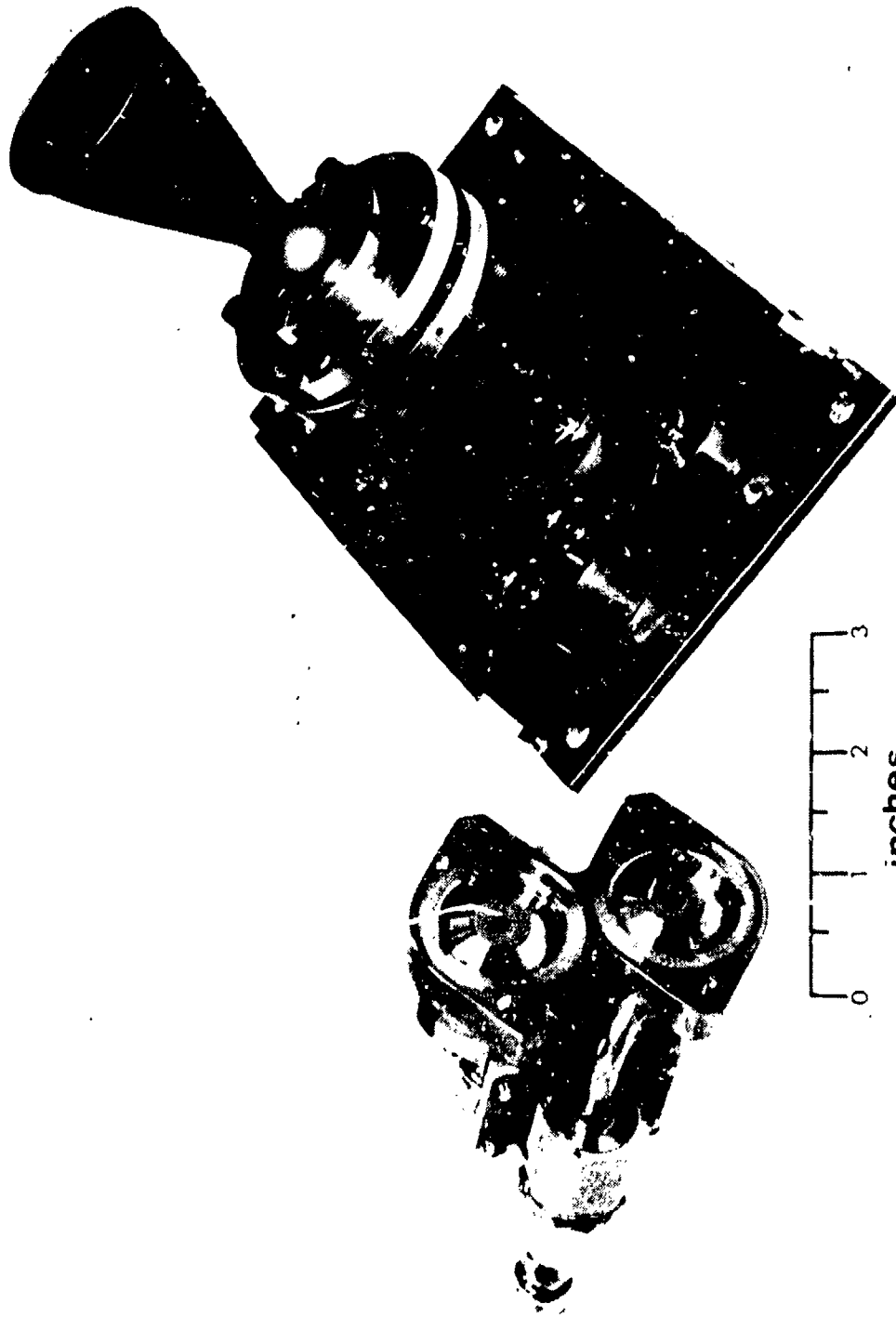


Figure 46. Partially Assembled 5 Lbf. Thruster, Configuration No. 2

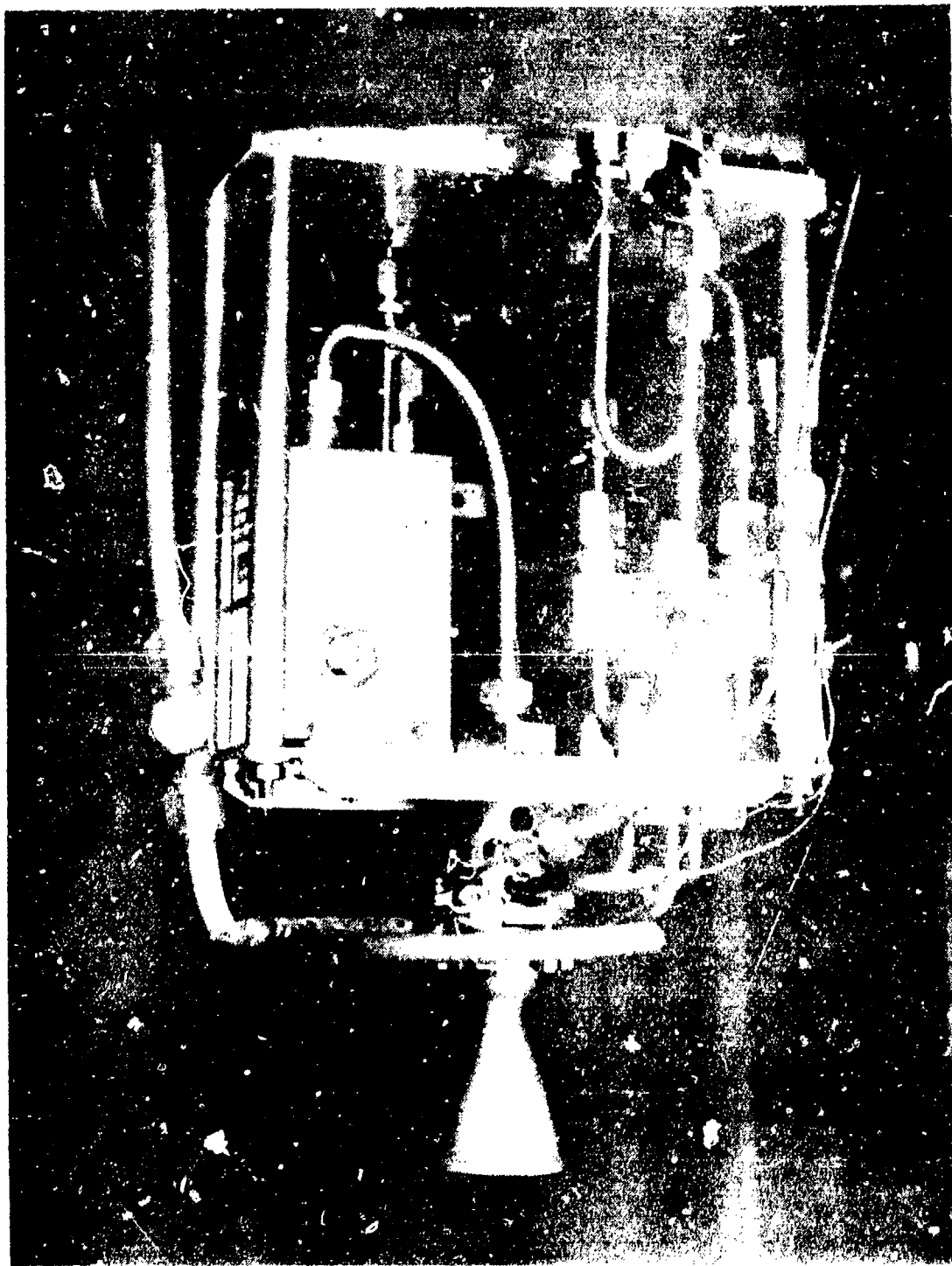


Figure 1. 5 lb. Diesel engine.

(2) Test Program and Results

Baseline performance tests of Configuration No. 2 (Figure 43) showed a specific impulse of 353 seconds and an equilibrium wall temperature at steady state of 2400°F. Following completion of the baseline performance and thermal test series, the life test was initiated. At initiation of the life test, 765 seconds of firing time and 328 ignitions had been accumulated. Table 7 documents the test conducted on this thruster.

(a) Life Test

A series of pulse firings of various durations and rates were accomplished on Configuration No. 2 in an effort to accumulate 150,000 starts and 5 hours of firing duration. Three pulse rates and widths were used:

Series A - .05 seconds on, .45 seconds off (had 3000 firings per sequence)

Series B - .10 seconds on, .90 seconds off (had 1130 firings per sequence)

Series C - .25 seconds on, .75 seconds off (had 865 firings per sequence)

This series was to be repeated 6 times at 5 pressure levels.

At the end of the first day's testing and after 742 seconds and 8,260 firings, an inspection of the thruster was made. A white deposit was observed in the area of the throat but no other anomalies were observed. During the second day's testing, sparks were being ejected from the thruster, but a baseline test after an additional 1,721 starts and 1,177 seconds of firing indicated no throat erosion. Inspection of the thruster indicated that the C-103 injector had suffered hydrogen embrittlement and numerous cracks were observed, especially around the film cooling orifices. The thruster was removed from the test cell for failure investigation after 2,684 seconds of operation and 20,309 starts.

(b) Failure Investigation

Upon disassembly of the thruster, the following anomalies were observed:

TABLE 7. SUMMARY OF DATA FROM C-103 INJECTOR TESTS

<u>RUN</u>	<u>ON TIME</u>	<u>F</u>	<u>O/F</u>	<u>C*</u>	<u>ISP</u>
430	2.0	5.0	8.05	6634	350
433	60.0	4.8	8.10	6388	345
435	20.0	5.13	7.96	6830	360
436	2.0	5.43	5.97	7240	381
437	2.0	5.33	6.88	6990	369
438	2.0	5.03	7.96	6733	355
439	2.0	5.03	8.55	6513	346
440	2.0	4.60	10.00	6134	322
441	2.0	3.55	7.85	6615	337
443	2.0	2.36	7.84	6303	321
451	6.0	5.06	8.02	6763	355
452	2.0	5.3	7.08	6976	366
453	2.0	5.24	6.17	7000	363
454	2.0	4.63	8.51	6185	324
455	2.0	4.35	9.91	5859	307
456	2.0	6.16	8.10	6766	356
457	2.0	6.63	5.99	7364	384
458	2.0	5.62	9.97	6151	326
459	2.0	7.21	7.94	6824	362
460	2.0	4.79	8.04	6354	331
461	2.0	6.68	10.00	6298	333
462	2.0	3.90	8.03	6607	337
463	2.0	4.10	6.08	6827	356
464	2.0	3.70	10.00	6143	323
465	2.0	2.78	8.0	6342	327
466	2.0	3.01	6.17	6856	351
467	2.0	2.63	10.10	5949	310
468	2.0	1.78	7.90	6096	333
470	2.0	1.60	10.37	5497	281

- A white deposit was present in the combustion chamber and throat portions of the molybdenum combustor (see Figure 48).
- Numerous cracks were observed in the injector, especially around the film cooling holes. One large crack was evident at the spark plug hole. In addition, a white deposit was observed on the face of the injector and in the six premix orifices (see Figure 49).
- The MS5033-14 bolts and M521043-4 nuts holding the chamber to the injector were overtorqued by 75 inch-pounds. The nominal value was 25 inch-pounds. The actual value was 100 inch-pounds.

The deposit on the combustion chamber was analyzed and determined to be Columbium oxide, while the cracks in the injector face were determined to be intergranular and were caused by hydrogen embrittlement of the Columbium C-103.

It was concluded that the injector failed along the intergranular grain boundaries due to the overstress condition caused by overtorquing of the chamber attach bolts. The brittle failure was brought on by hydrogen embrittlement at temperatures above 1000°F. The Columbium oxide deposit was the result of oxidation of the Columbium in the premix orifices.

c. Configuration No. 3

Analysis of the results of the tests and failure investigation conducted on Configuration No. 2 showed that the use of Columbium was not suitable for the design. The design is oriented toward maintaining the exciter and valve at relatively low temperatures (250°F). In isolating these components, the injector by necessity will attain temperatures of 1000°F. (Later tests verify that the equilibrium temperature at the injector during pumping pulse duty cycles is 900-1000°F.)

The most suitable material for use in this range was found to be nickel (which was also used on Configuration No. 1). It has good oxidation resistance and a high thermal conductivity which minimizes thermal stress.

The Configuration No. 3 design was modified to utilize a Nickel 200 injector. All other design criteria were identical to that used on the prior configurations. Figure 50, P/N X28680, shows the thruster assembly. It is essentially identical to Configuration No. 2 except that:

- The combustor is attached to the injector using long bolts and the valve mount plate as the support.

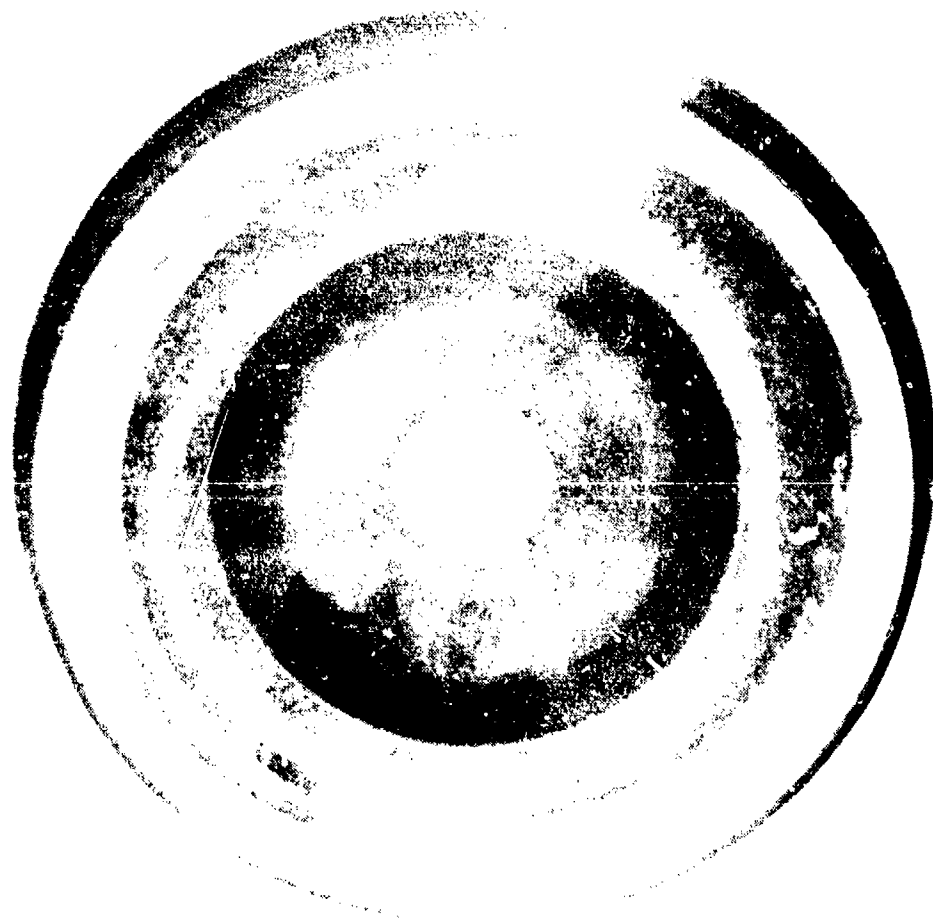


Figure 16. (Left) Cross-section of a tube, (Right) After Test

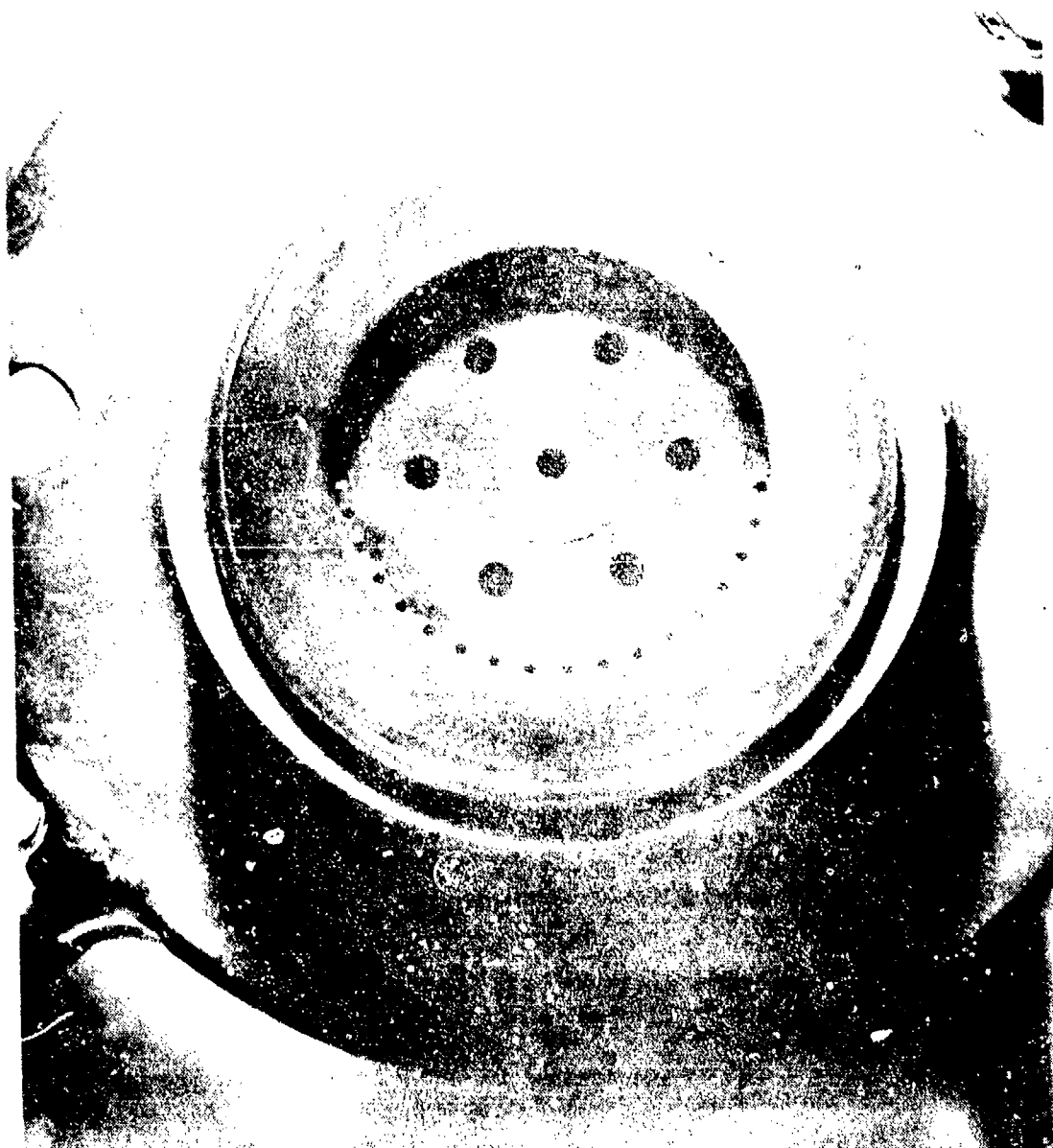


FIG. 1. Filter element, 100 mm diameter.

- The trim orifices were changed to fit into AN fittings.

Figures 51 and 52 show the assembled thruster prior to installation in Cell 9.

(1) Pretest Calibration and Thruster Evaluation

The thruster was weighed, leak checked, and cold flow calibrated prior to installation in Cell 9. Table 8 lists the weight of the individual parts, part number, and the projected flight weight. The actual weight of the thruster is 4.5 pounds (less exciter) with a projected weight of 2.9 pounds.

Cold flow calibration and orificing resulted in a thruster which uses approximately 60% of the fuel as film coolant. The thruster was designed to give 5 pounds of thrust at 200 psia inlet, but the final tests indicated a thrust of 4.8 pounds at 200 psia. This was due to a variation in the point at which the inlet pressure was measured.

(2) Test Program

The test program conducted on the Configuration No. 3 thruster was nearly identical to that conducted on Configuration No. 2. A series of steady state and pulse firings were accomplished prior to the life test to document both performance and thermal characteristics. Figures 31, 32, and 53 show the steady state and pulse performance of the thruster as a function of mixture ratio, thrust, and electrical pulse width. The specific impulse of the thruster at nominal thrust ($O/F = 7.934$) is 355 seconds.

Following the conclusion of the performance and documentation tests, a life test series was conducted for the purpose of accumulating 150,000 pulses and 5 hours of life. The life test run consisted of 50 and 100 millisecond firings plus steady state firings. Blowdown tests were not conducted since this characteristic had been demonstrated during the life test with Configuration No. 1.

(a) Performance

The results of the performance tests conducted on Configuration No. 3 are shown on Figures 31, 32, and 53.

Figure 53, specific impulse versus mixture ratio, indicates a specific impulse of 355 seconds at the stoichiometric mixture ratio of 7.934. Performance increases as thrust is increased and mixture ratio is decreased due to the change in reaction kinetics (as it affects thrust) and a change in theoretical performance. The maximum heat release increases as the mixture ratio decreases. The performance of the thruster as a function of thrust is shown on Figure 31. Performance

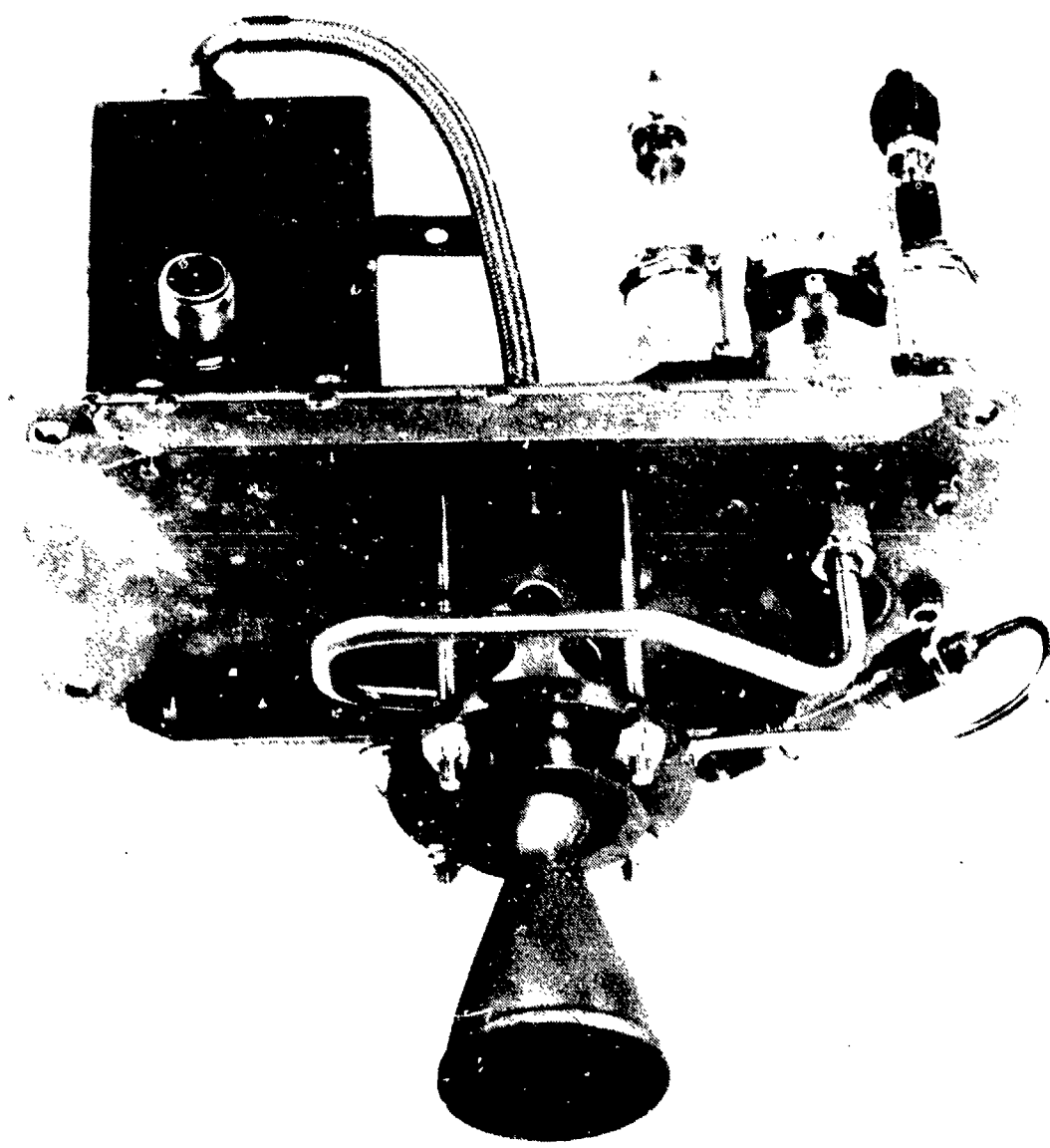
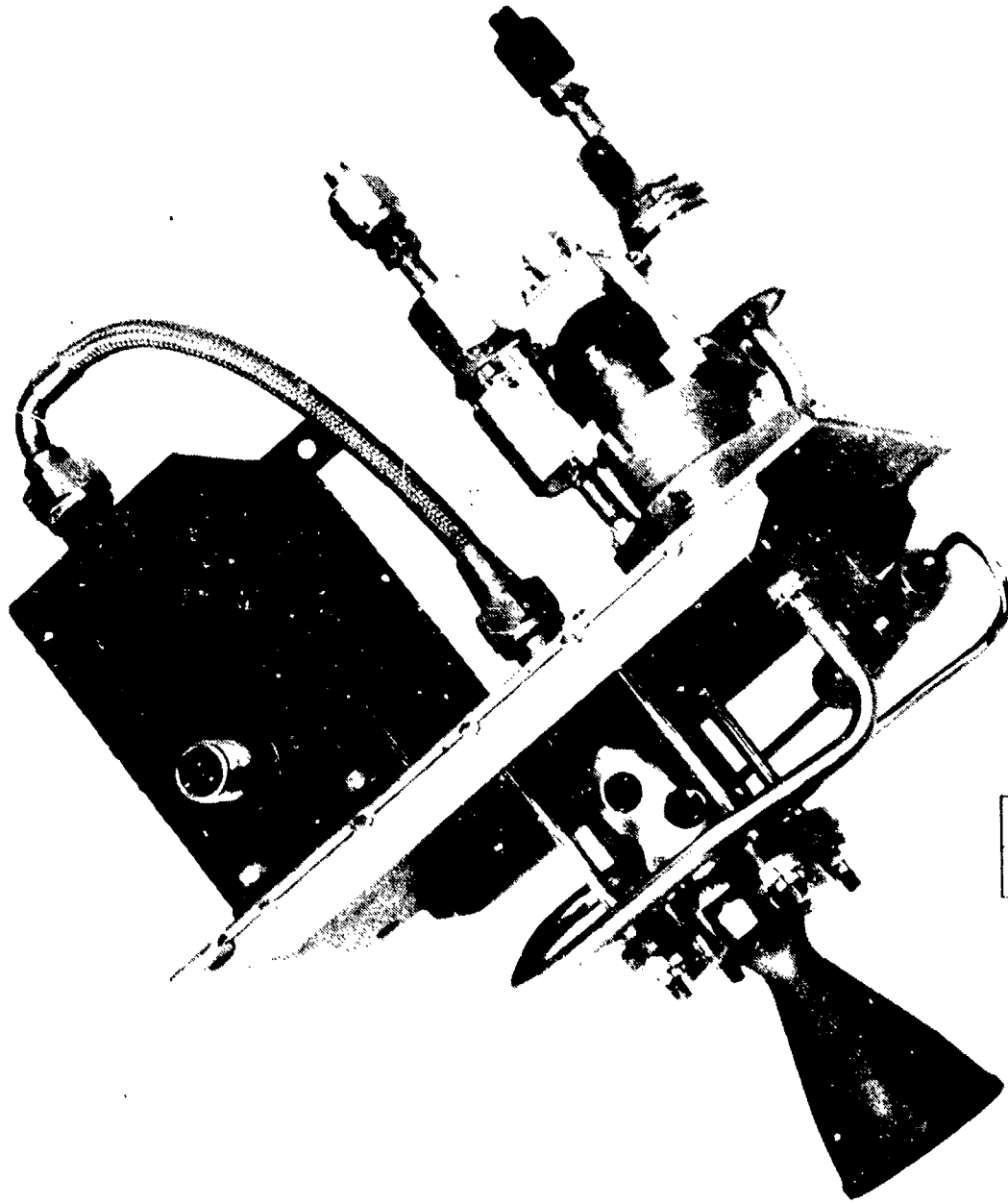


Figure 51. Assembled 5 Lbf. Thruster, Configuration No. 3



0 1 2 3 4 5 6 7 8 9 10 11 12 13 14 15 16 17 18 19 20 21 22 23 24 25 26 27 28 29 30 31 32 33 34 35 36 37 38 39 40 41 42 43 44 45 46 47 48 49 50 51 52 53 54 55 56 57 58 59 60 61 62 63 64 65 66 67 68 69 70 71 72 73 74 75 76 77 78 79 80 81 82 83 84 85 86 87 88 89 90 91 92 93 94 95 96 97 98 99 100

Figure 52. 5 Lbf. Thruster, Configuration No. 3

NE 01 74-341-40

TABLE 8. 5 LBF THRUSTER PART NUMBER AND WEIGHT SUMMARY

Orifice	X28686	NIL	NIL
Solenoid Valve, Bipropellant	X29258	1.95 lbs.	1.1 lbs.
Spacer	X29378	NIL	NIL
Ring, Split	X29382	.31 lbs.	.20 lbs.
Ring, Attach	X29381	.31 lbs.	.20 lbs.
Insulator	X29386	NIL	NIL
Combustion Chamber	X29383	.33 lbs.	.30 lbs.
Spark Plug	X28687	.06 lbs.	.06 lbs.
Spacer	X28684	NIL	NIL
Plate, Mounting	X28683	.70 lbs.	.35 lbs.
Standoff Assembly	X28682	.13 lbs.	.13 lbs.
Plate Assembly Spacer	X28685	.13 lbs.	.13 lbs.
Injector Assembly	X28681	.60 lbs.	.43 lbs.
<hr/>			
Rocket Engine Assembly	X28680	4.52 lbs.	2.9 lbs.

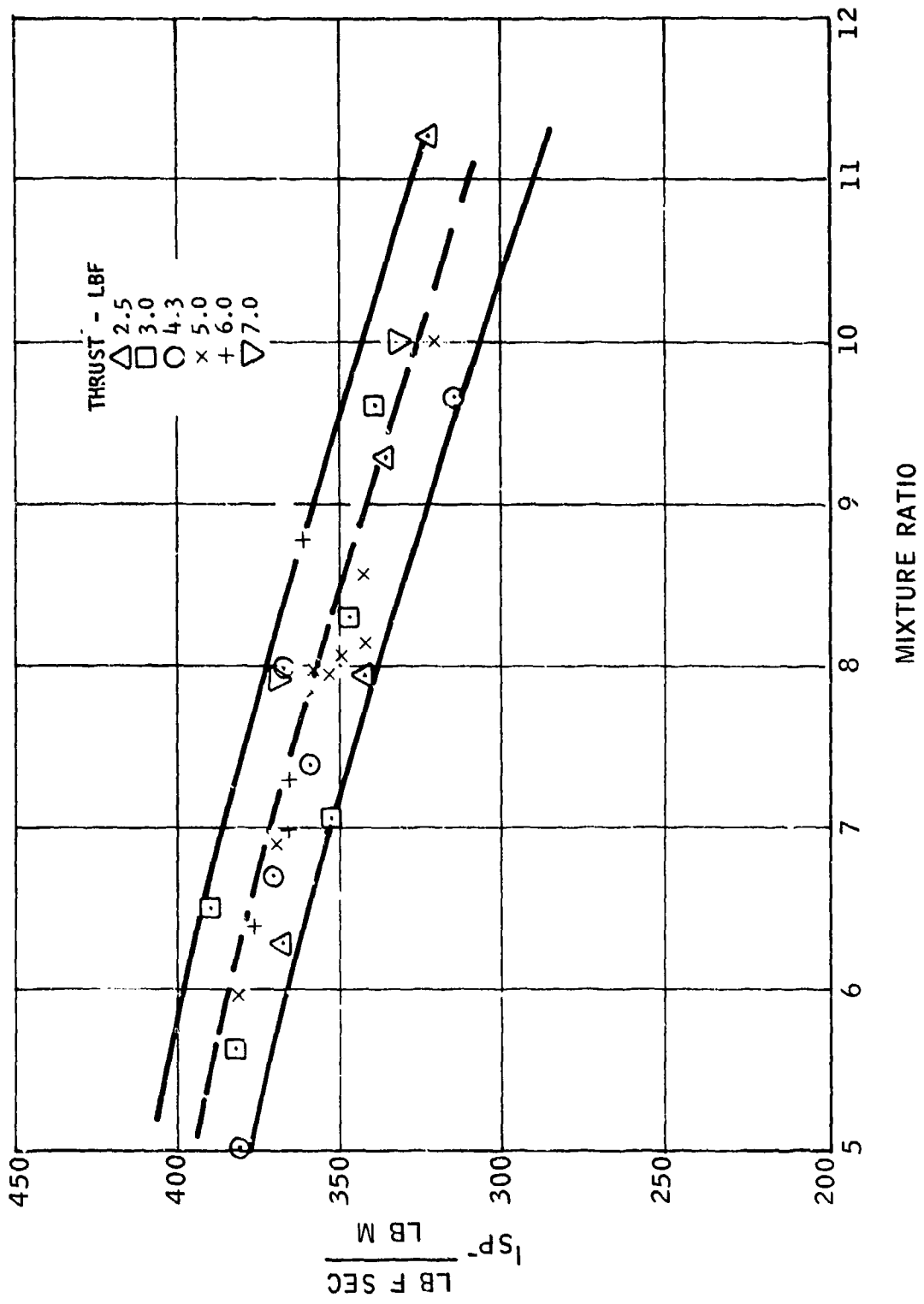


Figure 53. Performance of 5 Lbf. Thruster, Configuration No. 3

characteristics down to 1.5 pounds were documented. Below 1.5 pounds, ignition of the thruster was not attained. This lower limit is identical to that obtained in the prior program using an identical design (Reference 1).

Tables 9 and 10 list the data applicable to the performance evaluation for both steady state and pulse firing conditions. The pulse performance data shown in Table 10 is also plotted on Figures 32 and 54. Figure 54 shows the impulse bit as a function of thrust level and electrical pulse width, while Figure 32 shows the specific impulse as a function of the same parameters. As the inlet pressure increases, the valve opens slower and thus the same electrical pulse width at the higher inlet pressure results in a shorter valve open time (VOT). As the VOT decreases, the performance would decrease because a greater percent of the time is devoted to the ignition process.

Figure 55 shows that the valve is sensitive to inlet pressure. In fact, the valve would not open at 300 psia inlet pressure, which corresponds to 7.5 pounds thrust.

As a result, when a 50 ms. firing is conducted, the valve delay may affect the impulse bit, since the time to close is relatively constant. This is reflected in the time to 90% where the delay is significant at 6-7 pounds, while the time to 10% is relatively constant.

Figures 56 through 59 show typical engine firing records for various pulse widths. The thrust trace and chamber pressure trace show very little roughness and, in fact, the roughness over the entire thrust and mixture ratio range was less than 5%.

(b) Test Results - Thermal

The use of 60% fuel film cooling results in a maximum chamber temperature of 2500°F. Figure 60 shows the results of the thermal runs where maximum chamber temperature is plotted against thrust. The maximum injector temperature that occurs during steady state operation, and is nearly the same during pulsing cycles of significant duration, is approximately 1000°F. In all cases, the valve and exciter temperature is well below 200°F.

(c) Life Test

The Configuration No. 3 thruster successfully completed 150,000 cycles and approximately 4.2 hours of firing time during the life test. The maximum run duration was 3600 seconds while a majority of the

TABLE 9. STEADY STATE PERFORMANCE, 5 LBF CONFIGURATION NO. 3

<u>RUN</u>	<u>DURATION</u> (Sec.)	<u>F</u> (Lbs.)	<u>O/F</u>	<u>C*</u> (Ft/Sec)	<u>ISP</u> (Sec.)
545	4	4.55	8.05	6404	337
546	6	4.67	8.04	6541	349
547	6	4.68	8.10	6560	350
548	5	4.78	7.93	6630	357
554	1	4.84	8.11	6702	359
555	3	4.66	8.10	6616	348
563	1	4.74	8.37	6479	344
565	1	6.82	8.15	6826	364
566	1	6.86	8.15	6836	366
595	2	4.77	8.11	6604	354
596	2	4.80	8.11	6660	356
597	2	4.68	8.11	6688	347
598	2	4.81	8.04	6752	360
599	2	4.78	8.10	6743	358
600	5	4.74	8.10	6645	355
601	5	4.70	8.10	6574	352
611	2	4.83	8.16	6679	359
612	2	4.60	8.16	6469	342
613	2	4.81	8.16	6693	357
614	2	4.64	8.16	6553	345
618	2	4.69	8.04	6471	351
619	2	4.69	8.04	6499	351
620	2	4.69	8.04	6541	350
621	2	3.02	7.86	6375	348
622	2	2.99	7.38	6499	347
623	2	3.04	7.45	6572	352
624	2	2.17	7.36	6566	360
629	2	2.27	7.07	6533	375
630	2	2.02	7.16	6842	335
635	2	.736	7.16	No Data	118 No Ignition
636	2	.769	7.22	No Data	125 No Ignition
637	2	.701	7.38	No Data	114 No Ignition
338	2	.769	7.07	No Data	110 No Ignition
639	2	1.70	7.35	No Data	339
640	2	1.75	7.66	No Data	337
641	2	1.83	8.00	No Data	339
642	2	1.86	8.62	No Data	334
643	2	1.92	11.63	No Data	310
644	2	.78	5.41	No Data	203 No Ignition
645	2	.81	4.71	No Data	207 No Ignition

TABLE 9. (Continued)

<u>RUN</u>	<u>DURATION</u> (Sec.)	<u>F</u> (Lbs.)	<u>O/F</u>	<u>C*</u> (Ft/Sec)	<u>ISP</u> (Sec.)
646	2	.93	7.50	No Data	143 No Ignition
647	2	2.10	7.26	6461	347
648	2	2.18	8.43	3074	330
649	2	2.18	11.00	5117	314
650	2	2.02			-
651	2	.816			-
652	2	2.812	7.94	6352	342
653	2	2.898	9.3	6078	335
654	2	2.96	12.1	5798	323
655	2	2.681	6.3	6781	367
656	2	2.545	3.5	6744	354
657	2	3.615	7.10	6451	352
658	2	3.73	8.3	6297	347
659	2	3.86	9.6	5976	339
660	2	3.62	6.4	7241	390
661	2	3.51	5.7	7204	382
662	2	4.85	7.4	6632	359
663	2	5.11	8.05	6643	366
664	2	4.96	9.71	6100	313
665	2	4.80	6.73	6873	370
666	1	4.63	5.1	7174	379
669	1	7.05	8.75	6438	362
670	1	6.01	7.29	6848	365
671	1	5.87	6.37	7061	376
672	1	6.14	7.0	6744	366
677	1	4.69	8.1	6562	348
678	1	4.78	8.1	6646	355
679	1	4.65	8.1	6493	345
680	1	4.58	8.1	6549	348
687	1	4.54	8.1	6297	336
694	1	3.60	7.3	6403	352
701	1	2.80	7.3	6455	351
702	1	2.3	7.4	6364	330
704	1	2.29	7.3	6428	331
711	1	1.93	6.9	6375	341
718	1	4.18	8.2	6265	310
725	1	3.24	7.3	6329	317
732	1	2.33	7.5	6406	326
739	1	1.81	7.1	6498	323
746	1	1.57	8.22	2615	117
748	1	4.52	8.22	6348	336

TABLE 9. (Continued)

<u>RUN</u>	<u>DURATION</u> (Sec.)	<u>F</u> (Lbs.)	<u>O/F</u>	<u>C*</u> (Ft/Sec)	<u>ISP</u> (Sec.)	
755	1	3.35	7.3	6454	331	
762	1	2.33	7.5		327	
769	1	1.90	6.86		380	
776	1	4.51	8.21	6387	337	
783	1	3.44	7.15	6568	342	
790	1	2.36	7.59	6362	331	
797	1	1.87	8.4	6425	323	
804	1	4.56	8.10	6476	341	
811	1	3.35	8.30	6312	338	
818	1	2.32	7.32	6382	332	
						<u>TEMP.</u> °F
825	2	1.95	7.0		348	
832	2	4.42	7.97	5627	333	
836	2	3.36	7.15	6550	335	
837	3600	1.42	6.86	6600	336	2180
838	2	3.61	8.53	6151	310	
839	90	3.73	8.05	5192	335	2480
840	2	4.50	8.04	6415	337	
841	60	4.54	7.97	6406	342	2450

TABLE 10. PULSE PERFORMANCE, 5 LBF CONFIGURATION NO. 3

<u>RUN</u>	<u>ON TIME</u> (MS)	<u>OFF TIME</u> (MS)	<u>O/F</u>	<u>IMPULSE</u> <u>BIT</u> (Lb-Sec)	<u>ISP</u> (Sec.)
550	.05	.45	8.23	.189	272
551	.10	.90	8.37	.411	296
552	.25	.75	8.31	1.084	315
553	.50	2.5	8.24	2.201	322
556	.05	.95	8.24	.201	294
557	.10	.90	8.24	.489	357
558	.25	.75	8.24	1.223	358
559	.50	.50	8.16	2.526	375
560	.025	.975	8.06	.068	200
567	.05	.45	12.3	.18	195
568	.10	.90	12.4	.574	310
569	.25	.75	12.53	1.549	333
570	.50	.50	12.53	3.468	377
571	.05	.45	8.09	.193	232
572	.10	.90	8.07	.523	316
573	.25	.75	8.06	1.349	327
574	.50	.50	8.06	2.998	363
575	.05	.45	6.88	.224	334
576	.10	.90	6.78	.458	344
577	.25	.75	6.80	.955	290
578	.50	.50	6.74	2.442	373
579	.05	.45	8.23	.166	290
580	.10	.90	8.29	.388	339
581	.25	.75	8.29	.935	330
582	.50	.50	8.13	1.93	344
583	.05	.45	6.76	.127	320
584	.10	.90	6.69	.238	362
585	.25	.75	6.74	.681	344
586	.50	.50	6.70	2.750	347
587	.03	.45	7.02	.103	347
588	.10	.90	7.02	.208	350
589	.25	.75	7.02	1.079	363
590	.50	.50	7.02		

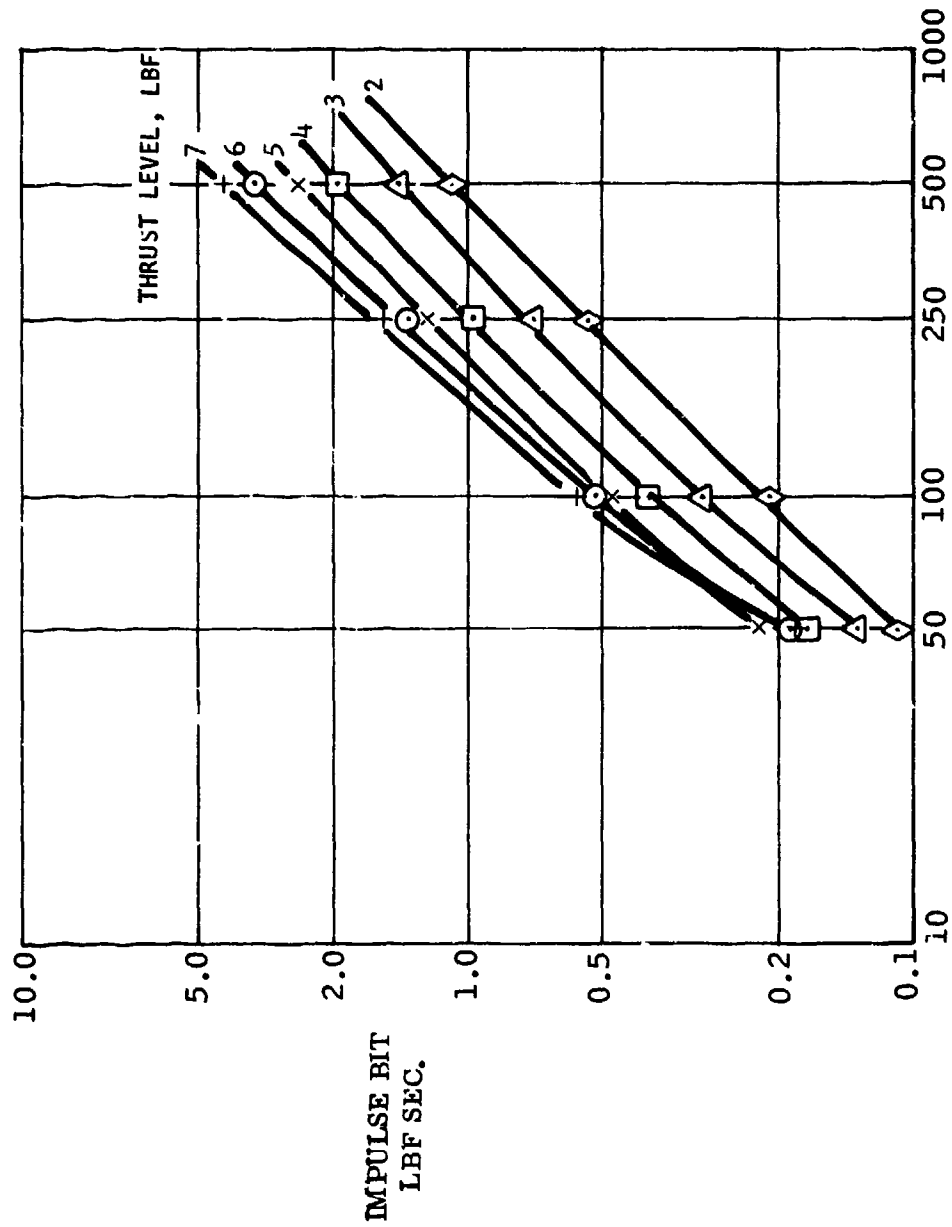


Figure 54. Impulse Bit of 5 Lbf. Thruster, Configuration No. 3

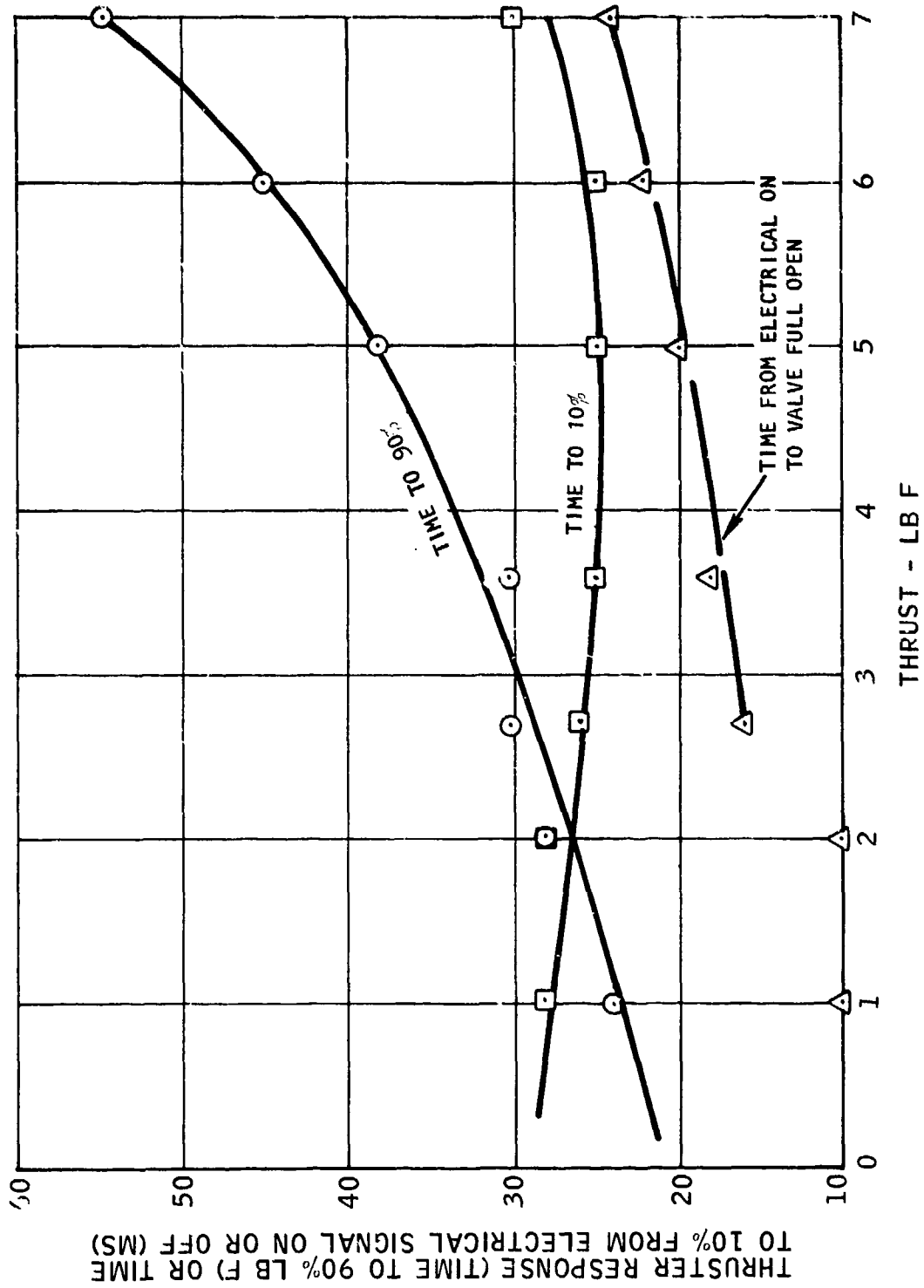


Figure 55. Valve Response Vs. Thrust Level

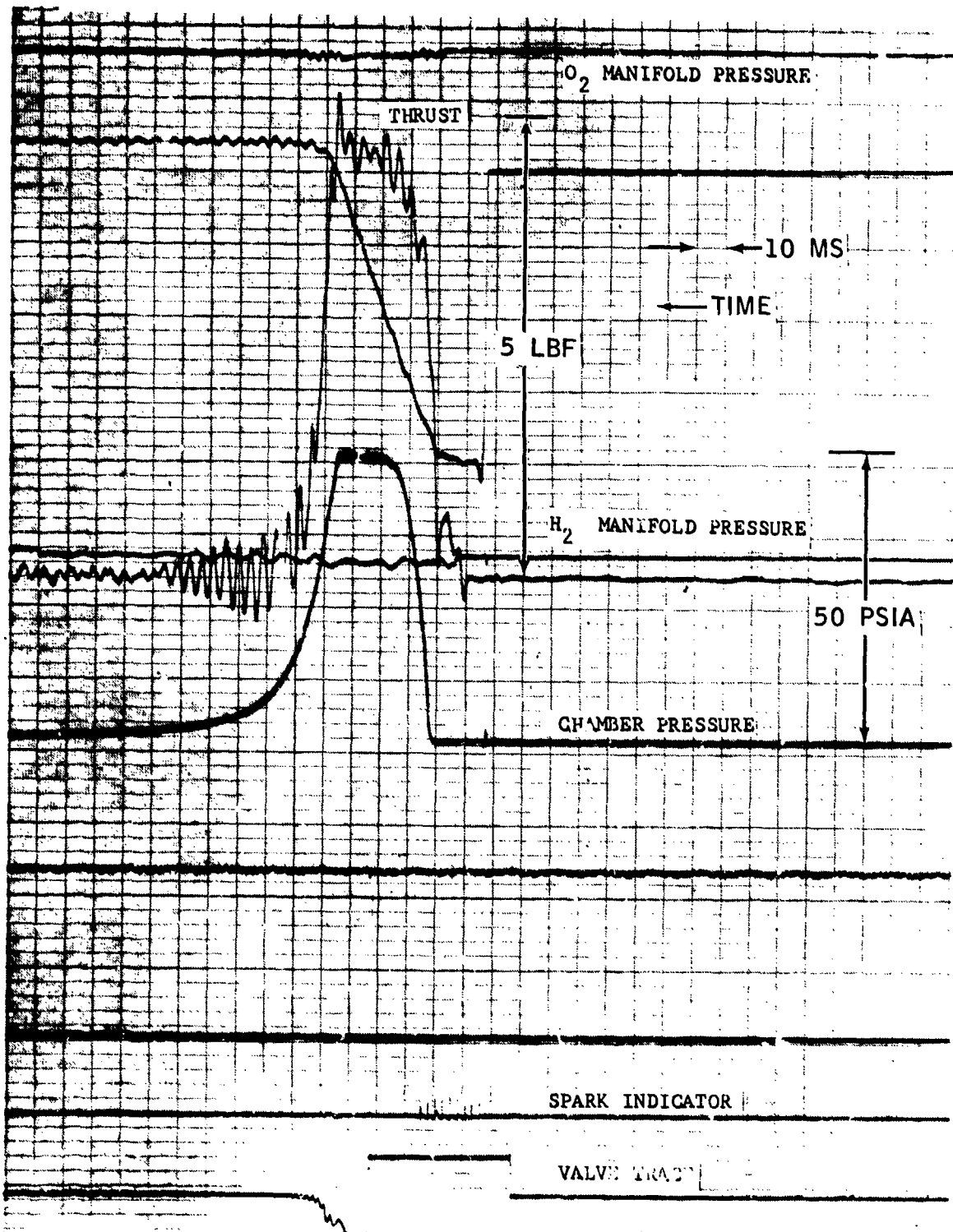


Figure 56. 5 Lbf. GO₂/GH₂ Rocket Engine Firing Record - 50 Ms Firing

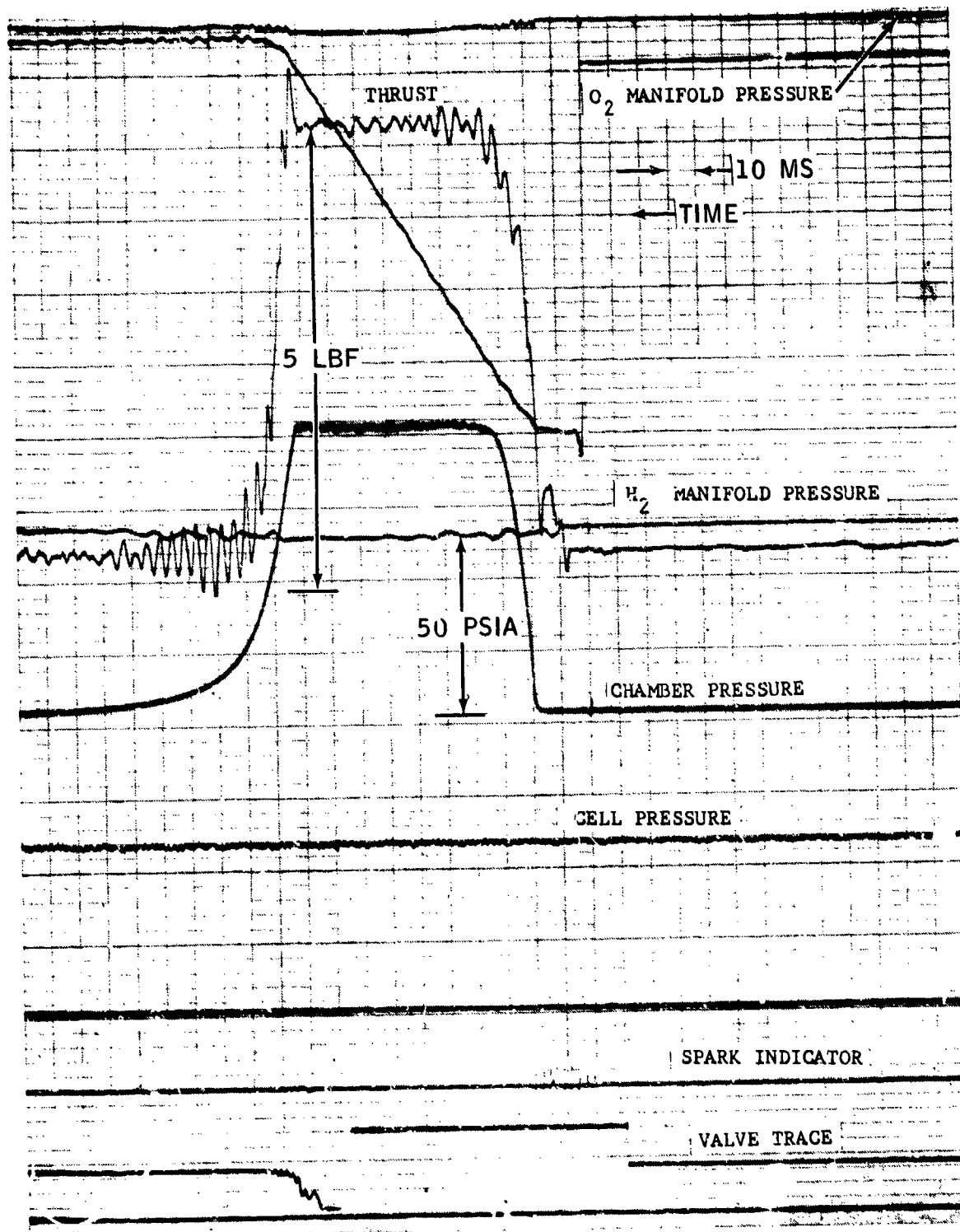


Figure 57. 5 Lbf. GO₂/GH₂ Rocket Engine Firing Record - 100 Ms Firing

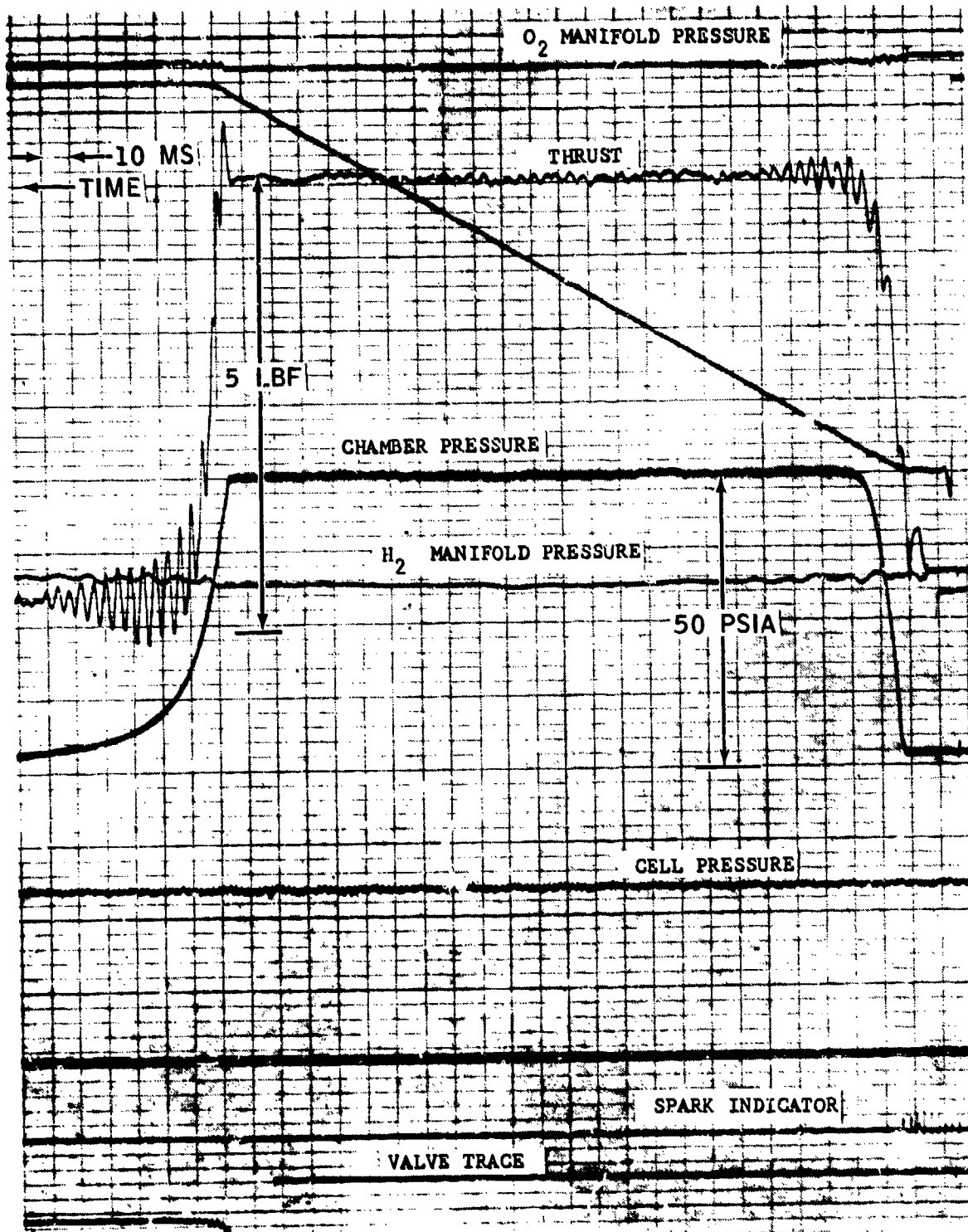


Figure 58. 5 Lbf. GO₂/GH₂ Rocket Engine Firing Record - 250 Ms Firing

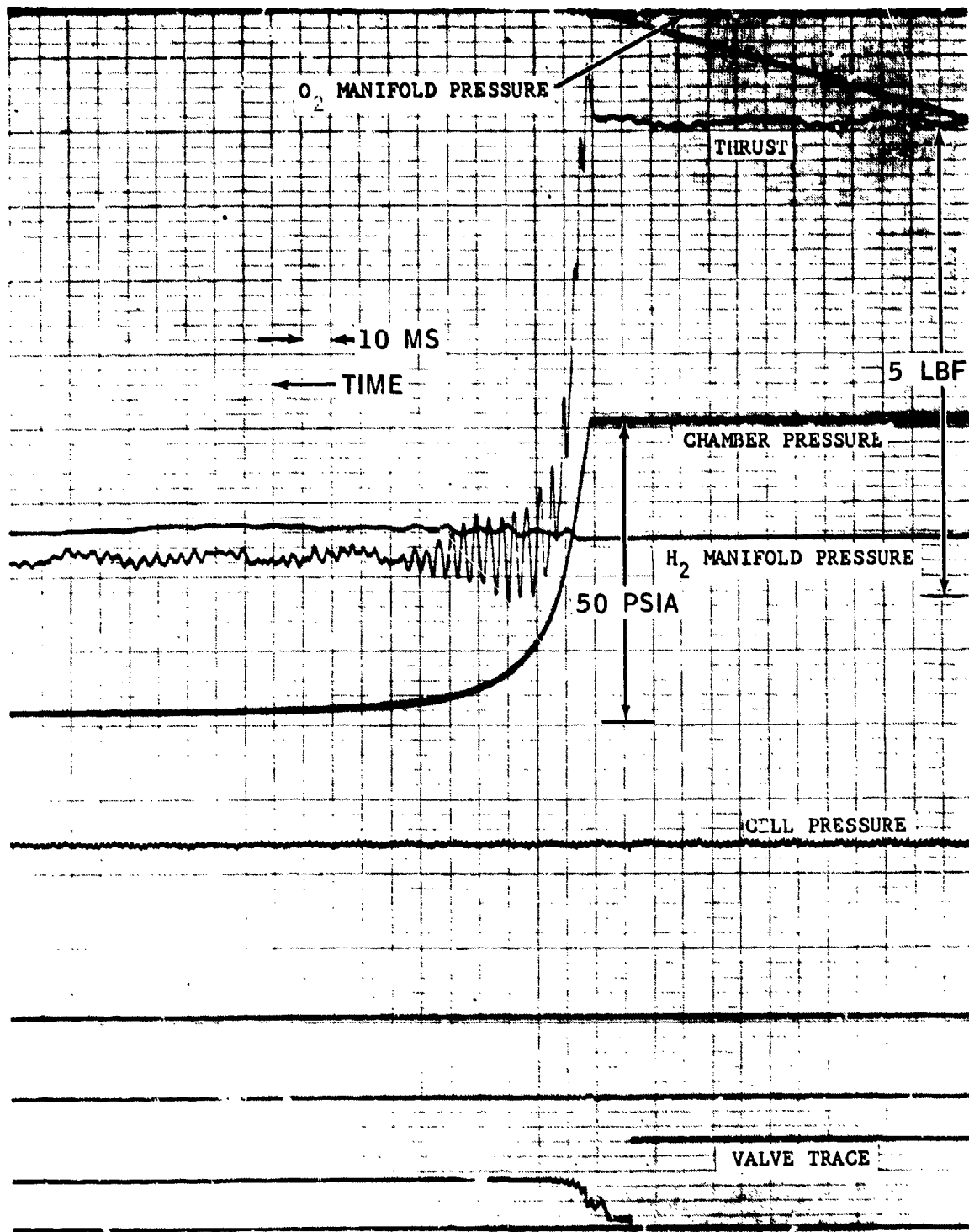


Figure 59. 5 Lbf. GO₂/GH₂ Rocket Engine Firing Record - End of Steady State Firing

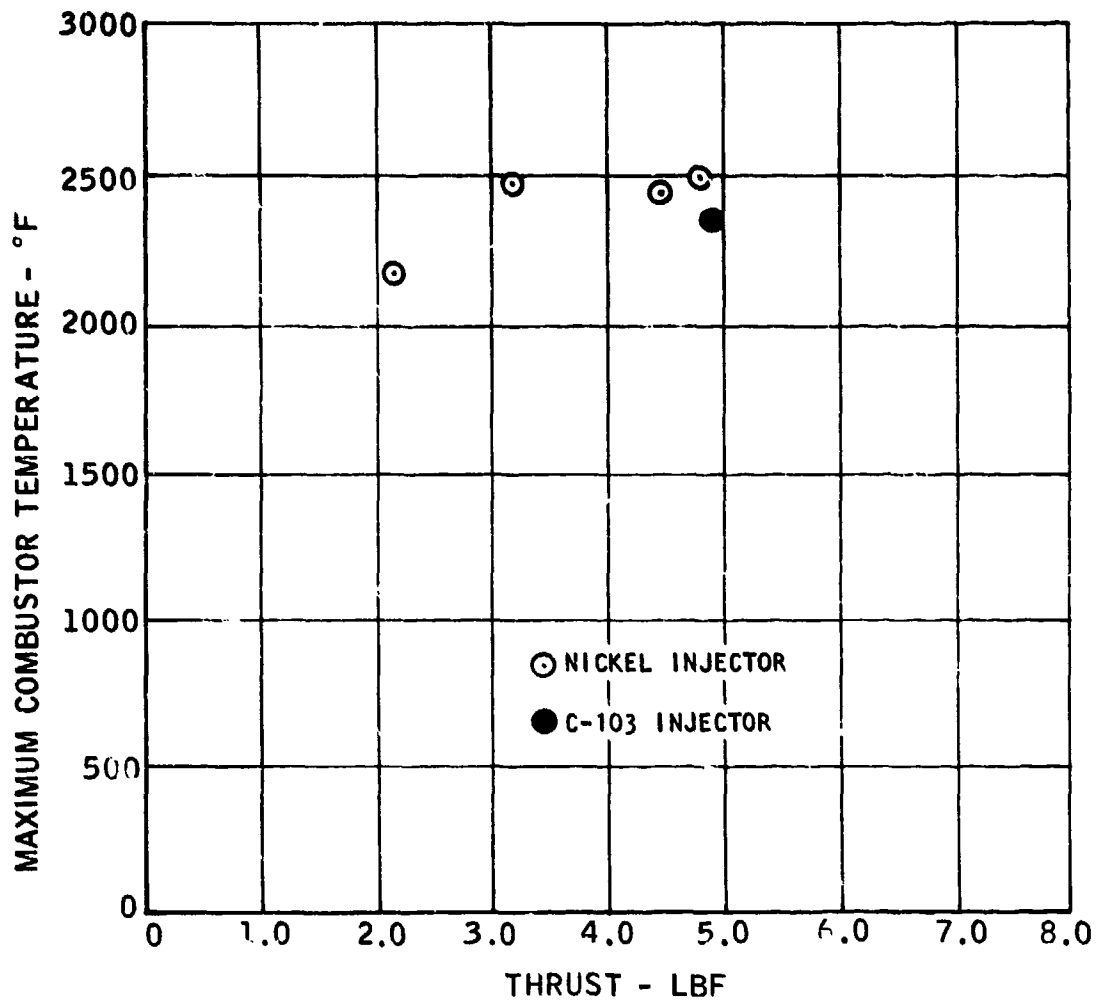


Figure 60. Maximum Combustor Temperature of 5 Lbf, Thruster

firings were made at 50 and 100 ms. with repetition rates of 1-5HZ. During this life test, all engine firings were successfully ignited and test to test repeatability at the start and end of the program was identical.

(d) Teardown and Inspection

Upon completion of the test, the thruster was visually and functionally checked for variations in characteristics. The bipropellant valve exhibited zero leakage in GN_2 at 0-250 psia with snoop, and the response is identical to that obtained at the start of the program.

Figure 61 shows the disassembled thruster at the end of the program, while Figures 62, 63, and 64 show the injector face, the spark plug, and the chamber, respectively. No cracks are visible on the face of the injector, and the combustion chamber shows only some heat stains. The white spots are columbium oxide which was the result of tests on Configuration 2. Figure 64 shows the tip of the spark plug after 150,000 cycles. The anode (inside portion of the plug) has miniscule globules of material deposited on it. The deposits are due to erosion of the cathode and redeposition on the anode. No degradation of spark efficiency was noted visually. The thruster ignition was also 100% reliable at the end of the 150,000 firings.

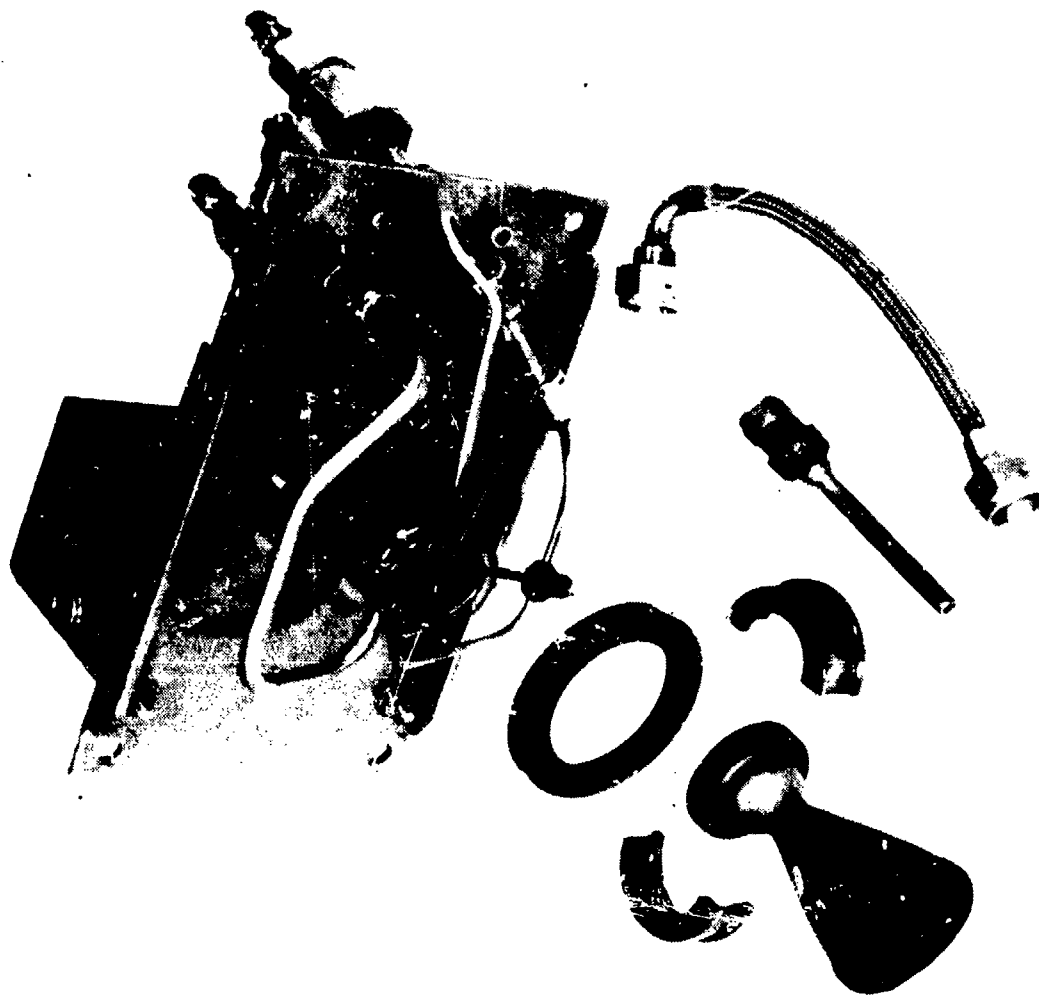


Figure 61. Disassembled 5 Lbf. Thruster, Configuration No. 3, After Test

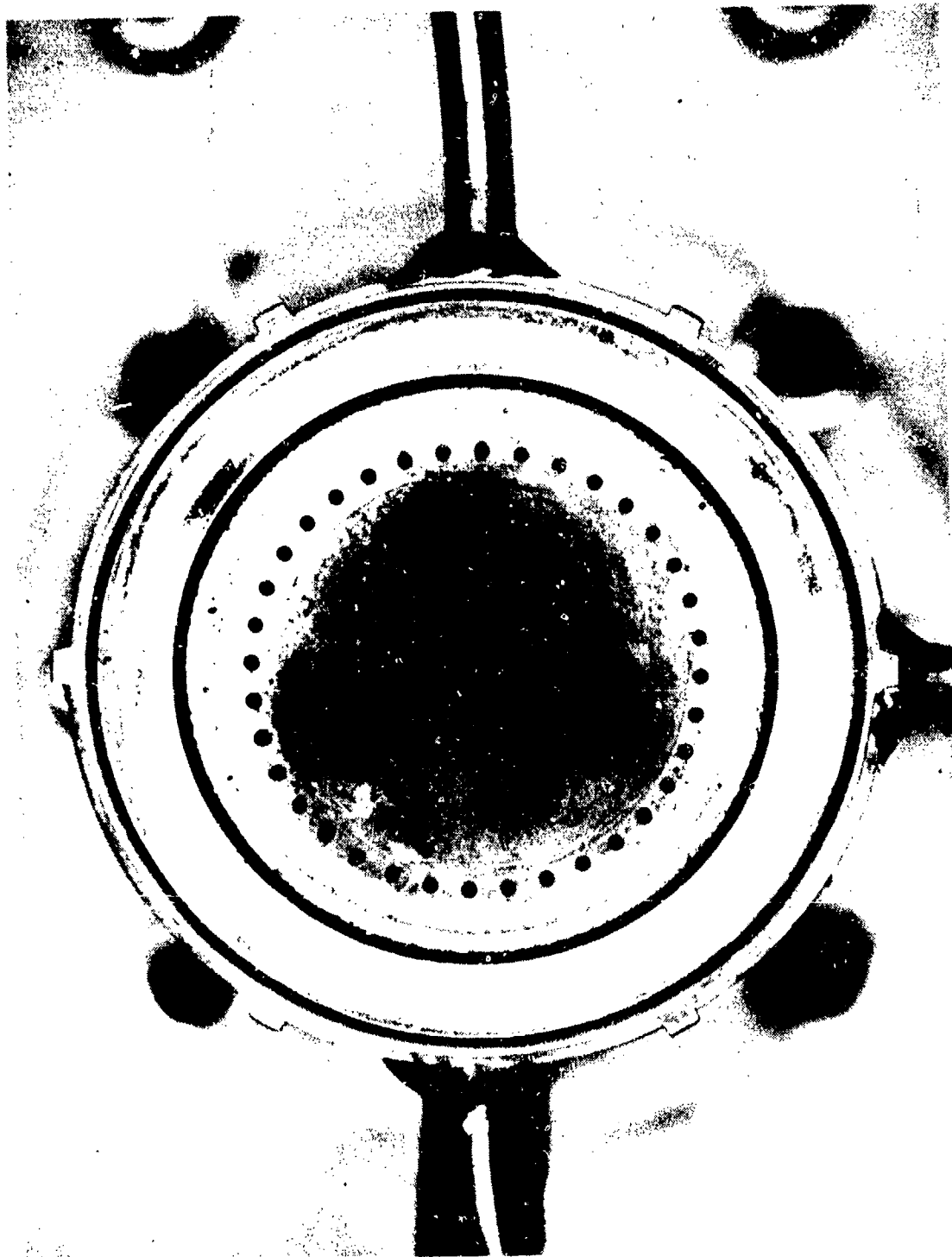


Figure 62. 5 Lbf. Injector Face, Configuration No. 3, After Test

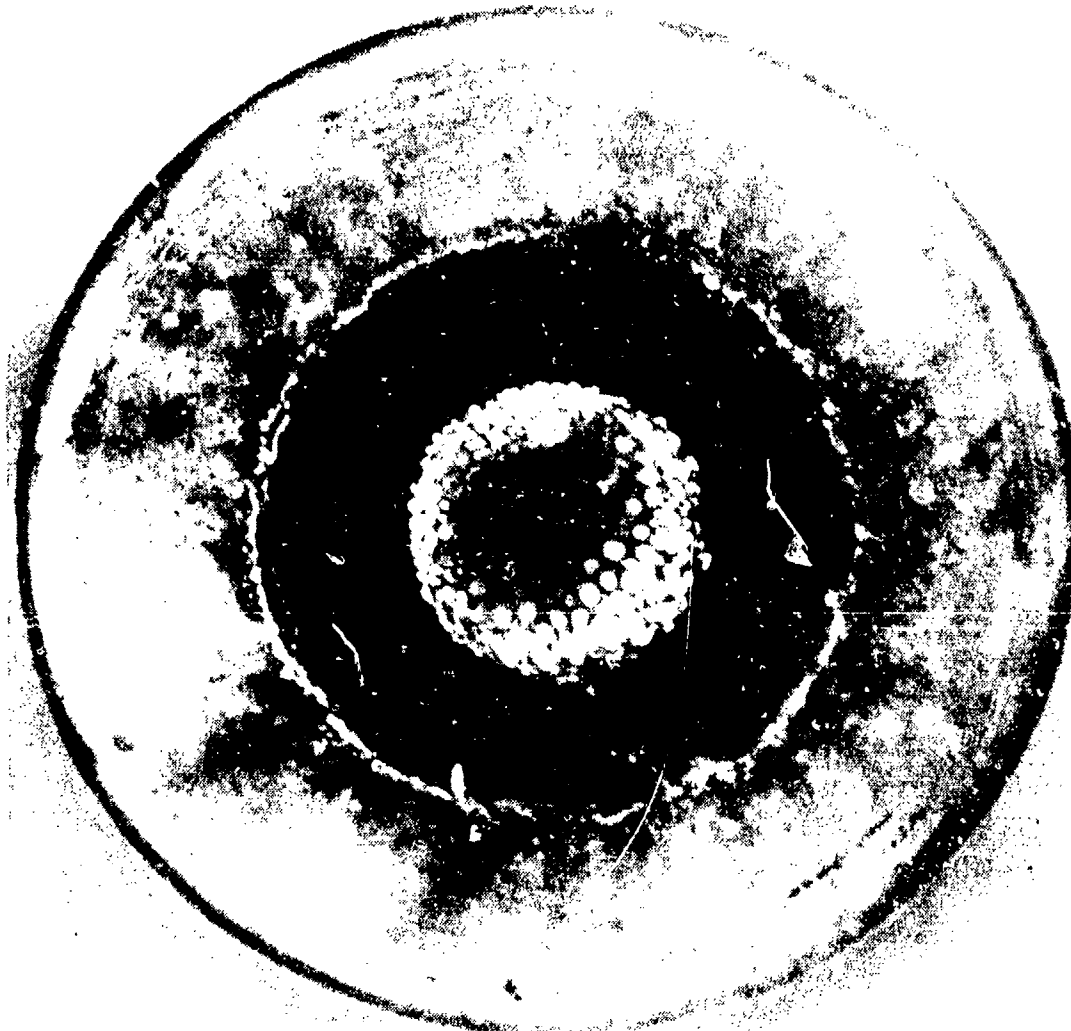


Figure 63. Spark Plug From 5 Lbf. Thruster, Configuration No. 3, After Test

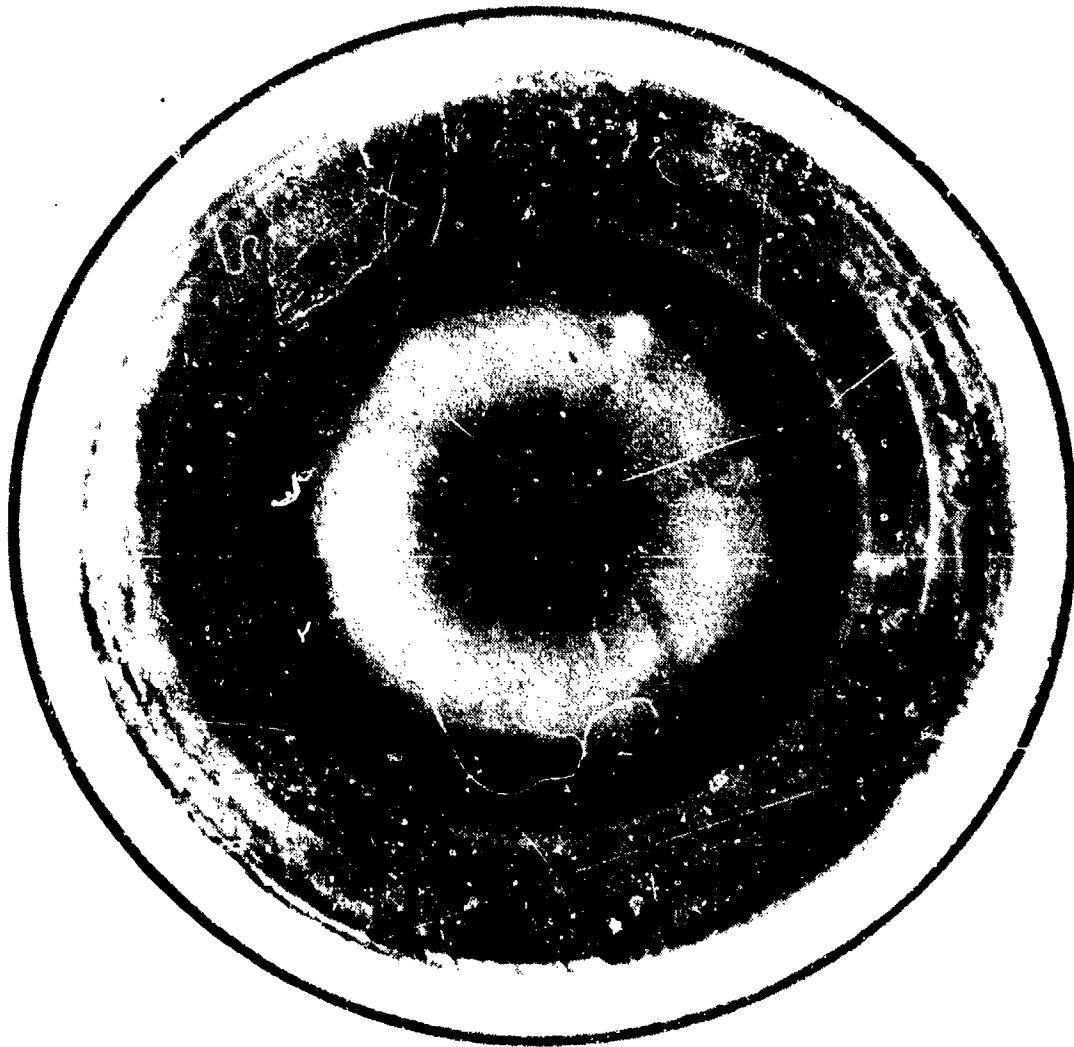


Figure 64. 5 Lbf, Combustor, Configuration No. 3, After Test

SECTION IV

ONE-TENTH POUND THRUST ROCKET ENGINE

A heavyweight 0.1 lbf engine had been developed on a previous contract (Reference 1). Design characteristics of the heavyweight engine were as follows:

Nominal Chamber Pressure	80 psia
Mixture Ratio	8
Chamber Cooling	Radiation
Chamber Material	Coated Molybdenum
Ignition Source	Spark Plug
Injector	Single Element
Flow Control	Sonic Orifices
Valves	Marquardt R-1E

Two different flightweight 0.1 pound thrust engines were built and tested on this program. One engine design had the spark plug located in the injector, while the second design had the spark plug located in a separate adapter. The latter design was similar in concept to the heavyweight engine developed on the previous contract which also had a separate spark plug holder between the injector and chamber. The principle difference between the two design approaches is that the injector with the integral spark plug receives convective heating from the combustion gas whereas the injector using the separate spark plug holder does not.

Both flightweight engine designs were based on the design limit temperatures developed on the previous contract, which are summarized in Table 11.

The injector injects hydrogen radially through a thin (0.002 inch) axisymmetric slot into the oxygen flowing through a 0.038 inch diameter passage. The gas mixture in the mixing section is greater than the flame speed of hydrogen/oxygen, so that combustion in the combustion chamber cannot propagate through the mixing section.

1. FLIGHTWEIGHT DESIGN NO. 1

The injector design used on Flightweight Design No. 1 is shown in Figure 65. The assembled engine is shown in Figure 66, which shows the large size of the Moog Valve and the spark plug relative to the rest of the engine.

The injector mixes propellants by injecting the hydrogen radially inward into the oxygen stream. The mixed gases then pass through a 0.030 inch diameter mixing section (shown in Figure 65). A Champion FHE 231 spark plug in the injector is

**TABLE 11. DESIGN CHARACTERISTICS
FLIGHTWEIGHT 0.1 POUND THRUST ENGINE**

Chamber Pressure (Maximum)	75 psia @ 0.1 Lb. Thrust
Chamber Pressure (Minimum)	25 psia @ 0.03 Lb. Thrust
Contraction Area Ratio	8:1
Expansion Area Ratio	100:1
L*	9 Inches
L/D Premix	8
Cooling	Radiation/Regenerative
Injector	Single Element Coaxial Premix
Valves	Moog Bipropellant
Spark Plug	Champion FHE 231A (Modified)
Injector	Radial Hydrogen Injection Into Oxygen Stream

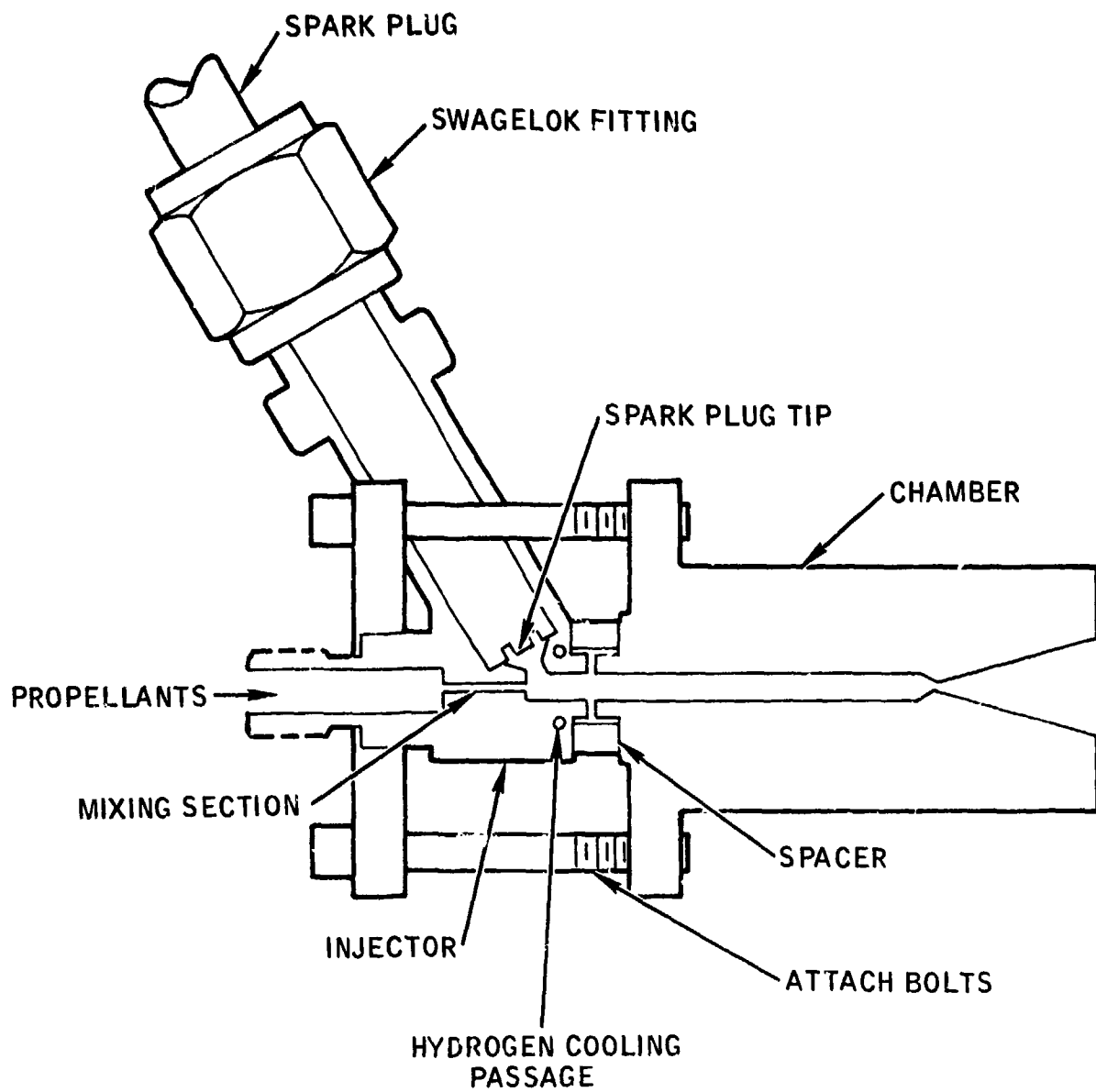


Figure 65. Flightweight 0.1 Lbf. Engine No. 1 Design

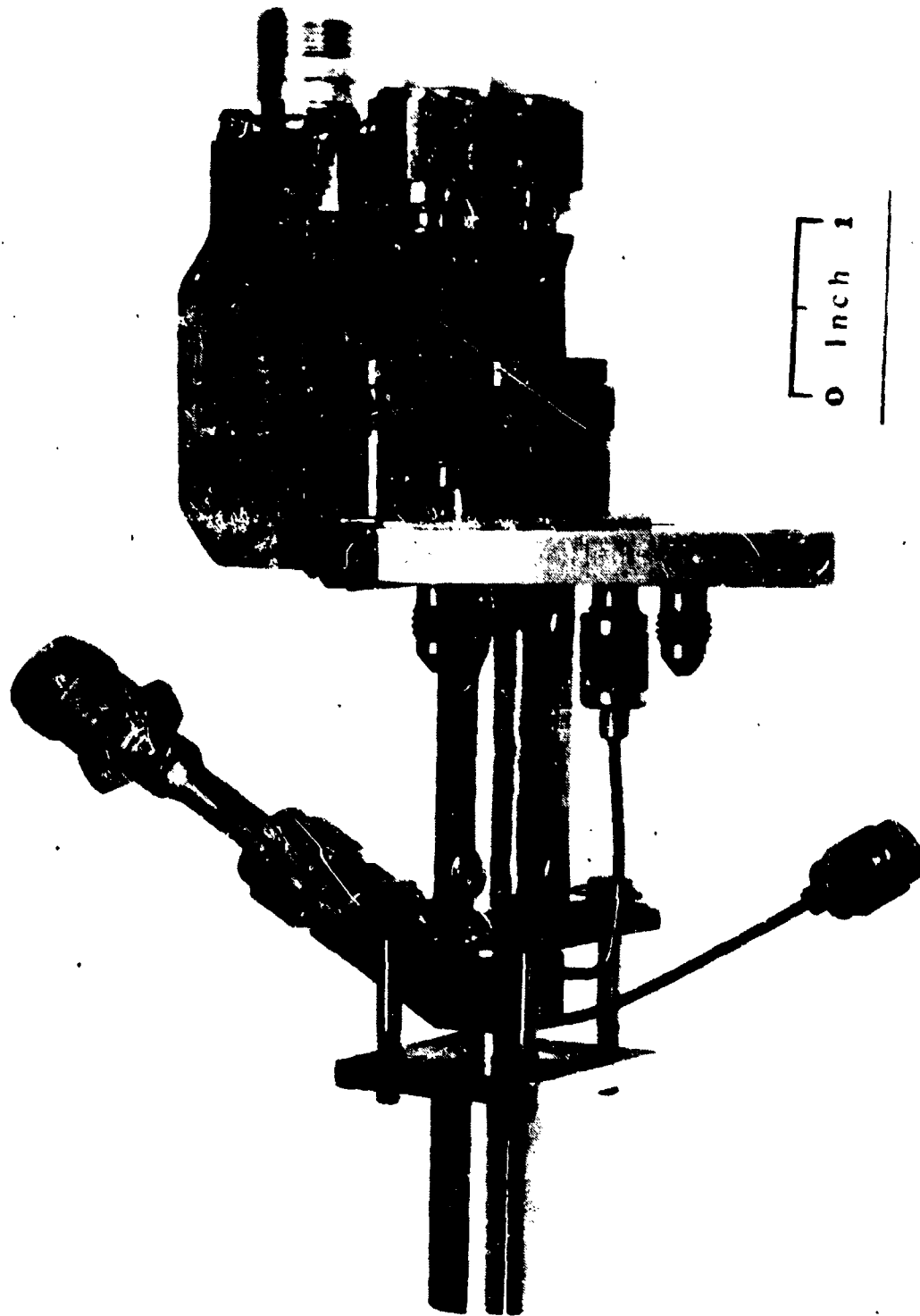


Figure 66. Assembled 0.1 Lbf. Flightweight Engine No. 1

exposed to the combustion chamber through a 0.060 inch diameter access port in the upstream corner of the injector. The hydrogen passes through a cooling passage in the injector before mixing with the oxygen. The combustion chamber and injector are not in direct contact but are separated by a spacer. The amount of heat conducted from the chamber to the injector can be reduced by using a spacer with a high thermal resistance. However, this raises the possibility of overheating the spacer where it contacts the chamber, since that point would be much hotter than the injector as the spacer has a high thermal resistance. Locating the spark plug in the injector necessitates exposure of some portion of the injector head to convective heating from the combustion gas because of the relative sizes of the spark plug and the combustion chamber diameter.

a. Temperature Limits

Heat transfer analysis of the Flightweight Engine No. 1 was made to develop a design that would meet the following approximate temperature limits:

Combustion Chamber	2300 ^o F
Injector	1600 ^o F
Mixing Section	1300 ^o F
Valve	250 ^o F

The temperature limit of the coated chamber (molybdenum or Columbium) was not critical because of the temperature capability of the chamber itself, but because of the effect of chamber temperature on the tensile and creep strengths of the attach bolts and spacer which contact the chamber.

The 1300^oF temperature limit upstream of the 0.030 diameter mixing section was set to avoid autoignition in the small volume where the hydrogen and oxygen meet. Tests on the previous contract had shown that the propellants would autoignite in the combustion chamber whenever the combustion chamber was 1300^oF or higher. It is not known whether or not the propellants could autoignite in the mixing section or in the very small manifold volume upstream of the mixing section if that portion of the injector reached 1300^oF. However, it was thought advisable to try to keep the mixing section below 1300^oF to avoid the possibility of autoignition, which would cause an unacceptable pressure drop through the mixing section.

The 1600^oF temperature limit of the injector mass surrounding the tip of the spark plug is based on the fact that 1600^oF is the softening point of a pressure seal in the spark plug. There would be a temperature drop from the spark plug tip to the seal, but the magnitude was unknown.

b. Heat Transfer Analysis

Heat transfer analysis of the Flightweight Engine No. 1 was made to predict the effect of the following design variables: (1) Radiation area and emissivity of injector, (2) Thermal resistance of spacer, and (3) Radiation area and emissivity of combustor.

(1) Effective Radiation Area of Injector

The relationship between engine temperature and the effective radiation area (radiating area x emissivity) of the injector is shown in Figure 67.

The predicted temperatures for the basic design were 1500°F for the injector and 2150°F for the combustor, using an injector with a radiating area of 1 in.² and an emissivity of 0.45, or an effective radiation area of 0.45 in.². In order to reduce the injector below the autoignition temperature of 1300°F, the effective area would have to be increased by a factor of 10. This could be achieved by using a radiation fin on the injector or simply by increasing the outside diameter of the injector. Either approach would entail added weight.

(2) Thermal Resistance of Spacer

The relationship between engine temperatures and the thermal resistance of the spacer between the combustor and injector is shown in Figure 68. The injector temperature can easily be reduced by increasing the thermal resistance of the spacer. However, this raises the problem of creep strength if a metallic spacer is used, or the problem of material brittleness if a ceramic spacer is used.

(3) Effective Radiation Area of Combustor

The relationship between engine temperatures and the effective radiation area of the combustor is shown in Figure 69. An increase in the effective radiation area of the combustor by a factor of about three would be required to reduce the injector temperature below 1300°F. This would entail an appreciable weight penalty.

c. Test Firings

The Flightweight Engine No. 1 (Figure 65) was test fired using an uncooled nickel 200 combustor. Testing was performed during April and May 1973.

FLIGHTWEIGHT 0.1 LB ENGINE NO. 1

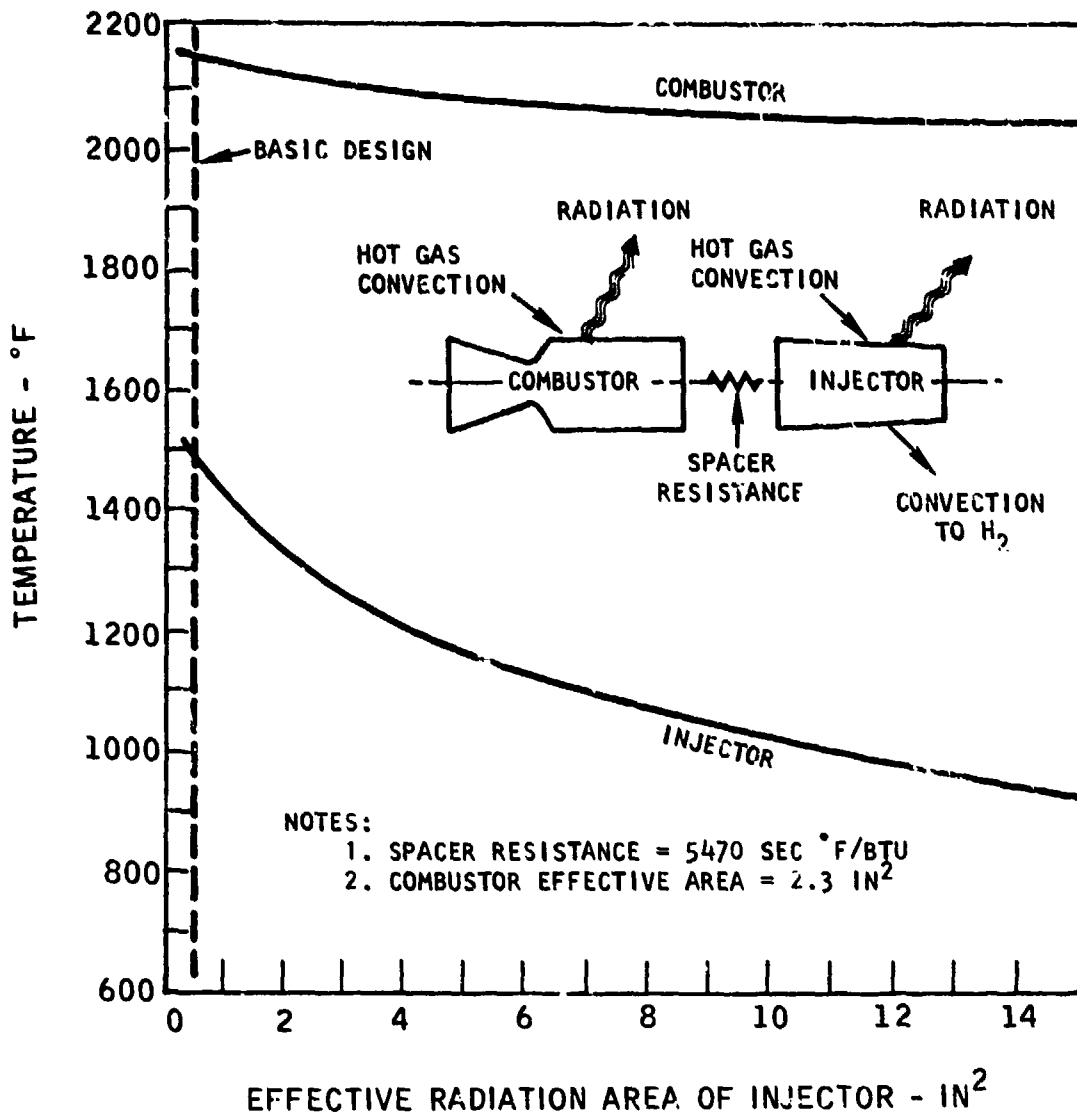


Figure 67. 0.1 Lbl. Engine Temperatures Vs. Injector Effective Radiation Area

FLIGHTWEIGHT 0.1 LB. ENGINE NO 1

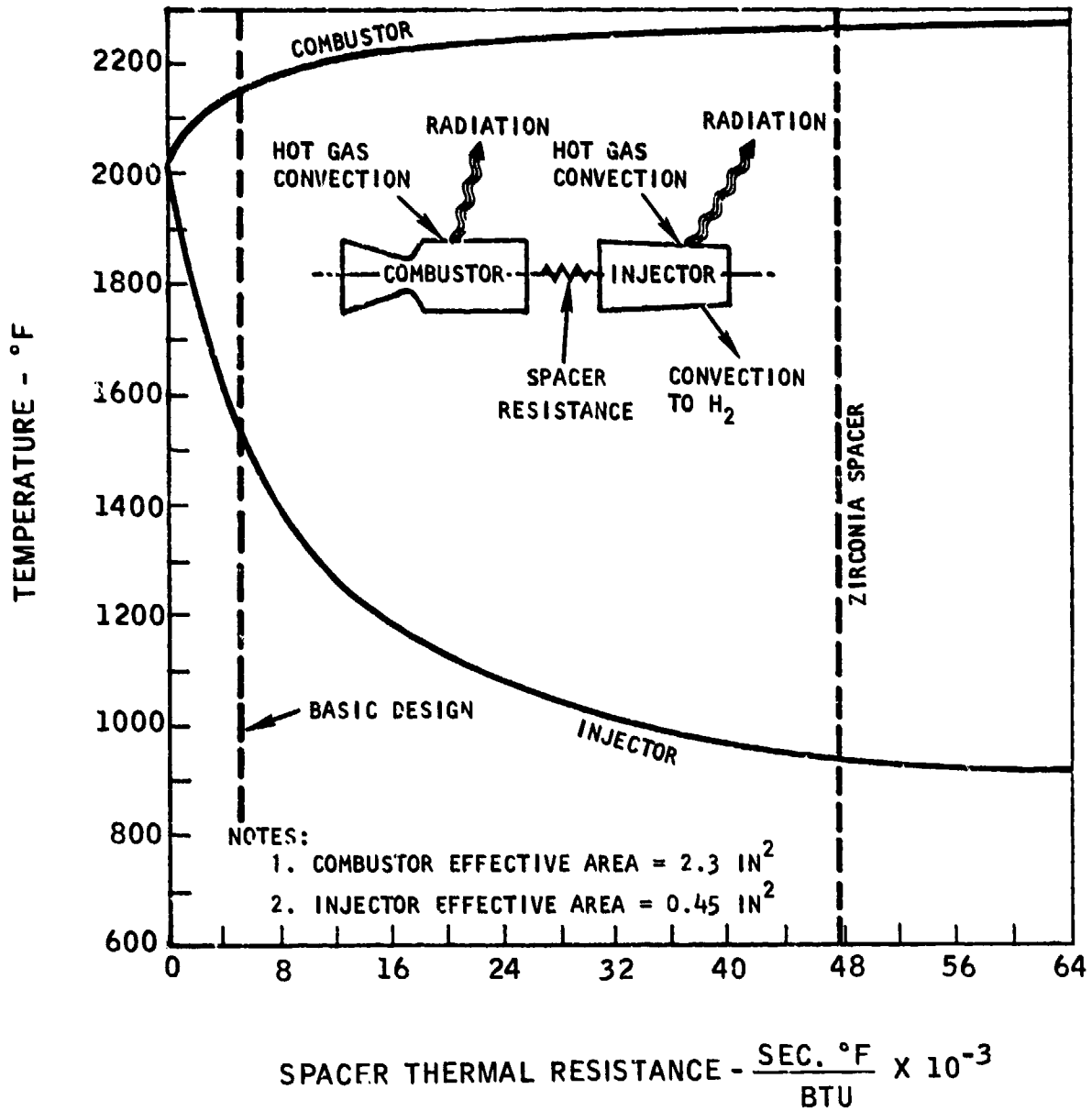


Figure 68. 0.1 Lbf. Engine Temperatures Vs. Spacer Thermal Resistance

FLIGHT WEIGHT 0.1 LB. ENGINE NO. 1

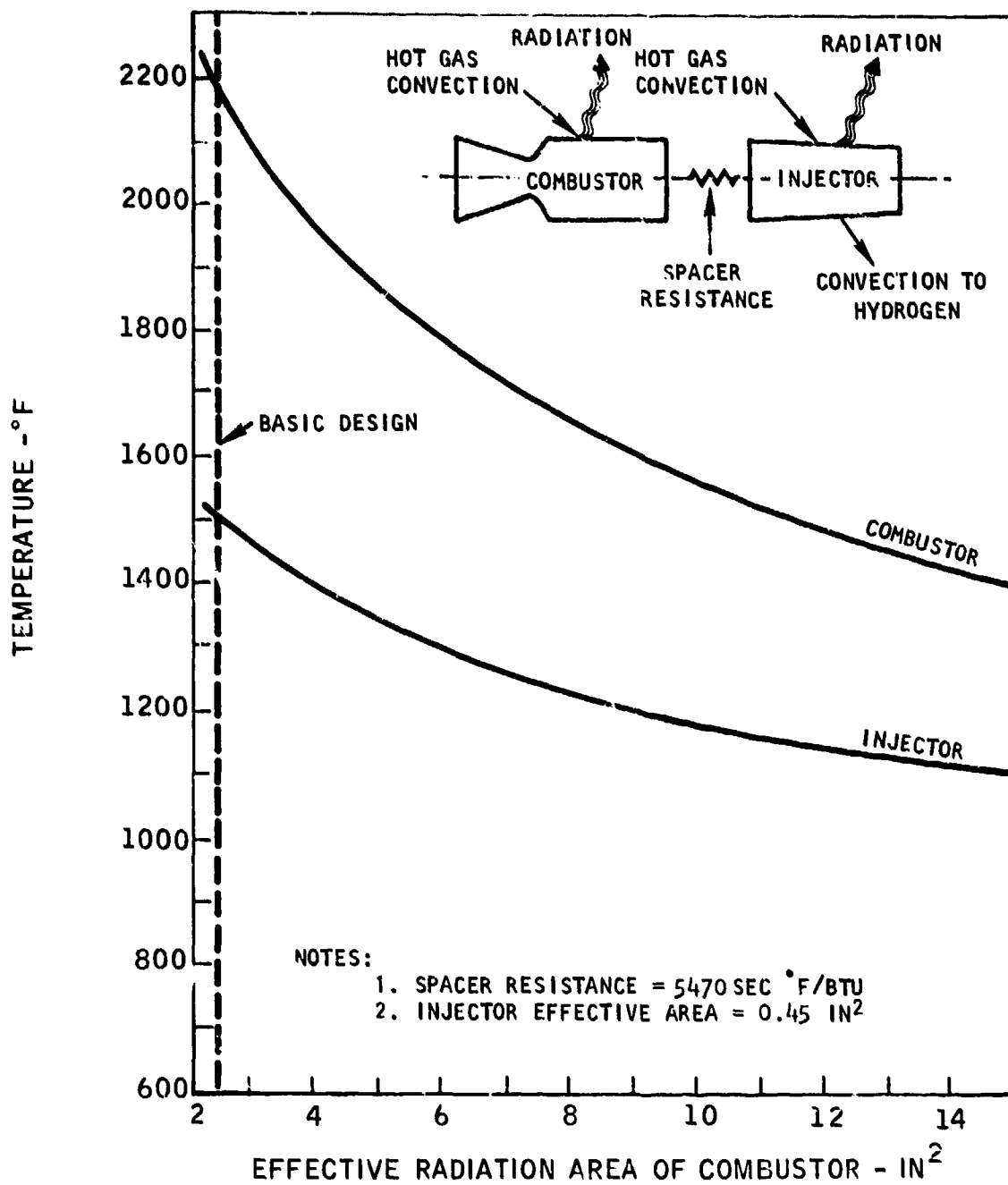


Figure 69. 0.1 Lbf, Engine Temperatures Vs. Combustor Effective Radiation Area

Runs 1-8

The flightweight engine was initially tested with nominal high supply pressures near 200 psia. The GLA spark igniter was used with a spark duration of 10 ms. The first tests with spark delays of 10 ms and 20 ms did not achieve ignition. Subsequent tests with a spark delay of 50 ms showed sporadic ignition. On Run 8, only 5 of 20 pulses ignited. It was observed on these tests that chamber pressure was going above the linear range, and the P_c transducer was found to be inoperative after Run 8. After Run 8, the combustor throat diameter was measured and found to be only 0.026 inch instead of the required 0.0294 inch, which explained the excessive chamber pressure which had probably also been peaking high because of the ignition delay.

Runs 9-31

The throat diameter of the nickel chamber was enlarged to 0.0294 inch before Run 9. The pressure transducer from P_{om} , oxygen manifold, was moved to measure P_c and the P_{om} port was capped. The Bel Air igniter was installed in place of the GLA igniter. It had been observed during Runs 1-8 that the chamber pressure trace was greatly perturbed at the time of sparking, and since the GLA igniter dissipates 10 times more energy at the tip of the spark plug than the Bel Air igniter, the possibility of flame suppression by the GLA spark, which completely filled the combustion chamber, was being considered.

Good ignition was obtained at high supply pressure settings (188 psig), but ignition could not be achieved at low supply pressures from 50 psig to 90 psig. At supply pressure of 100 psig and 150 psig, 100 percent ignition was obtained with 50 pulses. These results seemed to indicate that the Bel Air igniter was giving much better ignition than the GLA igniter since the spark duration to get ignition on these tests was only 10 ms. However, several other changes had also been made after Run 8, i. e., capping P_{om} and opening the throat diameter. Therefore, more tests were required to compare the two igniters.

Runs 32-56

The GLA igniter was reinstalled after Run 31. Good ignition was obtained at 189 psig down to 100 psig supply pressure. However, erratic ignition was obtained at 90 psig and lower, although ignition was obtained on all 50 pulses at 80 psig supply pressure, using a spark delay of 5 ms and a duration of 10 ms.

Runs 57-64

The GLA igniter was also used for the next series of tests with a spark delay of 5 ms and a sparking duration of 10 ms. At supply pressures of 199 psig for O_2 and 189 psig for H_2 , all pulses of a 59 pulse train ignited, although the rise in chamber pressure was slow on 3 pulses.

Ignition on all 100 pulses was achieved at low supply pressures of 52 psig for O₂ and 50 psig for H₂. Single performance runs were made at supply pressures near 100 psig and 150 psig, and a sparking duration of 10 ms. Performance was 80 to 85 percent of shifting C*.

Runs 65-91

Additional documentation of ignition characteristics during these runs showed unreliable ignition with supply pressures below 100 psig. Two long firings were made to get injector temperature data. On Run 75, a 47 second firing was made, during which time the injector rose to 1020°F and was still rising at shutdown. The Bristol Recorder was respaced and a 50 second run was made on Run 76, during which the injector temperature reached 1400°F and was still rising at the end of the run.

Runs 92-106

The hydrogen manifold pressure pickup was capped for the next series of tests. It was found that ignition reliability was worse than when the hydrogen manifold pressure was being recorded. This indicated that the transient mixture ratio is important in determining ignition. A large increase in manifold volume results when the pressure transducers are connected. Apparently an oxygen rich condition is conducive to ignition, based on the test results.

Runs 107-118

An engine configuration made of the lightweight injector with a spark plug holder and nickel nozzle from the prototype engine was assembled. This configuration allowed a comparison of the ignition characteristics with either a rear mounted spark plug or a side mounted spark plug.

Runs 107 and 118 were made with the side spark plug and both P_{om} and P_{hm} capped. Ignition was poor at 100 psig supply pressures and below. For example, at 100 psig, ignition was not obtained at spark durations up to 40 ms.

Runs 119-129

The P_{hm} port was connected to a transducer for this series of runs with the side spark plug. This would result in a higher initial mixture ratio. Good ignition was obtained at supply pressures down to 100 psig. However, ignition was erratic at 70 psig supply pressure.

Runs 130-148

The rear spark plug was used for these tests, keeping P_{hm} connected to get a comparison in ignition characteristics between the side and rear locations.

The results were about the same as with the side plug, with 10 out of 10 ignitions at supply pressures of 100 and 200 psig, and erratic ignition at 70 and 80 psig.

d. Discussion

The ignition tests indicated that ignition probability is about the same with either the rear or side spark plug locations. The tests also showed that the greater energy release at the spark tip provided by the GLA igniter had not significantly improved ignition probability at supply pressures below 100 psia, compared to results with the Bel Air igniter on last year's prototype engine. The solution proposed last year was to raise the nominal chamber pressure from 50 psia to 80 psia and limit the 0.10 pound engine to a 2:1 blowdown instead of a 3:1 blowdown. This would provide a minimum supply pressure of about 100 psia instead of 67 psia, so that the 0.10 pound engine should always ignite reliably. The convection heating to the injector occurs in the initial .190 inch length of the combustion chamber, and it was uncertain whether the full combustion temperature and heat flux would actually occur so close to the injector. However, the high injector temperatures on Runs 75 and 76 were in approximate agreement with the analysis. Review of the analysis revealed that the conduction resistance of the spacer between the injector and combustor had been calculated incorrectly, since the final design had a larger contact area than originally assumed in the analyses. The corrected analysis predicted an injector temperature of 1650°F instead of 1500°F.

The engine was not run long enough to reach steady state temperatures because of the hot injector, but the rate of injector heating indicated that the injector could reach 1800°F or higher, definitely above the injector limit temperature. Therefore, two steps were taken: (1) a copper radiation fin was installed on the injector of Flightweight Engine No. 1, and (2) a new engine (Flightweight Engine No. 2) was designed, fabricated, and tested.

e. Copper Radiation Fin

A six inch diameter, 0.10 inch thick copper radiation fin was brazed to the Flightweight Injector No. 1. The engine assembly with the radiation fin is shown in Figure 70. The side of the fin facing toward the engine exit was grit-blasted and coated with black matt chrome to produce a high emissivity coating. The other side of the fin facing the valve was smooth and polished to produce a very low emissivity coating to eliminate thermal radiation back toward the valve or mounting plate. Tests of the black matt chrome coating on copper and nickel had shown that the coating is stable in a vacuum at 1500°F, but is not stable at 1975°F. Other tests in air at 1200°F had shown that the coating was stable on nickel 200 but was not stable on copper. A copper fin would be much lighter than a nickel fin for the same radiation

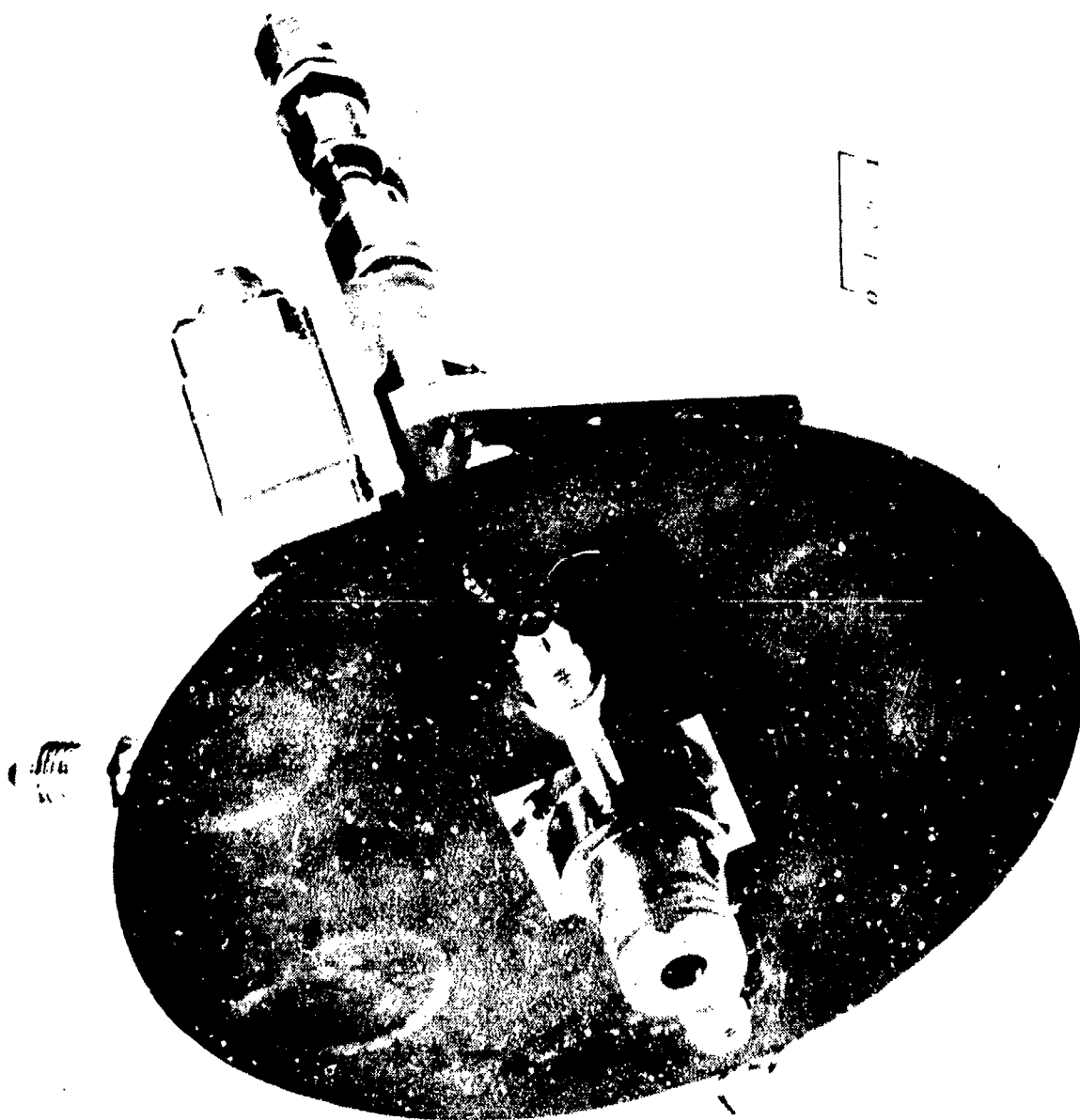


Figure 70. Flightweight 0.1 Lbf. Engine No. 1 With Radiation Fin

effectiveness because of the higher thermal conductivity of copper. Therefore, a copper fin was used because it would be usable for operation in space vacuum and would probably also be usable in the altitude test cell.

Flightweight Engine No. 1 with the copper fin on the injector was tested with a water-cooled combustor, using three thermal resistance spacers between the combustor and the injector. The water cooled combustor was made by adding a cooling passage to the thick-walled uncooled nickel combustor used in the preceding tests.

Run 159

A Rene' 41 spacer was used during a 175 second run during which the injector rose to 840°F. However, it was clear that a spacer with higher thermal resistance than Rene' 41 was required.

Run 164

A pyrolytic graphite spacer was used during a 110 second run during which the injector rose to 640°F. However, a leak developed between the combustor and the pyrolytic graphite washer, terminating the run prematurely.

Run 167

A thin L-605 spacer with a thermal resistance of 52,000 second °F/BTU was used during Run 167 with a firing duration of 15 minutes. This high thermal resistance reduced conduction between the injector and the combustor to a negligible amount.

The engine temperatures, essentially stabilized at the end of the run, were as follows:

Injector	1100° F
Spark Plug	460° F
Valve	130° F
Copper Fin, inside diameter	810° F
Copper Fin, outside diameter	790° F
Water-Cooled Chamber	340° F

The engine was thermally isolated from the thrust stand so that the above temperatures are a good indication of steady state temperatures. The area of the copper fin could be reduced by a factor of 2, based on the above data, and keep the injector below 1300°F. Therefore, a fin with a diameter of 1/2 inches, weighing 0.4 pounds, would be adequate to meet all temperature limits of the Flightweight Engine No. 1.

2. FLIGHTWEIGHT DESIGN NO. 2

a. Engine Description

The design of Flightweight Engine No. 2, shown in Figure 71, was a flight-weight version of the prototype engine developed on the previous contract. The spark plug was inserted into a spark plug holder located between the injector and the combustion chamber. The injector was not exposed to direct convective heating by the combustion gas, and the area on the spark plug holder exposed to combustion gas heating was reduced as much as possible. The access port to the spark plug tip, formerly a 0.060 inch diameter hole, was changed to a rectangular 0.018 x 0.036 inch hole so that the axial length of the spark plug holder exposed to the combustion gas heating could be reduced to 0.075 inch compared to the 0.190 inch length of injector exposed on Flightweight Engine No. 1.

Hydrogen flows through a cooling passage within the spark plug holder and then through a mixer section. The hydrogen and oxygen are mixed in the same way as in the prototype engine and the Flightweight Engine Design No. 1. The 0.002 inch deep radial injection slot for hydrogen injection into the oxygen stream is in the front tip of the injector which bears on the mixer. The mixer was initially used as a separate component to allow removal for possible design changes. The mixer section was lapped to seal with the spark plug holder and the injector. However, the lapped seal to the spark plug holder was on a 45-degree cone and was not leak tight. Poxalloy sealant was used to seal the mixer joint for initial tests. The mixer section was subsequently welded into the spark plug holder after Run 200. The engine components are shown in Figure 72 and the assembled engine is shown in Figure 73.

A lapped circular L-605 insert welded into the spark plug holder was used to form a seal against the lapped face of the combustion chamber. The L-605 insert was used to give higher creep strength at high temperature, while the remainder of the spark plug holder was made of nickel 200 for good thermal conductivity. A low volume holder for the chamber pressure transducer was attached to the spark plug holder.

Two combustion chambers were made, one using C-103 columbium alloy with a R512E silicide coating, and the other using unalloyed molybdenum with a Durak B silicide coating. Initial life testing was performed with the molybdenum chamber, which originally provided a better sealing surface when lapped than the columbium. The columbium silicide coating exhibited a more granular structure, which appeared to provide very small leak paths over the short distance (about 0.030 inch) across the sealing surface against the L-605 insert. The final life testing was performed with the columbium chamber and was very successful after the columbium chamber was carefully lapped.

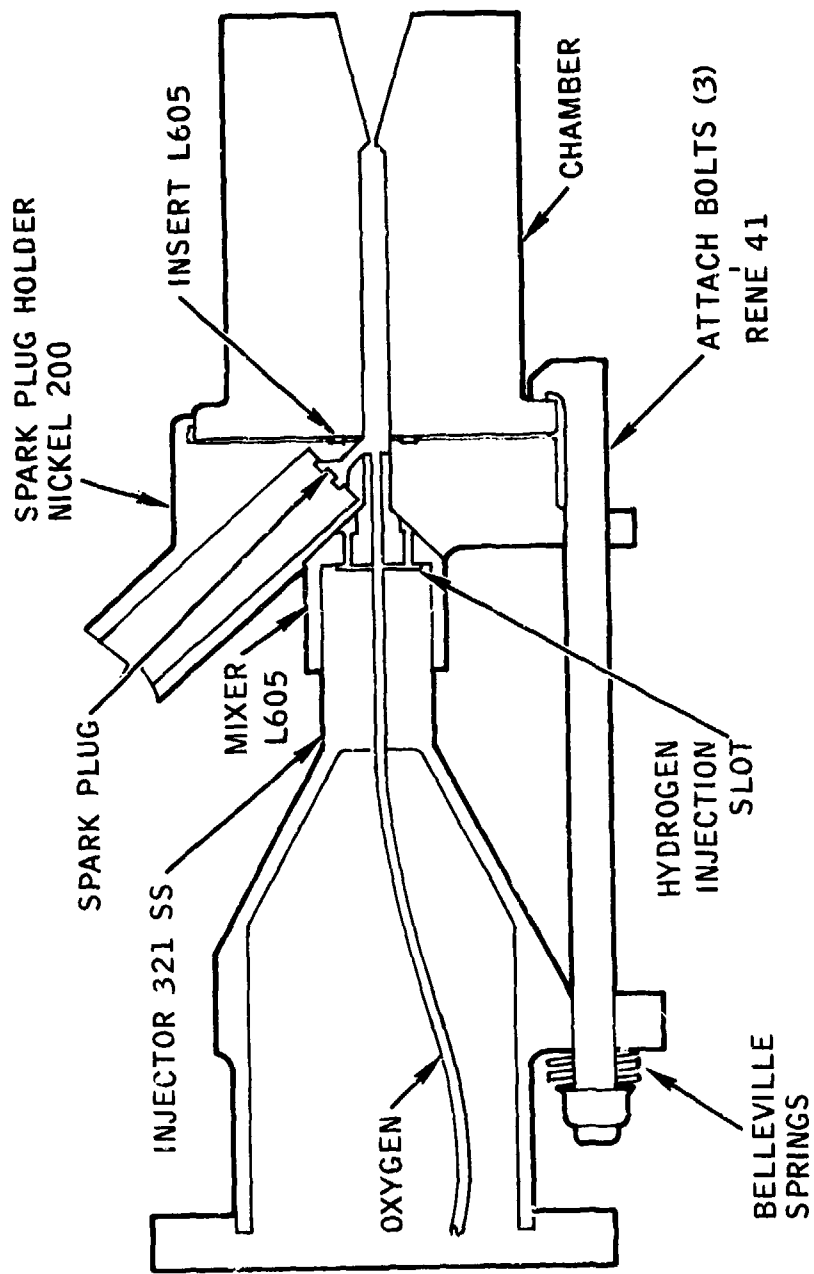


Figure 71. Flightweight 0.1 Lbf. Engine No. 2 Design

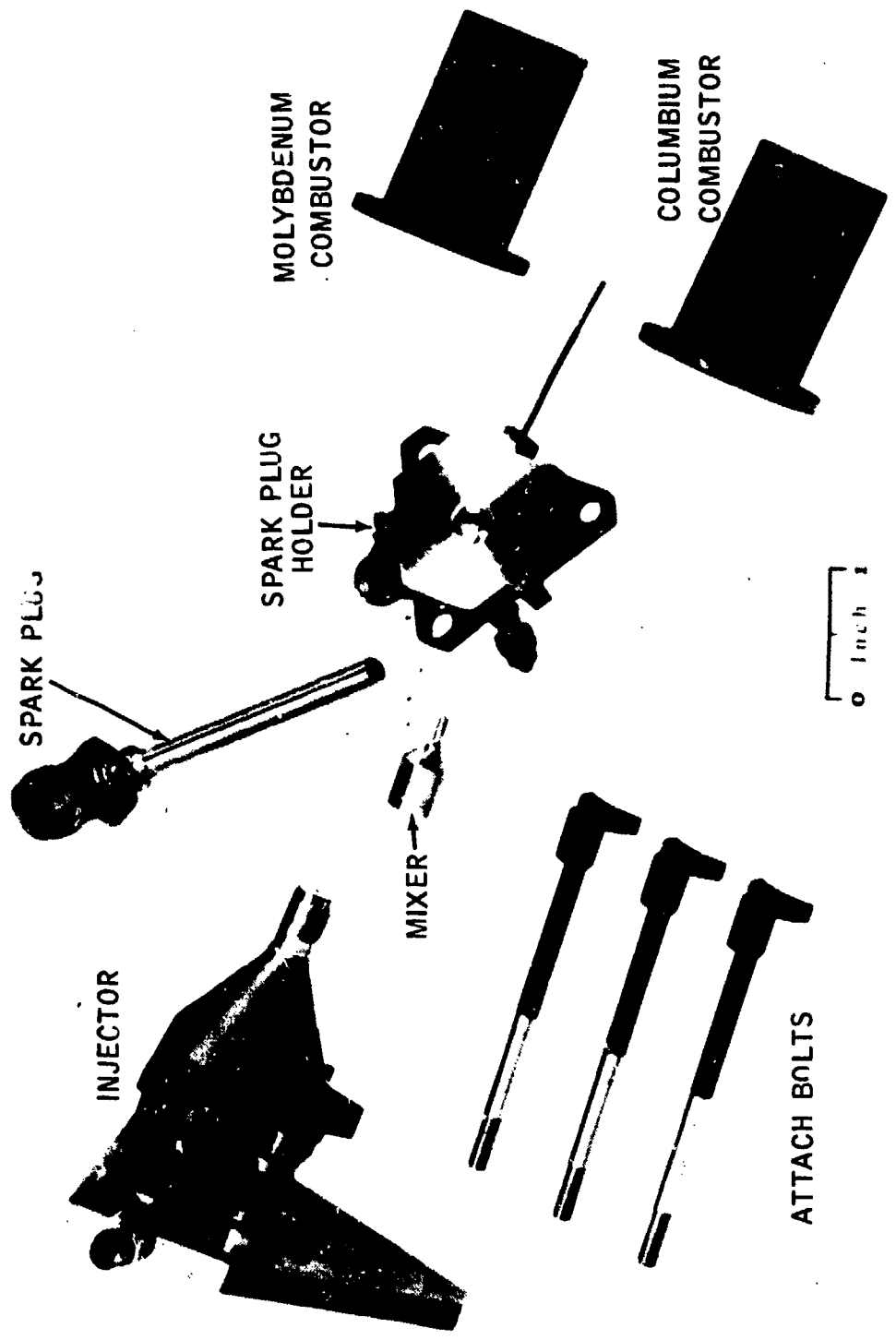


Figure 72. Components of Flightweight 0.1 Lbf. Engine No. 2

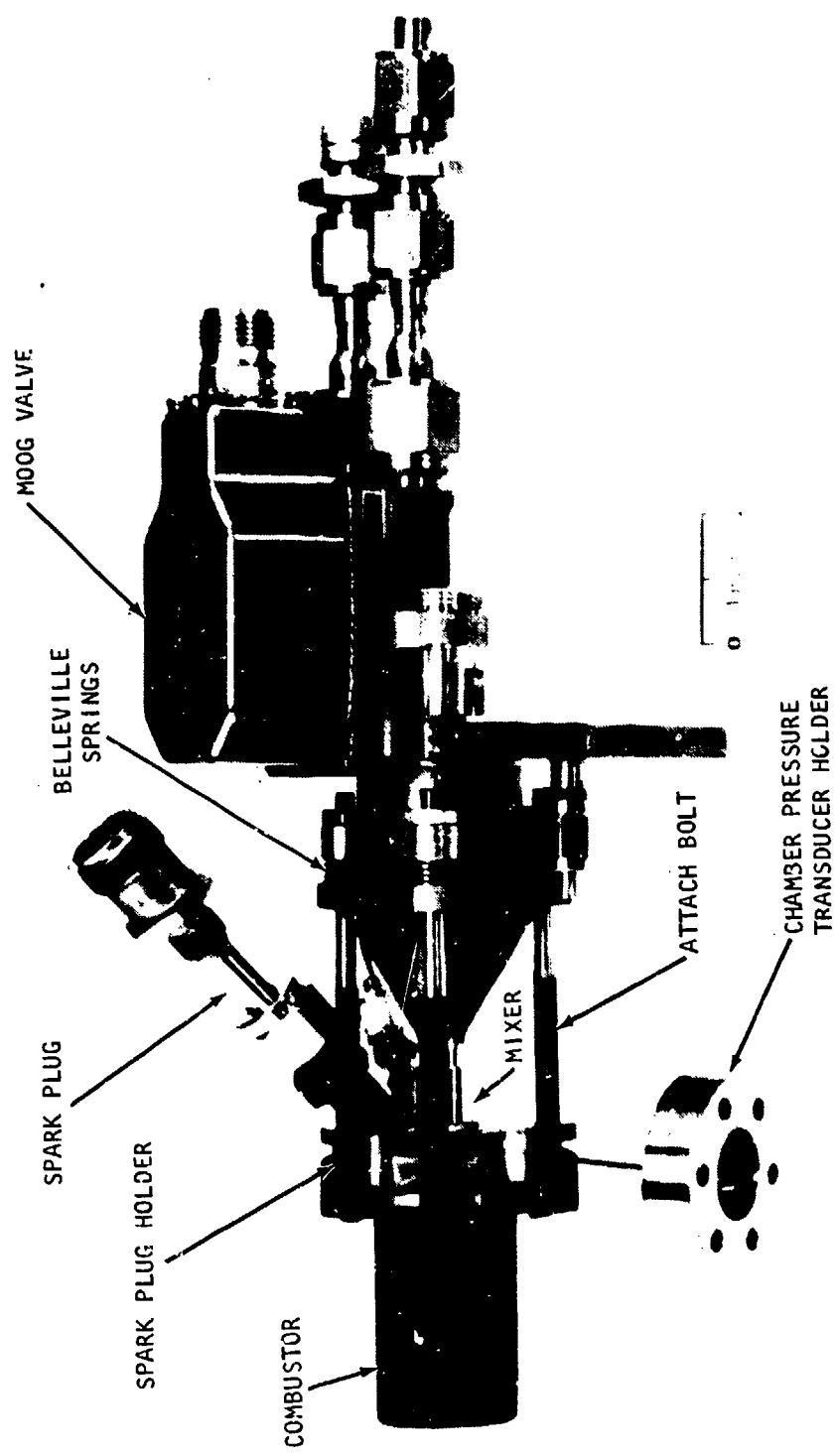


Figure 73. Flightweight 0.1 Lbf. Engine No. 2 Assembly

Three Rene' 41 attach bolts were designed to grip the chamber flange. The bolts were held in controlled tension by Belleville springs to accommodate differential thermal expansion of the bolt and the engine components.

The Champion FHE 231A spark plug used on the previous contract was used on the flightweight engine. Although this spark plug is much longer than required, the critical design parameter for installation in the 0.10 pound engine is the diameter, which could not be decreased significantly by any redesign. The Moog valve, P/N 8477-470650-11, was used because of availability and mature development status, although its 0.84 pound weight is not flightweight for this engine.

The temperature limits for Flightweight Engine No. 2 at the locations shown in Figure 74 are as follows:

Combustion Chamber	2300 ^o F
Spark Plug Holder	1600 ^o F
Mixer	1300 ^o F
Bolt Head	1650 ^o F
Injector (Belleville Springs)	400 ^o F
Valve	250 ^o F

The reasons for selection of temperature limits on the combustion chamber, spark plug holder (i. e. , injector on Flightweight Engine No. 2) and mixer (i. e. , mixing section) were the same as for Flightweight Engine No. 1. The bolt head limit temperature of 1650^oF was set to avoid excessive creep of the bolt head under bending. The temperature of the injector flange supporting the Belleville springs should not exceed 400^oF because of long duration temperature limits of the Belleville springs.

The preload on the three bolts was set by using a gage block to measure the correct stack height of the Belleville springs. The preload was calculated to maintain a seal between the chamber and spark plug holder under a random vibration specification which produced a transverse acceleration of 140 g's. Each bolt head had two raised land areas of 0.0025 in², each bearing on the chamber flange. This small contact area controlled the amount of heat transfer from the chamber to the bolt so that the bolt head could be kept below 1650^oF.

Heat transfer analyses were made to select critical design dimensions so that all temperature limits would be satisfied. The most critical component was the spark plug holder, with the same heating problems, convection from the combustion gas and conduction from the combustion chamber, that had handicapped the injector of Flightweight Engine No. 1. The convective heating was

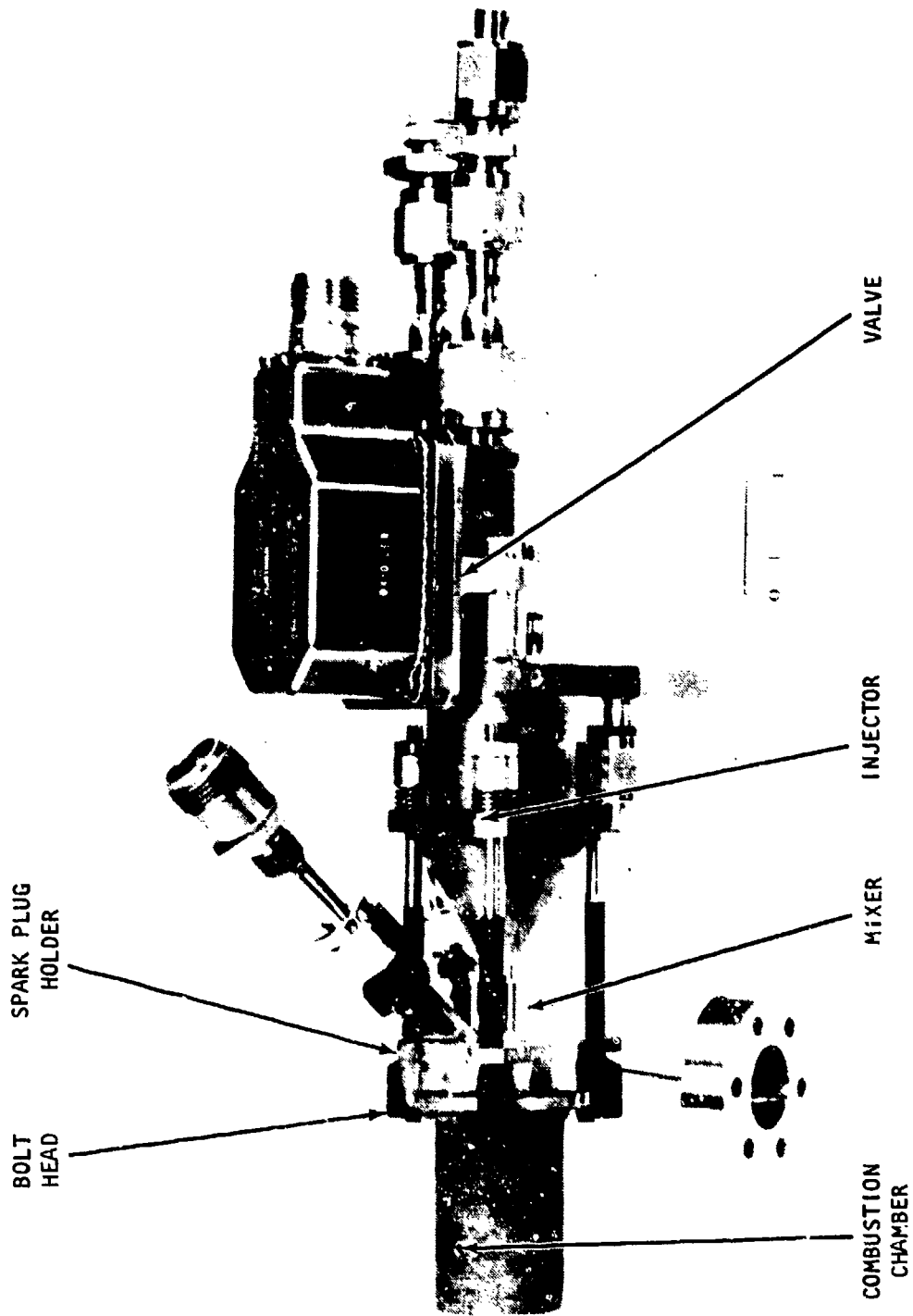


Figure 74. Location of Thermocouples on Flightweight Engine No. 2

NEG. 74-483-10

minimized by using a rectangular spark plug port which minimized the area exposed to the combustion gas. The conduction heating from the chamber was reduced by using a smaller bearing area of 0.02 in². It was calculated that the maximum bearing stress would be 12,300 psi which would not cause excessive creep of the L-605 seal insert at the 1600°F temperature limit. At the same time, the contact resistance of the 0.02 in² bearing area was calculated to reduce conduction heating sufficiently to meet the temperature limit of 1600°F for the spark plug holder.

The outside surfaces of the spark plug holder, except for the surface facing the combustion chamber, were grit-blasted to get a good emissivity (estimated at 0.6) for radiation cooling. The outside surface of the injector was also grit-blasted.

Outward facing portions of the attach bolts were grit-blasted and also coated with a black chrome finish for high emissivity, as shown in Figures 72 and 73.

The weight of the components of Flightweight Engine No. 2 are as follows:

Moog Valve	0.84 lb.
Injector, Mounting Plate (nonflightweight)	0.78 lb.
Chamber, C-103 (flightweight)	0.46 lb.
Spark Plug Holder, Mixer (flightweight)	0.23 lb.
Bolts, Belleville Springs, etc. (flightweight)	0.13 lb.
Spark Plug, Swagelok Fitting (flightweight)	0.09 lb.

The estimated weight of a completely flightweight engine, using the above flightweight components together with two flightweight valves (0.25 pound each) and a flightweight injector (estimated 0.3 pound) would be 1.71 pounds, not including an igniter. The flightweight igniter weighing 1.56 pounds could probably serve a number of engines

b. Preliminary Testing

Runs 168-174

The columbium C-103 chamber was used for a series of runs to demonstrate performance and ignition reliability. The engine ignited on all of 20 pulses but chamber pressure was low during both hot firings and cold flows.

Pressure testing of the engine after the test firings revealed a leak through the lapped seal between the spark plug holder and the combustion chamber. The engine was disassembled and inspected. The L-605 insert was found to be imperfectly lapped. In addition, the lapped surface of the C-103 chamber

exhibited a granular structure. It was not clear whether the surface was perfectly smooth or whether small leak paths existed around the grain boundaries of the coating. It was apparent that most of the leakage was due to the poor lapping of the L-605 insert. However, the molybdenum chamber was used for the next series of tests because of its apparently smoother lapped surface.

Runs 175-189

A series of runs were made with the molybdenum chamber to determine engine performance. The engine leak had been eliminated by relapping the L-605 insert. Ignition was obtained on each of 10 pulses (1 second ON, 1 second OFF) at supply pressures of 200 psia and 100 psia. Ten pulses were then attempted at each of the supply pressures 70 psia, 90 psia, and 200 psia. The engine failed to ignite on any of these firings.

Runs 190-200

A different CLA igniter (S/N 004) unit of the same model was used for the next series of tests. Ignition was obtained on all tests over a range of supply pressures from about 200 psia to 70 psia.

A seven-minute firing was made on Run 200 with supply pressures near the nominal maximum of 200 psia. After three and one-half minutes of firing, the chamber pressure dropped from 74 psia to 58 psia, and the chamber temperature dropped from 2000°F to 1600°F. It was determined after the run that Poxally sealant on the mixer had been dislodged, undoubtedly by overheating, and had allowed leakage of hydrogen, with subsequent loss of performance and chamber temperature. All engine temperatures were well below design limit temperatures. Therefore, it was concluded that Flightweight Engine No. 2 should be used for the life testing.

c. Life Testing - Molybdenum Chamber

Life testing of Flightweight Engine No. 2 was begun using the molybdenum chambers. The mixer was welded into the spark plug holder before beginning life testing.

The objective of the tests was to accumulate ten hours of firing time and 300,000 pulses. These life requirements were to be demonstrated over a very short period of time, compared to a seven-year satellite mission. Therefore, the engine temperature would be much higher than it would on a satellite because of the absence of cool down time between firings. A total of 100,070 pulses and 3.52 hours of hot firing were actually accomplished with the molybdenum chamber.

(1) Performance Characterization

A series of firings were made at three levels of propellant supply pressure to determine engine performance and steady-state temperatures.

Runs 201-209

During a series of test firings made at the high propellant supply level, about 200 psia, engine performance was found to produce a C* efficiency of 82.2% of shifting equilibrium and an Isp of 329 seconds. During pulsing at .2 seconds ON, .2 seconds OFF, ignition was achieved on only 26 of 30 pulses.

Runs 210

A pulse train of 999 firings at .2 seconds ON, .2 seconds OFF was made at the high supply pressure. The engine failed to ignite on one-third of the first 100 pulses, but ignited on all subsequent pulses.

Runs 211-215

A series of firings were made at an intermediate propellant supply pressure (about 150 psia). The engine produced a C* efficiency of 79.8% of shifting equilibrium and an Isp of 326 seconds. During pulsing at .2 seconds ON, .2 seconds OFF, ignition was obtained on 9 to 10 pulses on Run 211, on 48 of 50 pulses on Run 213, and only 5 of 15 pulses on Run 215.

Runs 216-217

The engine failed to ignite on all 10 pulses with the high propellant supply pressure near 200 psia. The test cell was opened and the spark plug was observed while sparking, which appeared normal. The electrical system between the pulser and igniter was examined, and no reason for the erratic ignition could be found.

Run 218

No changes were made for the next run, during which a pulse train of 999 pulses was made at the intermediate supply pressure near 150 psia. The engine ignited on all 999 pulses.

Runs 219-221

Twenty pulses were made at .2 seconds ON, .2 seconds OFF at a low supply pressure near 70 psia. Ignition was not achieved on any of the 20 pulses. One engine design criterion was operation at a supply pressure one-third of nominal (200 psia). Therefore, operation at a supply pressure of 67 should be possible. However, it had been found impossible on the preceding contract to ignite reliably at such a low supply pressure, and the same situation was found to exist with the flightweight engine. However, by raising the supply pressure slightly, reliable ignition should be possible, based on tests of the heavyweight engine.

Runs 222-224

The supply pressure was raised to about 90 psia, at which condition ignition was obtained on all of 10 pulses during Run 222 and on 997 of 999 pulses on Run 224.

Engine performance during a five second firing on Run 223 produced a C* efficiency of 70.5% of shifting equilibrium and an Isp of 282 seconds.

The performance of Flightweight Engine No. 2 is shown in Figure 75 superimposed on performance for the heavyweight 0.1 pound engine developed on the previous contract. There was no significant difference in performance of the two engines.

Runs 225-232

A 10-minute steady-state firing was made at each of three propellant supply pressures. The engine temperatures at the locations shown in Figure 74 are shown in Table 12. The engine temperatures were all below the design maximum temperature limits. In particular, the spark plug holder temperature at the high chamber pressure condition was only 1250°F, compared to the design limit temperature of 1600°F.

Difficulty in ignition was again experienced during this series of runs. Therefore, the igniter, S/N 001, was installed with the engine. This igniter had been previously used on over 150,000 pulses with the flightweight five pound engine. Despite this change, difficulty in ignition was still experienced.

Runs 233-239

A total of 96,869 pulses of .1 second ON, .1 second OFF were accumulated using the high propellant supply pressures near 200 psia.

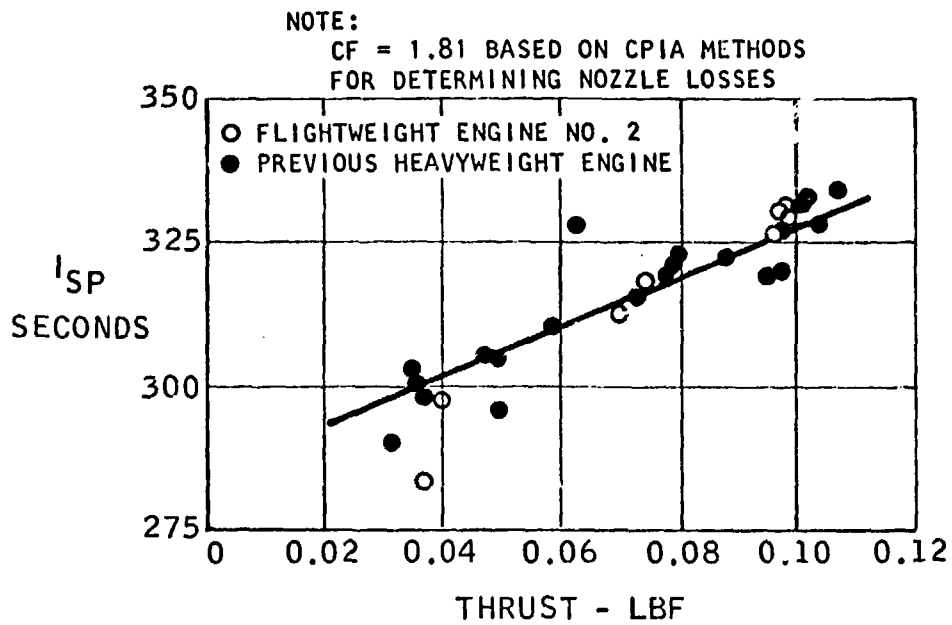


Figure 75. Performance of 0.1 Lbf. Flightweight Engine No. 2

TABLE 12. STEADY-STATE TEMPERATURES WITH 0.1 POUND MOLYBDENUM CHAMBER

	Temperatures °F			Design Limit Temperatures °F
	Low Pressure Run 225 $P_c = 25.5$ psia	Intermediate Pressure Run 229 $P_c = 47$ psia	High Pressure Run 232 $P_c = 68.6$ psia	
Combustion Chamber	1600	1800	2000	2300
Spark Plug Holder	1060	1180	1250	1600
Mixer	1040	1160	1200	1300
Bolt Head	880	1020	1336	1650
Injector (Belleville Springs)	300	320	375	400
Valve	120	115	120	250

The engine is shown during this pulsing in Figure 76. The chamber temperature was 1600°F during pulsing with the 50% duty cycle.

The 96,869 pulses were accumulated during three days of testing. On the first day, during Run 234, a total of 56,000 pulses were made. On the second day, 11,951 pulses were made on Run 237. Difficulty was experienced in getting the first ignition for Run 237, but once started, all pulses ignited. This again suggested that some type of erratic electrical problem existed in the ignition system. Therefore, a new spark plug was installed before Run 239. Reliable ignition was shown on this run, during which 28,918 pulses were accumulated. It was concluded, based on sparking and ignition tests at sea level as well as the erratic ignition at altitude, that the spark plug was the source of ignition problems. It was hypothesized that a cracked insulator might be causing arcing to occur internally rather than at the spark plug tip.

The testing was terminated on Run 239 when the chamber pressure suddenly jumped from about 70 psia to 90 psia and the spark plug holder and chamber suddenly rose in temperature by several hundred degrees. By this time, the molybdenum chamber had accumulated 100,070 pulses and 3.52 hours of hot firing.

(2) Post-Test Examination

Post-test examination of the engine showed that the throat was partially blocked by a silver colored globule. When the engine was disassembled, it was found that a black deposit of metallic appearance had collected in the short length of 0.086 diameter combustion chamber within the spark plug holder. The walls of the access port between the spark plug tip and the combustion chamber were spotted with a black deposit.

The entrance of the molybdenum combustion chamber showed evidence of a coating failure. The chamber was sectioned down the center-plane and it was found that the chamber had eroded near the entrance end as shown in Figure 77.

The thickness of molybdenum disilicide coating buildup at the beginning of the test program had been only 0.0005 inch, compared to an expected coating buildup of 0.003 inch. This thinness of coating might have contributed to the coating failure. However, a second factor, relating to the spark plug discharge energy, is thought to have been the principal problem. The spark igniters used for development of the heavyweight engine released only one millijoule at the spark plug tip. The flight-weight igniters made by General Laboratory Associates were designed to release ten millijoules. It was expected that this higher energy



Figure 76. Flightweight 0.1 Lbf. Engine No. 2 During Firing

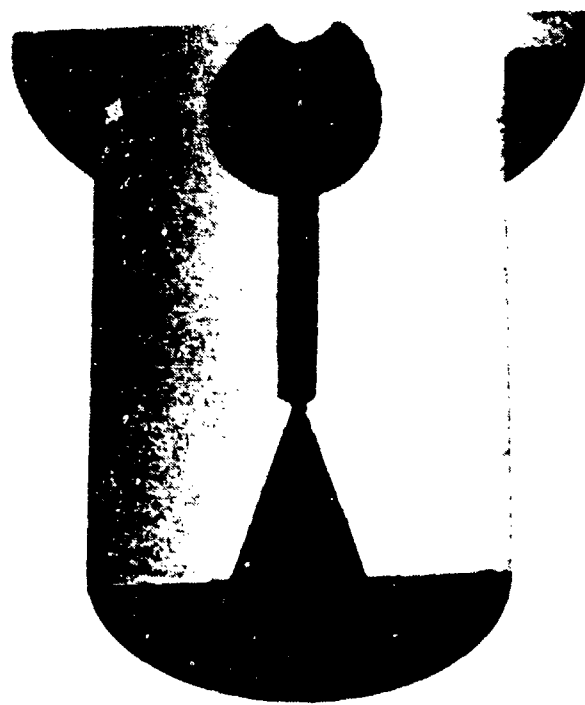


Figure 77. Cutaway View of 0.1 Lbf. Molybdenum Chamber After Firing

release per spark would allow ignition at significantly lower supply pressures than had been feasible with the heavyweight engine. However, this was not the case, as supply pressures of about 90 psia were required. The greater energy released from the GLA igniter was visually observed to cause emission of glowing sparks from the spark plug tip much more frequently than observed with the heavyweight igniters.

It is suspected that the glowing particles were accumulated in the spark plug well and combustion chamber near the spark plug. Some chemical reaction between the chamber coating and the deposited particles could have led to the coating failure.

The two spark plugs used for life testing of the molybdenum chamber had both accumulated a deposit on the center electrode during testing. A greater amount of deposit was found on the plug used for only 28,918 pulses on Run 239, as shown in Figure 78, than found on the plug used for the previous 71,152 pulses, shown in Figure 79. It is surmised that the heavier deposit on the second plug might be due to condensation of products from the chamber oxidation after coating failure.

The ceramic insulator between the center electrode and spark plug shell of the two spark plugs had been removed to a depth of 0.060 inch. This allowed more wear on the center electrode while maintaining a sparking surface, but also exposed more area on the center electrode to the hot combustion gas.

The GLA igniter was supposed to limit sparking to a 15 millisecond duration, but was not terminating the sparking duration. Therefore, the control pulser was set up to limit energy to the igniter to 30 milliseconds duration.

It was concluded that since emitted particles from the spark plug had evidently contributed to the coating failure, that future testing should be done with as short a sparking duration as possible. It was also concluded that the depth of ceramic removal should be reduced, in case overheating of the electrode had been a contributing factor to particulate emission from the spark plug.

d. Life Testing - Columbium Chamber

Life testing of Flightweight Engine No. 2 was continued with the C-103 columbium chamber. The sealing surfaces of the chamber and the L-605 insert in the spark plug holder were carefully relapped, after which a good seal was obtained. The columbium disilicide coating buildup thickness at the entrance to the columbium chamber, expected to be 0.005 inch, was actually



Figure 78. Spark Plug After Run 239 (28,918 Accumulated Pulses)



Figure 79. Spark Plug After Run 237 (71,152 Accumulated Pulses)

0.007 inch, much thicker than the coating buildup on the molybdenum chamber. A spark plug with the ceramic insulator removed to a depth of only 0.020 inch was used for life testing of the columbium chamber.

The igniters used on the previous contract to develop the heavyweight 0.1 pound engine were no longer in operating condition. Therefore, the GLA flight-weight igniters had to be used despite an indication from the molybdenum chamber failure that increased spark energy of the GLA igniter was undesirable. The duration of sparking was reduced to 5 milliseconds to minimize the amount of particles emitted by the spark plug.

A total of 301,726 firing pulses and 10.07 hours of hot firing time were accumulated with the columbium chamber. The test history of the columbium chamber is summarized in Table 13.

Runs 241-242

Two runs were made to determine the minimum spark delay that would be sufficient to obtain ignition with a 5 millisecond spark duration. It was found that zero delay was not satisfactory but ignition was obtained with a 10 millisecond delay.

Run 243

A single five second firing was made to determine engine performance. An Isp of 331 seconds and a C* efficiency of 82.8% were obtained at the high propellant supply pressure.

Run 244

A train of 999 pulses was made with 0.2 seconds ON, 0.2 seconds OFF, to determine ignition reliability. Ignition was obtained on all but one pulse.

Run 246

A 600 second run was made to determine steady state engine temperatures with the columbium chamber. The engine temperatures, shown in Table 14, were all below the design limit temperatures. Comparing the engine temperatures for the columbium chamber (Run 246, Table 14) and the molybdenum chamber (Run 225, Table 12), it is seen that the columbium chamber was 220°F cooler than the molybdenum chamber. This was probably due to the higher emissivity of the columbium coating compared to the emissivity of the molybdenum coating, as had previously been predicted.

TABLE 13. RUN SUMMARY FOR LIFE TEST OF 0.1 POUND COLUMBIUM CHAMBER

Run No.	Date	Engine Time		No. Pulses	Supply Pressures		Chamber Pressure	C* Eff. %	ISP	Thrust	Remarks
		Sec.	Off		psia	psia					
240	8/5/74	30	-	1	O ₂ 194	H ₂ 218	25.5				Cold flow
241	"	.2	.2	10	"	"					O delay, 5 ms spark, no ig.
242	"	.2	.2	10	"	"					10 ms delay, 5 ms spark, ig.
243	"	5	-	1	"	"	68.6	82.8	331	.0964	Performance run
244	"	.2	.2	999	"	"					Ignite 998
245	8/6/74	30	-	1	"	"	25.5				Cold flow
246	"	600	-	1	"	"					Steady state temperature
247	"	.1	.1	110,891	"	"					15 ms delay, 5 ms spark
248	8/7/74	30	-	1	"	"					Cold flow
249	"	5	-	1	"	"	69.0	81.9	328	.098	Performance run
250	"	.1	.1	127,872	"	"					
251	8/8/74	30	-	1	"	"	25.5				
252	"	.1	.1	61,938	"	"					
253	"	1,800	-	1	O ₂ 87	H ₂ 96	27.5	74.5	298	.0395	Normal performance
254	"	1,800	-	1	O ₂ 150	H ₂ 167	49.0	78.5	314	.0704	Normal performance
255	"	1,800	-	1	O ₂ 194	H ₂ 218	68.6	82.8	331	.098	Coating failure at 1320 sec.

TABLE 14. STEADY-STATE TEMPERATURES WITH 0.1 POUND COLUMBIUM CHAMBER

Location	Temperatures ° F				Design Limit Temperatures ° F	
	High Pressure Run 246	Low Pressure Run 253	Intermediate Pressure Run 254	High Pressure		
				Run 255 Beginning		*End
Combustion Chamber	1780	1440	1660	1780	1200	2300
Spark Plug Holder	1350	1160	1300	1740	1520	1600
Mixer	1160	1030	1180	1700	1450	1300
Bolt Head	1250	1020	1180	1270	1040	1650
Injector	360	420	480	600	560	400
Valve	120	180	180	180	200	250
Spark Plug	450	490	560	670	620	Unknown

*After coating failure.

Run 247

A series of 110,891 pulses of 0.1 second ON, 0.1 second OFF were made during Run 247. A 15 millisecond delay was used with a 5 millisecond sparking duration for this and all subsequent testing to insure ignition on all pulses.

Run 249

The day after Run 247 was made, a performance check was made during a 5 second firing on Run 249. Engine performance was unchanged by the previous performance check on Run 243.

Runs 250, 252

A series of 127,872 pulses of 0.1 second ON, 0.1 second OFF were made on Run 250 and the next day a series of 61,939 pulses were made on Run 252 to complete the pulsing requirement of 300,000 pulses.

Runs 253-255

Three continuous firings of 30 minutes duration were made to accumulate a total of 10 hours of firing on the engine. The steady state engine temperatures measured during these runs are shown in Table 14.

Engine performance, determined at the beginning of each run, was found to be the same at each pressure level as measured previously. The Isp for low, intermediate, and high supply pressures was 298, 314 and 331 seconds, respectively.

Engine temperatures throughout Runs 253 and 254 were steady and compatible with the reduced heating rates at these reduced pressures. Engine temperatures at the beginning of Run 255 were similar to the temperatures on the previous Run 246 at high supply pressure, with the exception of the spark plug holder which was 1740°F (higher than the 1600°F design limit and higher than the 1350°F temperature measured on Run 246). The reason for this higher temperature is not known, but might be related to buildup of particles emitted by the spark plug.

After 22 minutes of Run 255, the chamber pressure suddenly rose and the engine temperatures started dropping. By the end of the 30 minute run, the chamber temperature had dropped to 1200°F. The hydrogen manifold pressure also rose high enough to unchoke the sonic orifice controlling hydrogen flow rate. The measured parameters indicated that partial blockage of the throat had occurred. The reduced propellant flow rates, despite the higher chamber pressure, resulted in less heating of the engine.

The engine was disassembled and inspected. A slag-like deposit was found all over the throat wall with a small hole in the center, as shown in Figure 80. The chamber was sectioned in half, and a coating failure was found in about the same location as the failure in the molybdenum chamber, at the entrance end near the spark plug holder. The sectioned columbium chamber is shown in Figure 81. A hard, dark green deposit, probably an oxidation product of columbium, was found on the chamber inside surface. A hard, dark green deposit was also found in the combustion zone within the spark plug holder. The access port to the spark plug was completely closed by this dark green deposit. The tip of the spark plug was in good condition (Figure 82) with much less buildup of deposit on the center electrode than on the spark plugs used with the molybdenum chamber.

The test data and post-test examination lead to the conclusion that engine operation was normal throughout a total of 301,726 pulses, and all but the last eight minutes of the 10.07 hours of hot firing.

A failure of the columbium disilicide coating occurred sometime during the last 30 minute run. Therefore, the engine fulfilled the life goal of 300,000 pulses, but fell just short of the 10-hour life. The combination of the thicker coating on the columbium chamber, plus the reduced sparking duration, resulted in a much longer engine life. The engine testing was more severe than the 10 hours of life over a seven-year satellite mission would require, because of the lack of engine cooling between pulse trains. During Runs 247, 250, and 252, during which a total of 300,701 pulses of 0.1 second ON, 0.1 second OFF were accumulated, the temperature of the combustion chamber was 1400°F for a total of 16.7 hours.

Inasmuch as both the columbium and molybdenum chambers failed in the same general location, it seems likely that the same cause of failure was in effect. The most likely cause is chemical reaction between the coatings and the particles deposited from the spark plug. It seems likely that this could be corrected by using a lower spark energy similar to that used for development of the heavyweight engine.

e. Pulsing Performance

A low volume holder for the chamber pressure transducer was connected to the spark plug holder through a 0.026 inch ID tube. The volume in the chamber pressure transducer on the heavyweight engine had been 10.6 times as large as the combustion chamber volume. The time to reach 90% of chamber pressure had been observed to be as much as 500 milliseconds for a cold heavyweight combustor. Pressure rise was faster with a hotter combustor. It was surmised that the combustion gas entering the pressure transducer line was being quenched, causing a slow chamber pressure rise.

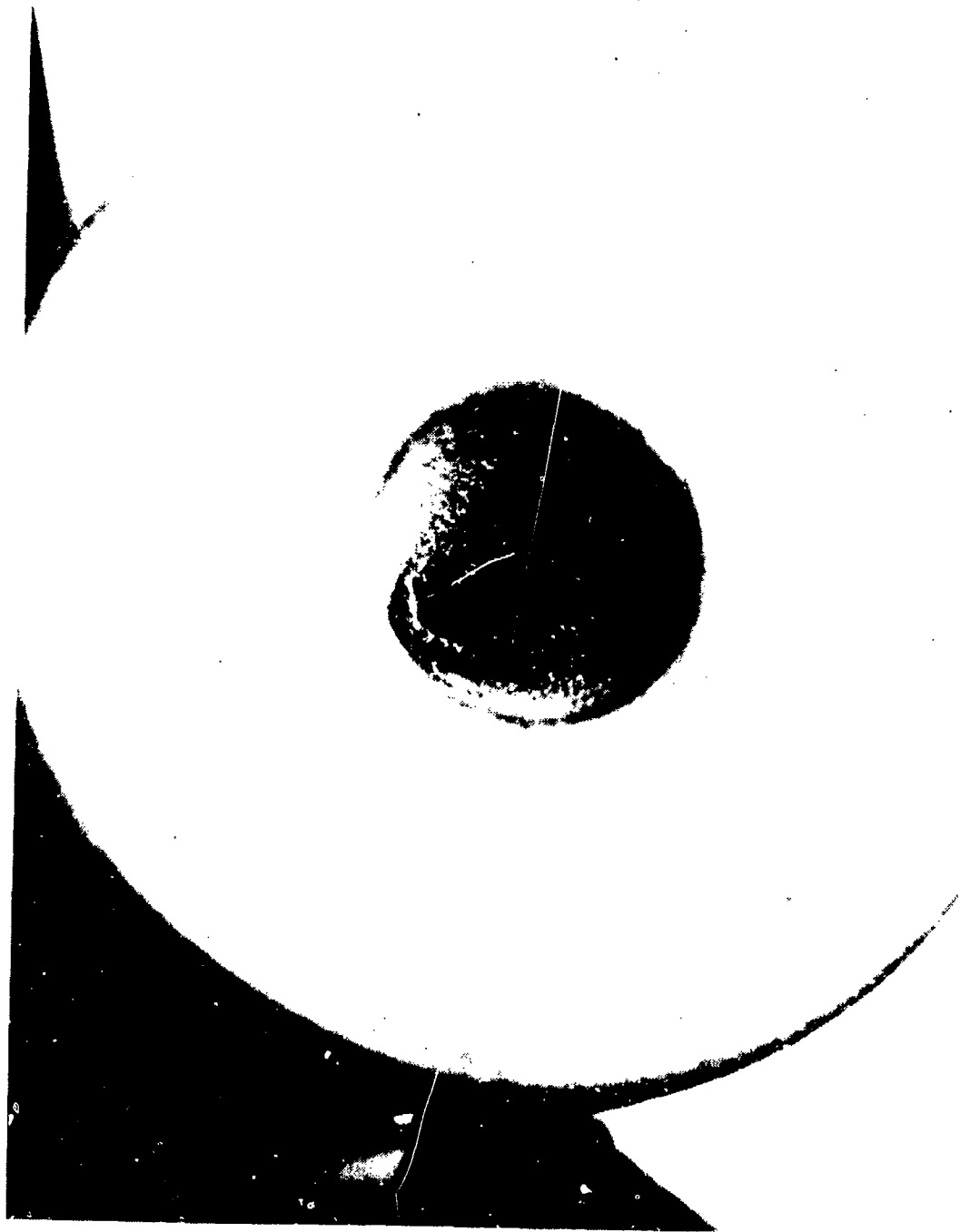
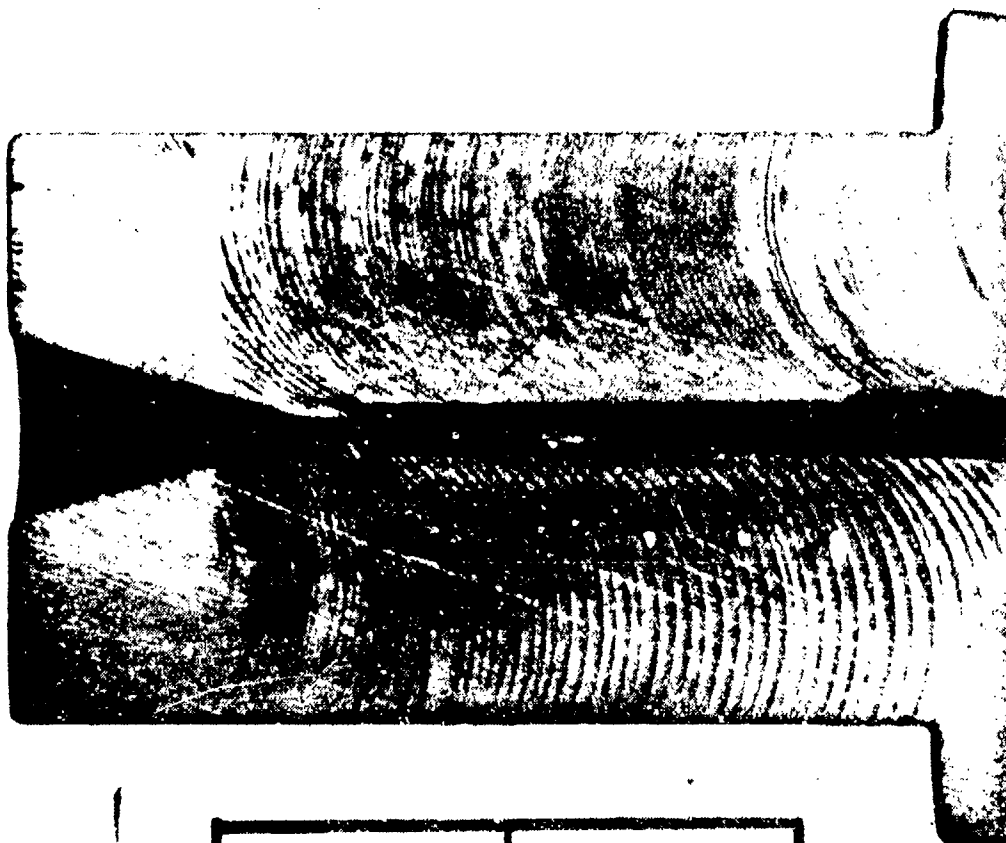


Figure 80. Deposit in Throat of 0.1 Lbf. Columbium Chamber



0 Inch 1

Figure 81. Cutaway View of 0.1 Lbf. Columbiuim Chamber After Firing

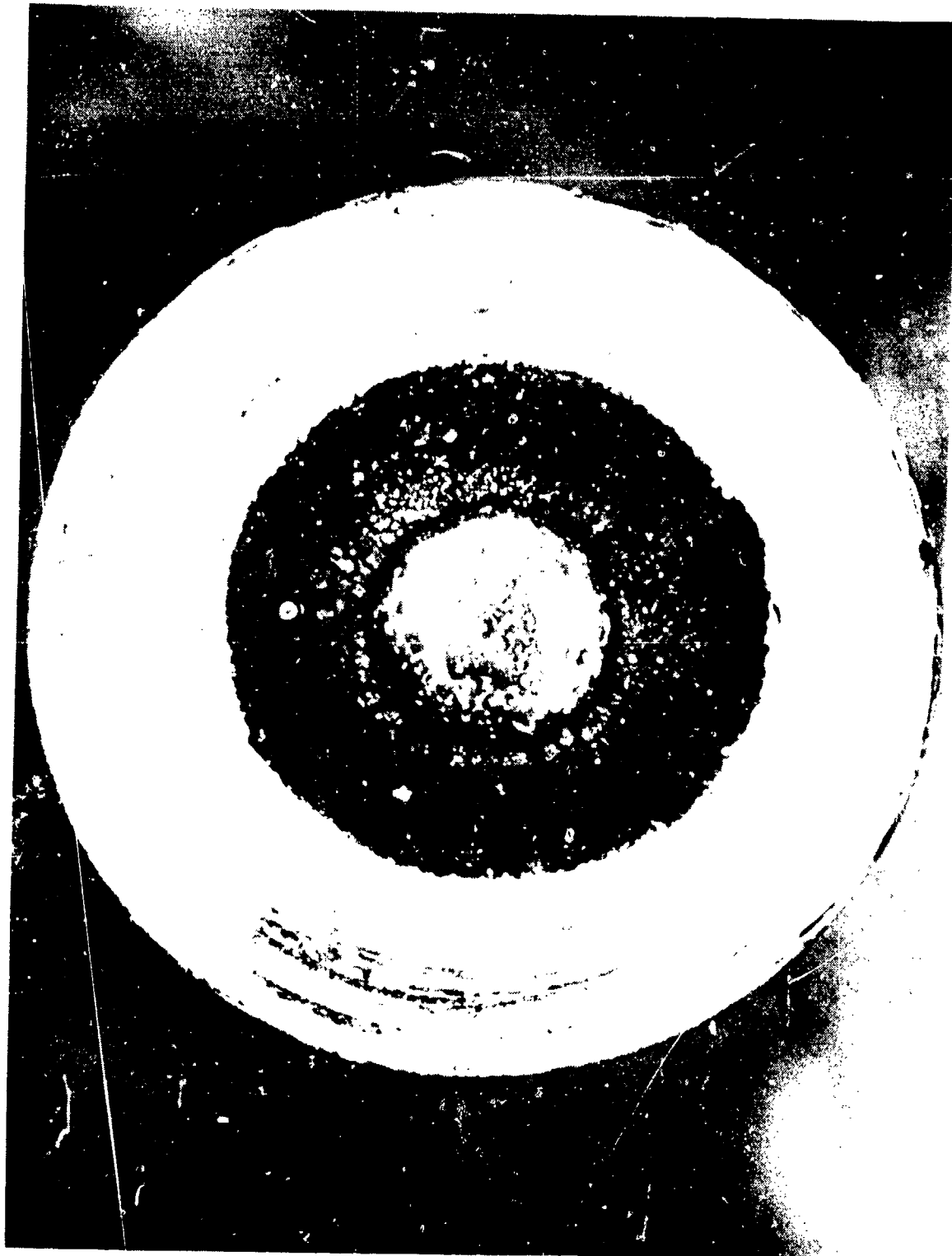


Figure 82. Spark Plug After Run 255 (301,728 Accumulated Pulses)

Testing with the Flightweight Engine No. 2, which had a chamber pressure transducer system volume only 1.1 times as large as the combustion chamber showed that the pressure rise time was still long, i. e. , on the order of 500 milliseconds for a cold combustor.

The chamber pressure rise characteristics of Flightweight Engine No. 2 are shown in Figure 83. The chamber pressure rises much more quickly if the combustor is hot, reaching 90% of the steady state value in 30 milliseconds if the chamber is initially 1400°F, compared to about 1000 milliseconds if the chamber is cold. The pressure rise is even faster if the chamber temperature is near the steady state value (1789°F for a columbium chamber).

Subsequent to obtaining test firing data, heat transfer and performance analysis was done which showed that the slow pressure rise is due to heat loss to the combustor walls. The heat loss, radiation from the combustor and spark plug holder, was calculated to be .475 BTU/second for a coated columbium chamber with a temperature of 1780°F and an emissivity of .72. The theoretical heat release from the propellant flow rate of 3.03×10^{-4} pound/second is 1.75 BTU/second. Therefore, the heat loss in steady state is 27% of total combustion energy. This leads to a predicted C* efficiency of about 85%. The 85% C* efficiency observed during steady state test firings indicates that the additional performance loss due to incomplete mixing and combustion was only about 3%.

Even greater heat loss will occur whenever the combustor temperature is colder than the steady state value, which would explain the observed relationship between combustor temperature and rate of chamber pressure rise.

The unusually large effect of heat loss on performance of the 0.1 pound engine is caused by the large ratio of combustor inside surface area to chamber volume, due primarily to the very small chamber diameter of this size engine. With a chamber ID of 0.086 inch, a chamber length of 1.25 inches, and a throat diameter of 0.031 inch, the chamber L^* is 9.6. The chamber length and contraction ratio were chosen to maximize steady state performance. A reduction in chamber length in an attempt to reduce heat loss would involve a trade-off between steady state Isp and transient pressure rise rate. However, the present configuration which produced a high performance (331 seconds Isp) is probably preferable for most applications.

Since the combustor and attach bolt temperatures were considerably below their temperature limits, the combustor OD could be reduced somewhat. This would reduce weight and give some improvement in pulsing and steady state performance.

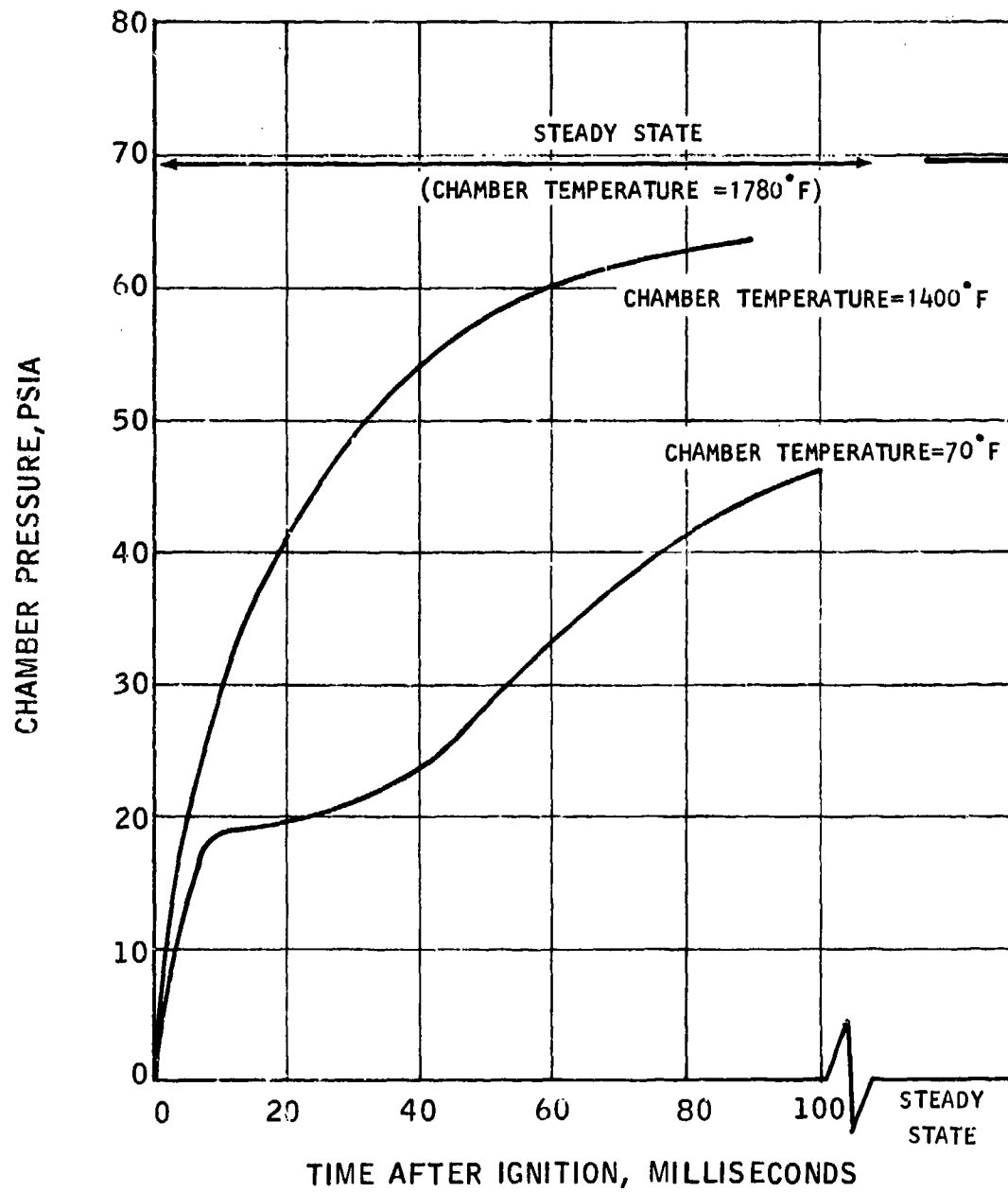


Figure 83. 0, 1 Lbf. Engine Chamber Pressure Rise

SECTION V

SPARK IGNITION AND EXCITER SYSTEM

1. SYSTEM DESCRIPTION

The 0.0 lbf and 0.1 lbf thrust GO_2/GH_2 rocket engines used to provide the attitude control and ΔV maneuvers for the water electrolysis system are ignited by a spark plug located in the combustion chambers of the engine. Figure 84 shows the spark plug used in the two engines. The Champion Spark Plug Company's FHE 231A is a standard item used for ignition of reciprocating and jet engines. A semiconductor material is located on the tip between the anode and cathode. This material is removed prior to use on the rocket engines so that a high voltage, low total energy spark is produced, rather than a low voltage, high total energy which is characteristic of a "shunt" type plug. During the design phase of this program, the possibility of changing the spark plug material was investigated but heat transfer studies indicated that the temperature of the spark plug and igniter tip could be kept at a temperature which was well below the temperature at which spark plug performance would degrade.

The principle purpose of the igniter/ignition phase of this program was to develop an ignition system which was both reliable and flight type. Prior studies with the Bel Air Igniter, described in Reference 1, showed that the engines could be ignited with one millijoule of energy, but under certain conditions of mixture ratio and temperature that a greater energy would be required.

The flight type exciter to provide energy to the spark plug was made by General Laboratory Associates of Norwich, New York. The design and operating characteristics of the flightweight exciter are presented in Appendix A.

2. TEST PROGRAM RESULTS

Three flight type and one boiler plate exciter systems were supplied by GLA for the test program. The boiler plate system was used to test the 5 lbf thruster which was built for the system test and this exciter supplied 10 millijoules of energy but did not have EMI suppression as a control circuit. The three flight systems contained a control system which delayed the spark for 4-5 milliseconds after electrical signal. The spark rate was 500 Hz with 7 sparks supplied in 15 milliseconds. Figures Nos. 85, 86 and 87 show the acceptance test records for the three flight type exciters.

EXAMINATION OF PRODUCT

INITIAL	DATE	PARA. NO. & TEST	ACTUAL READING
<i>J</i>	9/1/57	2.2 Dimensions	
<i>J</i>	9/1/57	2.2 Marking	
<i>J</i>	9/1/57	2.2 Weight	

ELECTRICAL PERFORMANCE

INITIAL	DATE	PARA. NO. & TEST	ACTUAL READING			
<i>RB</i>	9/1/57	2.3.1 Output Circuit Resistance	8.5K ± K Ohms			
<i>RB</i>	9/1/57	2.3.2 Insulation Resistance	1200 Megohm			
			Input	24 VDC	28 VDC	32 VDC
<i>RB</i>	9/1/57	2.3.3 Spark Delay		4.9 MS	4.3 MS	4 MS
<i>RB</i>	9/2/57	2.3.4 Burst Length		14.2 MS	14 MS	15 MS
<i>RB</i>	9/2/57	2.3.5 Sparks/Burst		6 SPB	7 SPB	10 SPB
		2.3.6 Discharge Peak Current	35 Amps			
<i>RB</i>	9/2/57	Duration	40 Micro-Sec			
<i>RB</i>	9/2/57	2.3.7 Open Circuit Output Voltage	5.6 KV			

ADDITIONAL TESTS

INITIAL	DATE	PARA. NO. & TEST
(HG)	9/1/57	2.4.1 Leak Test

Figure 85. Acceptance Test Record for S/N 001 Exciter

EXAMINATION OF PRODUCT

INITIAL	DATE	PARA. NO. & TEST	ACTUAL READING
<i>RB</i>	<i>9/10/73</i>	2.2 Dimensions	X
<i>RB</i>	<i>9/10/73</i>	2.2 MARKING	
<i>RB</i>	<i>9/10/73</i>	2.2 Weight	

ELECTRICAL PERFORMANCE

INITIAL	DATE	PARA. NO. & TEST	ACTUAL READING			
<i>RB</i>	<i>9/10</i>	2.3.1 Output Circuit Resistance	<i>91.2</i> K Ohms			
<i>RB</i>	<i>9/10</i>	2.3.2 Insulation Resistance	<i>1100</i> Megohm			
			Input	24 VDC	28 VDC	32 VDC
<i>RB</i>	<i>9/10</i>	2.3.3 Spark Delay		<i>4.7</i> MS	<i>4.3</i> MS	<i>3.9</i> MS
<i>RB</i>	<i>9/10</i>	2.3.4 Burst Length		<i>14</i> MS	<i>14.5</i> MS	<i>15.5</i> MS
<i>RB</i>	<i>9/10</i>	2.3.5 Sparks/Burst		<i>6</i> SPB	<i>8</i> SPB	<i>9</i> SPB
		2.3.6 Discharge Peak Current	<i>38</i> Amps			
<i>RB</i>	<i>9/10</i>	Duration	<i>12</i> Micro-Sec			
<i>RB</i>	<i>9/10</i>	2.3.7 Open Circuit Output Voltage	<i>5.5</i> KV			

ADDITIONAL TESTS

INITIAL	DATE	PARA. NO. & TEST
<i>RB</i>	<i>9/10/73</i>	2.4.1 Leak Test

Figure 86. Acceptance Test Record for S/N 002 Exciter

EXAMINATION OF PRODUCT

INITIAL	DATE	PARA. NO. & TEST	ACTUAL READING
<i>[Signature]</i>	9/17/77	2.2 Dimensions	X
<i>[Signature]</i>	9/18/77	2.2 Markings	
<i>[Signature]</i>	9/17/77	2.2 Weight	

ELECTRICAL PERFORMANCE

INITIAL	DATE	PARA. NO. & TEST	ACTUAL READING			
<i>RB</i>	9/20	2.3.1 Output Circuit Resistance	10 K Ohms			
<i>RB</i>	9/20	2.3.2 Insulation Resistance	700 Megohms			
			Input	24 VDC	28 VDC	32 VDC
<i>RB</i>	9/20	2.3.3 Spark Delay		48 MS	4.25 MS	3.8 MS
<i>RB</i>	9/20	2.3.4 Burst Length		14 MS	15 MS	15 MS
<i>RB</i>	9/20	2.3.5 Sparks/Burst		6 SPB	8 SPB	9 SPB
		2.3.6 Discharge Peak Current	35 Amps			
<i>RB</i>	9/20	Duration	38 Micro-Sec			
<i>RB</i>	9/20	2.3.7 Open Circuit Output Voltage	575 KV			

ADDITIONAL TESTS

INITIAL	DATE	PARA. NO. & TEST
<i>[Signature]</i>	9/16/77	2.4.1 Leak Test

Figure 87. Acceptance Test Record for S/N 004 Exciter

SECTION VI

CONCLUSIONS

The results of the life testing of the water electrolysis propulsion system, the 5 lbf. flightweight engine and the 0.1 lbf. flightweight engine lead to the following conclusions:

1. Initial life testing of the water electrolysis unit revealed design inadequacies after 19 weeks of testing. The design inadequacies were eliminated and the modified electrolysis unit operated without any change in performance for 14 weeks of continuous testing.
2. All components of the propellant supply system operated satisfactorily after substitution of a Carpenter 20 check valve in the oxygen outlet line.
3. The propellant supply system does not require a water deionizer or water filter.
4. The flightweight 5 lbf. engine satisfactorily met all performance requirements including a high specific impulse, repeatable impulse bits and high ignition reliability at a 3 to 1 blowdown ratio.
5. The flightweight 0.1 engine demonstrated the capability to operate for more than 10 hours life and 300,000 pulses. Increased life should be possible with a reduced spark energy.
6. The flightweight 0.1 lbf. engine demonstrated high specific impulse and high ignition reliability for supply pressures as low as 100 psia, corresponding to a 2:1 blowdown from a 200 psia system.

SECTION VII

RECOMMENDATIONS

The following recommendations are based on the fact that the water electrolysis satellite propulsion system possesses significant weight advantages for attitude control and ΔV of large, long-life satellites.

1. Further life testing of the modified water electrolysis unit should be accomplished with 100,000 pound-seconds being the primary goal.
2. A single cell, lightweight water electrolysis system combined with the 0.1 and 5.0 pound thruster should be designed, built, and tested to demonstrate its weight and performance advantage.

APPENDIX A

FLIGHTWEIGHT IGNITER

The General Laboratory Associates of Norwich, New York, successfully developed a flight type exciter (Figure A1) for use in the water electrolysis system. This exciter weighs 1.5 pounds and has an integral timer circuit and EMI suppression. Figures A2 and A3 show the wiring schematic and installation.

EXCITER OPERATION

The exciter consists of six basic sections, each performing a required function. They are as follows: (Reference Block Diagram Figure A4)

The Input Section contains the reverse polarity diode for reverse input protection and a current limiting resistor. Also in this section are the voltage dropping resistors for the zener regulator of the Delay Section.

The function of the Delay Section is to sense the application of input voltage and generate a signal after the proper interval of time to activate the Burst Length Control circuit.

The Burst Length Control determines the length of time the Charging Circuit and Discharge Circuit will function. These circuits yield a burst of high voltage-high current discharges at the igniter gap for a fixed time period. The EMI Filter Section provides filtering of interference pulses generated in the Charging and Discharge Sections.

The application of 28 ± 4 VDC of proper polarity to the input of the Input Section results in the reverse biasing of the reverse polarity diode D1-1. Thus, it appears as an "open" and allows exciter operation. However, if the polarity of the input is reversed, the diode will be forward biased, appearing as a short circuit with R1 in series. This will draw sufficient current to trip a circuit breaker or cause a fuse to open. Protecting the exciter with a circuit breaker or fuse of 2 to 3 amperes will be adequate.

Applying 28 ± 4 VDC to the input in the proper polarity will initiate the Delay Circuit as follows: Current will flow from B pin through R1, R2-1, C4-1, D3, C4-2, and R2-2 to A pin; D3 is a zener diode, R2-1 and R2-2 are the dropping resistors for D3. The combination of R2-1, C4-1 and R2-2, C4-2 form small EMI filters. The voltage across D3 will rise rapidly. The Delay Circuit operates from the regulated source D3.

The Delay Circuit is basically a programmable Unijunction Oscillator (Q3). Its standoff ratio is set by the ratio of R13/R14. The delay is set by the RC network R17, C5. When the charge on C5 reaches the firing point, Q3 conducts.

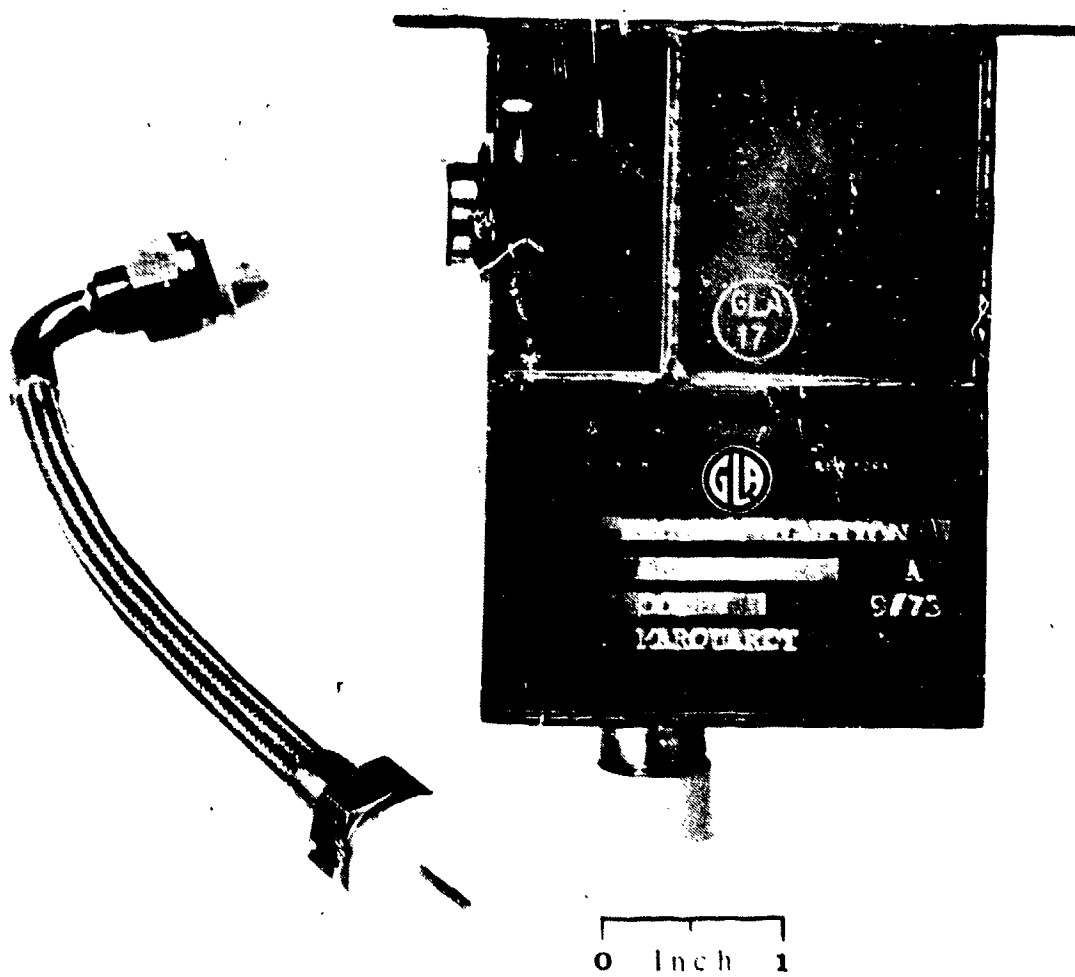


Figure A1. Flight Type Exciter

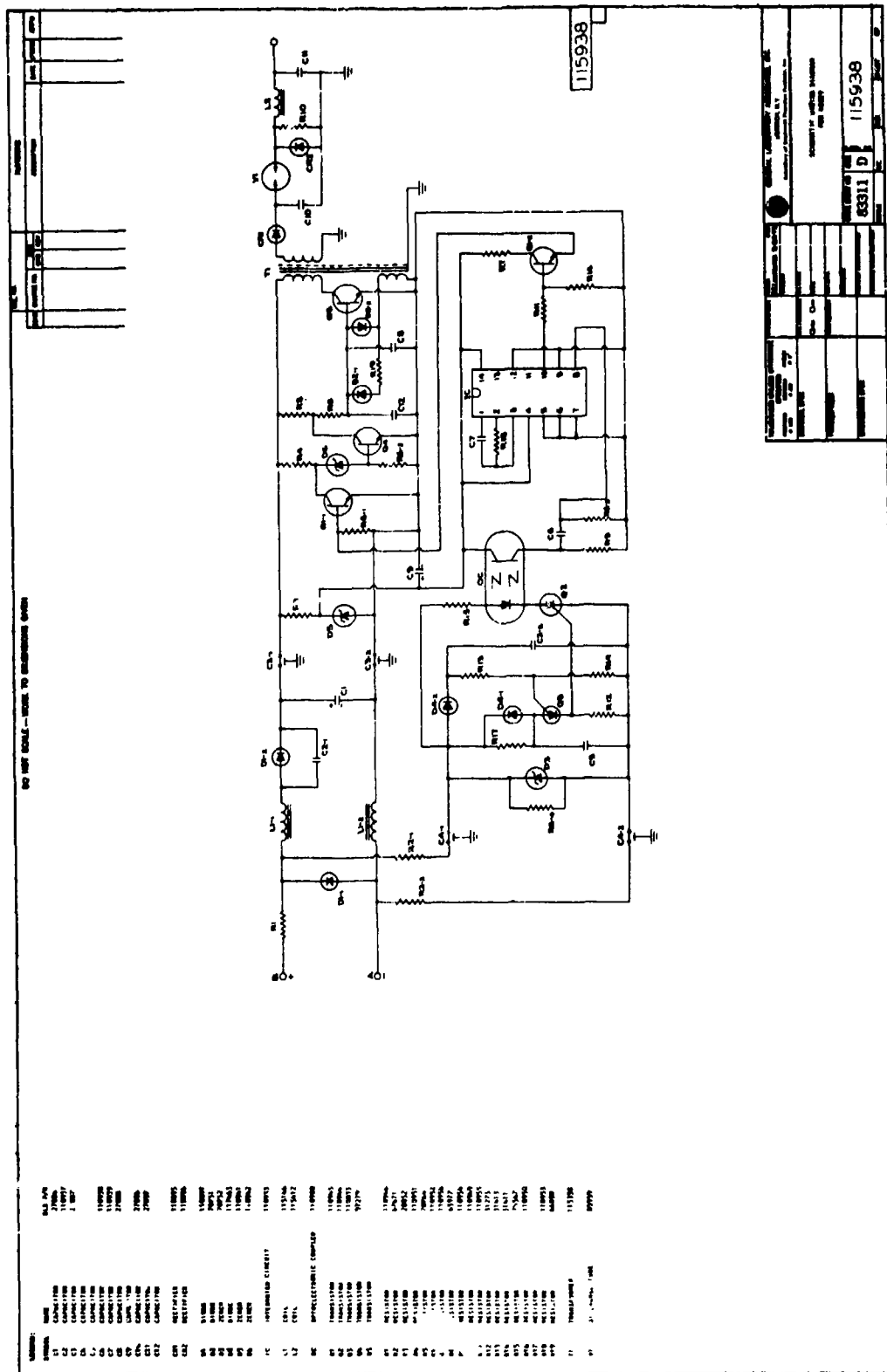


Figure A2. Schematic Wiring Diagram for Flightweight Igniter

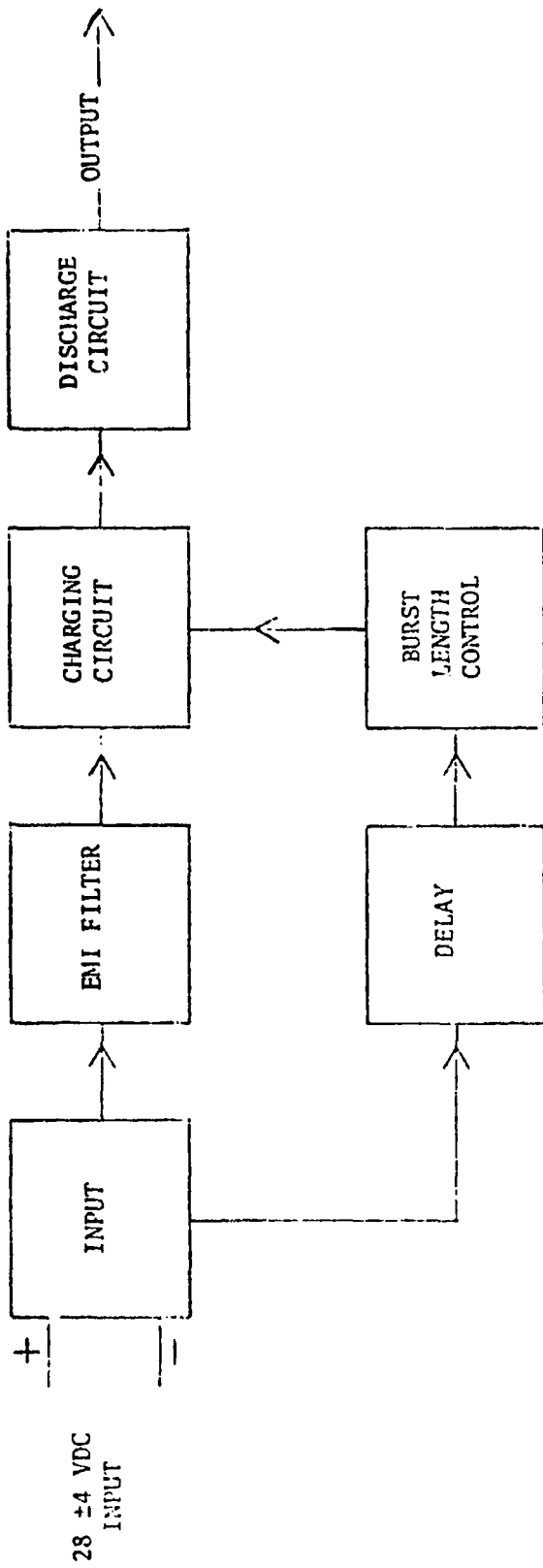


Figure A4. Block Diagram of Flightweight Exciter

The discharge of C5 produces a pulse at the gate of Q2 SCR. This pulse "gates" Q2 to the "ON" state. The unijunction oscillator continues to operate as long as there is voltage on the input. However, Q2 "latches" in the ON stage until the input voltage is removed. When Q2 is ON, the input diode (a light emitting diode in the optoelectronic coupler, OC) is activated. The output of the OC is in the Burst Length Control Circuit. The OC is a device to couple one circuit to another with a high degree of electrical isolation, thus the Delay circuit is electrically isolated from the Burst Control Circuit and will respond only to conditions at the input to the exciter.

Other components in the Delay Section are protection against false firing of Q3 due to switch or relay contact bounce; to prevent this false firing, C5 must discharge faster than C2-2. This is done by making the time constant of C5, R6-4 faster than the time constant of C2-2 x (R13 + R14).

The delay is set for 2.2-2.4 milliseconds. During this delay time, C1 will charge to near input voltage through L1-1, D1-2, and L1-2. D1-2 prevents discharge of C1 back to the input and prevents activating the Delay Circuit when input power is removed. C2-1 "softens" the switching characteristics of D1-2 for EMI. C1 serves two purposes. It is an effective filter for the audio susceptibility requirements (AC voltages impressed on the DC line) and tends to cancel the reactance of the EMI Filter Inductors L1-1 and L1-2.

C3-1 and C3-2 are feed-through capacitors which, in conjunction with L1-1 and L1-2, comprise the major EMI filtering elements of the exciter.

At the end of approximately 2.4 milliseconds after application of input voltage, a pulse has been generated to turn on Q2 and cause the LED (Light Emitting Diode) in the OC to light. This beam of light will activate the photo transistor (output portion) of the OC.

This transistor receives its power from the zener diode (DS) regulated source (R3 is the zener dropping resistor). R9 is the transistor load resistor. When the transistor is turned on by the light from the LED, a pulse is coupled to pin 8 (positive edge trigger input of the Ic) through C6. The Ic is a monostable multivibrator, whose timing is set by the RC combination R18, C7. The Ic also shares the regulated power of zener D5.

When pin 8 is triggered, pin 10, which is normally low (at zero voltage), goes high and turns on the emitter follower Q1-2 and then Q1-1.

During the interval of the Delay Circuit operation, the charging circuit is inoperative because Q1-1 is off, causing current to flow through R4 and D6 to the base of Q4. This forward bias forces Q4 into saturation (turned on with low resistance). The starting current for the charging circuit flows through

R5 and R8 during the charging cycles. However, until the Q4 is turned off, current will flow through R5 and Q4 to the negative line, disabling the charging circuit. When Q1-1 is turned on, the bias on Q4 is removed, turning Q4 off and allowing the starting current to flow through R5 and R8 to the base of Q5.

This starting current (forward bias) on the Q5 base emitter junction causes current to flow through the primary of T (power transformer), the Q5 collector-emitter junction and return to the negative input line.

The current flow in the primary of T1 induces a voltage in the feedback winding of T1. Because the current increase in T1 primary is linear, the voltage out of the feedback winding will be basically a square wave in shape. This voltage causes current to flow through R19 and D2-1 to keep Q5 in the "ON" state.

When the loop gain of Q5, R19 and the feedback winding reaches zero, the collector current can no longer increase and the feedback voltage decreases to zero. Therefore, the current in the primary decreases to zero very rapidly. The polarity of the high voltage winding of T1 is such that the high voltage rectifier CR1 is blocking (reversed biased) when the current in the primary is increasing. When the current rapidly decreases, a high voltage pulse of the opposite polarity is induced in the winding. This energy pulse places a charge on the energy storage capacitor C10.

Concurrently with this pulse generation, the feedback winding produces a pulse of opposite polarity (-) which is applied through D2-2 to the base of Q5 (reverse bias) aiding in the turnoff of Q5. When all of the energy stored in the transformer has been "delivered" to C10, Q5 will again conduct and the charge cycle will repeat. C8 and C12 are bypass capacitors that eliminate Q5 response to high frequency pulses. This charging cycle will continue, and each time Q5 is turned off, the voltage on C10 will increase. When the voltage on C10 reaches the ionization point of the discharge tube, V1 will ionize and the discharge cycle will begin.

The Discharge Section serves two functions. The first is to provide a trigger (or ionizing) pulse (5KV) to the igniter. The second is the energy portion of the discharge which comprises the spark at the igniter tip. The trigger voltage is generated by the resonant charging of C11 through L2 (a high Q inductor). This places a voltage on C11, and also on the igniter electrodes that is 1.6 to 1.8 times that of the voltage on C10. (See following pages for a detailed description of Resonant Charging.) This trigger voltage appears at the igniter center electrode to ionize the igniter gap.

Upon ionization of the igniter gap, the main portion of the discharge occurs as follows: Current flows through L2, through the center conductor of the

output cable to the center electrode of the igniter, through the ionized gap of the igniter producing a spark, to the outer electrode, back to C10 through the outer conductor of the output cable and case. The characteristic of the discharge is Unidirectional (see following pages for a full description of Unidirectional Discharge).

When the voltage on C10 reaches zero, all of the energy stored in C10 has not been dissipated in the circuit. A large amount is stored in L2 $\left(E = \frac{L1^2}{2}\right)$. L2 now becomes an energy source. This remaining energy will now start to charge C10 in a negative direction. This will forward bias CR2 clamp rectifier. Due to the low forward drop of CR2, V1 and C10 are removed from the circuit and the remaining energy is dissipated at the igniter tip. R10 serves as a protective load in the event the igniter is quenched or the exciter is operated without the proper cable and spark igniter.

This charging and discharging of C10 will continue until the Burst Length Circuit switches to the off state. At this time, the starting current to Q5 will be removed, stopping oscillation and further charging of C10. The charging circuit will not function until input power is removed. Reapplication of power will again activate the exciter with the associated delay, burst duration and turnoff sequences.

The basic spark rate is set at 400 sparks/second at 28 VDC input. This yields a nominal 2.5 milliseconds between discharge pulses. Thus, in a 15 milliseconds burst duration, 6 pulses should be present.

Due to the characteristics of V1 discharger tube, the charge time per pulse will vary slightly. This is due to the high discharge rate. The discharge tube will vary slightly in its ionization point, yielding this variation in charge time. The charging time is also a function of the input voltage, so at 24 VDC input, the charge time will be longer, and at 32 VDC, it will be shorter. Therefore, the delay to the first output pulse will vary with the input voltage level. The delay circuit is designed to impart 2.3 milliseconds nominal delay. This designed delay plus the charge time is the total delay to the first pulse. Tests show a delay of 4.7 milliseconds at 28 VDC, becomes 5 milliseconds at 24 VDC and 4.1 milliseconds at 32 VDC.

Due to the high voltage involved in the Discharge portion, this method of delay was used. For greater accuracy, more complicated circuits would be involved and would increase the volume, weight, and cost of the exciter.

a. Resonant Charging

Figure A5 is a schematic of the components used in the discharge of the capacitor to provide energy to the spark plug. The monitor circuit and

resistors which have nothing to do with plug firing are omitted.

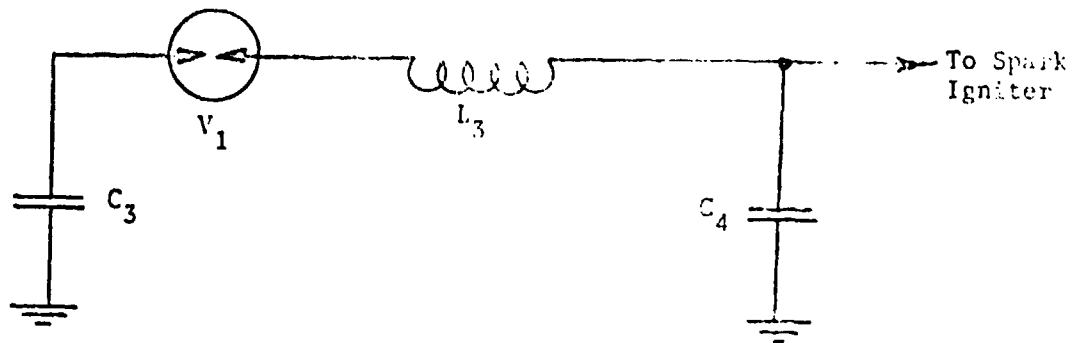


Figure A5. Resonant Charging Components

Capacitor C_3 , Inductor L_3 , and Capacitor C_4 form a resonant charging circuit, the purpose of which is (1) to increase the voltage applied to the spark plug, and (2) to control the rise time of the voltage to the spark plug so that the full voltage is not applied to the plug instantaneously.

The circuit of Figure A5 can be simplified for analysis as follows (see Figure A6). When the Gap V_1 fires, it is a short circuit and can be eliminated from the circuit. Capacitor C_3 has a much larger capacity than C_4 and can be considered a stiff DC source during the period of time we are considering (time from Gap firing to Plug firing). What remains is the resonant charging circuit of Figure A6.

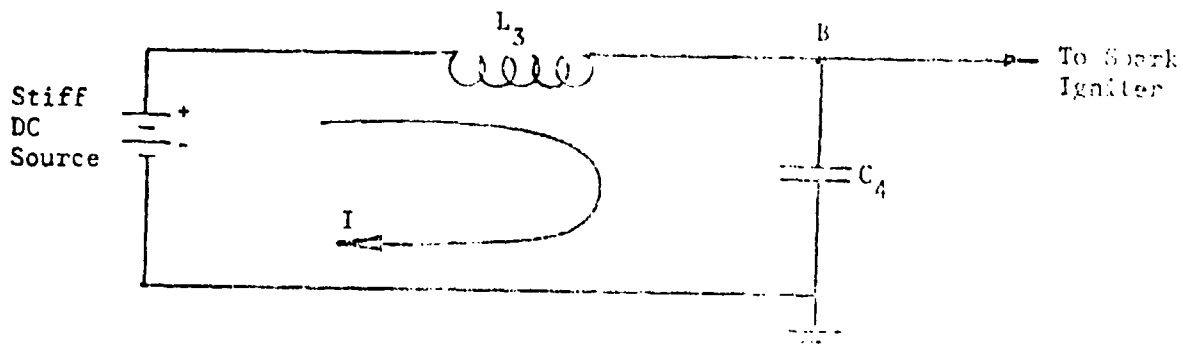


Figure A6. Resonant Charging Circuit

At the instant the gap fires, all the voltage appears across the inductor L3, and the voltage at point B is zero. Current will begin to flow, charging C4 to the value of the source voltage (see Figure A7). This charging current builds up a magnetic field about inductor L3. When the capacitor C4 has charged to the value of the source voltage, current would cease to flow if the inductor were not present. The magnetic field that has been built up about the inductor begins to collapse at this point and causes current to continue to flow in the same direction until the field has completely collapsed (Lenz's Law). This additional current flow in the same direction will theoretically charge C4 to twice the source voltage. Because part of the energy stored in the magnetic field is lost to heating and other losses, C4 actually charges to only 1.6 to 1.8 times the tank voltage.

If the circuit of Figure A-6 were allowed to continue undisturbed, C4 would discharge back to the source voltage with the discharge current again building up a magnetic field about L3. This field would begin to collapse when $V_B = V_A$ and cause the discharge current to continue flowing in the same direction. V_B is less than V_A when the field is completely collapsed, and C4 will again start to charge to the source voltage. This process would continue with energy being gradually lost until the condition is reached where $V_B = V_A$, and there is no energy stored in the magnetic field. The spark ignitor will fire somewhere between O and X on the V_B curve (see Figure A7).

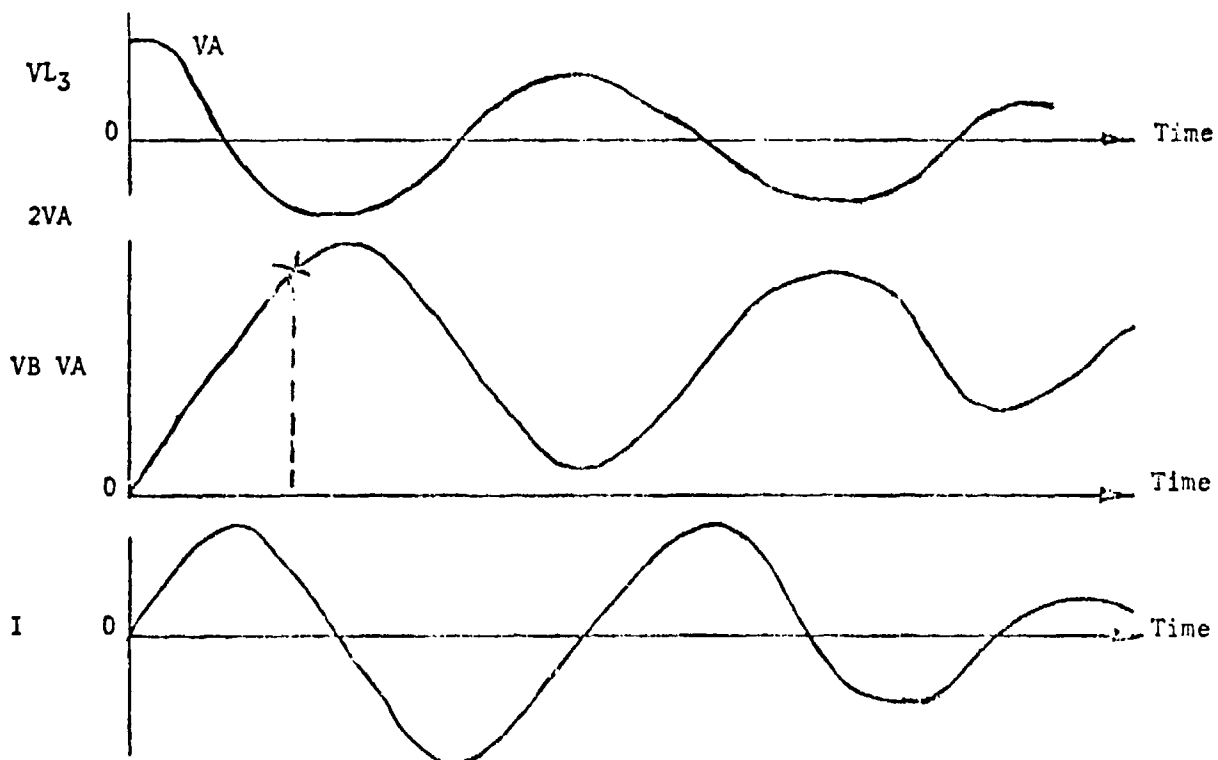


Figure A7. Voltage and Current Transients

Some of the advantages of the resonant charging augment circuit are listed below:

- (1) A simple means of providing an output voltage 1.6 to 1.8 times the storage capacitor voltage. This increased voltage extends the life of a semi-conductor surface gap type spark igniter. The higher voltage will ionize discontinuities in the semi-conductor surface and in the contact between electrodes and the semi-conductor.
- (2) The slower rate of rise of the output voltage increases the possibility of ionizing discontinuities in the contacts between semi-conductor surface and electrodes.
- (3) L3 also can be used to lengthen the discharge period of the storage capacitor. In some applications, this provides a gain in burner ignition characteristics.
- (4) L3 also can be adjusted to provide optimum energy transfer from the storage capacitor to the igniter tip. The discharge current can be controlled by the inductance. The inductance of the discharge circuit is normally very low without L3 and the discharge currents high. The high currents cause losses in the linear resistance of the circuit components and wiring.

By inserting the inductance of L3, the currents and losses are decreased. The Q of the inductor is kept high to minimize I^2R losses. The low limit on discharge current is dictated by practical size of the inductor, peak discharge power requirements of the burner, and igniter characteristics.

b. Oscillatory Discharge

The conventional method of converting input power to spark energy is to use an oscillatory discharge circuit of the type shown in Figure A8.

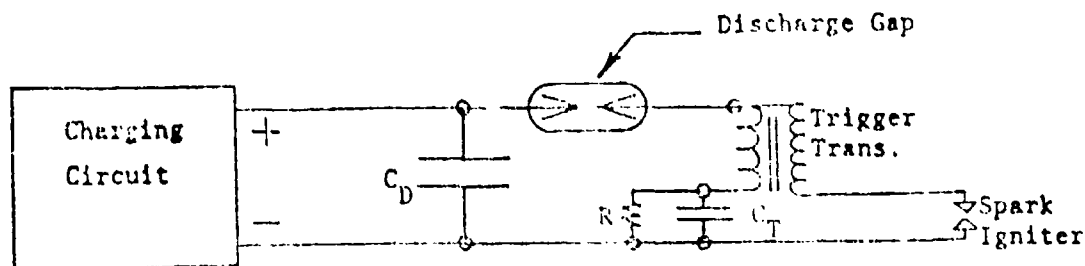


Figure A8. Oscillatory Discharge Circuit

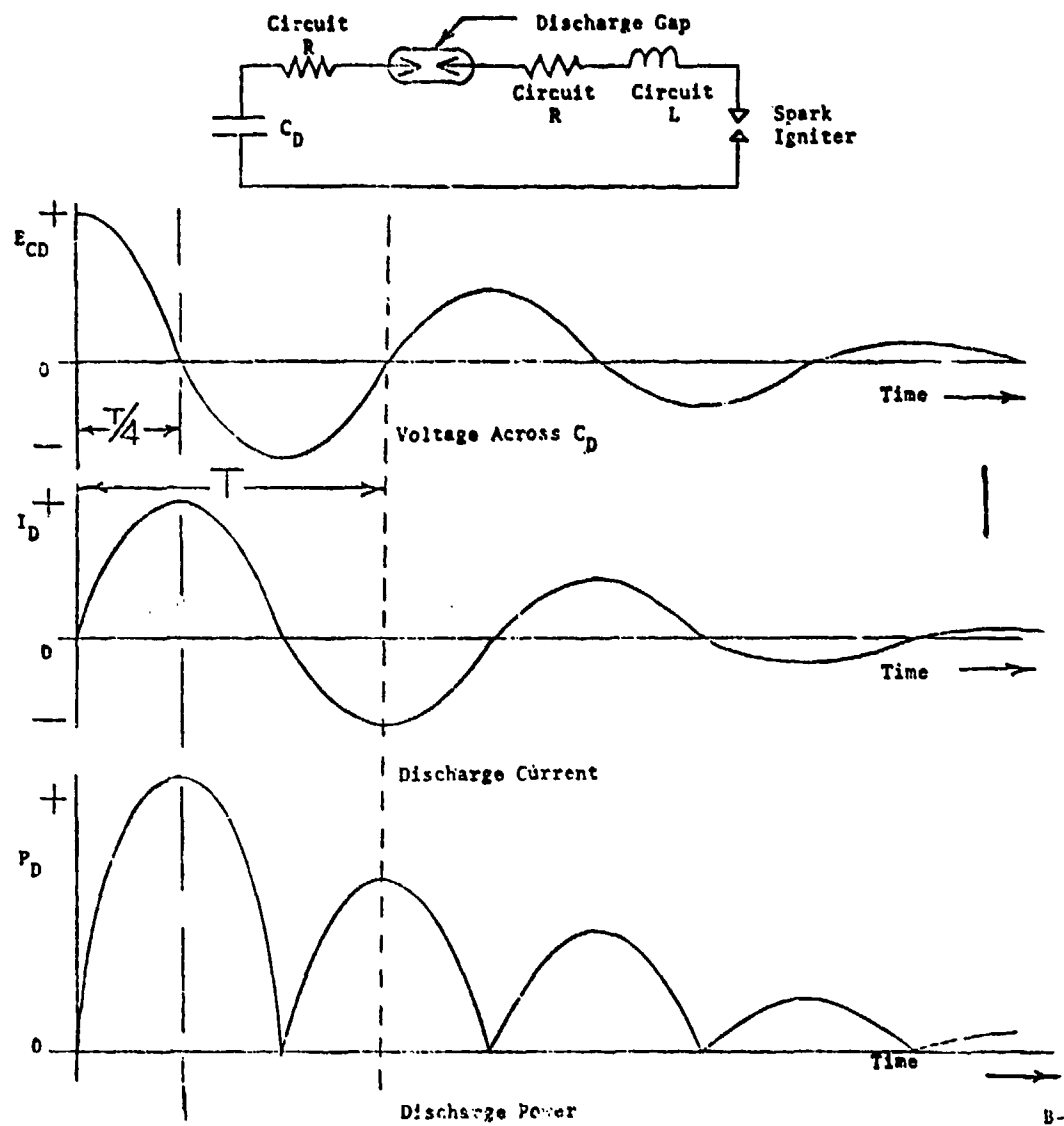


Figure A9. Characteristics of Oscillatory Discharge Circuit

The characteristics of an oscillatory discharge circuit are shown in Figure A9. When the voltage on C_D in Figure A8 reaches the breakdown voltage of the discharge gap, current flows from the positive terminal of C_D through the gap, the circuit inductance and resistance, and the spark igniter to the other terminal of C_D . Some of the energy stored on C_D is dissipated in the circuit resistance, including the discharge gap, and some in the spark igniter. A large amount is stored in the circuit inductance L . This energy is transferred back to C_D as a negative voltage as shown by the C_D voltage waveform. The energy will continue to oscillate between C_D and L until it is dissipated in the circuit resistance and the spark igniter. In a typical exciter, 18 to 25% of the energy is dissipated at the igniter tip.

c. Unidirectional Discharge

A unidirectional discharge circuit is shown in Figure A10.

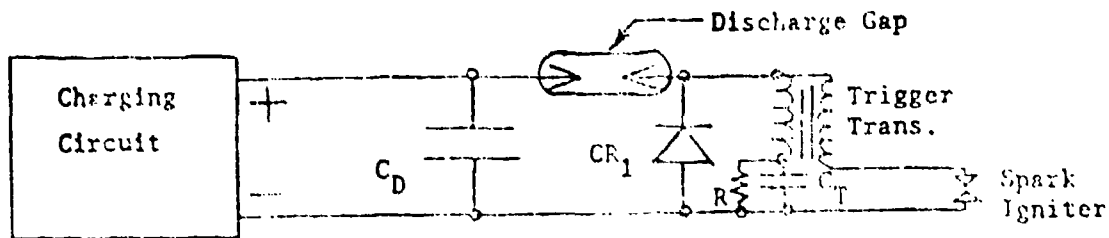


Figure A10. Unidirectional Discharge Circuit

The operating characteristics of a unidirectional discharge circuit are shown in Figure A11. Operation is the same as the oscillatory discharge circuit for the first one-quarter cycle of C_D voltage discharge current. When the voltage on C_D starts to reverse or go negative (point T/4) CR_1 is forward biased and the discharge current path switches from the discharge tube through CR_1 . The remaining energy is at this time stored in L and is dissipated in the circuit made up of the spark igniter gap, CR_1 , and the remaining circuit resistance.

The discharge gap and C_D are removed after the first quarter cycle, preventing the oscillation of energy and providing a nonreversing or unidirectional discharge pulse. The increase in efficiency is mainly due to the elimination of the discharge capacitor and gap after the first quarter cycle. In the oscillatory circuit, the gap dissipates nearly as much energy as the spark igniter, as it has a similar arc voltage and the same current flows through it. Typical efficiencies range from 36 to 50% as compared to 18 to 25% with the oscillatory pulse.

The important component in the circuit is CR_1 . It must have a reverse voltage capability equal to the voltage on C_D (2000 to 3600 volts) and pass the discharge current in the forward direction (200-3000 amperes). The losses in the forward direction must be minimal to provide for the maximum efficiency.

The unidirectional discharge pulse exciter offers reduction in size and weight and reduced input power requirements. The reduced input power is also an advantage in miniature continuous duty exciters where heat dissipation is a problem. The concept can be used for both high tension and low tension exciters.

Bench tests on shunted surface gap spark igniters indicate a substantial increase in life can be expected with the unidirectional discharge.

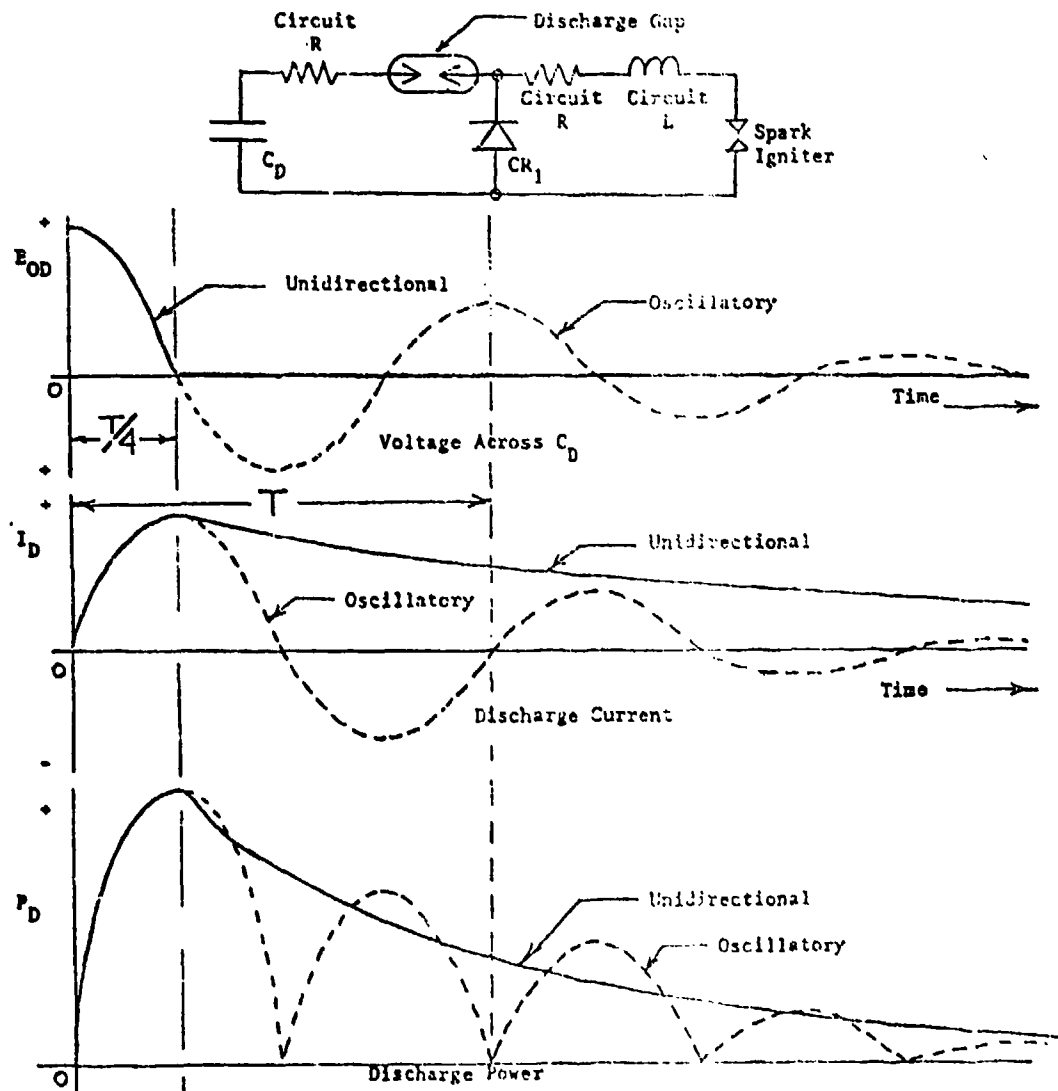


Figure A11. Characteristics of Unidirectional Discharge Circuit

APPENDIX B

TEST OF EXCITER CHARACTERISTICS

by

General Laboratory Associates, Inc.

TEST NO. 12103

DATE: 9-26-73

1.0 TEST SPECIMEN

<u>Part No.</u>	<u>Name</u>	<u>Serial No.</u>	<u>Qty</u>
48829	IGNITION EXCITER	003	1

2.0 TEST PURPOSE

- 2.1 Evaluate the prototype unit for EMI/EMC characteristics to MIL-STD-461A, Notice 3, Class A2.
- 2.2 Develop test procedures that will permit preparation of formal test plans for later phases of the program.

3.0 REQUIREMENTS

Perform EMI tests to Method CE-03 (20 KHz to 50 MHz Power Leads), Method RE-02 (14 KHz to 10 GHz Electric Field) and Method CS-01 (30 Hz to 50 KHz Conducted Susceptibility).

4.0 TEST DETAILS

4.1 Method CE-03

Figure B1 depicts the test setup. Measurements were made over the 20 KHz to 50 MHz frequency range using the slideback substitution method. Preliminary testing showed that the turn-on transient was much larger than the EMI due to sparking in the 15 MS burst. The transient was also found to be well above (nearly 40 DB) the specified limits. A 2 MH inductor was connected in series between the negative terminal of the 3 PPS solid state switch and the negative line 10 mfd feed-thru capacitor in order to reduce the transient to less than CE-03 broadband limits. The remaining transient was still larger than the EMI due to steady operation of the ignition circuit. Details of the solid state switch are shown in Figure B2. The rise time of the voltage across the load is in the order of 40 usec. A short duration transient is caused by the resonant charging of the 10 mfd F.T. capacitor of the EMI test setup (MIL-STD-461A required). Page B13 shows the conducted EMI levels at 20 KHz and 65 KHz using the switch only. Pages B14 thru B19 show acceptable EMI levels using the 2 MH series inductor to limit the on transient. Pages B20 thru B23 show conducted EMI levels on both the switch side (line)

TEST NO. 12103

DATE: 9-26-73

and exciter side of the 10 mfd F.T. capacitors with the drive to the switching transients of the solid state switch reduced such that the rise time of the voltage to the exciter was reduced to approximately 1 msec. It will be noted that the EMI is greater on the switch side of the capacitors.

The acceptable data of pages B14 thru B19 is plotted in Figures B3 and B4.

4.2 Method RE-02

No change in layout was made from that used for CE-03, except that excessive radiation was found to be originating in the 2 MH series inductor used for CE-03. The inductor was removed from the test setup and the solid state switch was modified to reduce the turn-on current surge as in 4.1. The radiated levels were reduced to less than RE-02 broadband EMI limits at all frequencies except those in the 14 KHz to 20 KHz range. This data is shown on pages B25 thru B28. Page B27 shows the radiated EMI levels in the 14 KHz to 150 KHz range with the 10 mfd. F.T. capacitor to exciter leads laying on the ground plane. This roughly simulated shielding these leads and shows that the conducted transient on the input leads was the source of the high radiated levels at 14 KHz to 20 KHz.

The data of pages B24 thru B29 is plotted in Figure B5.

4.3 Method CS-01

The conducted susceptibility test (30 Hz to 50 KHz power leads) was performed outside the shielded enclosure on open bench space.

Delay time (time to first spark) and the number of sparks in the burst were monitored by oscilloscope. A miniature accelerometer was installed on the igniter shield enclosure to pick up the spark shock impulse. The oscilloscope sweep was synchronized to start at the moment the solid state switch applied power to the exciter. Synchronized pickup was by means of an RFI current probe, loaded by 5 ohms, clamped over one of the power leads to the exciter.

Low frequency susceptibility signal levels were found to increase the jitter of the time delay to the first spark. This occurred mostly in the frequency range where the time per cycle of the susceptibility signal either approached or exceeded the delay time. Pages B30 and B31 show the delay time vs. test signal frequency and level. Page B32 shows that a variation in the number of sparks per burst could not be detected at any of the three DC input voltages.

TEST NO. 12103

DATE: 9-26-73

as a result of injecting the required RMS test voltage. Page B33 presents data to show the level at which the delay jitter increase could just be detected.

4.4 Additional Susceptibility

Tests were not performed to Methods CS-02 (50 KHz to 400 MHz Power Leads), CS-06 (Spike, Power Leads), RS-02 (Magnetic Induction Field) or RS-03 (14 KHz to 10 GHz Electric Field). These tests must be performed at an outside test facility. In view of the nature of the test sample which works at high energy levels, is contained in a hermetically sealed magnetic material case and is provided with a high performance integral power line filter; these four requirements become insignificant and the performance of these tests would not produce meaningful results at this stage of the program.

5.0 SUMMARY

The P/N 48829 Exciter demonstrated that the requirements for Conducted EMI (CE-03) and Radiated EMI (RE-02) can be met in accordance with the broadband limits of MIL-STD-461A, Notice 3, Class A2, except for high levels of conducted EMI during the switching transients. The radiated transients may be reduced to acceptable levels by shielding the power input wiring. Conducted transient levels were found to be a function of the rate of rise of the power applied to the exciter and can be reduced to acceptable levels by controlled switching. The conducted transients are, to a degree, a function of insertion of the 10 mfd feed-thru capacitors in the power input leads. These do not exist in the actual installation. The EMI test of the complete subsystem as called for in MIL-STD-461A, Notice 3, Section 4.1.1, thus becomes significant in importance.

Conducted susceptibility at low frequencies presented some jitter problems.

6.0 RECOMMENDATIONS

The next phase of the program must include resolution of the following EMC areas in terms of performance vs. cost conscious design:

- 1) Can short duration turn-on transients be tolerated?
- 2) Is controlled step function switching of the power desirable or necessary?

TEST NO. 12103

DATE: 9-26-73

- 3) Are the CS-01 required susceptibility levels realistic at low frequencies? If they are, then the circuit must be designed to produce the maximum delay at 24 VDC minus the susceptibility voltage and the minimum delay at 32 volts plus the susceptibility signal. At 30 Hz the half cycle time approaches the full "ON" operational time.
- 4) The impact of MIL-STD-461A, Space Shuttle Amendment (now in proposed form) on the present exciter design.
- 5) Since it is recognized that the characteristics of the power switch have an effect on the transient EMI and that the 10 mfd. feed-thru capacitor disturbs the circuit, the use of the actual switch, or simulation thereof, between the 10 mfd. F.T. capacitors and the test specimen should be considered in preparing an EMC test plan.

NAME OF TEST EMI RE02 CE03 TEST NO. 12103
 TEST PLAN NO. _____ PARA. NO. _____ PAGE 2 OF 2
 TECHNICIAN G. Rudd DATE 9-24-73

EQUIPMENT USED FOR TEST:					
NAME	MANUFACTURER	TYPE NO.	SER. NO.	LAST CALIB.	CALIB. DUE
NF-105 Noise & Field Intensity Meter, Basic Unit	Singer Metrics (Empire)	BA	3314	7-9-73	10-5-73
Tuning Unit NF-105	Singer Metrics (Empire)	T _A	2683	7-5-73	10-5-73
"	"	T _B	3314	7-5-73	10-5-73
"	"	T ₁	3314	7-5-73	10-5-73
"	"	T ₂	3314	7-6-73	10-5-73
"	"	T ₃	2336	7-6-73	10-5-73
41" Vertical Ant.	Singer Metrics (Empire)	VA-105	1126	4-5-73	7-5-74
"	"	VA-105	1126	4-5-73	4-5-74
Biconical Ant.	Honeywell Inc.	7B25	131	Factory	Cal.
Conical Loop Ant.	Electro Mechanics	CLP, A	2004	"	"
Current Probe	Stadart	91197-1	553-7	4-4-73	4-4-74
"	"	91550-1	277-200	4-4-73	4-4-74
Shielded Enclosure	Acc		HR1011 10K-G-3		

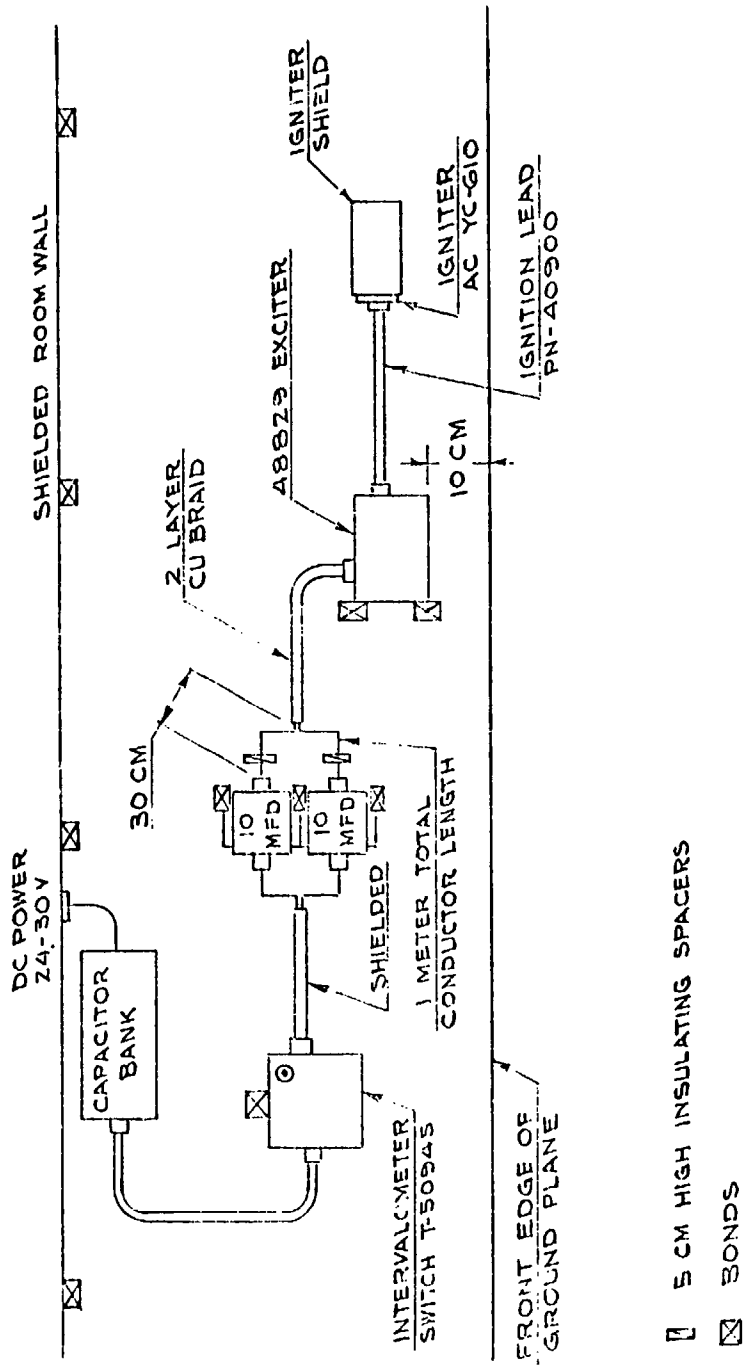
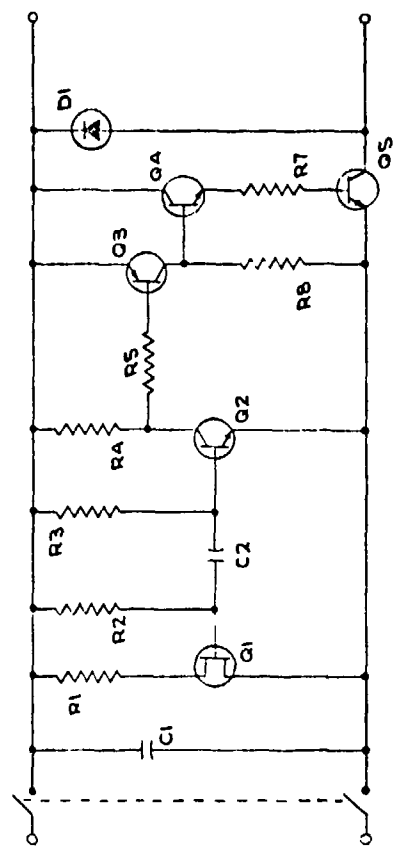


Figure B1. Test Setup

T-50945

LEGEND:		DO NOT SCALE — WORK TO DIMENSIONS GIVEN		REV. NO.		REVISIONS	
SYMBOL	NAME	DESCRIPTION	CHANGE NO.	SYM	CHG	REV	DESCRIPTION
C1	CAPACITOR	1.0 MFD ± 100V					DATE
C2	CAPACITOR	5 MFD ± 50V					D'AMAN
D1	DIODE	1N5001					APP D
Q1	TRANSISTOR	2N491					
Q2	TRANSISTOR	2N5172					
Q3	TRANSISTOR	ACA 40319					
Q4	TRANSISTOR	2N3054					
Q5	TRANSISTOR	2N3773					
R1	RESISTOR	270 OHMS, 1/2W					
R2	RESISTOR	22K OHMS, 1/2W					
R3	RESISTOR	680K OHMS, 1/2W					
R4	RESISTOR	150K OHMS, 1/2W					
R5	RESISTOR	10K OHMS, 1/2W					
R6	RESISTOR	5.3K OHMS, 1/2W					
R7	RESISTOR	20 OHMS, 10W					
R8	RESISTOR	1500 OHMS, 1W					



TOLERANCES UNLESS OTHERWISE SPECIFIED DIMENSIONS ± 1/32" & 1/16" ANGLES ± 1°		STANDARD CODE YES <input type="checkbox"/> NO <input type="checkbox"/>		DATE 3-25-73	
MATERIAL SPEC		STOCK PROCEDURE		ORDER CHECKER GENERAL LABORATORY ASSOCIATES, INC. NORWICH, N.Y. Subsidiary of Summa Products, Inc.	
PROCESS SPEC		MEET ASSEMBLY		PROD. APPD.	
ENGINEERING SPEC		PREPARED UNDER CONTRACT		FURNISHED UNDER CONTRACT	
SWITCH-INTERVALMETER		CODE IDENT NO 83311		SIZE B	
SCALE		WT.		REF.	
SHEET		OF		T-50945	

Figure B2. Solid State Switch

RUNNING LOG

P/N 48829
S/N 003

TEST NO. 12103
TEST PLAN
SHEET 1 OF 1
DATE 9-24-73

DATE	TIME	TOTAL OPERATING HOURS	REMARKS
9-24-73	0745	—	STARTED TEST SET UP
	0850		BEGAN CE 03 TESTING
			DETERMINED THAT SWITCH TRANSIENT WAS LARGER THAN STEADY STATE BME
			INSTALLED 2MH INDUCTOR IN NEW SWITCH LEAD.
	1000		BEGAN CE 03 SMOOTH DATA RUN.
	1130		COMPLETED CE 03 " " "
	1210		BEGAN RE 02 PRELIMINARY TEST.
			FOUND THAT 2MH INDUCTOR USED IN CE-03 CAUSED EXCESSIVE RADIATION.
			MODIFIED ELECTRONIC SWITCH TO LIMIT INPUT CURRENT SURGE & CONTROL RISE TIME
		1300	
	1530		COMPLETED RE 02
	1540		BEGAN CE 03 TEST TO SHOW LEVELS WITH MODIFIED SWITCH AND LEVELS ON SWITCH SIDE OF 10MFD F.T. CAPACITORS.
	1700		COMPLETED CE 03 TESTING
9-25-73	0300		STARTED CS 01 TEST SETUP
	1330		BEGAN CS 01 TEST.
	1700		SECURED FOR 9-25-73
9-26-73	0800		RESUMED CS 01 TEST.
	0930		COMPLETED CS 01

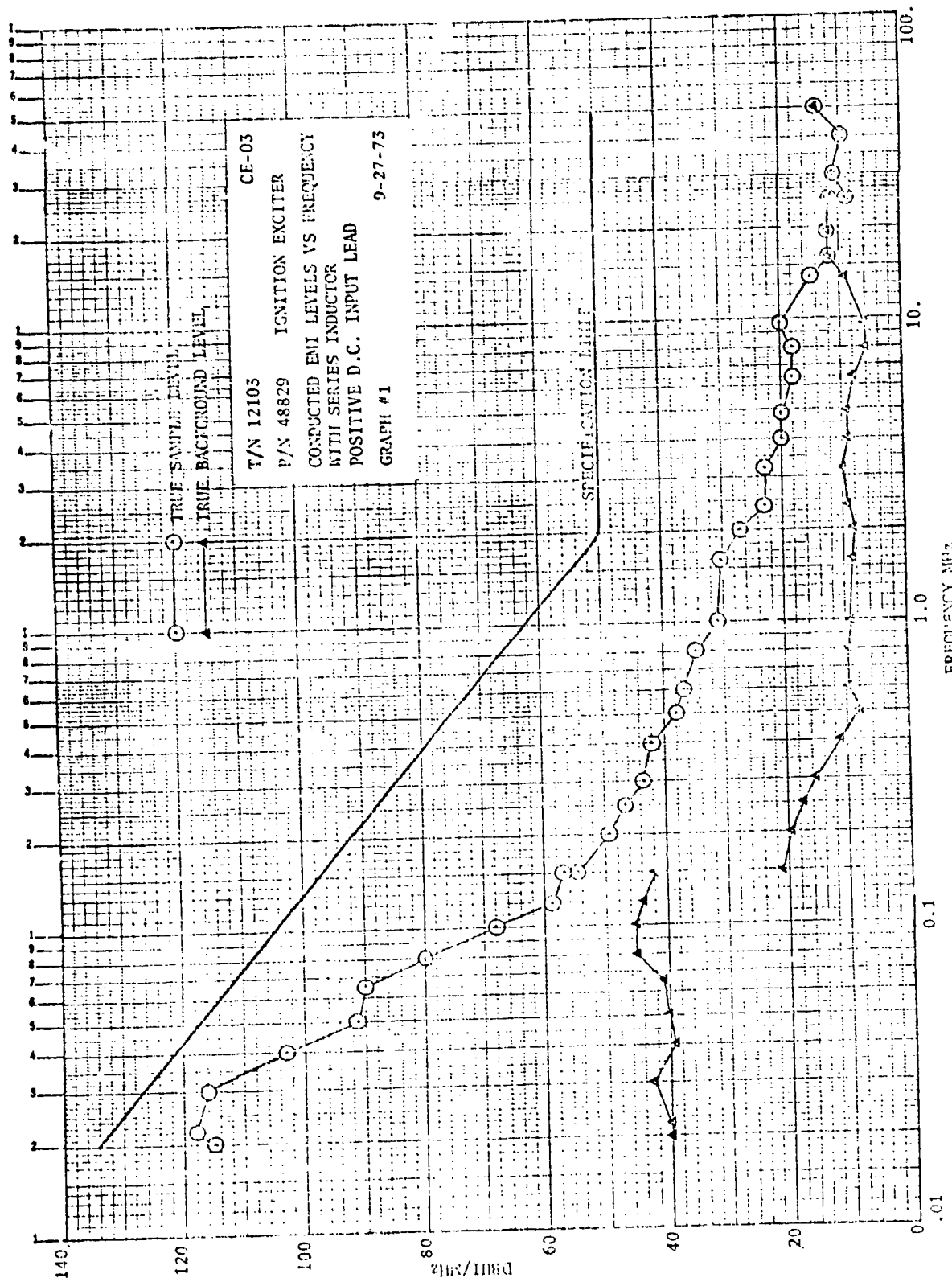


Figure B3. EMI Levels Vs. Frequency, Positive D.C. Input

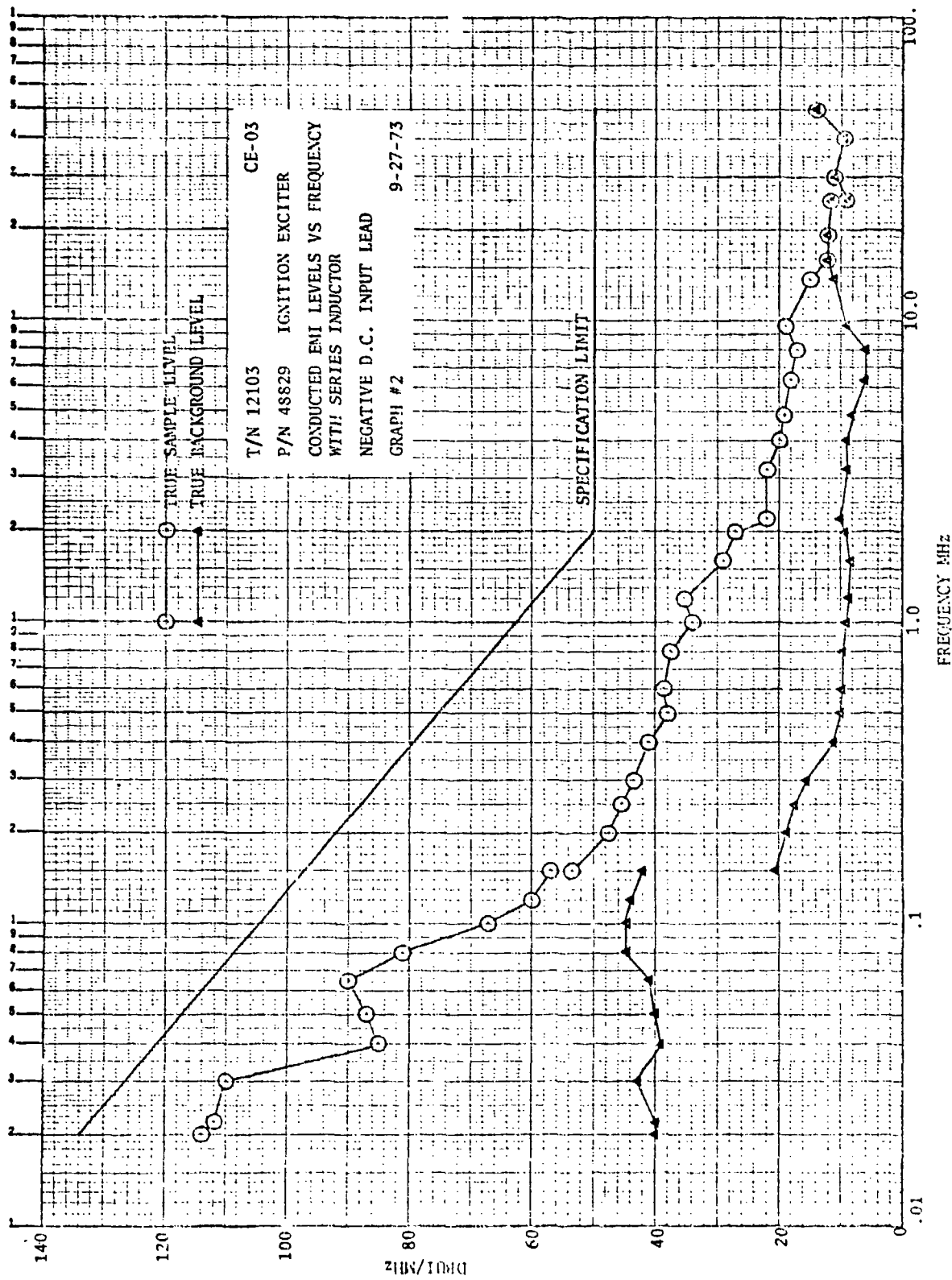


Figure B4. EMI Levels Vs. Frequency, Negative D.C. Input

TEST NO. 12103

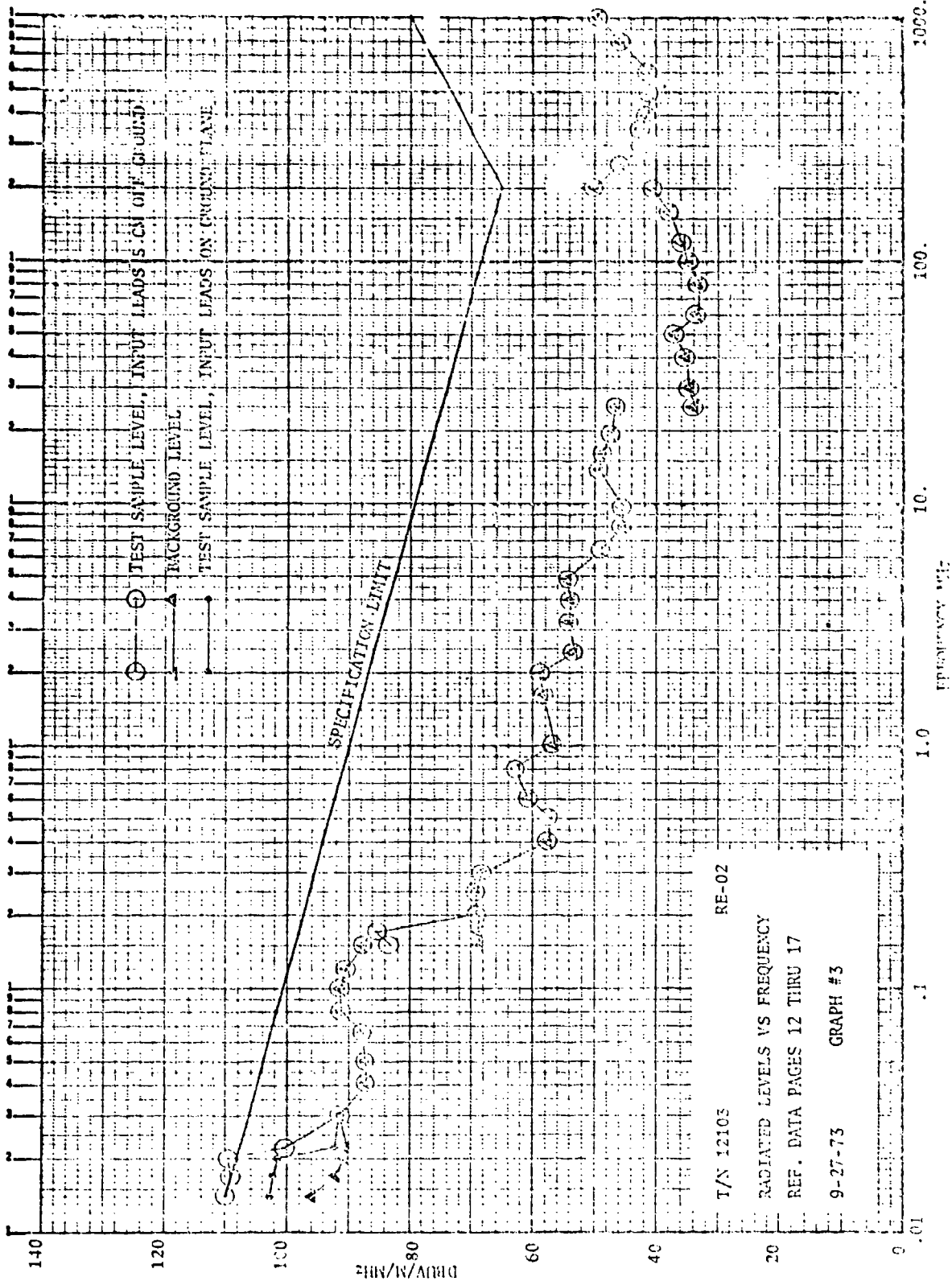


Figure B5. Radiated Levels Vs. Frequency

CONDUCTED BROADBAND RADIO INTERFERENCE TEST DATA

ITEM EXCITER NW 48829 SERIAL NO. 003
 ACCESSORIES IGNITION LEAD 40900 IGNITER AC.-Vc-610
 TEST NO. 12103 DATE 9-24-73 TECHNICIAN G. Ruck
 PURPOSE OF TEST PROTOTYPE EVALUATION
 TEST EQUIP. NE-105 AY SER. 3314 LAST CAL. 7-9-73
 TEST EQUIP. TR/NE-105 SER. 3314 LAST CAL. 7-5-73
 PROBE/TEST TR-10501 4N371-360 FUNCTION Peak FREQ. RANGE 100 MHz. to 25 MHz
 INPUT 30 VDC SPEC. 46.1 A (30) CONTRACT _____
C.E. 03 FAST SWITCH WITH Z-MAT INDUCTOR

FREQ	READING	BACKGROUND LEVEL	TRANSFER IMPEDANCE	TRUE BACKGROUND LEVEL	TRUE SAMPLE LEVEL	SPEC LIMIT	REMARKS
MHZ	DBU V /MHZ	DBU V /MHZ	SUB DB	DBU I /MHZ	DBU I /MHZ	DBU I /MHZ	DBUE = DB ABOVE 1 MICRO VOLT DBUI = DB ABOVE 1 MICRO AMP
1.50	60	26	5.2	20.8	54.8	97	
2.00	57	26	7.3	18.7	49.7	92	
2.50	55	26	8.5	17.5	46.5	88	
3.00	53	25	9.5	15.5	43.5	84	
4.00	53	22	11.0	11.0	42.0	79	
5.00	50	20	12.0	8.0	38.0	75	
6.00	49	22	12.5	9.5	36.5	72	
8.00	48	23	13.5	9.5	34.5	67	
1.00	45	23	14.0	9.0	31.0	62	
1.60	45	23	14.5	8.5	30.5	54	
2.00	42	23	14.8	8.2	27.2	50	
2.40	38	24	15.0	9.0	23.0	50	
3.20	38	25	15.0	10.0	23.0	50	
4.00	35	24	15.0	9.0	20.0	50	
4.80	35	24	15.0	9.0	20.0	50	
6.40	33	23	15.0	8.0	18.0	50	
8.00	33	21	15.0	6.0	18.0	50	
9.60	35	21	15.0	6.0	20.0	50	
13.80	30	24	15.0	9.0	15.0	50	
16.00	27	27	15.0	12.0	≤ 12.0	50	
19.20	27	27	15.6	12.0	≤ 12.0	50	
25.00	26	26	14.5	11.5	≤ 11.5	50	

APPROVED: C. J. B.
 WITNESSING INSPECTOR _____

CONDUCTED BROADBAND RADIO INTERFERENCE TEST DATA

ITEM Exciter PIN 48829 SERIAL NO. 003
 ACCESSORIES 16.0VITER AC VC-610
 TEST NO. 12103 DATE 9-24-73 TECHNICIAN G. R. Wood
 PURPOSE OF TEST PROTOTYPE EVALUATION
 TEST EQUIP. NF-105 XY SER. 3314 LAST CAL. 7-9-73
 TEST EQUIP. T₂/NF-105 X SER. 3314 LAST CAL. 7-5-73
 PROBE/TRANS Mag. 915507 2M827-200 FUNCTION Peak FREQ. RANGE 150MHZ to 25MHZ
 INPUT 30 VDC SPEC. 761A (3) CONTRACT FE03
FAST SWITCH WITH 2 MH INDUCTOR

FREQ	READING	BACKGROUND LEVEL	TRANSFER IMPEDANCE	TRUE BACKGROUND LEVEL	TRUE SAMPLE LEVEL	SPEC LIMIT	REMARKS
MHZ	DBU V /MHZ	DBU V /MHZ	DB	DBU I /MHZ	DBU I /MHZ	DBU I /MHZ	DBUE = DB ABOVE 1 MICRO VOLT DBUI = DB ABOVE 1 MICRO AMP
150	59	26	5.2	20.8	53.8	97	
200	55	26	7.3	18.7	47.7	92	
250	54	26	8.5	17.5	45.5	88	
300	53	25	9.5	15.5	43.5	84	
400	52	22	11.0	11.0	41.0	79	
500	50	22	12.0	10.0	38.0	75	
600	51	22	12.5	9.5	38.5	72	
800	51	23	13.5	9.5	37.5	67	
1.00	48	23	14.0	9.0	34.0	62	
1.20	50	23	14.5	8.5	35.5	59	
1.60	44	23	14.8	8.7	29.2	54	
2.00	42	24	15.0	9.0	27.0	50	
2.40	37	25	15.0	10.0	22.0	50	
3.20	37	24	15.0	9.0	22.0	50	
4.00	35	24	15.0	9.0	20.0	50	
4.80	34	23	15.0	8.0	19.0	50	
6.40	33	21	15.0	6.0	18.0	50	
8.00	32	21	15.0	6.0	17.0	50	
9.60	34	24	15.0	9.0	19.0	50	
13.80	30	26	15.0	11.0	15.0	50	
16.00	27	27	15.0	12.0	≤ 12.0	50	
19.20	27	27	15.0	12.0	≤ 12.0	50	
25.00	26	26	14.5	11.5	≤ 11.5	50	

APPROVED: C 9/15

WITNESSING INSPECTOR _____

RADIATED BROADBAND RADIO INTERFERENCE TEST DATA

ITEM EXCITER P/W 47829 SERIAL NO. 003
 ACCESSORIES IGNITION LEAD 40900, 15 AMPER AC, 1/2-610
 TEST NO. 12103 DATE 9-24-73 TECHNICIAN G. Buell
 PURPOSE OF TEST PROTOTYPE EVALUATION
 TEST EQUIP. NF-105 AT SER. 3314 LAST CAL. 2-9-73
 TEST EQUIP. TU/NF-105 X SER. 3314 LAST CAL. 2-5-73
 ANT. VA-105 FUNCTION Peak FREQ. RANGE 100 kHz to 50 MHz
 INPUT 30 VDC SPEC MIL-577-461A(3) CONTRACT _____

RF 02

FREQ.	READING	BACKGROUND LEVEL	ANT. FACTOR	TRUE BACKGROUND LEVEL	TRUE SAMPLE LEVEL	SPEC. LIMIT	REMARKS
MHZ	DBUE /MHZ	DBUE /MHZ	dB	DBUE/M /MHZ	DBUE/M /MHZ	DBUE/M /MHZ	DBUE = OR ABOVE 1 MICRO VOLT
.100	41	26	42.5	68.5	83.5	98.6	
.154	43	26	42.5	68.5	85.5	98.6	
.200	26	26	42.6	68.6	≤ 68.6	97.5	
.250	26	26	42.8	68.8	≤ 68.8	96.5	
.300	25	25	43.1	68.1	≤ 68.1	95.5	
.400	22	22	35.7	57.7	≤ 57.7	94.0	
.500	20	20	37.2	57.2	≤ 57.2	93.0	
.600	22	22	36.4	60.4	≤ 60.4	92.3	
.800	23	23	37.9	62.9	≤ 62.9	90.8	
1.00	23	23	33.4	56.4	≤ 56.4	89.8	
1.60	23	23	35.2	58.2	≤ 58.2	87.5	
2.00	23	23	35.9	58.9	≤ 58.9	86.5	
2.40	24	24	29.5	53.5	≤ 53.5	85.7	
3.20	25	25	29.0	54.0	≤ 54.0	84.4	
4.00	24	24	29.8	53.8	≤ 53.8	83.2	
4.80	24	24	30.6	54.6	≤ 54.6	82.4	
6.40	27	23	25.9	48.9	≤ 45.9	81.0	
8.00	21	21	24.8	45.8	≤ 45.8	80.0	
9.60	21	21	24.9	45.9	≤ 45.9	79.0	
13.80	24	24	25.3	49.3	≤ 49.3	77.5	
16.00	27	27	22.0	49.0	≤ 49.0	76.8	
19.20	27	27	20.6	47.6	≤ 47.6	76.0	
25.00	26	26	20.4	46.4	≤ 46.4	74.7	
.150	37	26	42.5	68.5	79.5	98.6	POWER BLEEDER RESISTORS
.154	38	26	42.5	68.5	80.5	98.6	MOVED TO BACK OF BOD. PLATE

APPROVED: G. Buell
 WITNESSING INSPECTOR _____

SUSCEPTIBILITY TEST DATA

ITEM Exciter P/N 48829 CONTRACT A 2312
 ACCESSORIES Ignition lead P/N ⁴⁰⁵⁰⁰ 41414 Terminal AC VC-610
 TEST NO. 12103 DATE 9/15/53 9/16/53 TECHNICIAN J. J. Maternal
 PURPOSE OF TEST Prototype Evaluation
 INPUT VOLTS 24, 28, 32 VDC MIL. SPEC. MIL-STD-461A (3)

FREQ KHZ	DELAY TIME M.S.					
	24V	V _{rms}	28V	V _{rms}	32V	V _{rms}
0	4.8 to 5.6	2.4	4.3 to 5.0	2.8	3.9 to 4.5	3.0
.030	4.4 to 6.0	2.4	3.9 to 5.2	2.8	3.4 to 5.0	3.0
.050	4.6 to 6.0	2.4	3.8 to 5.3	2.8	3.5 to 5.0	3.0
.060	4.4 to 6.0	2.4	4.6 to 5.7	2.8	3.6 to 4.8	3.0
.075	4.5 to 6.0	2.4	3.8 to 5.2	2.8	3.6 to 4.7	3.0
.100	4.6 to 5.8	2.4	3.8 to 5.2	2.8	3.5 to 4.4	3.0
.120	4.7 to 5.6	2.4	4.2 to 5.0	2.8	3.6 to 4.6	3.0
.150	4.8 to 5.5	2.4	4.2 to 4.8	2.8	3.8 to 4.5	3.0
.200	4.8 to 5.4	2.4	4.4 to 4.8	2.8	3.8 to 4.5	3.0
.250	4.8 to 5.4	2.4	4.2 to 4.8	2.8	3.8 to 4.4	3.0
.300	4.7 to 5.4	2.4	4.2 to 4.6	2.8	3.8 to 4.4	3.0
.500	4.6 to 5.4	2.4	3.8 to 4.8	2.8	3.6 to 4.4	3.0
.750	4.8 to 5.4	2.4	4.2 to 4.8	2.8	3.6 to 4.4	3.0
1.0	4.8 to 5.4	2.4	4.0 to 5.0	2.8	3.9 to 4.5	3.0
2.0	4.9 to 5.6	2.30	4.1 to 5.0	2.65	3.9 to 4.5	2.8
3.0	5.0 to 5.7	2.15	4.2 to 5.0	2.45	3.9 to 4.6	2.6
5.0	5.0 to 5.7	1.95	4.1 to 4.9	2.20	4.0 to 4.5	2.3

CONCLUSIONS SEE PAGE 78

B31

WITNESS _____ APPROVED [Signature]

SUSCEPTIBILITY TEST DATA

ITEM Exciter P/N 43529 CONTRACT A 2312
 ACCESSORIES Ignition Lead P/N 40900 Igniter PC, YC-610
 TEST NO. 12103 DATE 9/5/73 9/6/73 TECHNICIAN F. J. Wehrlich
 PURPOSE OF TEST Proto type Evaluation
 INPUT VOLTS 24, 28, 32 VDC MIL. SPEC. MIL-STD-461A (3)

FREQ KHz	DELAY TIME MS.					
	24 V		28 V		32 V	
	V _{min}	V _{max}	V _{min}	V _{max}	V _{min}	V _{max}
7.5	5.0 to 5.6	1.75	4.2 to 5.0	2.0	3.9 to 4.4	2.10
10	4.9 to 5.6	1.65	4.2 to 5.0	1.85	4.0 to 4.4	1.95
15	5.0 to 5.6	1.50	4.2 to 5.0	1.65	4.0 to 4.4	1.70
20	5.0 to 5.6	1.35	4.2 to 5.0	1.50	4.0 to 4.4	1.55
25	4.9 to 5.6	1.30	4.2 to 5.0	1.30	4.0 to 4.4	1.40
30	5.0 to 5.6	1.20	4.2 to 5.0	1.25	4.0 to 4.4	1.30
40	5.0 to 5.6	1.10	4.2 to 5.0	1.10	4.0 to 4.4	1.10
50	5.0 to 5.6	1.00	4.2 to 5.0	1.00	4.0 to 4.4	1.00
LIMIT	5.2 MAX		4.3 NOM		3.75 MIN	

CONCLUSIONS LOW FREQUENCIES HAVE A SLIGHT AFFECT ON DELAY TIME JITTER.

WITNESS _____ APPROVED G. J. S.

SUSCEPTIBILITY TEST DATA

ITEM Exciter P/N 48829 CONTRACT A 2312
 ACCESSORIES Ignition Lead P/N ⁴⁰⁹⁰⁰ 4410 Igniter AC, YC-610
 TEST NO. 12103 DATE 9/5/73 7/16/73 TECHNICIAN J. McDaniel
 PURPOSE OF TEST Prototype Evaluation
 INPUT VOLTS 24, 28, 32 VDC MIL. SPEC. MIL-STD-461A (2)

FREQ KHz	Number of Sparks Per Burst					
	24V	V _{RMS}	28V	V _{RMS}	32V	V _{RMS}
0	6	2.4	8	2.8	9	3.0
.030	6	2.4	8	2.8	9	3.0
.10	6	2.4	8	2.8	9	3.0
.20	6	2.4	8	2.8	9	3.0
.30	6	2.4	8	2.8	9	3.0
1.0	6	2.4	8	2.8	9	3.0
2.0	6	2.3	8	2.65	9	2.8
3.0	6	2.15	8	2.45	9	2.6
10	6	1.65	8	1.85	9	1.95
20	6	1.35	8	1.50	9	1.55
30	6	1.20	8	1.25	9	1.30
40	6	1.10	8	1.10	9	1.10
50	6	1.00	8	1.00	9	1.00

CONCLUSIONS NO CHANGE IN SPARKS PER BURST
WITH SUSCEPT. SIGNAL

WITNESS _____ APPROVED G.P.

SUSCEPTIBILITY TEST DATA

ITEM Exciter P/N 48829 CONTRACT 11 2312
 ACCESSORIES Ignition Lead P/N 40900 Igniter AC, YC-610
 TEST NO. 12103 DATE 9/5/73 9/26/73 TECHNICIAN T. J. Mahan
 PURPOSE OF TEST Prototype Evaluation
 INPUT VOLTS 24, 28, 32 VDC MIL. SPEC. MIL-STD-461A (3)

FREQ KHz	Signal level for Threshold of Susceptibility		
	24V	28V	32V
	V _{RMS}	V _{RMS}	V _{RMS}
.030	1.10	1.35	1.80
.050	1.18	1.62	2.0
.060	1.12	1.45	1.9
.075	1.25	1.70	2.05
.100	2.00	1.90	2.40
.150	2.00	2.20	3.00
.200	2.20	2.25	
.250	2.10	2.30	
.300	1.95	2.05	
.500	1.50	2.20	
.750	1.55	2.50	
1.0	1.65	2.40	
2.0	2.30	2.80	

CONCLUSIONS NONE REQ'D

WITNESS _____ APPROVED QJB